MINERALOGY, GEOCHEMISTRY AND PETROLOGY OF PEGMATITIC GRANITES AND PEGMATITES AT RED SUCKER LAKE, NORTHEASTERN MANITOBA

Leonard Eugene Chackowsky

B.G.S. (Brandon University)
B.Sc. (University of Manitoba)

A thesis presented to the
Faculty of Graduate Studies of the University of Manitoba
in partial fulfillment of the requirements for the degree of

Master of Science
in
Geological Sciences

Winnipeg, Manitoba

June 3, 1987 (C)

MINERALOGY, GEOCHEMISTRY AND PETROLOGY OF

PEGMATITIC GRANITES AND PEGMATITES AT

RED SUCKER LAKE, NORTHEASTERN MANITOBA

BY

LEONARD E. CHACKOWSKY

A thesis submitted to the Faculty of Graduate Studies of
the University of Manitoba in partial fulfillment of the requirements
of the degree of

MASTER OF SCIENCE

© 1987

ABSTRACT

Before this study, pegmatitic rocks occurring in the Archean Sachigo subprovince at Red Sucker Lake and Gods Lake, northeastern Manitoba, had not been studied in any significant detail, so that little was known about their parageneses and genetic affiliations.

The pegmatitic rocks at Red Sucker Lake occur in a 3 by 15 km area in two separate, parallel, E-striking shear zones. They intrude low-grade metabasalts and metasedimentary rocks of the Hayes River and Oxford Lake Groups, respectively. The southern shear zone hosts an elongated intrusion of pegmatitic granites and the Eastern series pegmatites. The Western series pegmatites are hosted by transverse joints north of the western end of the chain of pegmatitic granite exposures. The northern shear zone hosts the Northern series pegmatites.

The pegmatitic granites, mostly pegmatitic leucogranites, show an extreme increase in fractionation from the eastern and western margins to the central parts of the exposures, which is in part reflected by the appearance of petalite (up to 25%) and tantalite. In this respect they have no analogs among other pegmatitic leucogranites worldwide.

In contrast, the Eastern and Western series pegmatites are highly fractionated whereas the central Northern series are geochemically barren. The Western rare-element pegmatites contain Rb-Cs-rich lithian muscovite, spodumene, beryl, microlite and cassiterite. Field and geo-

chemical evidence indicate that the pegmatitic granites and pegmatites are consanguineous.

The Gods River albite-spodumene pegmatite intrudes metabasalts of the Hayes River Group near the north shore of Gods Lake. The pegmatite is 3 to 10 m thick and extends 2 km along strike to a depth of at least 250 m. It consists of 20-25% subparallel bladed spodumene grains and is unique in terms of its mineralogy and texture: no other pegmatitic rocks were observed in the area.

The only element that attains potentially economic quantities in these pegmatitic rocks is the lithium concentrated in the petalite-bearing pegmatitic leucogranites at Red Sucker Lake and in the Gods River pegmatite. These occurrences are not economically exploitable at present, but may be significant as strategic reserves in the future, particularly if extended by continued exploration in both areas.

ACKNOWLEDGEMENTS

CONTENTS

LIST OF TABLES

LIST OF FIGURES

Chapter I

INTRODUCTION

1.1 **SCOPE OF STUDY**

This study deals with a swarm of pegmatitic granites and pegmatites exposed along the northern margins of Red Sucker Lake, and one spodumene-bearing pegmatite exposed near the north shore of Gods Lake. Figure 1.1 shows the locations of the study areas.

To date, these rocks have not been studied in any significant detail, and so far almost nothing has been known about their parageneses and genetic affiliation. The present study, which is based on the first detailed sampling and documentation of these rocks, was undertaken in order to gain insight into the mineralogy, geochemistry and petrogenetic relationships of the pegmatitic granites and pegmatites in the two areas, and to assess their economic potential.
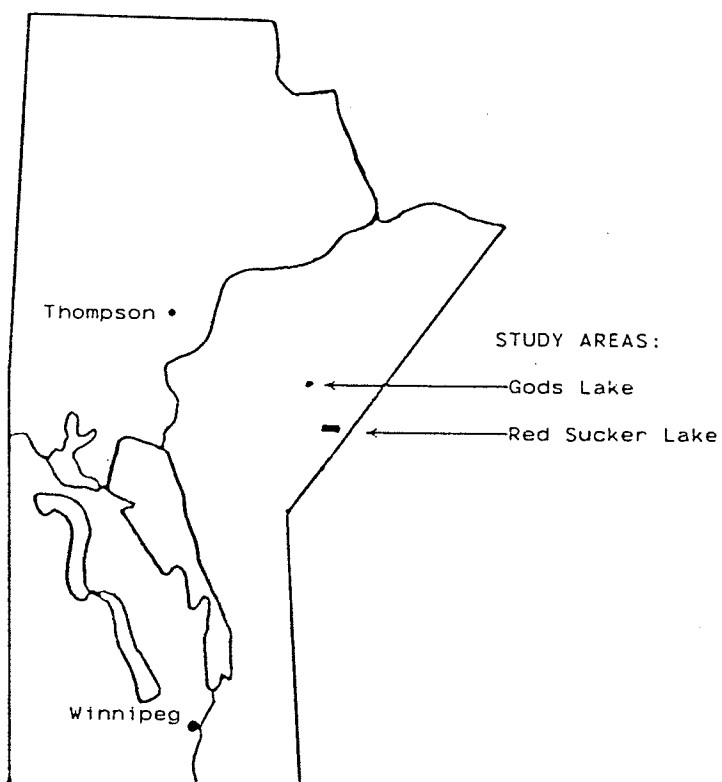
Figure 1.1: Map of Manitoba showing locations of the study areas.

1.2 PREVIOUS WORK

The general geology of the Stull Lake area, which includes Red Sucker Lake, was mapped by Downie (1963) at a scale of 1:253,400. The Boulton Lake-Red Sucker Lake area was mapped by Schledewitz and Kusmirski (1979), and the Red Sucker Lake area by Schledewitz (1980) at a scale of 1:100,000.

The cassiterite-bearing saccharoidal albite-rich dike at location TD (Figure 1.2) was discovered in 1928 (Bateman, 1943). Occurrences of cassiterite, topaz and indicolite in "albitite" were noted. By 1943,

279 m of diamond drilling was completed, but no ore-grade deposits of Sn were encountered. Bateman described a second pegmatite, trenched over a width of 16 m to a depth of < 0.3 m, containing a few bands of lithium minerals ("Either amblygonite or spodumene or both") along its footwall (Bannatyne, 1985), but no dikes in the area fitting that description were observed by this writer.

Pegmatitic rocks in northeastern Manitoba were examined by Bannatyne (1973). He made a brief note of the cassiterite-bearing saccharoidal dike on the north shore of Red Sucker Lake (the "Tin Dyke", location TD in Figure 1.2).

In 1980, five dikes on Red Sucker Lake were sampled by the Tantalum Mining Corporation of Canada, Ltd. (locations SQ, PK, TD, D, and the island immediately northeast of location D, Figure 1.2). These dikes were assayed for Ta_2O_5 and SnO_2. The pegmatite at location PK returned a high Ta_2O_5 assay but no further work was considered due to its small size. The pegmatite dike at location SQ yielded high Ta_2O_5 and SnO_2 assays from lepidolite which prompted Tanco to carry out a diamond drill study in 1981 in a futile attempt to determine the dike's lateral and/or vertical extent.

The Gods Lake area was mapped in 1971 to 1973 at a scale of 1:50,000 (Gilbert, 1985). The spodumene-bearing Gods River pegmatite, that out-crops near the north shore of Johnson Bay, was discovered in 1958 (Southard, 1977). Diamond drilling in 1959 by the Canadian Nickel Company showed that the dike continues for about 2 km eastward of the exposure along an east-west strike, and dips steeply to the north (Southard,
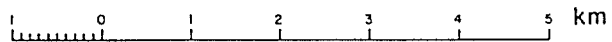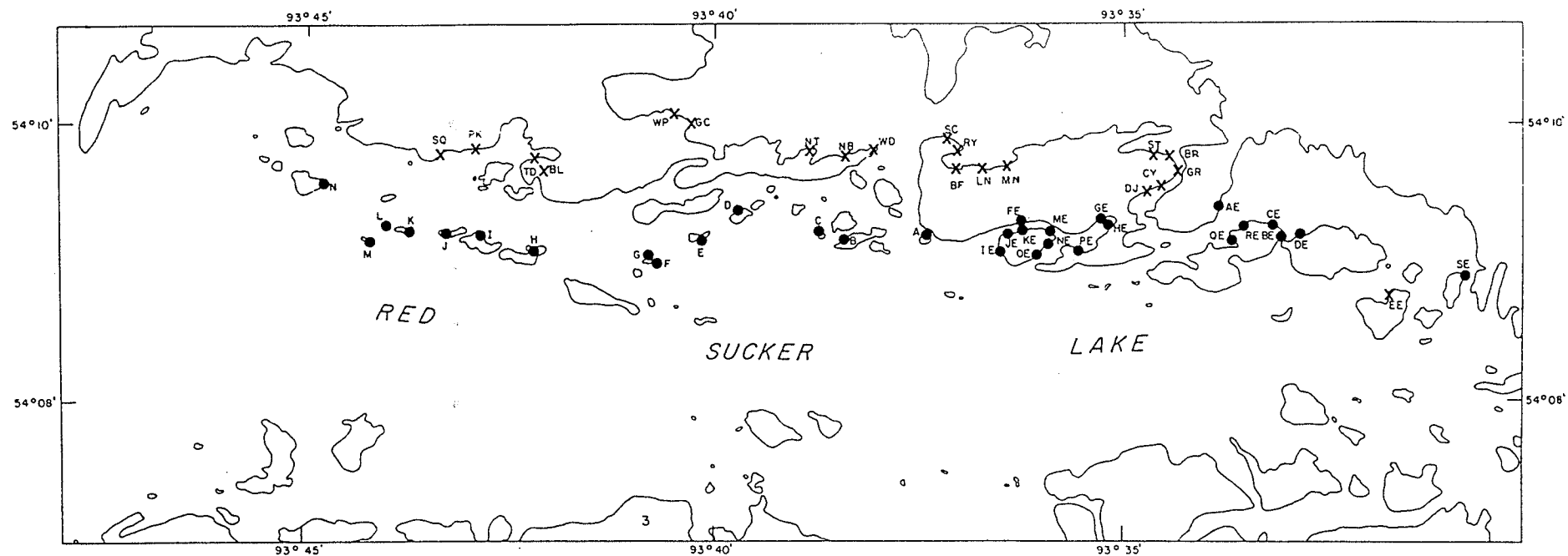
Figure 1.2: Sampling locations at Red Sucker Lake, Manitoba.
Modified after Chackowsky and Černý (1984).

1977;   see Manitoba Department of Energy and Mines Mineral Resources Division Open File 92618).

1.3   GENERAL GEOLOGY

Red Sucker Lake area

The pegmatitic granites and pegmatites are intruded into a 2 to 3 km wide east-trending belt of metavolcanic and metasedimentary rocks (Figure 1.3) that extends from the north shore of Red Sucker Lake to Pierce Lake, Ontario (Schledewitz and Kusmirski, 1979). The greenstone belt is one of many located in the Sachigo subprovince (synonymous with Gods Lake subprovince) of the Archean Superior province in the Canadian Shield (see Figure 1.4).   See Ermanovics et al. (1979) and Ermanovics and Wanless (1983) for more detailed information on the geology and complex thermal history of the Sachigo subprovince.

The oldest component of the belt is the Hayes River Group which is mainly composed of metavolcanic rocks intercalated with volcanogenic sedimentary rocks (Downie, 1936;   Schledewitz and Kusmirski, 1979). These rocks occur in the southwestern part of the belt at Red Sucker Lake where they are mostly composed of massive and pillowed metabasalts with local biotite-hornblende schists (Schledewitz, 1980, map unit 1a). Clark and Cheung (1980) reported a minimum (metamorphic) Rb-Sr whole-rock age of 2680 ±125 Ma for Hayes River Group rhyolite tuffs amd basalts in the Goose Lake area.

The Hayes River Group at Red Sucker Lake is in part overlain by younger metasedimentary rocks of the Oxford Lake Group to the north and east.   These are mostly garnetiferous biotite schists with subordinate
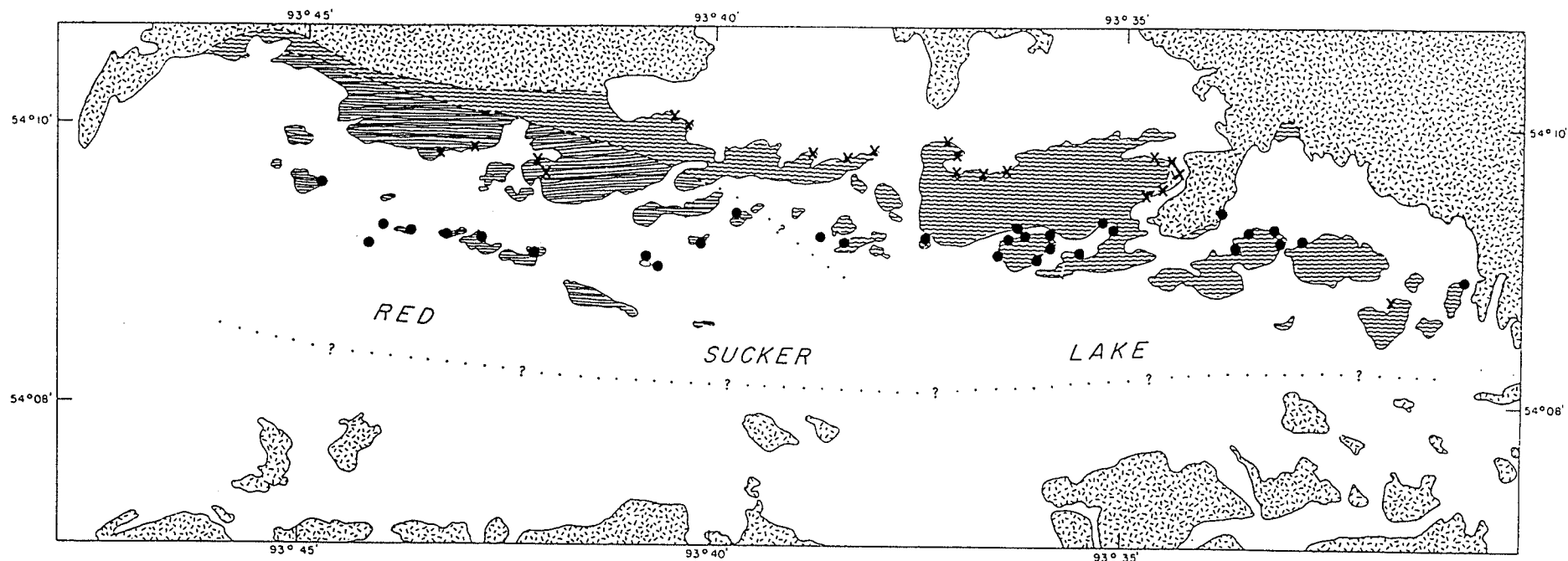
SYMBOLS:

● Pegmatitic granite – including pegmatitic leucogranite, fine-grained leucogranite and sodic aplite

x Pegmatite

---- Geological boundary (approximate, assumed)

LEGEND:

Hayes River Group: metamorphosed mafic volcanic and derived sedimentary rocks

Oxford Lake Group: arenaceous to pelitic metasedimentary rocks, pyroclastic rocks

Grey tonalite and granodiorite, pink granite

Figure 1.3: General geology of the Red Sucker Lake area. Modified after Chackowsky and Černý (1984).
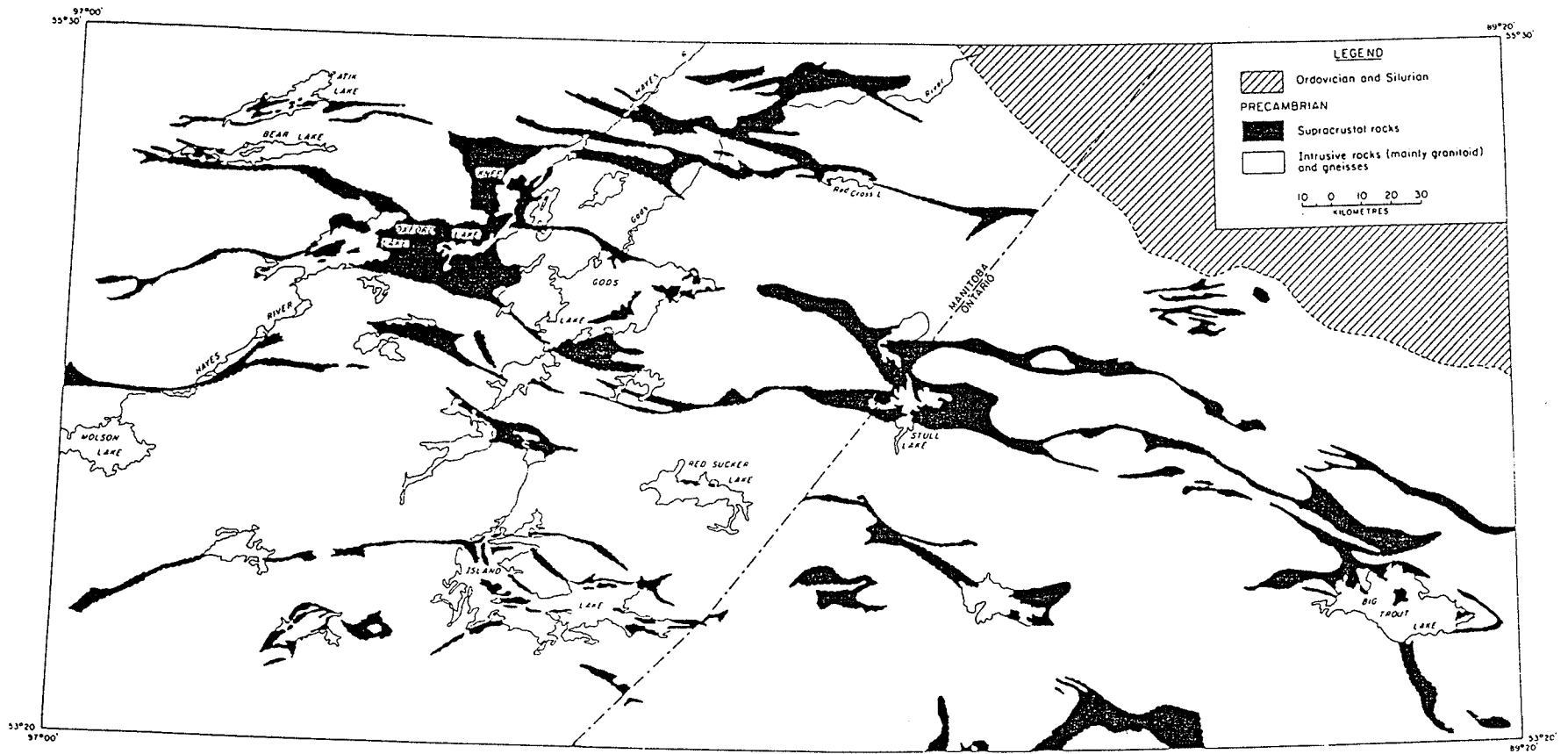
Figure 1.4: Distribution of greenstone belts (shaded) in the sachigo subprovince of the Canadian Shield in northeastern Manitoba. Modified after Gilbert (1985).

arenaceous lithologies.   Schledewitz (1980)   mapped these supracrustal rocks as "intermediate tuffaceous(?) rocks: layers of acicular amphibole, quartzo-feldspathic layers and muscovite-biotite-quartz-feldspar schists (± garnet, cordierite)" (unit 1c) with subordinate polymictic conglomerate (1h) and metagreywacke (1i).   Small, 0.5 to 1 m wide east-trending tonalitic dikes intrude the metasedimentary rocks.

The greenstone belt is flanked to the north and south by early plutonic rocks that are dominantly composed of leucotonalite (3d) with subordinate tonalite (2b), medium to coarse grained foliated hornblende (± biotite) tonalite to granodiorite (3a), and porphyroblastic granodiorite (3e) (Schledewitz, 1980).

The youngest rocks in the area are granitic batholiths (unit 7 in Schledewitz, 1980), and the pegmatitic granites and pegmatites. The batholiths are composed of pink, medium to coarse grained and locally porphyritic granite and are located several kilometers to the north and west of the study area.   High concentrations of U and Th are reflected by airborne radiometric anomalies of > 2 ppm eU (equivalent uranium) averaging approximately 10 ppm eU (Weber et al., 1982).   Clark and Weber (1987) report a Rb-Sr whole-rock age of 2495 ±30 Ma.

No isotopic age data are available for the pegmatitic rocks in the Red Sucker Lake area.   However, other pegmatitic rocks in the Sachigo subprovince have Rb-Sr whole-rock ages of between 2400 and 2500 Ma. The post-kinematic, highly fractionated Magill Lake granite has an age of 2455 ±35 Ma (Clark and Cheung, 1980), and preliminary results from late leucogranites in the Cross Lake pegmatite field give Rb-Sr ages from 2400 to 2500 Ma (Clark and Meintzer, in preparation).   By analogy to

these rocks, the late pegmatitic granites and pegmatites at Red Sucker Lake are inferred to be late Archean, but the age relationship between the pegmatitic and unit 7 batholithic rocks is uncertain.

Thick deposits of glacial drift leave only extremely limited exposure; it is generally restricted to shorelines.

Gods Lake area

The Gods River pegmatite intrudes a 3 to 10 km wide east-trending greenstone belt that is dominantly composed of sheared metabasalts (Figure 1.5). The greenstone belt is one of many in the Gods Lake-Oxford Lake area (see Figure 1.4).

The oldest component of the belt is the Hayes River Group, which, in the Gods Lake study area, is composed of metamorphosed mafic volcanic and related subvolcanic rocks and minor ultramafic and sedimentary rocks (units 1b, 1c, 1g and 1h in map GR83-1-8 in Gilbert, 1985). The pegmatite intrudes sheared metabasalts that occur in a small outcrop dominated by mafic to intermediate pyroclastic rocks (1f). Small amounts of younger felsic to intermediate volcanic fragmental rocks (2b) occur southeast of the pegmatite.

The youngest rocks in the area are metamorphosed tonalitic to granodioritic intrusive rocks of the Bayly Lake complex (units 4a, 4g and 7b, Gilbert, 1985), including the massive to porphyritic Gods River pluton located about 1 km southwest of Gods River, and the Gods River pegmatite (7i). Clark and Cheung (1980) reported a Rb-Sr whole-rock age of 2424 ±74 Ma for the massive to slightly foliated granodioritic Bayly Lake Pluton.

Figure 1.5: General geology of the northern part of the Gods Lake area. Modified after Chackowsky et al. (1985).

Chapter II

FIELD AND ANALYTICAL PROCEDURES

2.1 FIELD WORK

Outcrops of pegmatitic granites and pegmatites were sampled and docu-
mented in detail during the 1984 and 1985 field seasons. Documentation
consisted of describing the individual exposures in terms of size, atti-
tude, relationship to the host rock, mineralogical and/or textural zon-
ing, and mineral assemblages.

Sampling consisted of taking representative whole-rock and mineral
specimens from the pegmatitic granite and pegmatite outcrops for further
laboratory examination. As the pegmatitic granites at Red Sucker Lake
are generally similar to the pegmatites in terms of texture and nature
of the outcrops, the same sampling techniques were applied to both rock
types.

About 40 whole-rock specimens were collected at Red Sucker Lake and 4
from the Gods River pegmatite. An attempt was made to collect whole-
rock specimens from each of the locations shown in Figure 1.2, but this
was often impossible due to the smooth, relatively unfractured nature of
many of the outcrops. The pegmatitic granites at locations A, B, C, D,
I and L were too inhomogeneous and coarse-grained to take representative
samples due to the large quantities of rock that would be required (>100
kg). Instead, separate samples of the graphic K-feldspar megacrysts and

the matrix were collected, and modal analyses of the sample sites in terms of matrix vs graphic K-feldspar megacrysts (vs petalite megacrysts at locations B and C) were performed in the field. Normative mineral calculations on the analyses of the separate components were later used to estimate the densities of the samples. Multiplying the estimated densities by the modal (volume) proportions of the phases yields their weight proportions which were used to determine the whole-rock composi- tions at the above-mentioned sample sites. Due to the medium to coarse grained textures and homogeneous structures of the rocks at the remain- der of the pegmatitic granite and pegmatite locations, it was possible to collect representative, 3-5 kg whole-rock samples.

Approximately 700 mineral specimens were collected from the Red Suck- er Lake area, and 30 from the Gods River pegmatite. Blocky K-feldspars and garnets were collected from almost every sample location in Figure 1.2. Primary book muscovite was found at only a few localities, and, along with accessory minerals such as columbite-tantalite, apatite, gah- nite and tourmaline, was sampled wherever possible.

K-feldspars were collected for analysis only if they were blocky (i.e., non-graphic) in texture. They were collected from quartz pods if these features were observed at any given outcrop; otherwise the fresh- est and coarsest blocky K-feldspars were collected from unzoned bodies.

Coarse book muscovite samples were collected where present. Biotite samples were collected if they appeared to be exomorphic (in contact with metabasaltic host rocks), as these biotites are often extremely en- riched in Li, Rb and Cs.

Garnets were found at almost every outcrop in the Red Sucker Lake area, and were sampled from all rock types present at a given location. Notably, no garnets were observed in the most fractionated pegmatitic body in the area, the pegmatite at location SQ. Also, no garnet was observed in the Gods River pegmatite.

2.2   SAMPLE PREPARATION

Mineral specimens selected for non-microprobe chemical analysis were crushed to 1 to 3 mm fragments and separated by hand to provide 1 to 2.5 gram samples of pure material. The separated material was pulverized in a motorized agate mortar and pestle. Some of the powder was used to prepare smear mounts for x-ray diffraction analysis, the rest submitted for chemical analysis. 108 garnets, 8 opaque minerals, 6 apatites, and 3 gahnites selected for electron microprobe analysis were mounted in epoxy, ground flat, and polished. Final polishing was done using 0.25 micron grit.

44 whole rock samples were prepared for analysis by crushing in a jaw crusher, splitting off a 200 gram split, and pulverizing in a tungsten carbide mill. 5 and 10 gram splits of the powdered samples were submitted for analysis.

2.3   MINERAL ANALYSES

K-feldspar, mica and beryl

256 K-feldspars, 43 micas and one beryl sample were submitted for partial chemical analysis. K-feldspars were analyzed for Na, K, Ca, Fe, Li, Rb, Cs, Sr, Ba and Pb. Micas were analyzed for K, Ca, Mg, Na, Fe,

MN, Ti, Li, Rb, Cs and Be.   The beryl sample was analyzed for Fe, Mn, Ca, Na, Li, Rb and Cs. Samples > 2.0 grams were analyzed at the Manitoba Department of Energy and Mines Geochemical Laboratory, Winnipeg, Manitoba, using atomic absorption spectroscopy (AAS).   Samples < 2.0 but > 1.2 grams were analyzed at Bondar Clegg & Co. Ltd., Ottawa, using D C plasma and, for Cs, neutron activation.   Samples < 1.2 grams were analyzed at l'École Polytechnique, Montrèal, using AAS.

Electron microprobe analyses

Garnet, Ta-Nb oxide minerals, cassiterite, apatite, and gahnite samples were analyzed at the Department of Geological Sciences, University of Manitoba.   A MAC-5 microprobe operating in energy dispersive mode was used for all the analyses.   Operating conditions were: 15 kV, 5 nA for Ta-Nb-Sn oxides minerals, 10 nA for other minerals, and 200 second collection times.   The presence of internal zoning was determined by comparing spectra collected at the cores and rims of mineral grains.   If zoning was detected then 2 or more spectra were collected and the analyses averaged out for the grain.   Standards used to calibrate the analyses are listed in Table 2.1.

Fe concentrations were recalculated as FeO.   If the total number of cations per unit formula of garnet and the Nb-Ta-oxide minerals was higher than the ideal number, then some of the FeO was recalculated as Fe_2O_3 by normalizing to the ideal number of cations per unit formula, thus providing a calculated Fe^{3+}/Fe^{2+} ratio.   Calculated Fe^{2+}/Fe^{3+} ratios for wodginites have been shown to agree with ratios determined experimentally by Mössbauer spectroscopy (Ercit, 1986).

Table 2.1: Mineral standard used in electron microprobe analyses.

Element	Garnet	Apatite	Ta–Nb–Sn Oxides
Mg	pyrope		pyrope
Al	spessartine		
Si	pyrope		
P		apatite	
Ca	pyrope	pyrope	microlite
Sc			Sc_2O_3
Ti			titanite
Mn	spessartine	spessartine	Mn–tantalite
Fe	chromite		fayalite
Nb			Fe–columbite
Sn			cassiterite

Optical methods

Compositions of albite-twinned plagioclase in thin section were determined by the universal stage method of orienting the grains normal to x and measuring extinction angles between (010) and α' (Deer et al., 1966). The intersection of the (010) composition plane and the (001) cleavage plane defines the position of [100], the x axis. The inset in Figure 123 of Deer et al. (1966) shows a schematic diagram of a plagioclase grain oriented normal to x. If this grain is brought to extinction by a clockwise rotation then the extinction angle is positive in sign. This method gives data for low-temperature plagioclase only. The measured samples were assumed to be low-T due to the fully ordered nature of the K-feldspars (all maximum microcline) and the Archean age of the pegmatitic granites and pegmatites at Red Sucker Lake and Gods Lake. For more information on universal stage techniques, see Phillips (1971).

X-ray diffraction studies

X-ray diffraction methods were used in order to identify unknown minerals, determine microcline triclinicities and unit cell parameters, and to determine muscovite polytypes.

A Phillips automated powder diffractometer with a graphite monochromator was used for most of the x-ray work. The powder diffractometer was operated using Cu Kα radiation. Instrumental settings were 40 kV, 40 mA and scanning speeds of 0.1 °/s for triclinicity and polytype determinations, and 0.01 °/S for determination of unit cell parameters. Very small mineral grains were identified with a 114 mm Gandolfi camera using Cu Kα radiation, Ni filter, 35 kV, 20 mA and exposure times ranging from 1 to 8 hours depending on sample size.

Triclinicities of microcline samples were determined by measuring the separation of the (131) and (131) reflections which corresponds to the obliquity of the β angle. Triclinicity (Δ) is given by the formula of Goldsmith and Laves (1954):

$$\Delta = 12.5 \ (d_{131} - d_{1\bar{3}1}).$$

Unit cell parameters for microcline samples were determined using unambiguously indexed peak positions (output by the diffractometer computer) in the range 20° to 52° 2θ. LiF was used as the internal standard. Peak tip positions were corrected for $K\alpha_1$–$K\alpha_2$ overlap using a correction equation, calibrated for the x-ray goniometer at the University of Manitoba (Ercit, 1986):

$$y = ax^4 + bx^3 + cx^2 + x$$

where
$y = 2\theta$ (corrected)
$x = 2\theta$ (observed)
$a = -3.44 \times 10^{-8}$
$b = 3.92 \times 10^{-6}$
$c = -1.111 \times 10^{-4}$.

Unit cell parameters were refined using the least squares program (CELREF) of Appleman and Evans (1973).

2.4 WHOLE-ROCK ANALYSES

Whole-rock samples were analyzed at the Department of Geology, University of Ottawa, and Bondar Clegg & Co., Ldt., Ottawa.

All analyses at the University of Ottawa were done by x-ray fluorescence spectroscopy (XRF) and included the following elements: Si, Al, Fe (total Fe as Fe_2O_3), Mn, Mg, Ca, Na, K, Ti, P, S, Ba, Sr, Rb, Cr, Zr, Y, Nb, Zn, Ni and V.

Bondar-Clegg analyzed for the following elements: Li and Be (AAS), CO_2 and H_2O (gravimetric analysis), F (specific ion electrode), Hf, Ta, Th, U and Cs (neutron activation), FeO (volumetric analysis), and Ga and Sn (XRF).

Fe_2O_3 was calculated for each sample by converting the concentration of FeO (from volumetric analysis) to an equivalent amount of Fe_2O_3, and subtracting this from the concentration of total Fe reported as Fe_2O_3 (from XRF analysis).

2.5 RADIOGENIC [87]SR CORRECTIONS

Due to the decay of [87]Rb to [87]Sr over geologic time, much of the Sr re-
ported in mineral and whole-rock analyses from highly fractionated peg-
matitic rocks with high Rb/Sr ratios is radiogenic [87]Sr. This radiogen-
ic [87]Sr must be subtracted from the total Sr reported in an analysis
before it can be used to model igneous processes (Clark and Černý,
1987). Therefore, due to the extremely high Rb/Sr ratios encountered in
some of the whole-rock and K-feldspar samples, this correction was made
before using any of the Sr data. The concentration of radiogenic [87]Sr
in a sample is calculated using the equation

$$^{87}Sr = {}^{87}Rb \; X \; [\exp(1t) - 1]$$

where [87]Sr is the concentration of radiogenic [87]Sr, [87]Rb is the present
day concentration of [87]Rb, 1 is the [87]Rb decay constant (1.419×10^{-11}
y^{-1}) (Steiger and Jäger, 1977), and t is the assumed Rb-Sr age of the
sample. [87]Rb is calculated by multiplying the concentration of total Rb
in a sample by the present-day weight proportion of [87]Rb/total Rb ([87]Rb
= 0.2832 X total Rb). Common Sr is then determined by subtracting the
calculated radiogenic [87]Sr from the analyzed total Sr.

The least certain term in the calculation is t, since there are no
isotopic age data available for pegmatitic rocks in the study areas.
Analogous fertile granites and pegmatitic granites in the Superior and
Slave provinces give Rb-Sr whole-rock ages averaging approximately 2500
Ma (Clark and Černý, 1987; Clark and Cheung, 1980; Clark and Meintzer,
in preparation). These are probably minimum ages of primary crystalli-
zation which, in the Sachigo subprovince and the Yellowknife pegmatite

field, post-date corresponding U-Pb zircon ages by 100-200 Ma. In the Winnipeg River district, Rb-Sr ages of pegmatite K-feldspars were used by Clark and Černý (1987) to estimate the age of the pegmatites at 2575 Ma which is 175 Ma younger than U-Pb zircon ages of early granitoid rocks in the area. Based on all of this data, a value of 2500 Ma was chosen as a reasonable estimate of the Rb-Sr age of the whole-rock and feldspar samples from the Red Sucker Lake and Gods Lake areas.

Chapter III

PEGMATITIC GRANITES AT RED SUCKER LAKE

3.1 DISTRIBUTION AND INTRUSIVE RELATIONSHIPS

Pegmatitic granites occur throughout the Red Sucker Lake area in a long, narrow east-trending belt which may partly follow an axial shear zone in the greenstone belt (Chackowsky and Černý, 1984). Pegmatitic leucogranites are the most common type of pegmatitic granite at Red Sucker Lake, with lesser amounts of fine-grained leucogranites and sodic aplites (for nomenclature and rock-type descriptions see Černý et al., 1981).

Figure 3.1 shows the sampling locations and distribution of pegmatitic granites at Red Sucker Lake. The pegmatitic granites have been subdivided into Eastern and Western series at the eastern and western margins of the study area, and a central Main series which contains petalite-bearing pegmatitic leucogranites in its core.

The pegmatitic leucogranite dikes range from less than 1 m in width to several tens of m and attain up to 100 m in length. Exposures are generally concordant to the schistosity of the country rocks, with sharp contacts and no chill margins. Shear banding and boudinage occur in several outcrops as seen in Figures 3.2 and 3.3.

Sodic aplite commonly occurs as narrow layers intimately associated with the pegmatitic leucogranite. In a few locations, for example location KE, aplite predominates over pegmatitic leucogranite, at least within the limits of exposed outcrop.

Figure 3.1: Distribution of pegmatitic granite sampling locations at Red Sucker Lake. Modified after Chackowsky and Černý (1984).
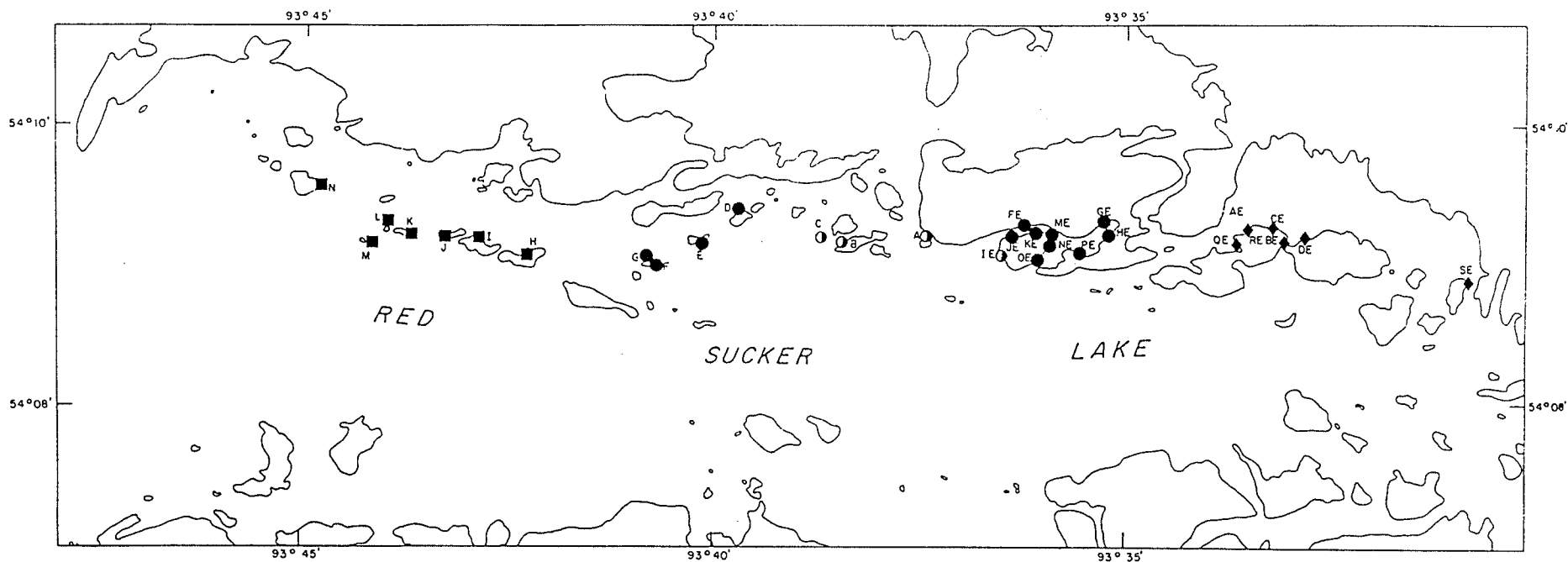
SYMBOLS:

♦ Eastern Series Pegmatitic Granites

■ Western Series Pegmatitic Granites

● Main Series Pegmatitic Granites

O Petalite-bearing Main Series Pegmatitic Granites

Fine-grained leucogranite is rare in the area. It occurs as small scattered exposures typically interlayered with pegmatitic leucogran-ites, as at location G.

Figure 3.2: Shear banding in pegmatitic leucogranite at location A. Note quartz 'eyes' (pale grey) and deformed K-feldspar (dark bluish-grey) near top of photo). Pencil is 14 cm long.

Figure 3.3:   Boudins in pegmatitic leucogranite at location E.   Sharp
intrusive contacts and lack of internal zoning are characteristic of
pegmatitic granites at Red Sucker Lake. Pencil is 14 cm in length.

3.2   INTERNAL STRUCTURE

In general, the pegmatitic granites in the Red Sucker Lake area are tex-
turally inhomogeneous.   Two types of pegmatitic granite commonly occur
in a single exposure (e.g., aplite and pegmatitic leucogranite at loca-
tions B and C, fine-grained leucogranite and pegmatitic leucogranite at
location G).   Large variations in grain size in the pegmatitic leuco-
granites are common,   but systematic textural and mineralogical zoning
was not observed.

The pegmatitic leucogranites commonly contain megacrysts of graphic K-feldspar + quartz intergrowths up to 30 cm in maximum exposed dimension (Figure 3.4). They are typically embedded in a finer grained matrix of quartz, feldspar and muscovite with accessory garnet. Large petalite megacrysts are locally abundant at locations B and C (Figure 3.5).

The pegmatitic leucogranites typically contain numerous small segregations of potassic pegmatite. These irregularly shaped blebs are 2 to 10 cm across, composed of blocky K-feldspar and massive quartz, with accessory micas, schorl and garnet.

Aplite typically comprises 10 to 20% of individual outcrops. They are usually banded, with the darker bands enriched in garnet (Figure 3.6).

(A)

(B)

Figure 3.4: (A): Graphic K-feldspar + quartz megacrysts embedded in finer-grained matrix of pegmatitic leucogranite at location C. Pencil is 14 cm long. (B): Close-up of the same rock type at location B. Field book is 20 cm in length.

Figure 3.5: Petalite (pale grey) and graphic K-feldspar + quartz (white) megacrysts embedded in matrix of pegmatitic leucogranite at location C.

Figure 3.6: Banded aplite at location A. Darker bands are enriched in garnet with respect to the lighter bands. Pencil is 14 cm long.

3.3   PETROCHEMISTRY

Sixteen chemical analyses of pegmatitic leucogranites, fine-grained leu-
cogranites and sodic aplites from Red Sucker Lake are listed in Tables
3.1 and 3.2, from which it can be seen that all of the rocks analyzed
are peraluminous. Various compositional parameters from the analyses of
the pegmatitic and fine-grained leucogranites are ploted in Figures 3.7
to 3.19.   These diagrams show a strong fractionation trend in terms of
increasing Li, Rb, Cs, Nb and Ta, and decreasing K/Rb, Nb/Ta and Al/Ga
from the marginal Eastern and Western series inward toward the Main se-
ries and the petalite-bearing pegmatitic leucogranites. K/Rb values are
consistently low, less than 100 for pegmatitic leucogranites, which in-
dicates advanced fractionation throughout the field.

The petalite-bearing pegmatitic leucogranites occupy distinct zones
on the K/Rb vs Li, Li vs F, Li vs Sn and Mg/Li vs Li diagrams.   These
diagrams show that the Main series pegmatitic granites, and especially
the petalite-bearing ones, also have high values of Rb, Cs, Nb, Ta and
Ga, and corresponding low values of K/Rb, Mg/Li, K/Cs, Nb/Ta and Al/Ga.
All these parameters indicate a fractionation trend toward the centre of
the Main series.   Ba, F and Sn do not show any significant variations
with increasing fractionation.

The K/Rb vs Sr diagram (corrected for radiogenic ^{87}Sr) in Figure 3.11
shows no systematic variation in Sr with fractionation.   Negative Sr
values are considered to be a result of post-crystallization migration
of radiogenic ^{87}Sr, or, at least in part, to analytical errors (Clark
and Černý, 1987).

Li in the pegmatitic leucogranites ranges from 8 ppm at location QE to 6900 ppm at location C. Li is also anomalously high at locations B (6050 ppm) and A (2650 ppm). These high values are due to the presence of petalite at these locations! Modal determinations in the field yielded 20% petalite at location B and 25% at location C.

Various geochemical parameters are plotted against K/Rb ratios for all of the analyzed pegmatitic leucogranites in Figure 3.20. Most of the data show fractionation trends from the marginal Eastern and Western series toward the central Main and petalite-bearing pegmatitic leuco-granites. Li, Cs, Sn and Ba increase while Al/Ga and Nb/Ta decrease with increasing K/Rb ratios. The erratic behavior of Li may in part re-flect the difficulty in obtaining representative whole-rock samples. Common Sr values are typically negative for these rocks and are there-fore not plotted in Figure 3.20.

Whole-rock contents of SiO_2, Al_2O_3, Li_2O, Na_2O and K_2O were recalcu-lated to 100% combined normative quartz, alkali feldspar and eucryptite, $LiAlSiO_4$ (Figure 3.21). Chemical data for the Bikita (petalite-bearing) and Kings Mountain (spodumene-bearing) pegmatites (Stewart, 1978) are plotted for comparison. Samples B and C plot in close proximity to the data for the Bikita and Kings Mountain pegmatites respectively, and plot within the general field of lithium-aluminosilicate-enriched units of zoned pegmatites, and the bulk compositions of the quasi-homogeneous al-bite-spodumene pegmatite type, as established by Stewart (1978).

Table 3.1: Whole-rock analyses of pegmatitic leucogranites at Red Sucker Lake.

Sample	A	B	C	D	F-09	I	L	QE-01
Wt.%:								
SiO_2	75.30	72.00	74.99	72.31	78.69	74.47	76.41	75.33
TiO_2	<0.01	<0.01	<0.01	0.01	0.01	0.01	0.02	0.00
Al_2O_3	15.53	16.52	15.84	15.70	12.37	14.39	14.12	15.12
Fe_2O_3	0.04	0.17	0.18	0.38	0.23	0.07	0.01	0.21
FeO	0.09	0.27	0.21	0.46	0.50	0.82	0.01	0.27
MnO	0.23	0.08	0.19	0.08	0.09	0.13	0.02	0.22
MgO	0.10	0.03	0.18	0.09	0.15	0.11	0.12	0.03
CaO	0.27	0.10	0.10	0.08	0.20	0.24	0.79	0.22
Na_2O	5.52	3.26	2.59	2.86	2.96	3.38	4.98	5.64
K_2O	1.58	4.31	3.59	6.91	4.11	6.00	2.72	1.37
P_2O_5	0.09	0.05	0.06	0.05	0.04	0.05	0.02	0.10
CO_2	0.02	0.04	0.05	0.09	0.04	0.10	0.09	0.02
H_2O^+	0.20	0.20	0.10	0.15	0.20	0.15	0.10	0.15
H_2O^-	nd	nd	nd	nd	nd	nd	nd	nd
S	<0.01	<0.01	<0.01	<0.01	<0.01	<0.01	<0.01	0.01
F	0.01	0.14	0.07	0.12	0.05	0.03	<0.00	0.01
Σ	98.98	97.11	98.12	99.24	99.62	99.93	99.41	98.61
PPM:								
Li	2650	6050	6880	221	100	39	14	8
Rb	1235	2800	2400	4723	662	795	369	377
Cs	54	80	108	57	11	12	14	18
Be	52	58	51	26	3	1	3	29
Sr	14	27	27	45	5	5	9	13
Ba	26	77	55	63	46	34	60	65
Ga	54	86	73	93	42	35	60	71
U	3	2	2	4	2	3	2	5
Th	5	4	5	7	5	4	9	5
Zr	<10	<10	<10	<10	<10	<10	<10	16
Hf	2	2	2	1	<1	<1	<1	3
Zn	29	122	110	129	49	37	30	30
Sn	15	50	81	252	22	15	19	34
Nb	62	71	91	64	30	17	33	61
Ta	213	64	66	29	12	6	11	89
Y	<10	<10	<10	<10	<10	12	33	<10
A/CNK	3.13	2.74	3.20	1.92	2.17	1.86	2.36	3.14
K/Rb	10.6	12.8	12.4	12.1	51.5	62.7	61.2	30.2
K/Cs	243	447	276	1006	3102	4151	1614	632
Rb/Cs	22.9	35.0	22.2	82.9	60.2	66.3	26.4	20.9
Ba/Rb	0.021	0.027	0.023	0.013	0.067	0.043	0.16	0.17
Al/Ga	1500	1000	1100	890	1600	2200	1200	1100
Nb/Ta	0.29	1.11	1.38	2.21	2.50	2.83	3.00	0.69

$A/CNK = Al_2O_3 / (CaO + Na_2O + K_2O)$

Table 3.2: Whole-rock analyses of fine-grained leucogranites and sodic aplites at Red Sucker Lake.

	Fine-grained leucogranites				Sodic aplites			
Sample	G-19	I-20	J-30	J-37	B-10	B-34	C-04	KE-24
Wt.%:								
SiO_2	75.03	76.20	73.93	76.24	74.40	74.04	74.00	72.36
TiO_2	0.02	0.02	0.03	0.03	<0.01	<0.01	<0.01	<0.01
Al_2O_3	14.52	14.11	14.66	13.71	15.50	16.01	15.76	16.29
Fe_2O_3	0.44	0.25	0.27	0.30	0.20	0.07	0.07	0.02
FeO	0.71	0.59	0.62	0.61	0.35	0.27	0.11	0.16
MnO	0.11	0.08	0.07	0.08	0.15	0.23	0.08	0.27
MgO	0.16	0.16	0.17	0.14	0.08	0.05	0.09	0.08
CaO	0.34	0.94	0.79	1.01	0.23	0.31	0.22	0.33
Na_2O	3.82	6.80	4.68	4.91	6.71	8.34	6.93	7.33
K_2O	3.77	0.47	4.25	2.75	1.51	0.31	2.09	2.66
P_2O_5	0.03	0.02	0.30	0.03	0.05	0.05	0.08	0.20
CO_2	0.04	0.14	0.04	0.10	0.04	0.14	0.00	0.12
H_2O^+	0.15	0.15	0.15	0.10	0.20	0.05	0.10	0.20
H_2O^-	nd	nd	nd	nd	nd	nd	nd	nd
S	<0.01	<0.01	<0.01	<0.01	<0.01	<0.01	<0.01	<0.01
F	0.07	<0.01	0.01	<0.01	0.09	0.02	0.02	0.02
Σ	98.18	99.93	99.96	100.01	99.47	99.98	99.54	100.03
PPM:								
Li	124	18	23	20	428	309	516	143
Rb	616	47	364	261	1052	183	1166	1268
Cs	13	3	8	7	32	27	29	37
Be	3	3	3	1	66	59	77	9
Sr	1	22	12	19	9	1	9	20
Ba	65	63	74	90	47	56	56	58
Ga	60	29	28	14	74	111	73	102
Zn	54	35	29	55	235	49	59	<10
U	5	10	13	17	3	3	4	2
Th	7	15	21	24	4	5	3	5
Zr	<10	31	40	58	<10	10	29	16
Hf	<1	2	2	2	2	7	4	10
Sn	31	6	9	6	38	11	75	11
Nb	61	35	25	21	89	87	113	78
Ta	17	22	4	7	73	110	179	181
Y	12	36	45	54	<10	<10	<10	<10
A/CNK	3.77	2.77	2.03	2.25	2.77	2.90	2.52	2.30
K/Rb	50.8	83.0	96.9	87.5	11.9	14.1	14.9	17.4
K/Cs	2400	1300	4400	3300	390	95	600	600
Rb/Cs	47	16	46	37	33	6.8	40	34
Ba/Rb	0.11	1.3	0.20	0.35	0.045	0.31	0.048	0.046
Al/Ga	1300	2600	2800	5200	1100	760	1100	850
Nb/Ta	3.6	1.6	6.3	3.0	1.2	0.79	0.63	0.43

$A/CNK = Al_2O_3 / (CaO + Na_2O + K_2O)$
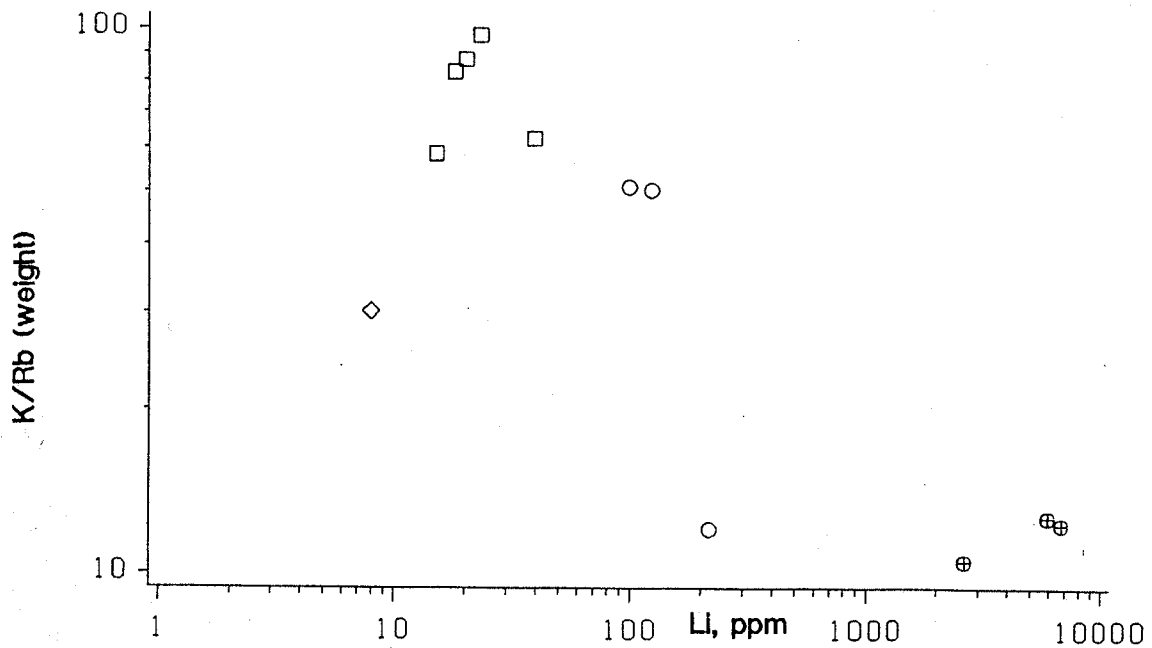
Figure 3.7: K/Rb vs Li plot for pegmatitic granites at Red Sucker Lake. Li increases with decreasing K/Rb ratio (increasing K/Rb fractionation). Note the extremely high Li contents of the petalite-bearing pegmatitic leucogranites. Data in this and following diagrams are grouped into the following units: Eastern (diamonds), Western (squares), Main (open circles), and petalite-bearing Main pegmatitic granites (crossed circles).
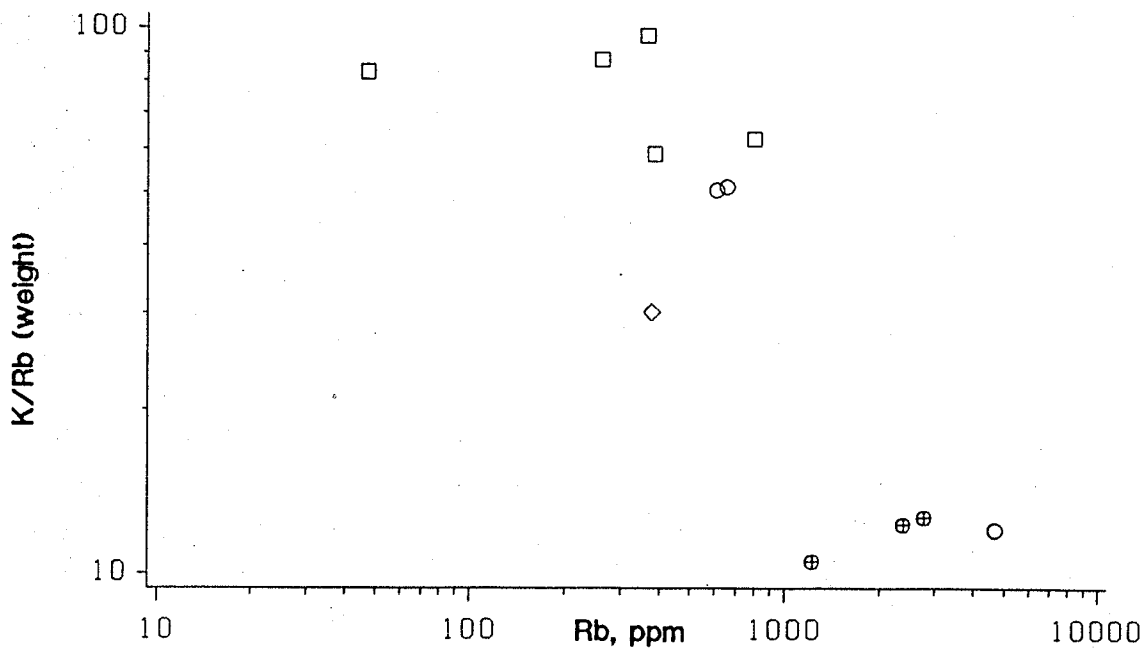
Figure 3.8: K/Rb vs Rb plot for pegmatitic granites at Red Sucker Lake. Rb increases with increasing K/Rb fractionation. Symbols as in Figure 3.7.
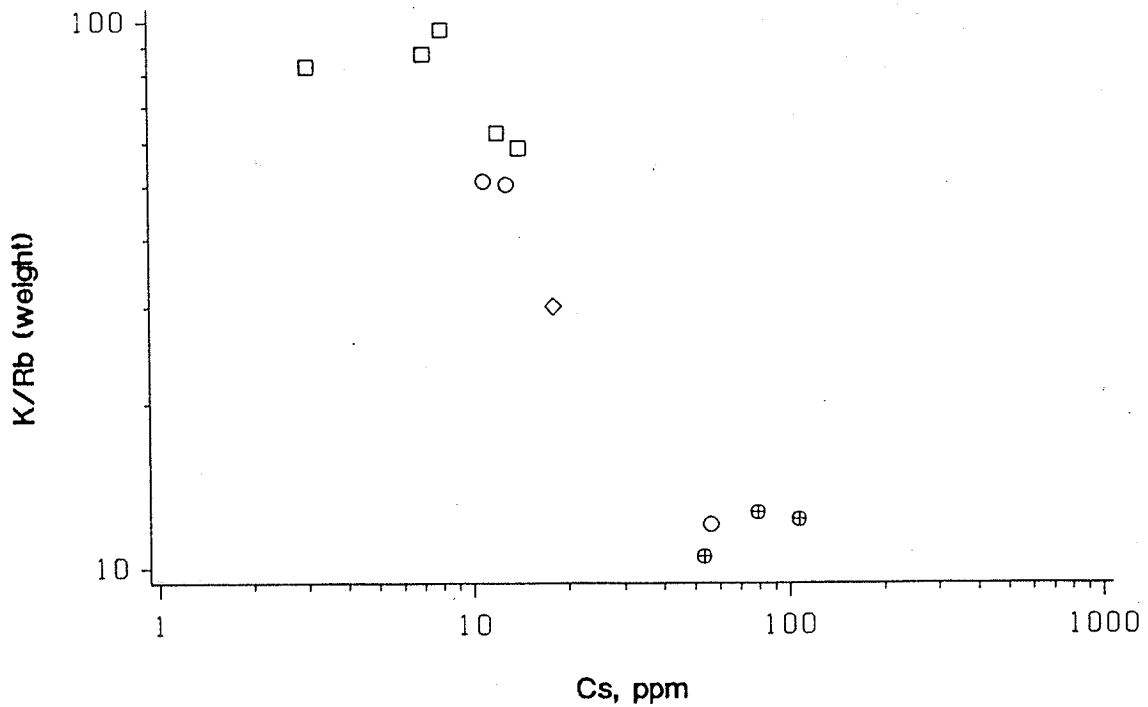
Figure 3.9: K/Rb vs Cs plot for pegmatitic granites at Red Sucker Lake. Increasing Cs values are very strongly correlated with decreasing K/Rb ratios. Symbols as in Figure 3.7.
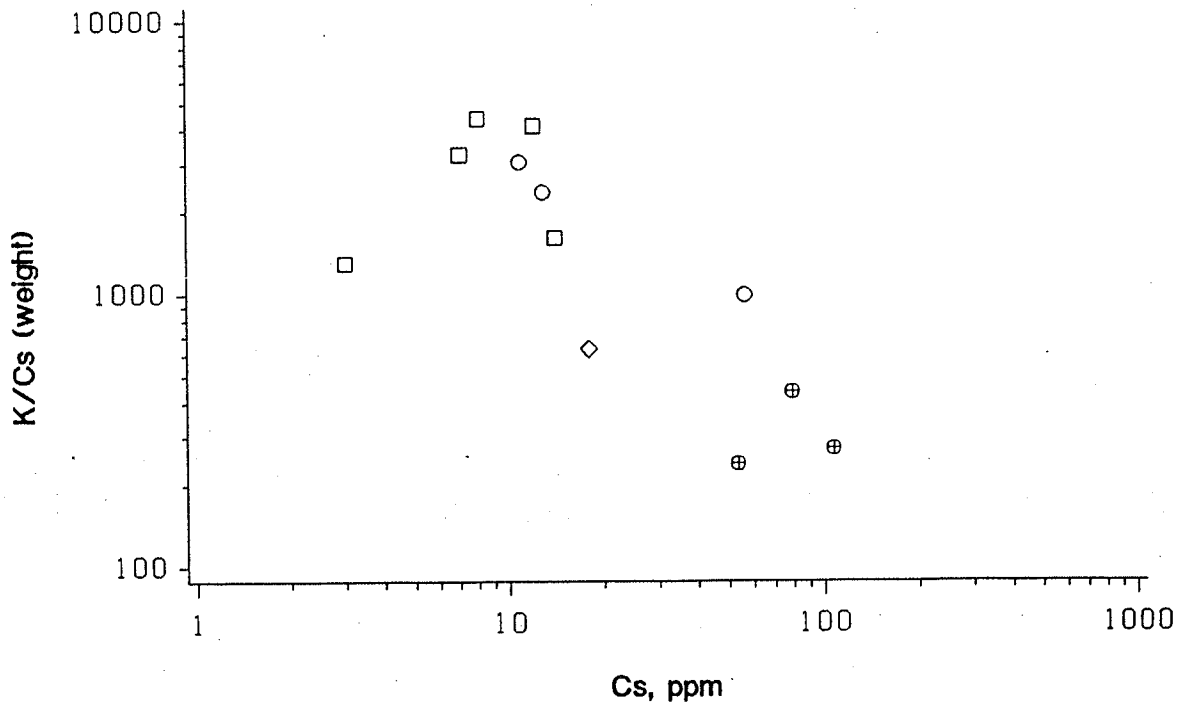
Figure 3.10: K/Cs vs Cs plot for pegmatitic granites at Red Sucker Lake. The petalite-bearing pegmatitic leucogranites show distinctly high levels of K/Cs fractionation. Symbols as in Figure 3.7.
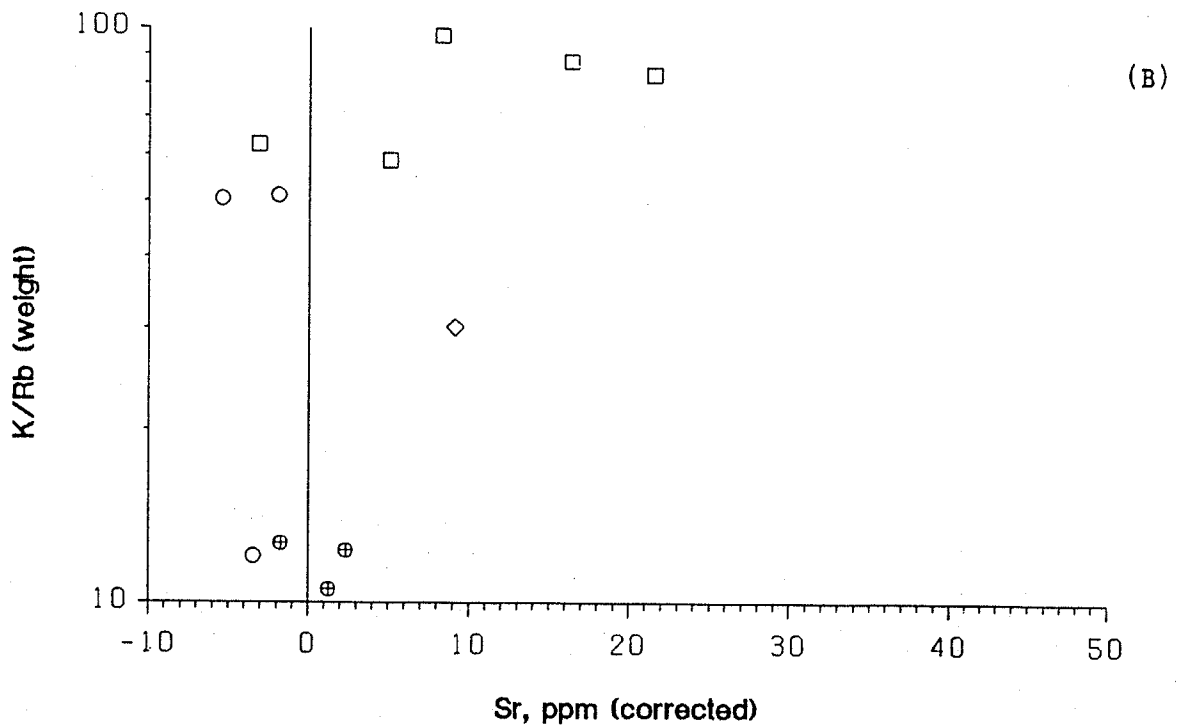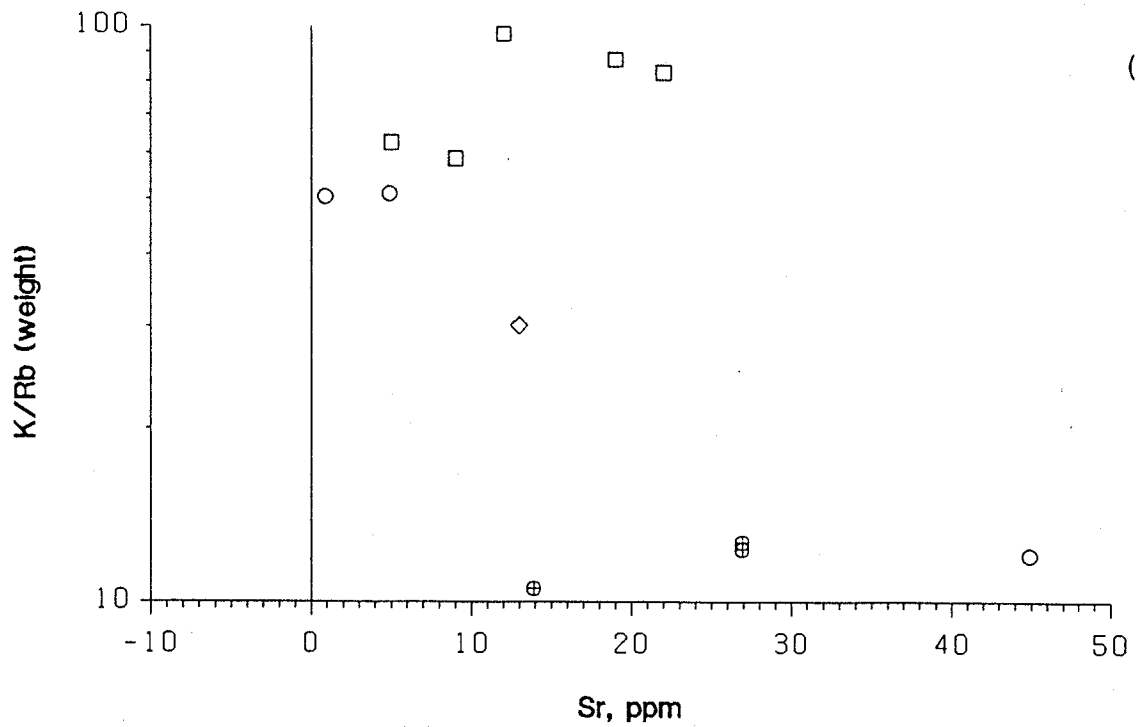
Figure 3.11: K/Rb vs Sr diagrams for pegmatitic granites at Red Sucker Lake. (A): Total Sr. (B): Sr corrected for radiogenic [87]Sr. Symbols as in Figure 3.7. See text for explanation of negative Sr values.
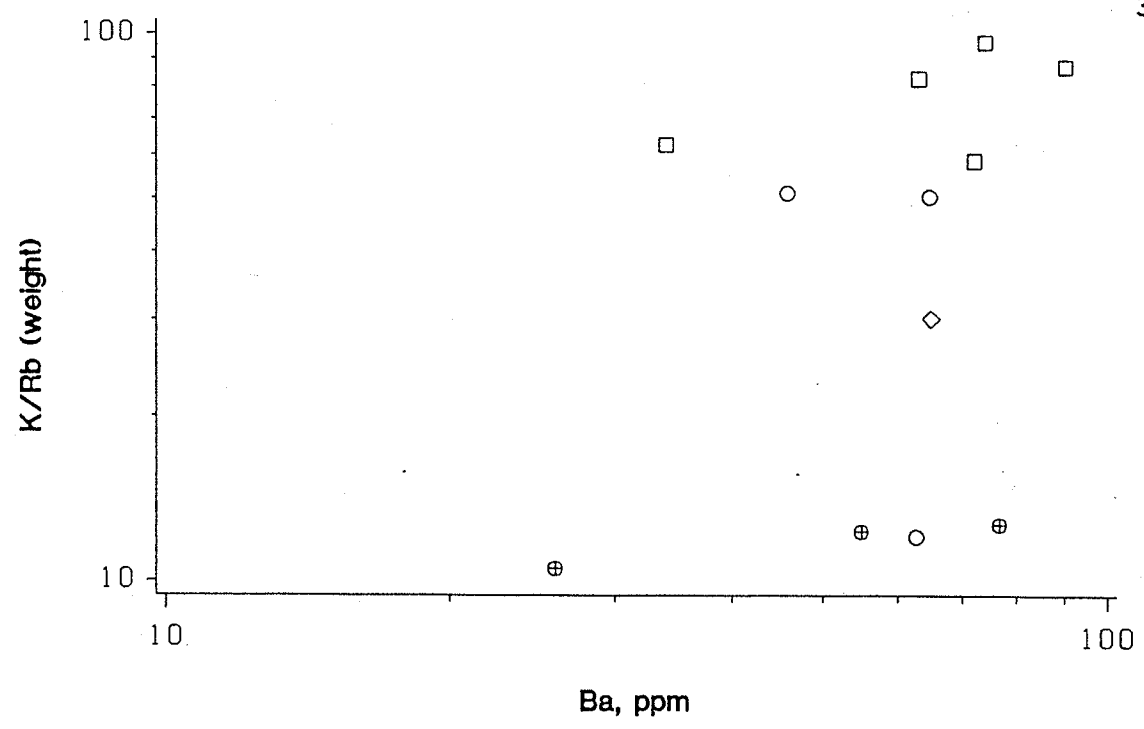
Figure 3.12: K/Rb vs Ba plot for pegmatitic granites at Red Sucker Lake. Note lack of correlation between K/Rb and Ba. Symbols as in Figure 3.7.
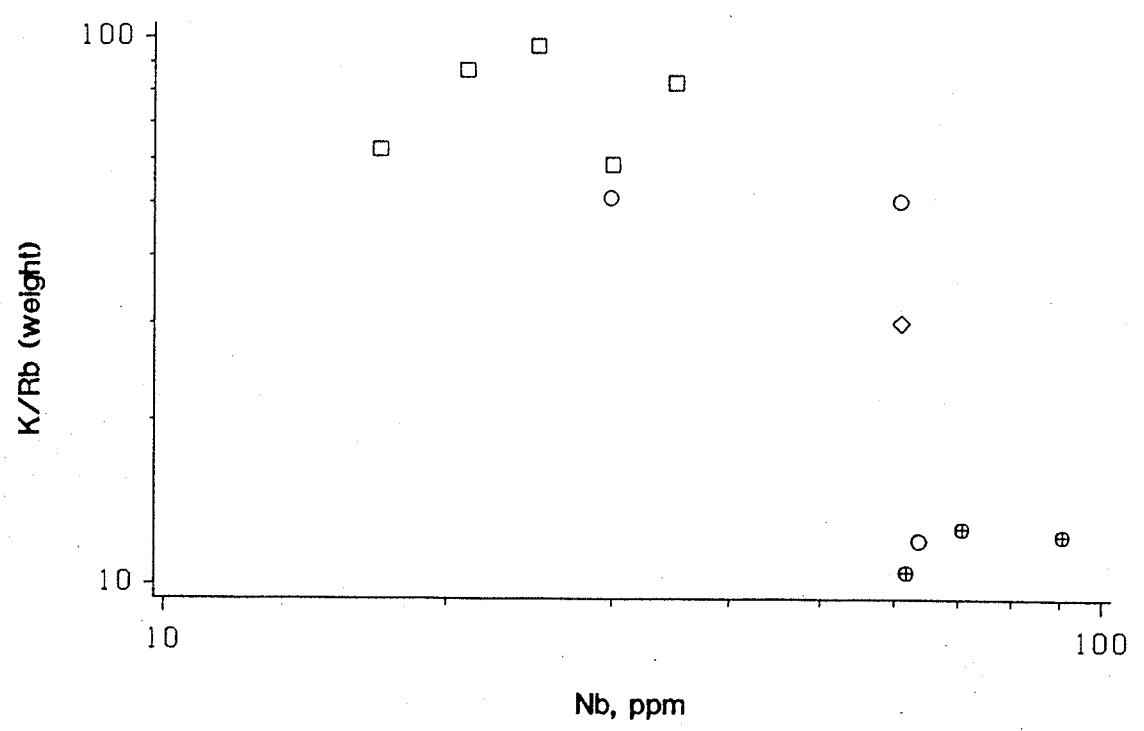
Figure 3.13: K/Rb vs Nb plot for pegmatitic granites at Red Sucker Lake. Main series and especially petalite-bearing pegmatitic leuco-granites are highly enriched in Nb. Symbols as in Figure 3.7.
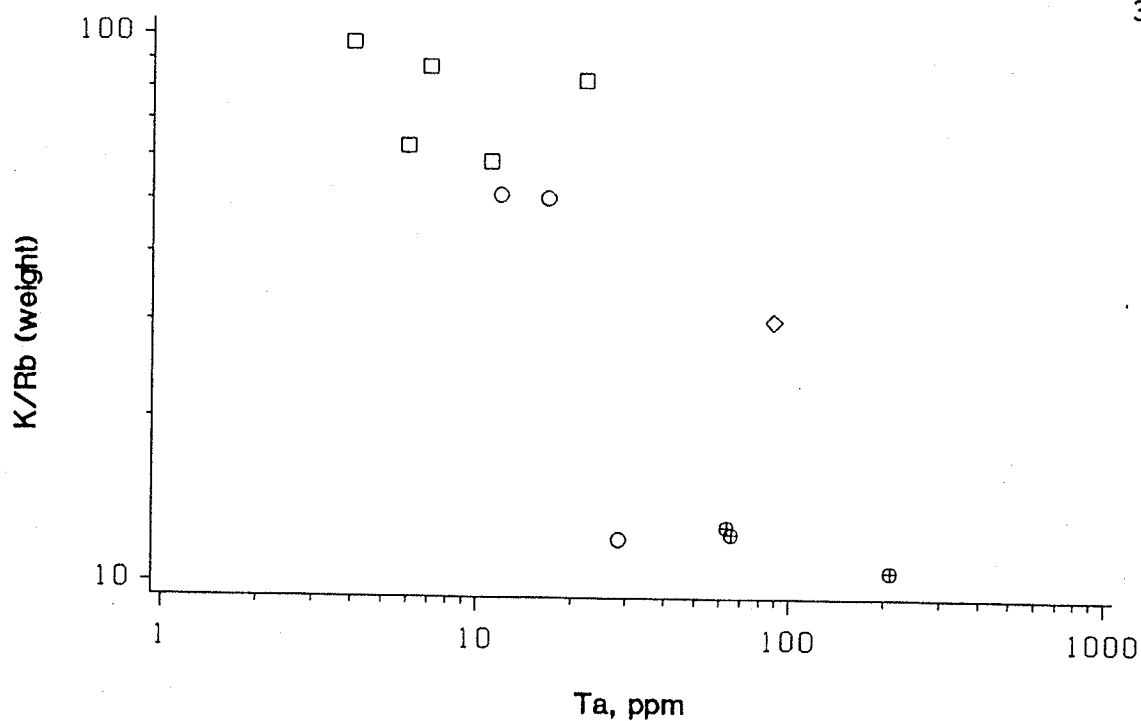
Figure 3.14: K/Rb vs Ta plot for pegmatitic granites at Red Sucker Lake. Ta increases with decreasing K/Rb ratios. The highest Ta values are found in the Main and petalite-bearing pegmatitic granites. Symbols as in Figure 3.7.
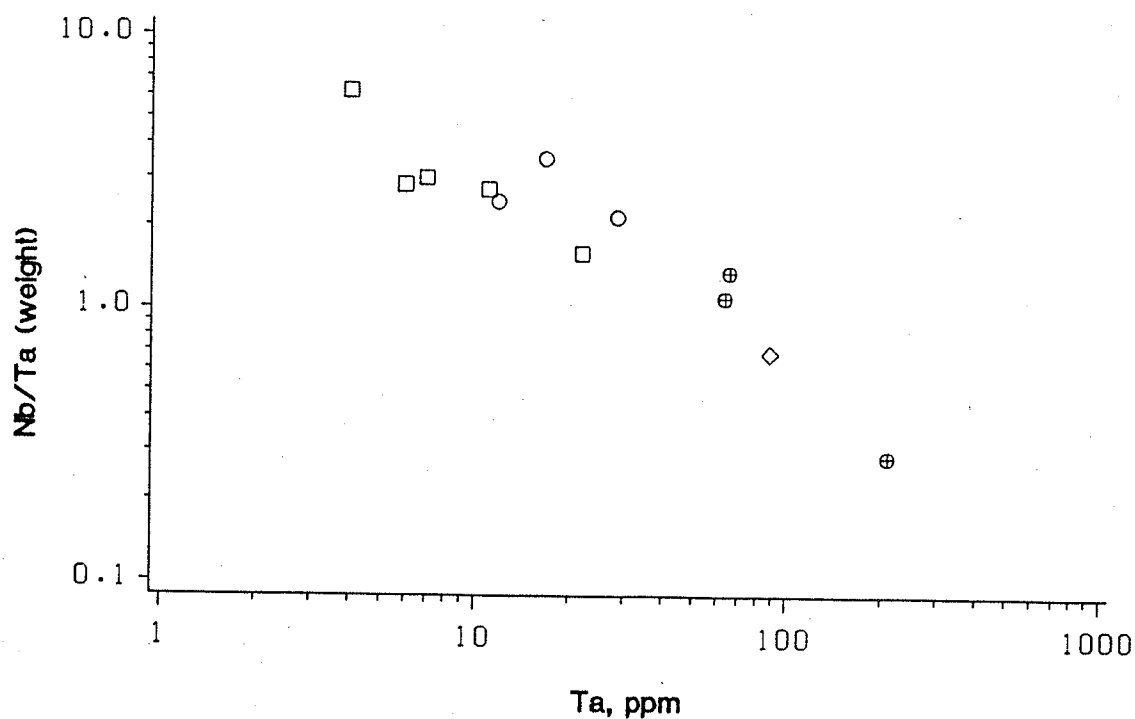
Figure 3.15: Nb/Ta vs Ta plot for pegmatitic granites at Red Sucker Lake. Highest Nb/Ta fractionation occurs in the Main and petalite-bearing pegmatitic granites. Symbols as in Figure 3.7.
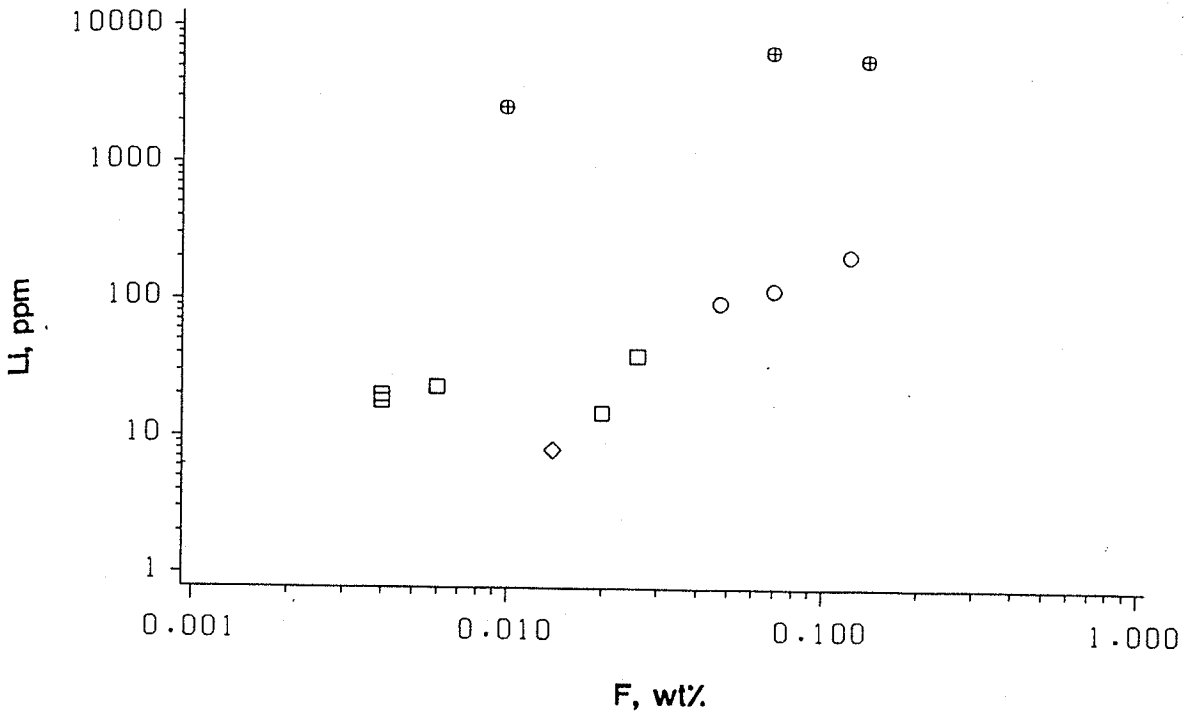
Figure 3.16: Li vs F plot for pegmatitic granites at Red Sucker Lake. All samples are F-poor. The samples with lowest Li values plot in the low F range of the diagram. Symbols as in Figure 3.7.
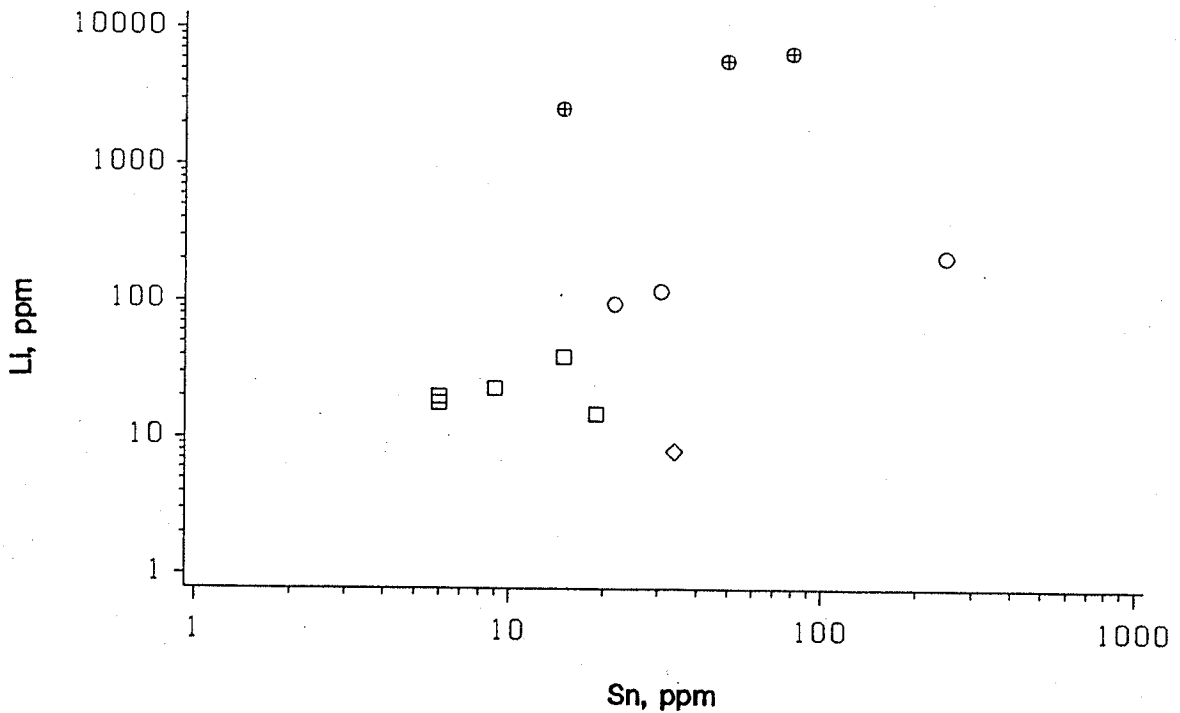
Figure 3.17: Li vs Sn plot for pegmatitic granites at Red Sucker Lake. There is a very weak positive correlation between Li and Sn. Symbols as in Figure 3.7.
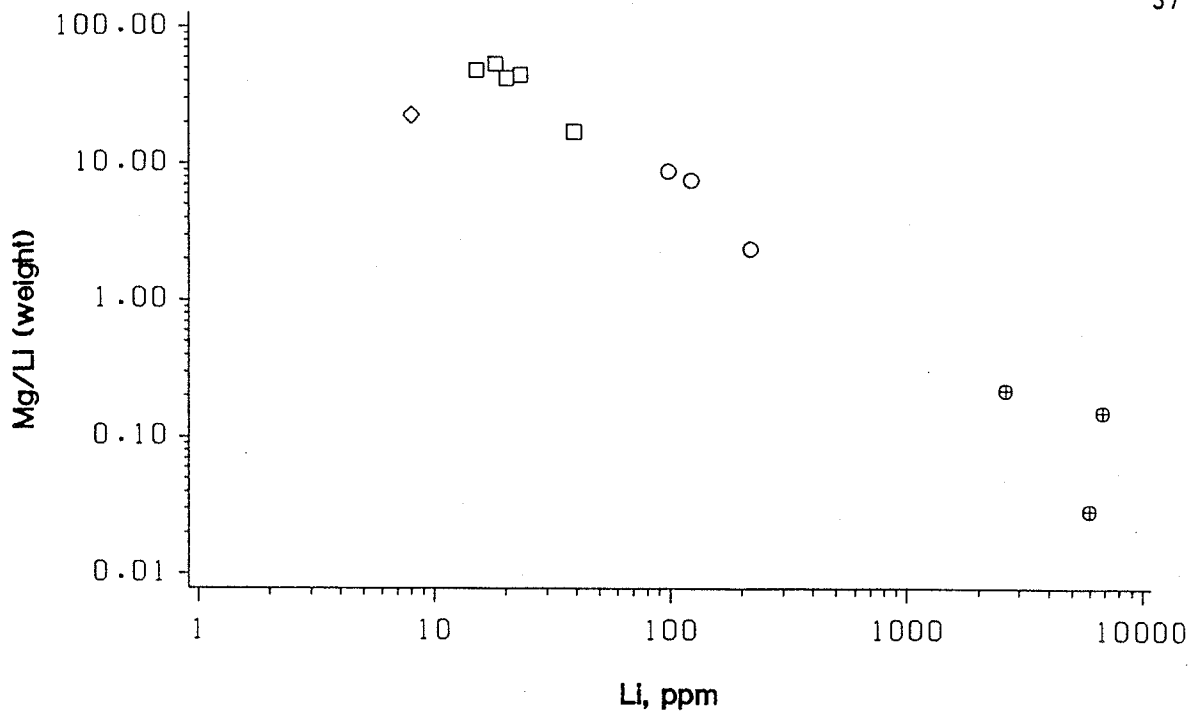
Figure 3.18: Mg/Li vs Li plot for pegmatitic granites at Red Sucker Lake, showing a very strong positive correlation between Mg/Li ratios and Li values. Symbols as in Figure 3.7.
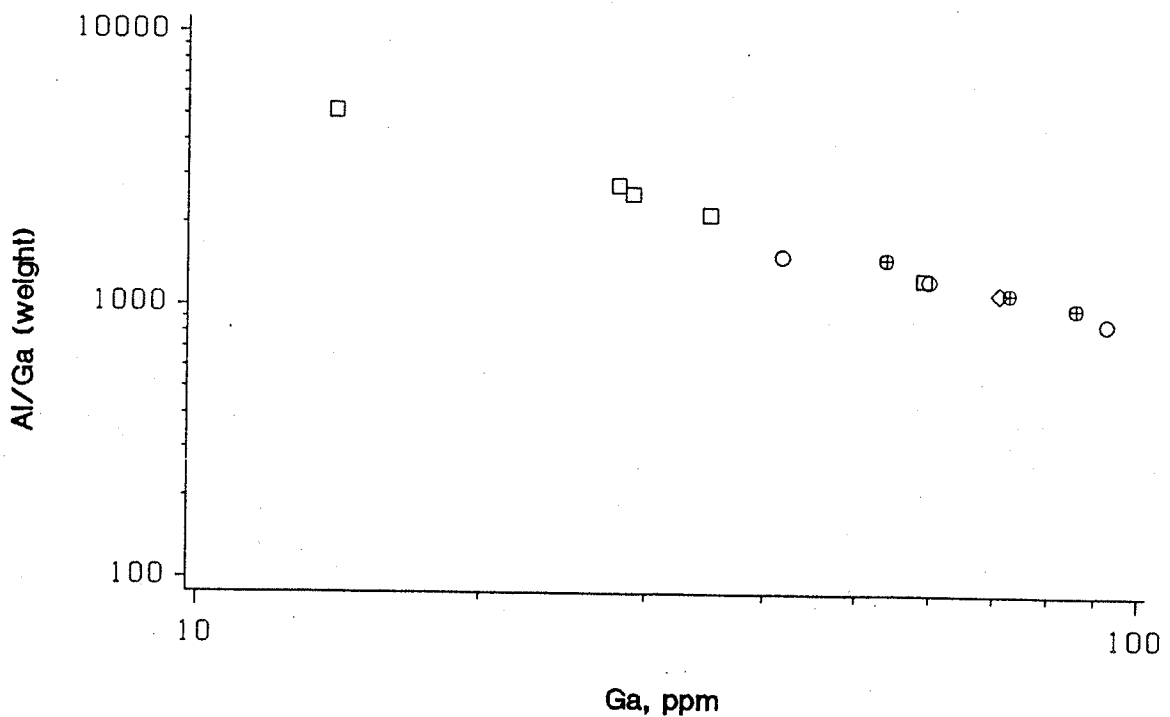
Figure 3.19: Al/Ga vs Ga plot for pegmatitic granites at Red Sucker Lake. Western series pegmatitic granites show low levels of Al/Ga fractionation compared to the Main and petalite-bearing pegmatitic leucogranites. Symbols as in Figure 3.7.
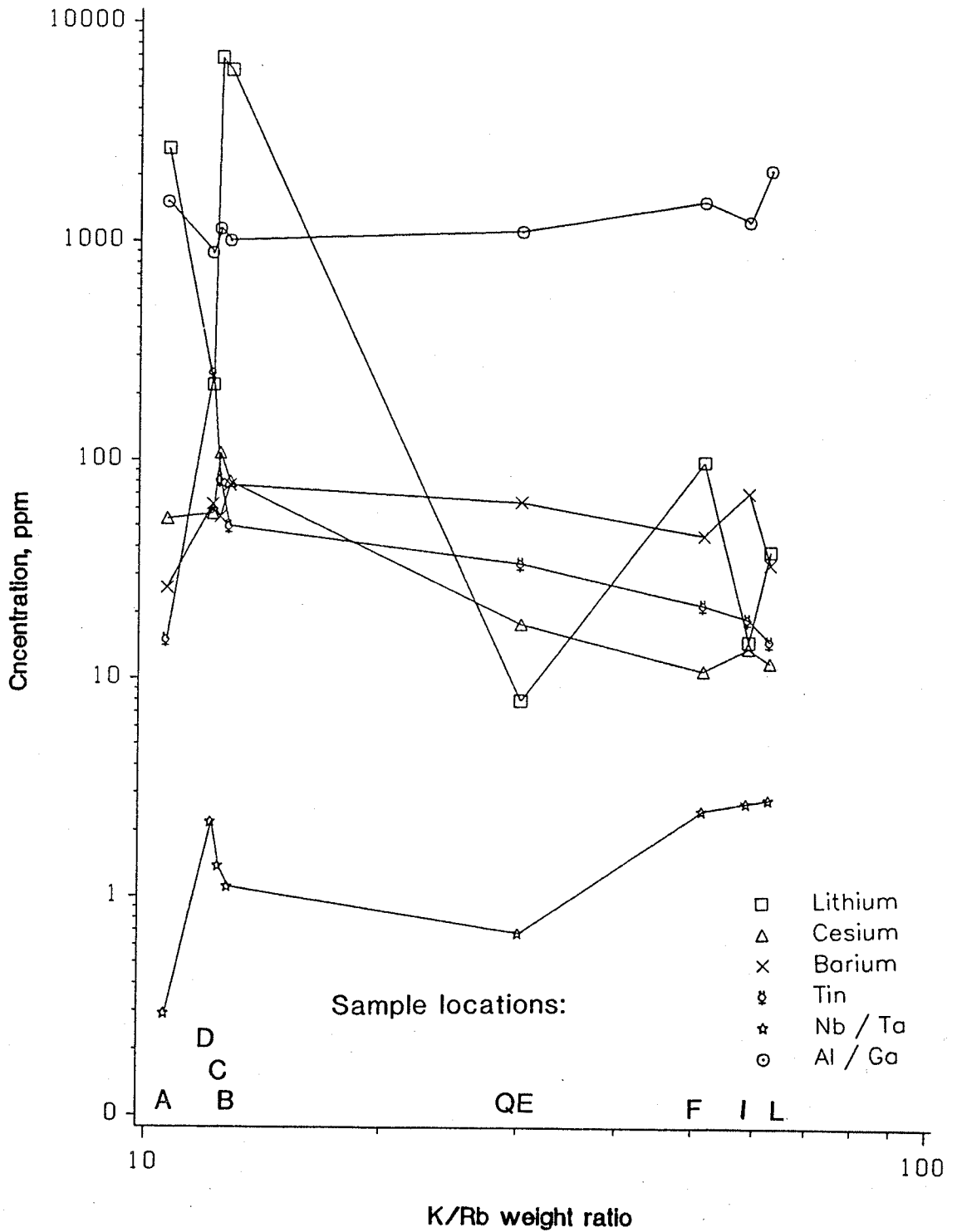
Figure 3.20: Various compositional parameters vs K/Rb ratios for pegmatitic leucogranites at Red Sucker Lake.
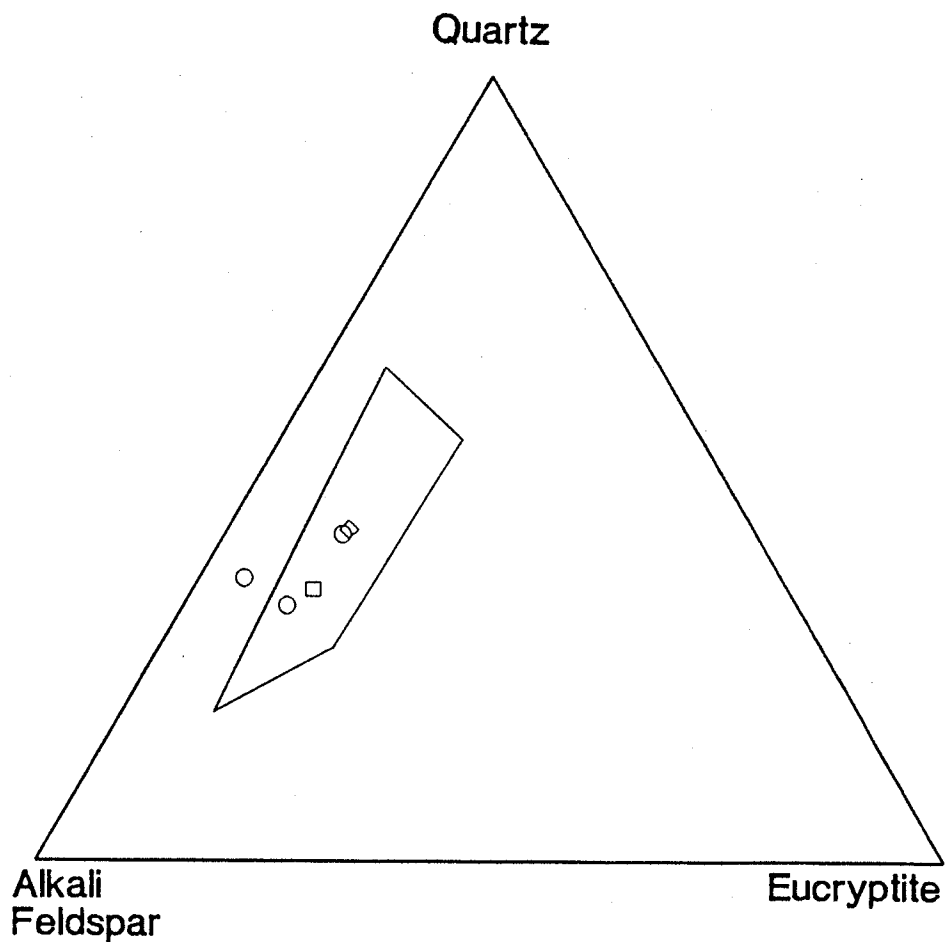
Figure 3.21: Compositions of petalite-bearing pegmatitic leucogranites from Red Sucker Lake (circles), and Bikita and Kings Mountain pegmatites (square and diamond) recalculated to 100 wt.% quartz, alkali feldspar (Or + Ab) and eucryptite. The large field shows the range of bulk compositions of spodumene and petalite pegmatites from Stewart (1978).

3.4   PARAGENESIS AND MINERALOGY

Parageneses of pegmatitic granites at Red Sucker Lake are listed in Table 3.3.   All rock types are pegmatitic leucogranites unless indicated otherwise. Relative mineral abundances are based on field observations. Note the presence of petalite and columbite-tantalite, and an increase in paragenetic diversity at locations A, B, C, IE and KE.   This correlates with the increase in geochemical fractionation that was discussed in the previous section on whole-rock geochemistry.

The pegmatitic leucogranites are dominantly composed of a graphic intergrowth of perthitic K-feldspar + quartz, quartz, plagioclase and subordinate muscovite.   They are typically very coarse-grained to pegmatitic in grain size.   Petalite occurs at locations IE, A, B and C. Accessory minerals are represented by garnet, tourmaline (schorl), biotite, arsenopyrite, löllingite, chalcopyrite, molybdenite and apatite. Ta-Nb oxide minerals are rare.

Fine-grained leucogranites are composed of K-feldspar, quartz, plagioclase and subordinate muscovite with accessory garnet and biotite.

Table 3.3: Paragenesis of pegmatitic granites at Red Sucker Lake.

SERIES	WESTERN							MAIN																EASTERN						
LOCATION	N	M	L	K	J	I	H	G	F	E	D	C	B	A	IE	JE	KE	FE	GE	ME	NE	PE	HE	AE	QE	RE	CE	BE	DE	SE
MICROCLINE	A	A	A	A	A	A	A	A	A	A	A	A	A	A	A	A	A	A	A	A	A	A	A	A	A	A	A	A	A	A
PLAGIOCLASE	a	a	S	a	a	S	a	S	a	S	A	S	S	S	A	A	A	A	S	S	A	A	A	S	A	S	S	A	a	a
QUARTZ	A	A	A	A	A	A	A	A	A	A	A	A	A	A	A	A	A	A	A	A	A	A	A	A	A	A	A	A	A	S
MUSCOVITE	S	S	S	S	S	S	r	A	A	a	S	a	a	a		a	a	a	a			A	a	a	S	S	a	S	S	S
BIOTITE		a	a		S	S	S	r	a	S	a	a	a	a	a			a	a				a	S		a	a	S	a	a
PETALITE												A	A	a	S															
GARNET	a	a	a	a	a	a	a	a	a	a	a	a	a	a	a		r	a		a	a	a	a	a	a	a	a	a	a	a
SCHORL		r		r				a	a		r	r	r					r			r								r	
DRAVITE								r																						
APATITE			r									r	a	r		r					r									
GAHNITE												r	r																	
COLUMBITE													r	r	r			r												
RUTILE																		r							r					
TITANITE																									r					
LOLLINGITE								r				r	r	r									r						r	
AESENOPYRITE						r						r												r	r	r			r	r
CHALCOPYRITE											r													r			r	r	r	
MOLYBDENITE													r						r											

A – abundant
S – subordinate
a – accessory
r – rare

K-feldspar

Graphic and blocky K-feldspar phenocrysts are abundant in most of the pegmatitic granite outcrops. Large graphic K-feldspar + quartz mega- crysts occur at locations A, B and C (Figure 3.4). Blocky K-feldspars range up to 5 cm in many of the pegmatitic leucogranite outcrops, and are generally equant to columnar and undeformed except in areas of in- tense shearing, as at location A. Coarse perthitic texture is visible in most specimens.

93 K-feldspar samples were selected for x-ray powder diffraction and partial chemical analyses. All samples turned out to be maximum micro- cline with triclinicities (Δ) ranging from 0.91 to 1.00. 12 samples were subsequently selected from this group for unit cell parameter de- terminations. The samples were chosen so as to cover the geographical extent of the pegmatitic granite exposures, and the ranges of Δ's and chemical variations in the microcline samples. The refined unit cell parameters are listed in Table 3.4 and ploted on determination diagrams in Figures 3.22 to 3.25. All 12 samples plot very close to the maximum microcline apices on all four diagrams, and no systematic variations in terms of chemistry or structural state of microcline from different lo- cations are evident.

The partial chemical analyses and Δ values of the 93 microcline sam- ples are given in Appendix A. Compositional parameters are plotted in Figures 3.26 to 3.31. From these diagrams it is seen that K/Rb, Li, Rb and Cs show strong fractionation trends from the marginal Eastern and Western series pegmatitic granites inward to the central Main and Petal- ite-bearing series. Ba shows little correlation with fractionation whereas Pb tends to decrease.

Table 3.4: Unit cell parameters and selected geochemical parameters of maximum microcline from pegmatitic granites at Red Sucker Lake.

Sample:	A-14	C-2	C-5	D-6	F-3	J-18
a	8.613(3)	8.590(2)	8.581(4)	8.567(6)	8.569(5)	8.555(6)
b	12.963(3)	12.970(4)	12.978(5)	12.965(4)	12.966(3)	12.966(5)
c	7.223(2)	7.223(2)	7.225(2)	7.224(3)	7.222(2)	7.223(3)
α	90.60(3)	90.59(3)	90.60(4)	90.61(4)	90.63(3)	90.69(4)
β	115.90(2)	115.97(2)	115.97(2)	116.01(4)	115.95(3)	115.98(5)
γ	87.77(2)	87.72(4)	87.72(4)	87.69(4)	87.67(3)	87.55(4)
vol.	724.9(3)	722.7(3)	722.7(3)	720.5(2)	720.9(3)	719.6(5)
a*	0.12916(5)	0.12957(3)	0.12973(6)	0.12998(9)	0.12988(6)	0.13014(9)
b*	0.07720(2)	0.07717(2)	0.07712(3)	0.07720(3)	0.07719(2)	0.07720(3)
c*	0.15392(4)	0.15398(4)	0.15397(4)	0.15404(7)	0.15399(5)	0.15402(6)
α*	90.41(3)	90.46(3)	90.45(4)	90.46(4)	90.43(3)	90.43(4)
β*	64.10(3)	64.05(2)	64.03(2)	64.00(4)	64.06(3)	64.02(5)
γ*	92.18(2)	92.28(4)	92.25(4)	92.28(4)	92.28(3)	92.39(4)
Ba	48	37	62	25	54	<10
Ba+Sr+Ca	340	150	170	140	140	160
Rb+Cs	13500	9200	8400	8500	1930	2830

Sample:	M-6	CE-12	DE-5	IE-4	KE-13
a	8.561(5)	8.556(7)	8.577(7)	8.579(4)	8.572(4)
b	12.965(5)	12.966(6)	12.960(7)	12.970(4)	12.973(3)
c	7.220(2)	7.220(2)	7.220(4)	7.224(2)	7.224(2)
α	90.92(4)	90.64(5)	90.65(6)	90.66(3)	90.61(3)
β	115.98(4)	116.00(6)	115.93(7)	115.95(3)	115.93(2)
γ	87.68(4)	87.63(5)	87.69(6)	87.69(3)	87.66(3)
vol.	719.8(4)	719.3(6)	721.1(6)	722.1(3)	721.9(3)
a*	0.13003(8)	0.1302 (1)	0.12975(8)	0.12974(6)	0.12982(5)
b*	0.07719(3)	0.07719(4)	0.07723(4)	0.07717(2)	0.07715(2)
c*	0.15409(6)	0.15410(8)	0.1540 (1)	0.15396(4)	0.15392(3)
α*	90.43(4)	90.44(5)	90.41(7)	90.39(3)	90.47(2)
β*	64.03(4)	64.01(6)	64.07(7)	64.05(3)	64.07(2)
γ*	92.27(4)	92.32(5)	92.26(6)	92.25(3)	92.31(3)
Ba	23	<10	<10	28	<10
Ba+Sr+Ca	820	370	230	450	510
Rb+Cs	1300	1310	1700	7300	10200

a, b and c in Å; vol. in Å^3; a*, b* and c* in Å^{-1}.
α, β, γ, α*, β* and γ* in degrees.
All chemical data in ppm.
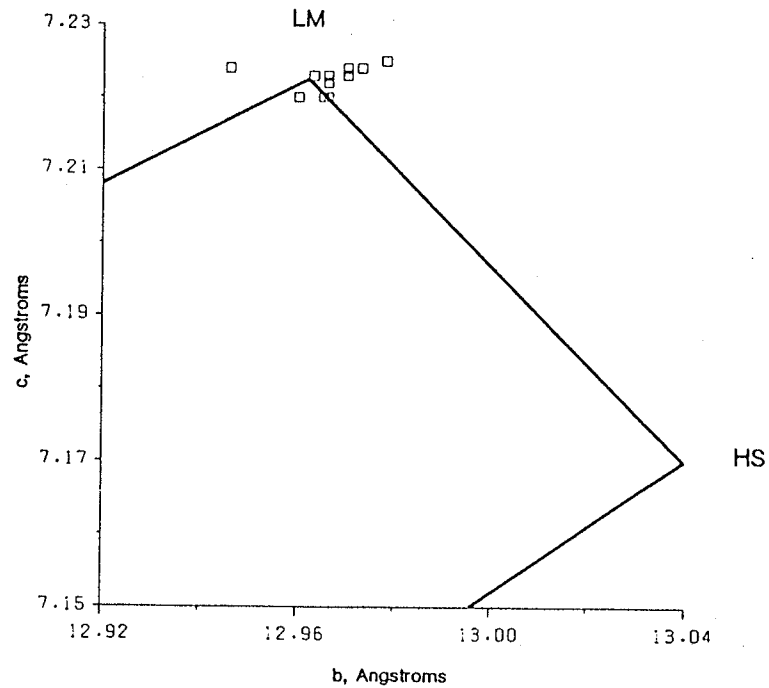
Figure 3.22 : c vs b cell parameters for maximum microcline from pegmatitic granites at Red Sucker Lake. Modified after Kroll and Ribbe (1983). All data plots near the maximum microcline corner indicating highly ordered structure and Or-rich composition of K-feldspar phases of perthitic samples.
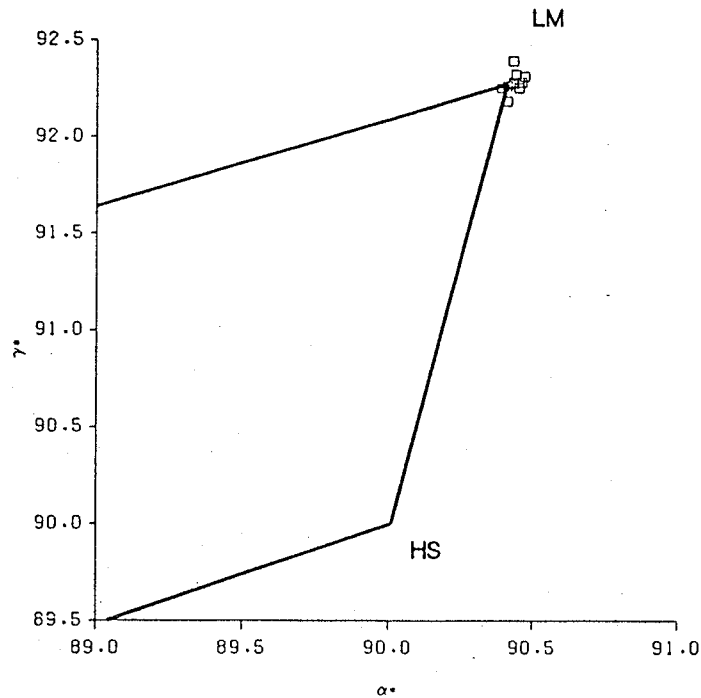
Figure 3.23 : $\gamma*$ vs $\alpha*$ for maximum microcline from pegmatitic granites at Red Sucker Lake. Modified after Kroll and Ribbe (1983). Data cluster tightly at the low microcline corner of the diagram.
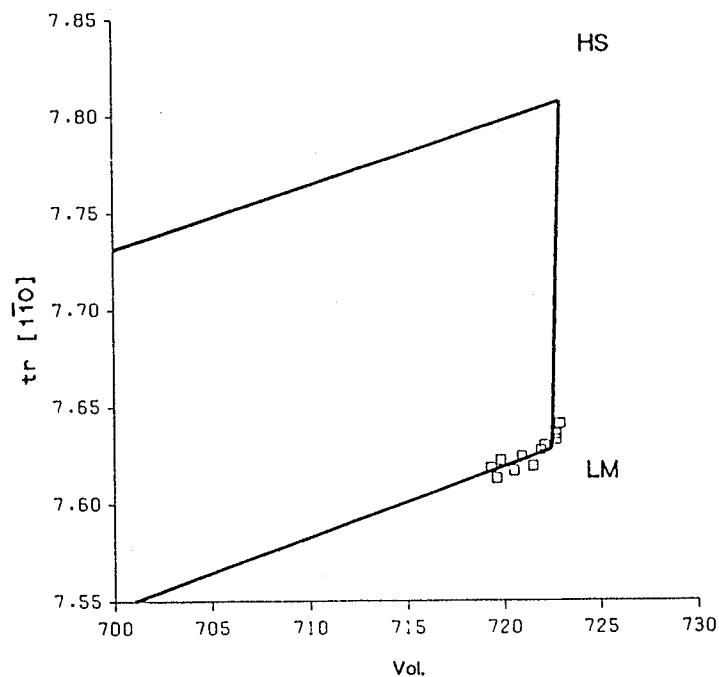
Figure 3.24 : tr[1Ī0] vs volume for maximum microcline from pegmatitic granites at Red Sucker Lake. Modified after Kroll and Ribbe (1983).
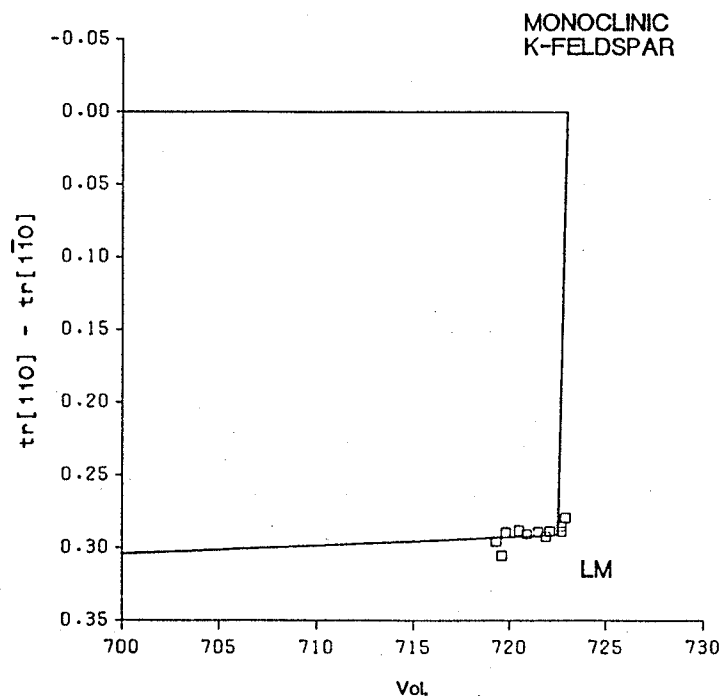
Figure 3.25 : tr[110] – tr[1Ī0] vs volume for maximum microcline from pegmatitic granites at Red Sucker Lake.   Modified after Kroll and Ribbe (1983).

The microcline samples analyzed range from $Or_{77.5}$ at location K to $Or_{96.5}$ at location KE. The most potassic microcline occurs in the central part of the Main series.

Li in microcline ranges from 2 ppm to 300 ppm with the highest values at locations A, B, C, FE, IE, KE and NE. Rb ranges from 400 to 13,400 ppm at location A and distinctly high values at the locations mentioned above for Li, except that Rb at location D is anomalously high (>8000 ppm) whereas Li and Cs display background values. Cs ranges from <1 ppm to 635 ppm with anomalously high values at locations A, B, C, FE, IE, KE, ME and NE.

The K/Rb vs Sr diagrams in Figure 3.29 show separate compositional fields for the Eastern and Western vs the Main and petalite-bearing pegmatitic granites. The total Sr (ie. not corrected for radiogenic ^{87}Sr) data show an apparent increase in Sr with decreasing K/Rb ratio which is opposite to what would be expected during fractional crystallization. The corrected data show an opposite trend - Sr decreases with fractionation, as should be expected. However, most of the corrected data have negative Sr values, for reasons discussed earlier. Determination of the Rb-Sr apparent age of each K-feldspar sample would be required to overcome the affect of post-crystallization migration of ^{87}Sr on the corrected Sr values. As isotopic analyses were not done on these samples, the Sr trends may be misleading.

Ba ranges from <20 ppm in the Eastern and Western series to 195 ppm at location E. There is a moderate enrichment in Ba toward the centre of the Main series. This trend parallels that shown by the whole-rock analyses.

Pb ranges from 7 to 108 ppm and tends to decrease with increasing fractionation of the rare alkali metals. The amount of radiogenic Pb in these and other feldspar samples in this study is insignificant due to the low concentrations of radiogenic Pb-generating isotopes in the samples and pegmatitic granite and pegmatite bodies (2-5 ppm U and 4-9 ppm Th in analyses of pegmatitic leucogranite).

Triclinicities of the microcline samples are plotted against various compositional parameters in Figure 3.32. These diagrams show that there are no systematic variations in Δ or significant effects of large cations on Δ in these samples.
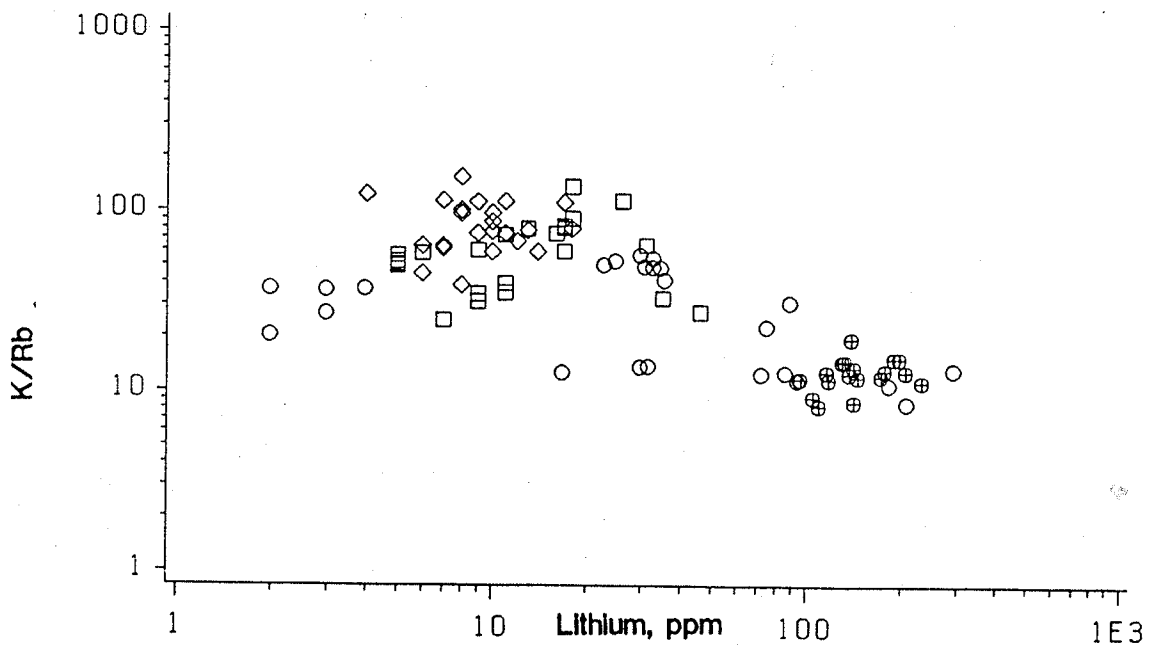
Figure 3.26 : K/Rb vs Li for microcline from pegmatitic granites at Red Sucker Lake. Data show increasing Li with decreasing K/Rb fractionation, and high levels of fractionation attained by the petalite-bearing pegmatitic leucogranites. Symbols as in Figure 3.7.
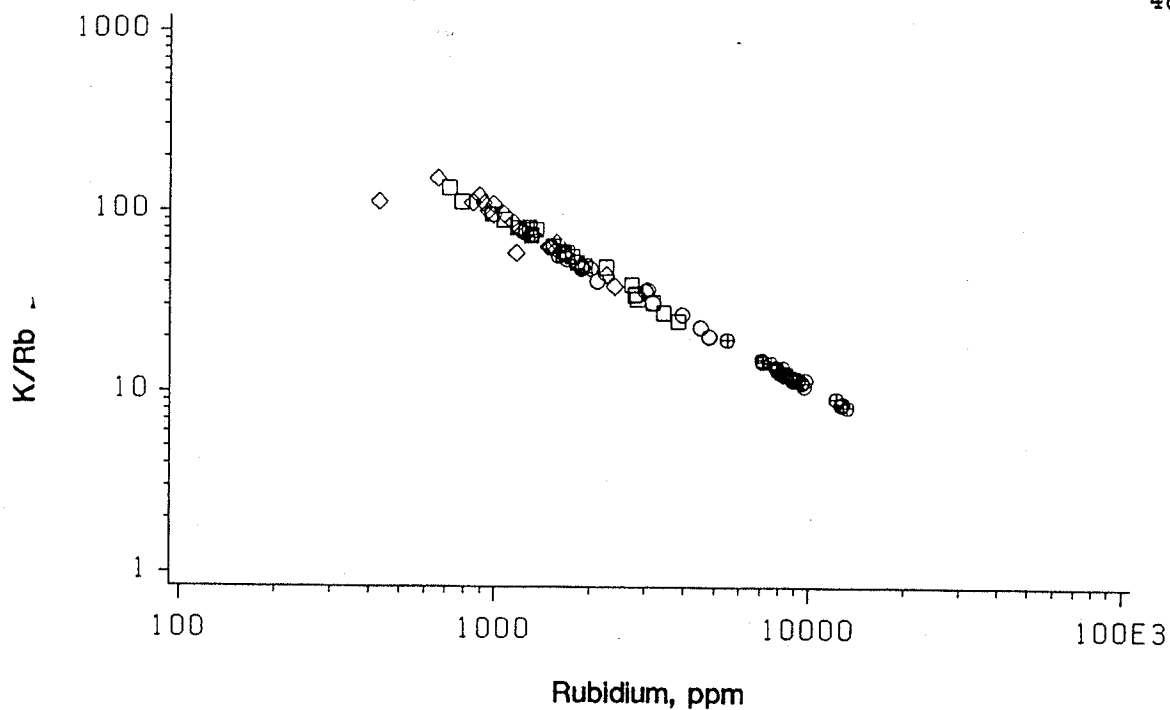
Figure 3.27 : K/Rb vs Rb for microcline from pegmatitic granites at Red
Sucker Lake. Highest levels of fractionation are attained by the
Main pegmatitic leucogranites. Symbols as in Figure 3.7.
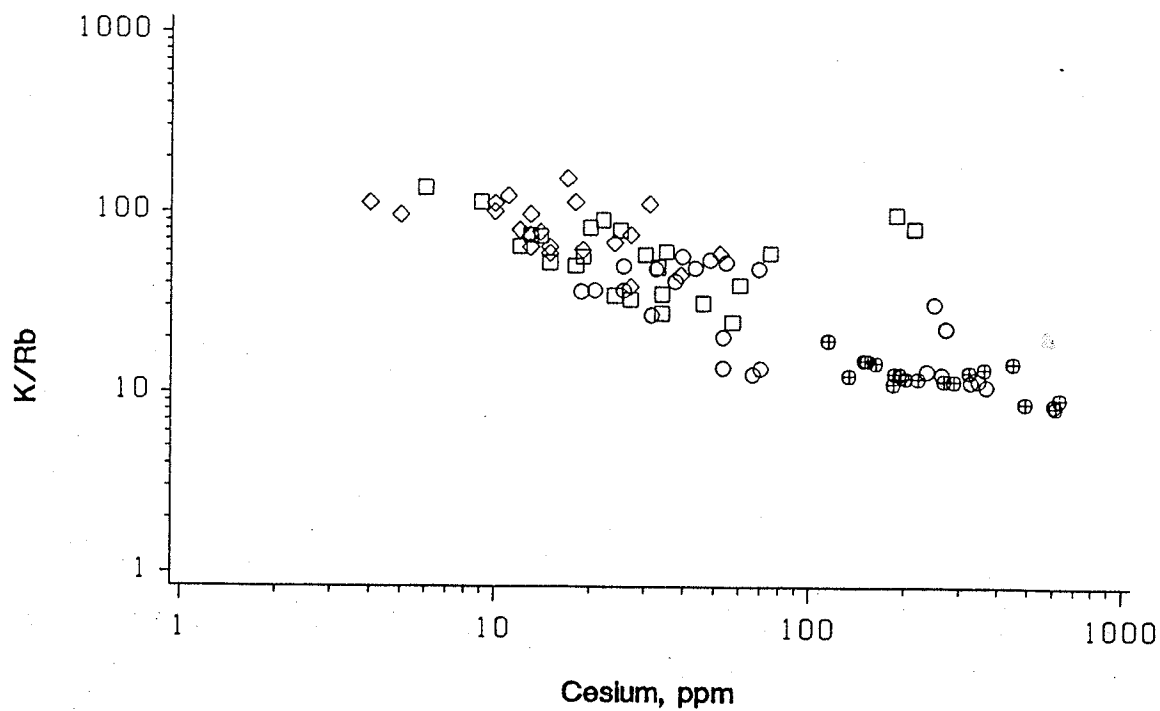
Figure 3.28 : K/Rb vs Cs for microcline from pegmatitic granites at Red
Sucker Lake. Highest levels of fractionation are attained by the pe-
talite-bearing pegmatitic leucogranites. Symbols as in Figure 3.7.
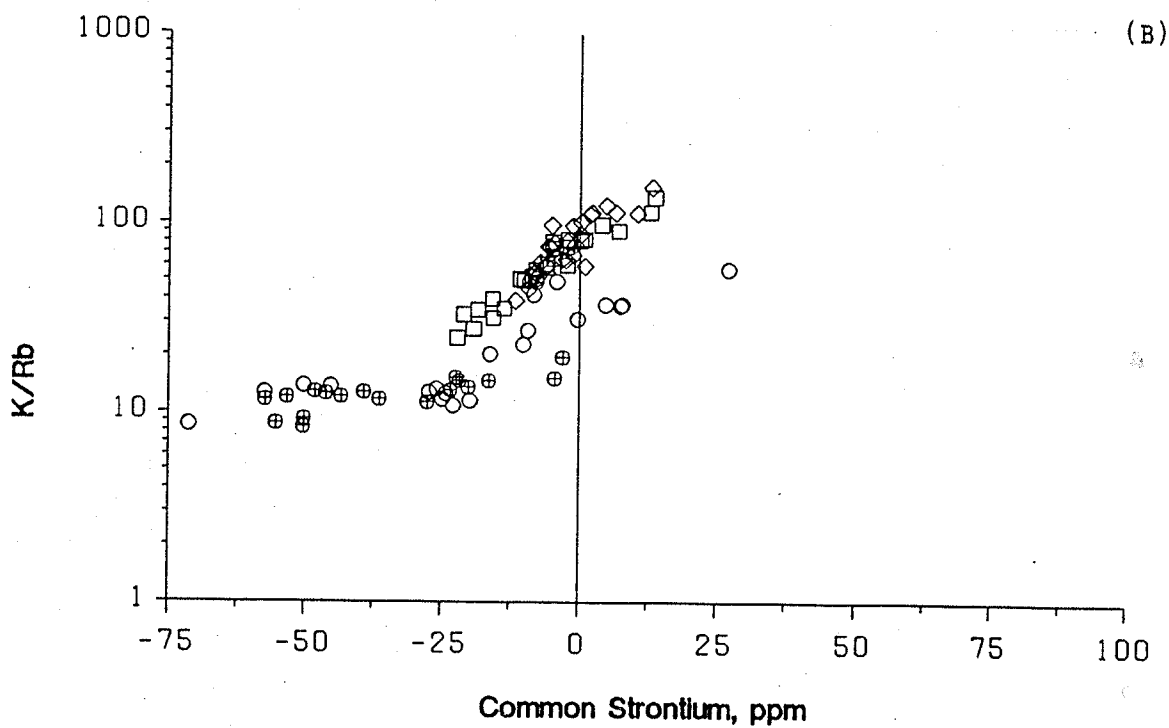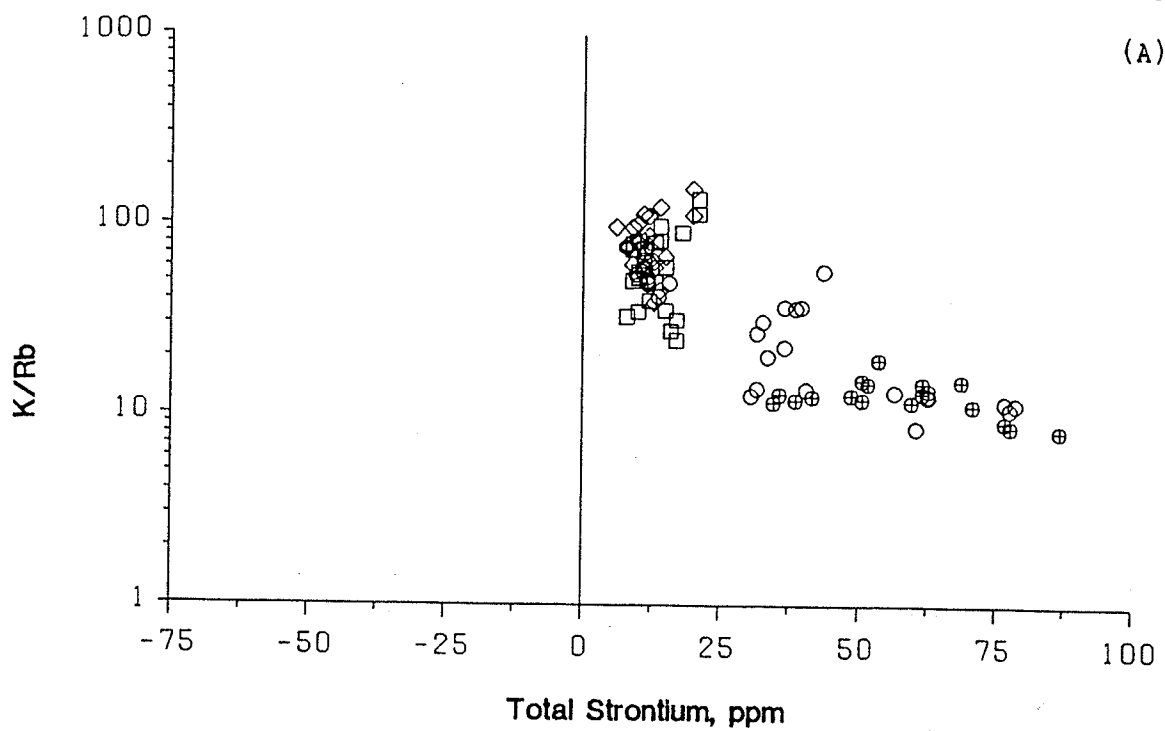
Figure 3.29 : K/Rb vs total Sr (A) and common Sr (B) for microcline from pegmatitic granites at Red Sucker Lake. Symbols as in Figure 3.7. Negative Sr values in (B) may indicate post-crystallization migration of [87]Sr. See text (p.27) for explanation of negative Sr values.
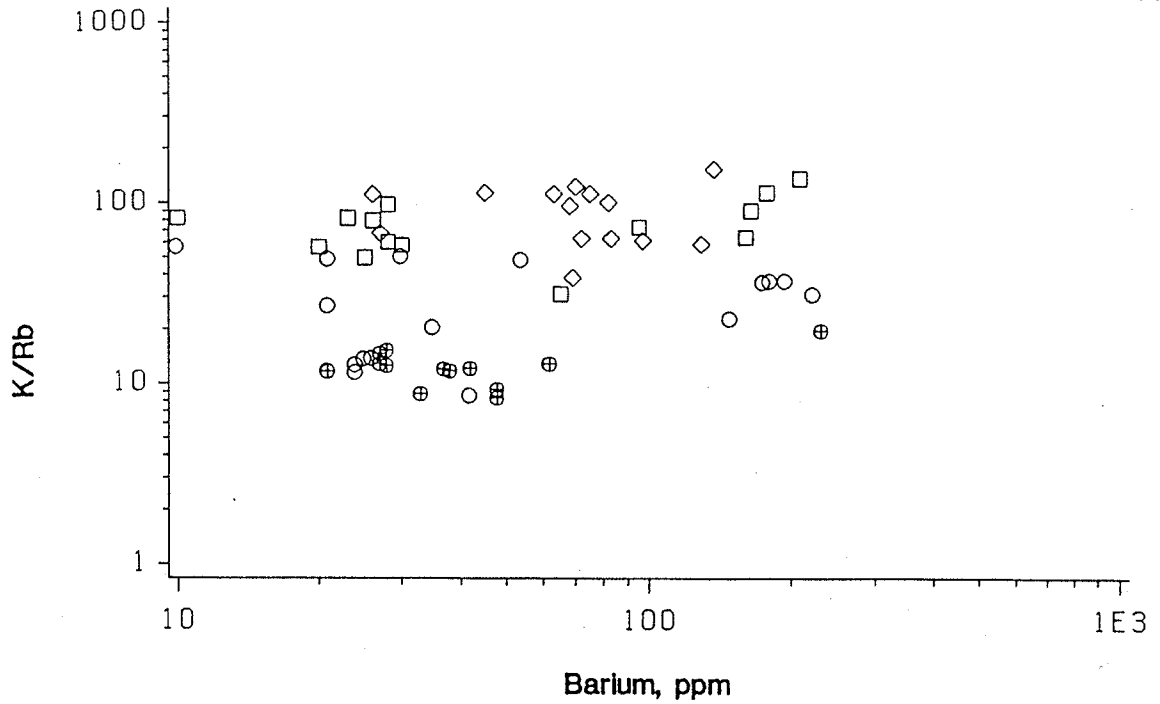
Figure 3.30 : K/Rb vs Ba for microcline from pegmatitic granites at Red
  Sucker Lake.   Data for the petalite-bearing pegmatitic leucogranites
  cluster at low K/Rb ratios and low Ba values.   Symbols as in Figure
  3.7.
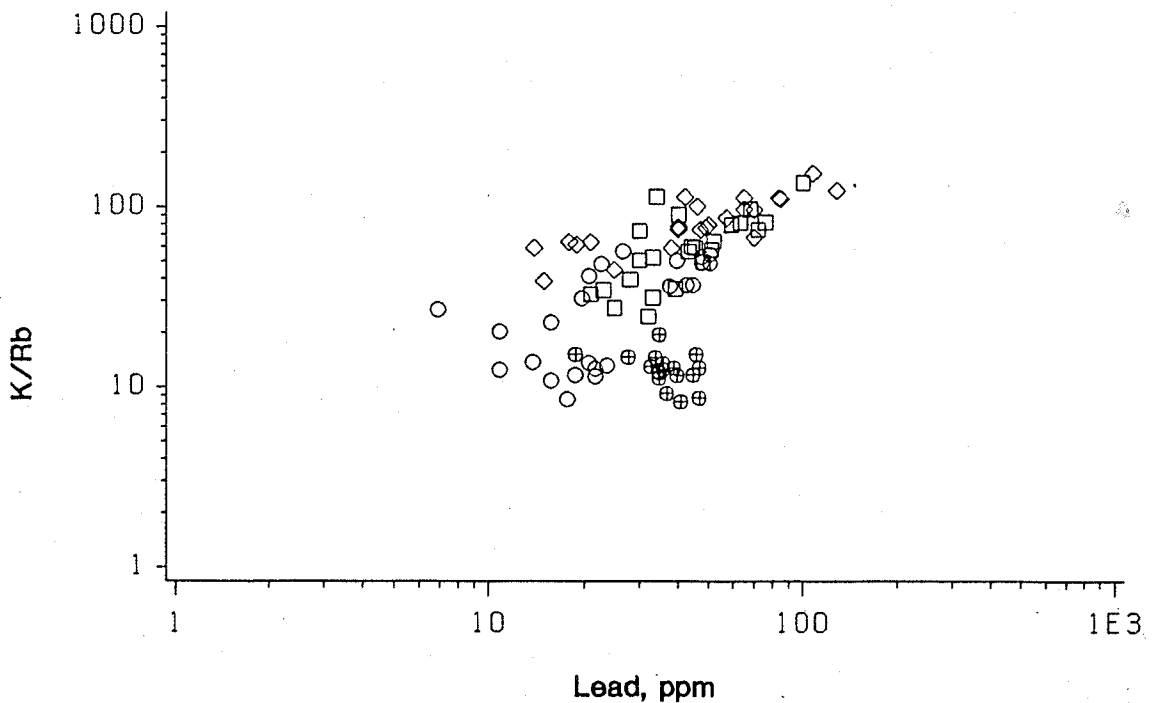
Figure 3.31 : K/Rb vs Pb for microcline from pegmatitic granites at Red
  Sucker Lake.   Data show decreasing Pb values with decreasing K/Rb
  ratios.   The petalite-bearing pegmatitic leucogranites have anoma-
  lously high Pb values. Symbols as in Figure 3.7.
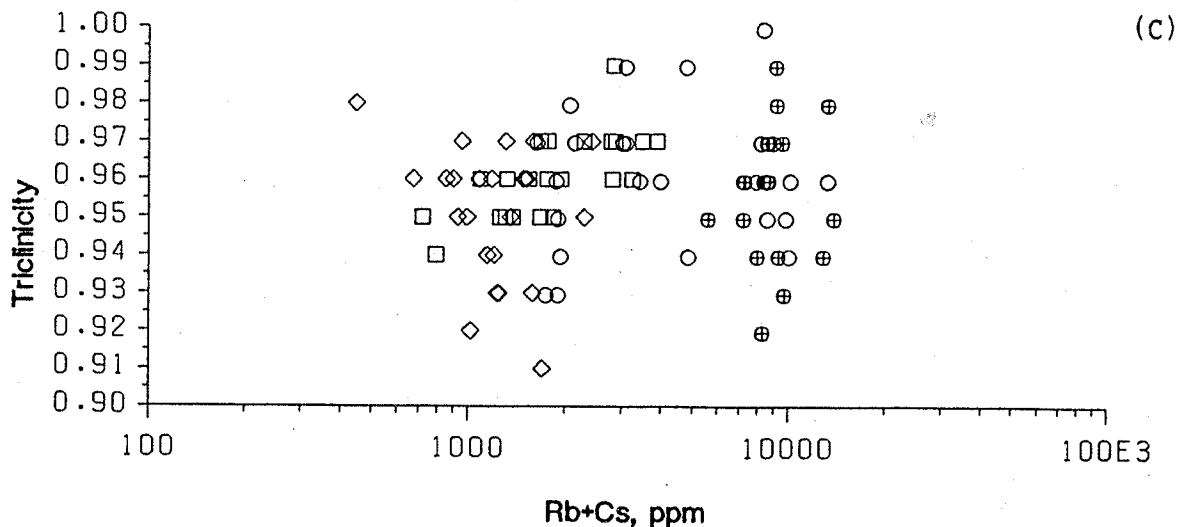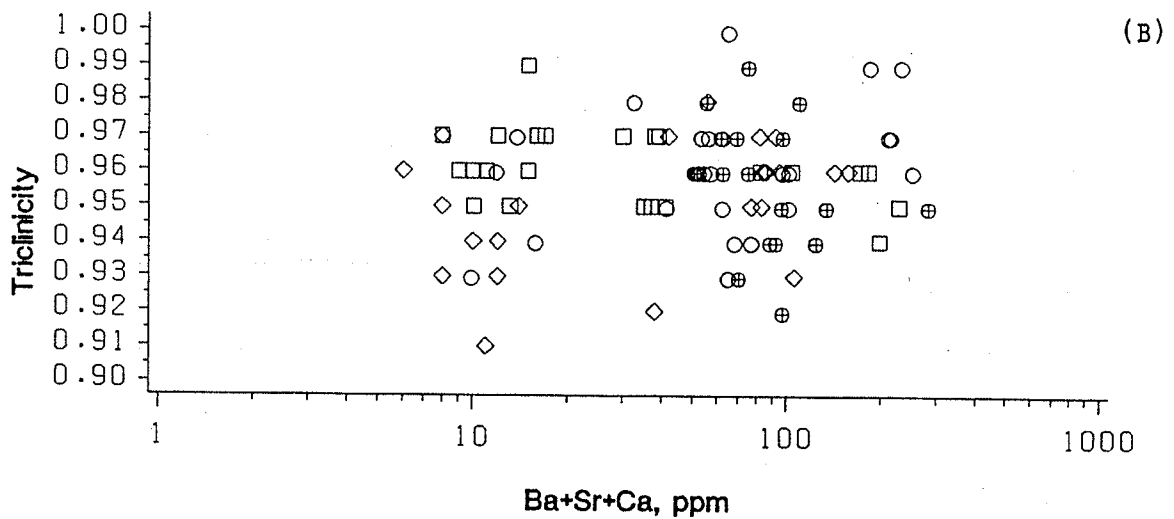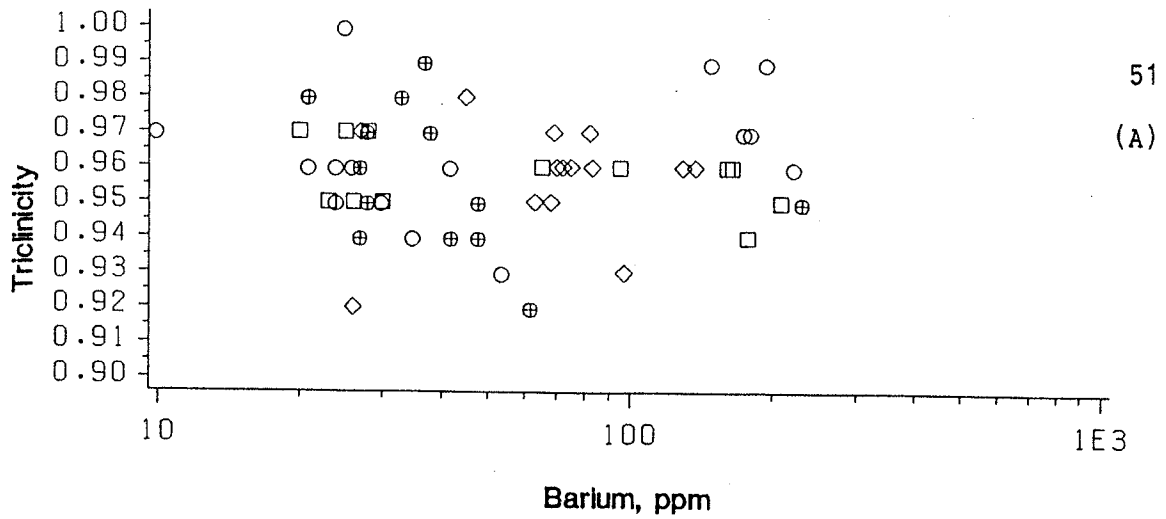
Figure 3.32 : Δ vs Ba (A), Δ vs Ca+Sr+Ba (B) and Δ vs Rb+Cs (C) for microcline from pegmatitic granites at Red Sucker Lake. Data indicate no correlation between Δ and concentrations of large divalent or rare alkali cations. Symbols as in Figure 3.7.

Plagioclase

Plagioclase occurs in the matrix of pegmatitic leucogranite, in fine-grained leucogranite and as the major constituent of sodic aplite. It rarely occurs as phenocrysts, as at location I. Clevelandite occurs rarely, associated with K-feldspar + quartz megacrysts.

Table 3.5 lists the optically derived compositions in terms of %An of selected specimens from the pegmatitic leucogranites. The samples range from relatively sodic albites (An_3 to An_7) in the Main series pegmatitic granites to calcic albites (An_8 to $An_1&$) in the Eastern and Western series.

Table 3.5: Compositions of plagioclase from pegmatitic granites at Red Sucker Lake.

Sample	Rock Type	Mol.% An	Series
DE-8	PLG	8	Eastern
BE-8	"	8	"
KE-5	SAP	6	Main
FE-1	SAP	3	"
B-10	PLG	4	"
B-33	"	5	"
C-4	SAP	4	"
C-6	PLG	4	"
D-4	"	7	"
I-21	PLG	10	Western
N-9	"	10	"

PLG – pegmatitic leucogranite
SAP – sodic aplite

Quartz

Quartz occurs interstitially in all of the pegmatitic granites, in massive quartz pods, potassic pegmatite segregations in pegmatitic leucogranite, and as blebs and graphic intergrowths in K-feldspar + quartz phenocrysts and megacrysts.

Muscovite

Muscovite occurs in all outcrops of pegmatitic granite, in a variety of paragenetic types: primary book muscovite, late fine-grained muscovite, fine-grained Fe-rich lithian muscovite at location B, and as fine-grained plumose aggregates (Figure 3.33).

Figure 3.33: Plumose muscovite aggregate from pegmatitic leucogranite at location F.

Primary book muscovite occurs sporadically, and rarely in quantities sufficient for geochemical sampling. As such, it is not a good petrogenetic indicator mineral in this area. It is usually silver-grey in colour, occuring in books ranging from 0.5 x 3 mm to 5 x 30 mm in size.

Plumose muscovite occurs at location F, G, I and J. The fine-flaked plumose aggregates are from 2 to 15 cm in maximum exposed dimension, and are composed of fine-grained, pale brown, fresh-looking bladed flakes that range from 0.5 to 5 mm in length.

Partial analyses of 11 book muscovite and 5 plumose muscovite samples are given in Tables 3.6 and 3.7 The plumose muscovites are depleted in Li, Rb and Cs with respect to the book muscovites. Polytype determinations show that all of these samples are $2M_1$.

The Fe-rich lithian muscovite occurs at the petalite-bearing localities as dispersed, thin, fine-grained, light brown interstitial flakes in the matrix of the pegmatitic leucogranite. It is the only mafic mineral at these locations. One sample from location B yielded 5.72 wt.% total Fe as Fe_2O_3, 1.3% Li_2O, 1.8% Rb, 0.6% Cs and 110 ppm Be. Its partial analysis is given in Table 3.7. The polytype is $2M_1$.

Table 3.6: Partial chemical analyses of book muscovite from pegmatitic granites at Red Sucker Lake.

Sample	F-1	F-13	F-14	G-2	G-13	G-24	J-7	J-8	J-23	K-4	N-2
wt.%:											
TiO_2	0.05	<0.01	0.01	0.07	0.04	0.05	0.04	0.10	0.10	0.15	0.11
TFe_2O_3	2.66	2.91	2.76	2.85	3.07	3.13	2.96	3.20	2.71	4.53	2.41
MnO	0.02	0.02	0.02	0.03	0.03	0.02	0.02	0.02	0.02	0.02	0.02
MgO	0.19	0.19	0.18	0.31	0.26	0.29	0.39	0.37	0.45	0.57	0.31
CaO	0.02	0.01	0.01	0.04	0.01	0.01	0.03	0.01	0.01	0.49	0.01
Na_2O	0.69	0.65	0.83	0.75	0.61	0.50	0.72	0.70	0.67	0.95	0.67
K_2O	8.55	9.42	9.33	10.40	9.53	9.92	9.41	9.54	9.60	9.21	9.04
Li_2O	0.24	0.25	0.24	0.14	0.31	0.29	0.18	0.23	0.12	0.03	0.06
ppm:											
Rb	2440	2940	2370	2140	2990	3470	2410	2760	2900	1320	1360
Cs	59	80	129	52	98	145	80	113	311	46	83
Be	10	12	12	8	7	11	8	9	13	10	11
K/Rb	29.1	26.6	32.6	40.3	26.5	23.7	32.5	28.7	27.5	58.1	55.3
K/Cs	1200	980	600	1700	810	570	980	700	260	1700	900
Rb/Cs	41	37	18	41	31	24	30	24	9.3	29	16

TFe_2O_3 = total Fe calculated as Fe_2O_3

Table 3.7: Partial chemical analyses of plumose and Fe-rich lithian muscovite from pegmatitic granites at Red Sucker Lake.

	PLUMOSE					LITHIAN
Sample	F-15	G-6	G-7	I-15	J-27	C-6
wt.%:						
TiO_2	0.05	0.03	0.04	0.05	0.12	n.d.
TFe_2O_3	2.45	2.34	2.02	1.70	2.00	5.72
MnO	0.04	0.06	0.03	0.02	0.04	0.22
MgO	0.26	0.22	0.20	0.26	0.34	0.04
CaO	0.11	0.05	0.01	0.01	0.07	0.03
Na_2O	0.52	0.25	0.35	0.34	0.64	0.72
K_2O	7.78	7.66	6.84	6.71	9.24	6.40
Li_2O	0.17	0.14	0.09	0.08	0.07	1.30
ppm:						
Rb	1590	1860	1060	1150	1110	18000
Cs	39	27	19	19	37	6000
Be	14	26	7	4	14	110
K/Rb	40.6	34.2	53.4	48.4	69.2	2.95
K/Cs	1700	2400	3000	2900	2100	8.85
Rb/Cs	41	69	56	61	30	3.00

TFe_2O_3 = total Fe calculated as Fe_2O_3

Biotite

Biotite occurs in most exposures of pegmatitic leucogranite and fine-grained leucogranite as small interstitial flakes, and rarely as large books (up to 2 cm) in pegmatitic leucogranite.

Exomorphic biotite was found on the south shore of the island at location C, at the contact between the pegmatitic leucogranite and the metabasalt country rock. It occurs in a 50 cm long 10 cm wide lens, as a monomineralic fine-flaked aggregate composed of 1 to 3 mm grains of fresh looking black biotite. Analysis of a sample of this biotite yielded 12800 ppm Rb and 1600 ppm Cs. The partial analysis is given in Table 3.8.

Table 3.8: Partial analysis of exomorphic biotite from pegmatitic leucogranite at location C.

Sample:		C-01			
Wt.%		ppm		ratios (wt.)	
TiO_2	2.21	Li	77	K/Rb	4.97
TFe_2O_3	17.10	Rb	12800	K/Cs	39.7
MnO	0.06	Cs	1600	Rb/Cs	8.00
MgO	4.26	Be	4		
CaO	0.46	Nb	105		
Na_2O	0.04	Ta	<8		
K_2O	7.66				

TFe_2O_3 = total Fe calculated as Fe_2O_3

Petalite

Petalite occurs in the pegmatitic leucogranite at locations A, B, C and IE, as mm-sized grains in the fine-grained matrix ranging continuously up to blocky megacrysts tens of cm's in maximum dimension (Figure 3.5). The crystals are equant to elongated in shape, anhedral to subhedral,

range from white to dark grey in colour and contain no visible inclusions. On outcrop surface, the dirty grey petalite is very inconspicuous and distinguished only by a relatively deep weathered relief, in contrast to the weathering-resistant and fresh-looking K-feldspar. On fresh broken surfaces the petalite is vitreous, translucent and pale grey to white, as opposed to the turbid to opaque, yellowish to white K-feldspar. Spodumene and spodumene + quartz intergrowths were not observed associated with the petalite, although minor amounts of spodumene were detected by x-ray powder diffraction of the pulverized rock samples.

Garnet

Garnet occurs in all types of pegmatitic granite at most outcrops as accessory grains ranging in diameter from <0.1 mm to 5 mm. They are mostly euhedral, equant and reddish to brown, rarely black. They occur in the matrix of pegmatitic leucogranite, in fine-grained leucogranite, and are concentrated in the dark bands that occur in many of the sodic aplites.

All garnets are almandine-spessartines in composition with spessartines occurring in the Main and petalite-bearing series pegmatitic granites.

Compositionally zoned and unzoned garnets occur throughout the pegmatitic granites. Two-spot microprobe analyses of zoned garnets show that the cores are enriched in Mn, and the rims enriched in Fe.

Analyses of 46 garnets from pegmatitic granites at Red Sucker Lake are given in Appendix A. The diagrams in Figure 3.34 show that Ca and Mg are anomalously enriched in the Western pegmatitic granites with respect to the other series. Ca and Mg in these garnets show no correlation with Fe/Mn ratios as would be expected from crystal-chemical considerations. This possibly indicates contamination of these pegmatitic granites from the host metabasalts. If the data points for the Western series pegmatitic granites are ignored, then Figure 3.34 shows that Mg decreases and Ca increases with increasing Mn content as is expected during igneous fractionation of rare-element pegmatites (Černý and Hawthorne, 1982). These trends are similar to those observed for garnets from the Winnipeg River pegmatite field (Černý et al., 1981), and from pegmatitic granites in the Winnipeg River district (Goad and Černý, 1981).

(A)
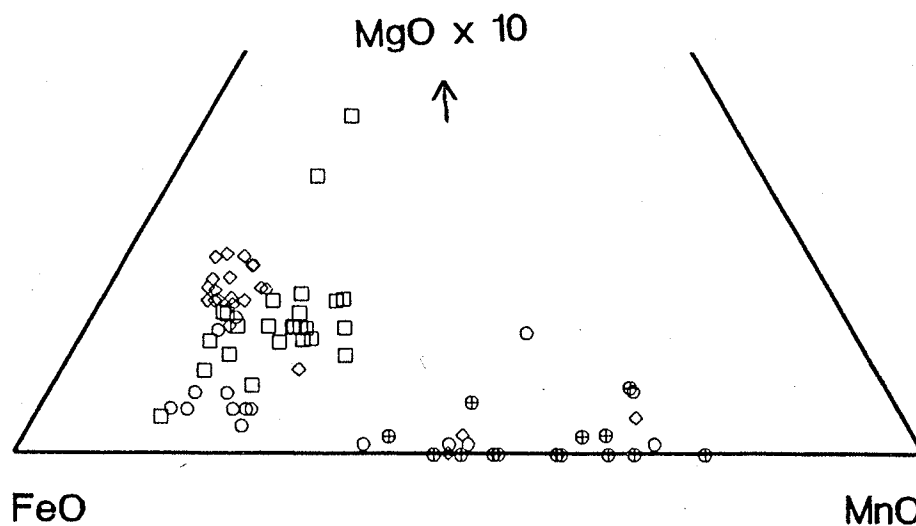
(B)
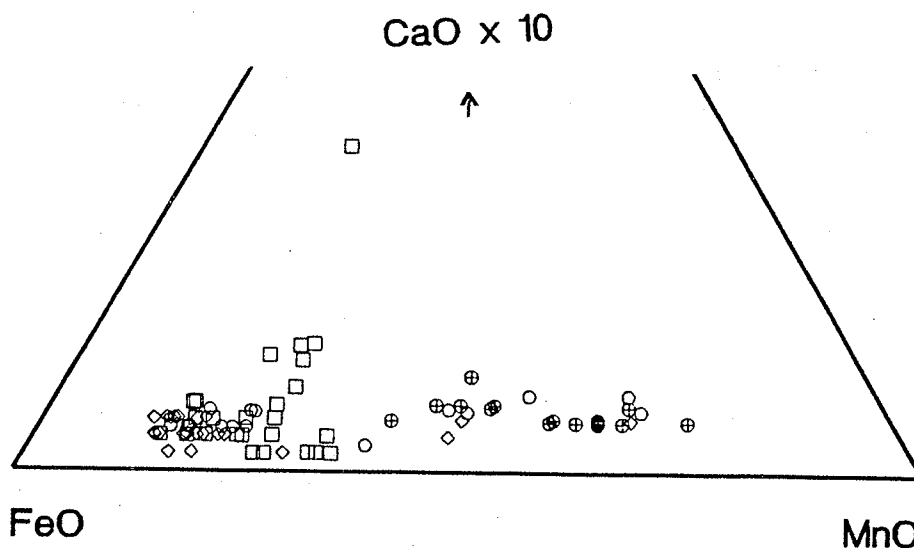
Figure 3.34: (A): FeO – MnO – MgOx10 diagram for garnet from pegmatitic granites at Red Sucker Lake. Symbols as in Figure 3.7. Note anomalously Mg-rich Western series that shows no correlation of Mg with Fe/Mn. The remaining data points show the expected positive correlation with Fe/Mn. (B): FeO – MnO – CaOx10 diagram. Note the anomalously Ca-rich Western series that shows no correlation of Ca with Fe/Mn. The remaining data points show a slight negative correlation with Fe/Mn, as would be expected during igneous fractionation.

Ta-Nb oxide minerals

Columbite-tantalite occurs at locations A, B, IE and KE. It is mostly very fine-grained and inconspicuous in outcrop, occurring as thin plates and stringers in the matrix of the pegmatitic leucogranite at A, B and IE, and in the aplite at KE. Grain size ranges form <0.1 mm to 2 mm.

Chemically these minerals range from ferrocolumbite to manganotantalite as shown in Figure 3.35. One specimen plots near the tapiolite-ferrotantalite miscibility gap and contains an internal zone bearing 11.0 wt.% SnO_2. This corresponds to either ixiolite or wodginite in composition, however the grain was too small for x-ray characterization. All columbite-tantalite analyses are listed in Table 3.9.

$FeTa_2O_6$ $MnTa_2O_6$

$FeNb_2O_6$ $MnNb_2O_6$
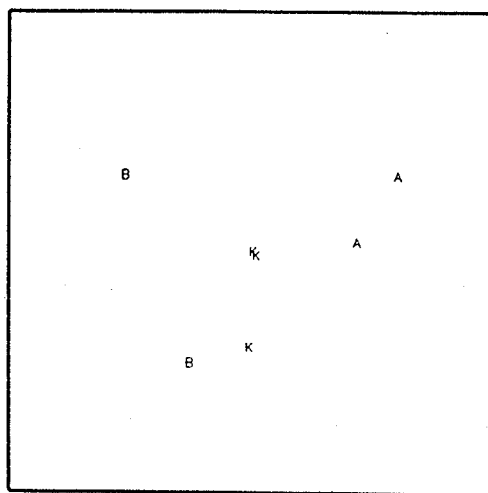
Figure 3.35: Compositions of columbite-tantalite in terms of atomic ratios of Fe/Mn and Nb/Ta, from mineralized pegmatitic leucogranites, and sodic aplite (location KE) at Red Sucker Lake. Letter symbols mark the sampling locations (K stands for KE).

Table 3.9: Microprobe analyses of columbite-tantalite from mineralized pegmatitic leucogranites, and sodic aplite (location KE) at Red Sucker Lake.

Sample	A-3	A-14	B-17	B-32	KE-9	KE-10	KE-18
wt.%							
Ta_2O_5	64.5	53.4	62.8	31.7	51.3	52.3	34.5
Nb_2O_5	20.1	29.6	19.5	51.9	31.8	31.3	48.2
TiO_2	<0.01	0.6	2.6	0.6	1.1	1.0	0.4
SnO_2	<0.01	<0.01	1.0	0.04	0.2	<0.01	<0.01
Sc_2O_3	<0.01	<0.01	<0.01	0.02	<0.01	<0.01	0.02
Fe_2O_3	<0.01	<0.01	<0.01	<0.01	0.8	<0.01	<0.01
FeO	2.9	4.6	11.6	11.8	7.8	8.3	9.3
MnO	11.5	11.4	3.6	6.9	8.7	8.3	9.0
Σ	99.1	99.7	101.1	103.0	101.7	101.2	101.4
Cations per 24 O's:							
Ta	5.35	4.14	4.99	2.14	3.84	3.95	2.40
Nb	2.77	3.81	2.57	5.82	3 95	3.93	5.57
Ti	——	0.13	0.58	0.10	0.23	0.22	0.07
Sn	——	——	0.11	0.004	0.02	——	——
Sc	——	——	——	0.004	——	——	0.004
Fe^{3+}	——	——	——	——	0.16	——	——
Fe^{2+}	0.73	1.09	2.84	2.45	1.79	1.92	1.99
Mn	2.97	2.76	0.89	1.44	2.02	1.95	1.95
Σ	11.82	11.93	11.98	11.96	12.00	11.97	11.98
Atomic ratios:							
Ta/Ta+Nb	0.659	0.521	0.660	0.269	0.493	0.501	0.301
Mn/Mn+Fe	0.802	0.717	0.239	0.370	0.510	0.503	0.495

Tourmaline

Tourmaline occurs sporadically throughout the pegmatitic granites as the schorl species. It is black in color, fresh-looking, equant and anhedral to subhedral. It is usually found along the margins of quartz cores and surrounding blocky K-feldspars in potassic pegmatitic segregations in pegmatitic leucogranites. Grain size ranges from a few mm's to 5 cm.

Apatite

Apatite was observed at locations A, B, C and K in pegmatitic leucogranite, and at KE and PE in sodic aplite.   It occurs as 0.1 - 1.0 mm anhedral interstitial grains. Microprobe analyses of four grains are listed in Table 3.10.   Mn was detected in all 4 grains, ranging up to 5.4 wt.% MnO. No minor elements other than Mn and Fe were detected.

Table 3.10:   Microprobe analyses of apatites from pegmatitic leucogranites at Red Sucker Lake.

Sample	P_2O_5	CaO	MnO	FeO
A-10	35.9	51.9	5.4	<0.1
A-2a	41.3	52.7	4.1	<0.1
A-13b	34.5	54.1	2.9	<0.1
B-17a	35.3	53.8	2.0	0.3

Gahnite

Gahnite was observed at locations B, C and DE, occurring as 0.5 to 2 mm euhedral grains in the matrix of the pegmatitic leucogranite.   They are dark bluish-green in color.   Qualitative microprobe analysis of one grain revealed a small amount of Fe, and no internal zoning.

Arsenopyrite and löllingite

Arsenopyrite and löllingite occur as accessory phases at several locations.   Löllingite occurs more frequently in the central parts of the pegmatitic leucogranite (locations A, B and C), whereas arsenopyrite occurs only in the Eastern and Western series.

3.5   DESCRIPTION OF THE GEOCHEMICAL ANOMALY

A geochemical anomaly occurring in the Petalite-bearing and Main series of pegmatitic granites is defined by high whole-rock and K-feldspar values of Li, Rb and Cs, high Mn/(Mn+Fe) ratios in garnets, and by the occurrence of petalite, columbite-tantalite and lithian ferromuscovite. The anomaly covers 16 outcrops over 9 islands and is roughly 2 to 3 km in length.   Figures 3.36 to 3.45 illustrate the linear extent of the anomaly within the pegmatitic granites, its shape and variability in values of the pertinent geochemical parameters.   It is gradational with respect to most chemical parameters and coincides approximately with the Main series of pegmatitic leucogranites.   Unlike the other geochemical parameters, Li content of whole-rock samples shows an extremely abrupt change; it increases dramatically in the centre of the Main series, coinciding with the occurrence of petalite.

In general, the Main series pegmatitic granites are silicic and peraluminous, with highly variable K_2O/Na_2O ratios.   In comparison with values for Ca-poor granites (Turekian and Wedepohl, 1961), they are enriched in Li, Rb, Cs, Ga, Sn, Nb and Ta, and depleted in Fe, Mg, Ca, Ba, Sr, Ni, Zr, Ti, V and S.   Low K/Rb, K/Cs, Rb/Cs, Al/Ga, Zr/Hf and Nb/Ta ratios are also characteristic.

Table 3.11 summarizes the geochemical data characterizing individual sample locations in terms of K-feldspar, garnet and whole-rock compositions, and compares them with data characterizing the most fractionated pegmatite in the Red Sucker Lake area (location SQ), and the Tanco pegmatite of southeastern Manitoba (Černý, 1982). The anomalous pegmatitic granites approach fractionation parameters of the most highly evolved rare-element pegmatites.

This anomalous mineralization has no analog among other occurrences of pegmatitic leucogranite worldwide. It is similar to the highly evolved pegmatitic cupolas of granitic intrusions of the Montebras and Échassières type (Aubert, 1969; Burnol, 1974), but the mineralogy, geochemistry and textural style are unique.

Table 3.11: Geochemical characteristics of the anomalous zone of pegmatitic granites at Red Sucker Lake.

Location	K-feldspar					Garnet $\frac{MnO}{MnO + FeO}$	Bulk Rock					
	Li	Rb	Cs	K/Rb	Rb/Cs		Li	Rb	Cs	Be	Nb	Ta
A	120	12 400	582	9	22	0.73	2 650	1 235	54	52	63	216
B	149	8 000	269	14	30	0.56	6 050	2 800	80	58	67	58
	–	–	–	–	–	–	[370]	[1 050]	[32]	[66]	[88]	[90]
C	149	8 700	217	13	41	0.61	6 780	2 400	108	51	66	48
	–	–	–	–	–	–	[400]	[1 150]	[45]	[76]	[113]	[150]
D	26	8 300	64	14	130	0.52	200	4 720	57	26	64	30
E	3	3 090	22	38	141	–	–	–	–	–	–	–
F	30	1 860	42	53	44	0.24	180	660	11	2.5	30	12
G	31	1 090	47	89	23	0.24	(120)	(620)	(13)	(2.5)	(61)	(17)
FE	73	8 500	199	13	43	0.41	–	–	–	–	–	–
HE	3	4 400	43	24	102	0.19	–	–	–	–	–	–
IE	189	7 440	157	15	49	0.53	–	–	–	–	–	–
KE	169	9 360	323	12	29	0.62	[140]	[1 270]	[37]	[9]	[78]	[180]
ME	250	5 500	260	20	21	0.48	–	–	–	–	–	–
NE	211	12 400	613	88	21	0.73	–	–	–	–	–	–
OE	–	–	–	–	–	0.51	–	–	–	–	–	–
PE	–	–	–	–	–	0.52	–	–	–	–	–	–
SQ	110	17 500	1 000	6	17	–	–	–	–	–	–	–
Tanco	200	18 000	900	8	18	–	–	–	–	–	–	–

All values in parts per million
No brackets – pegmatitic lencogranite
[ ] – sodic aplite
( ) – fine grained lencogranite
Tanco – approximate averages of data from all pegmatite units, not weighted for relative abundances.
SQ – averages of data from the central part of the pegmatite outcrop.

K-feldspar: Li, ppm
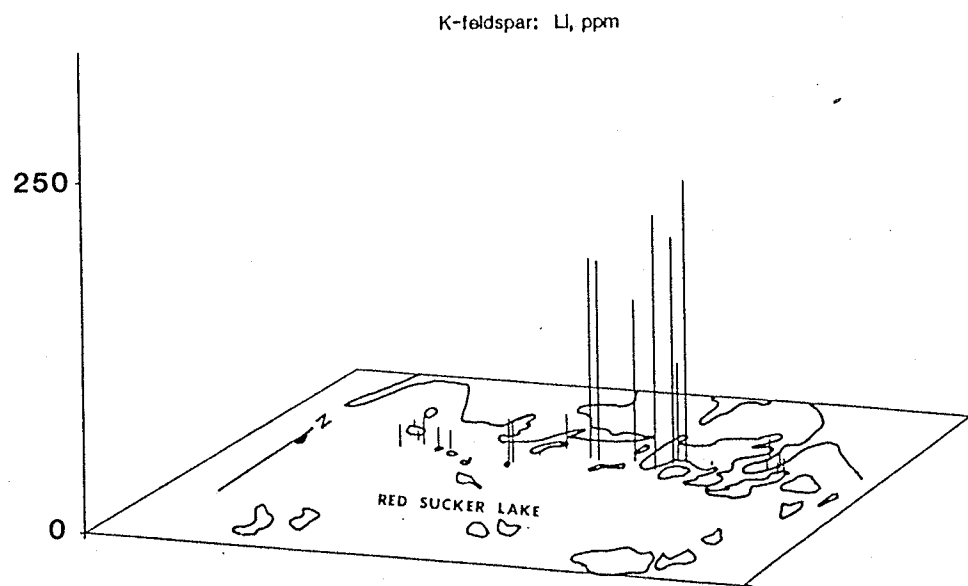
Figure 3.36: Li contents of blocky microcline from pegmatitic leuco-
granites at Red Sucker Lake. Highest values occur 1-2 km east of the
petalite-bearing pegmatitic leucogranites.

K-feldspar: Rb, ppm
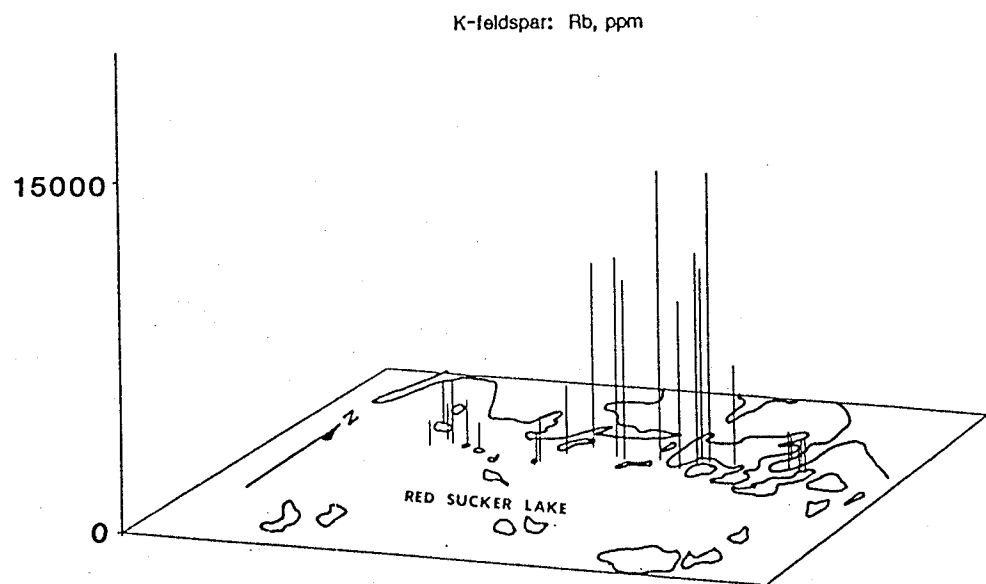
Figure 3.37: Rb contents of blocky microcline from pegmatitic leuco-
granites at Red Sucker Lake. Highest values occur at the eastern ex-
tent of the petalite-bearing pegmatitic leucogranites.

K-feldspar: Cs, ppm
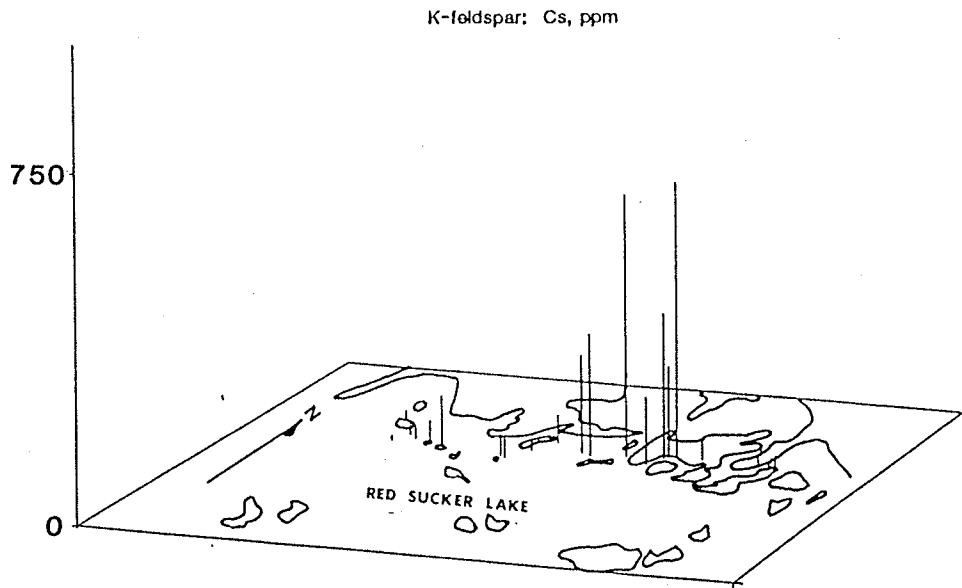
Figure 3.38: Cs contents of blocky microcline from pegmatitic leuco-granites at Red Sucker Lake. Highest Cs-contents occur just east of the petalite-bearing pegmatitic leucogranites.

K-feldspar: K/Rb
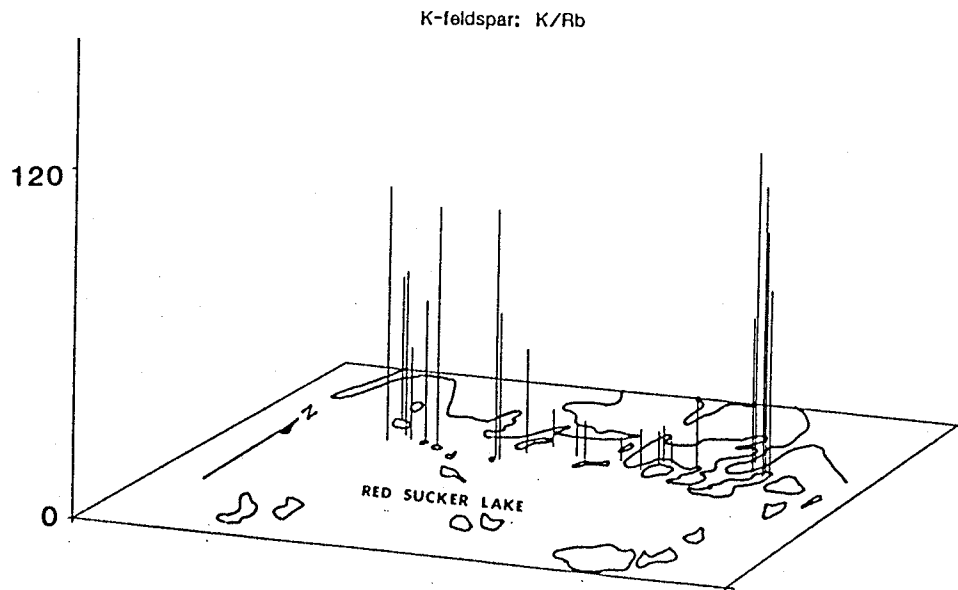
Figure 3.39: K/Rb ratios of blocky microcline from pegmatitic leuco-granites at Red Sucker Lake. Lowest K/Rb ratios occur in the petal-ite-bearing pegmatitic leucogranites.

Garnet: 100*MnO / (FeO + MnO), wt.%
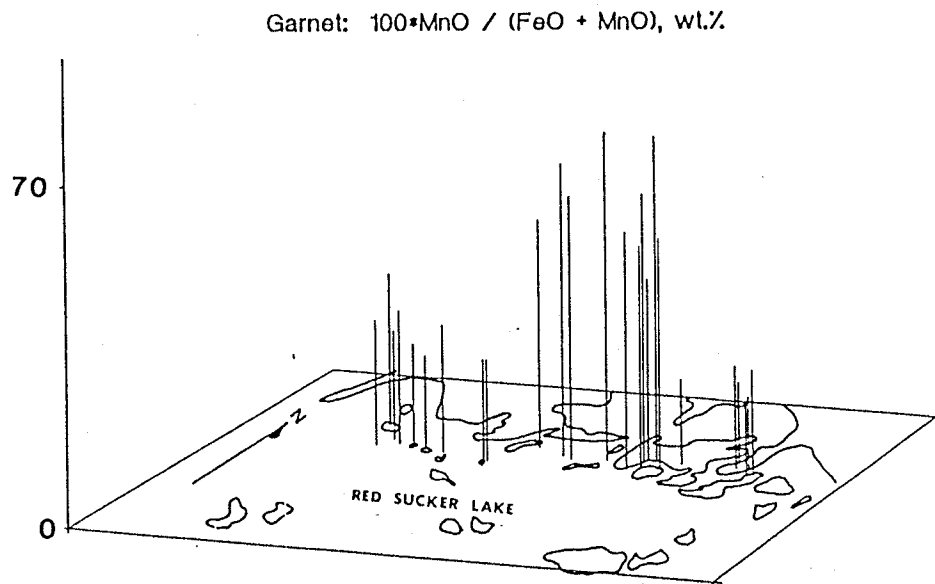
Figure 3.40: Mn/(Mn+Fe) ratios of garnet from pegmatitic granites at Red Sucker Lake. Greatest Fe/Mn fractionation occurs 1-2 km east of the petalite-bearing pegmatitic leucogranites.

Whole rock: Li, ppm
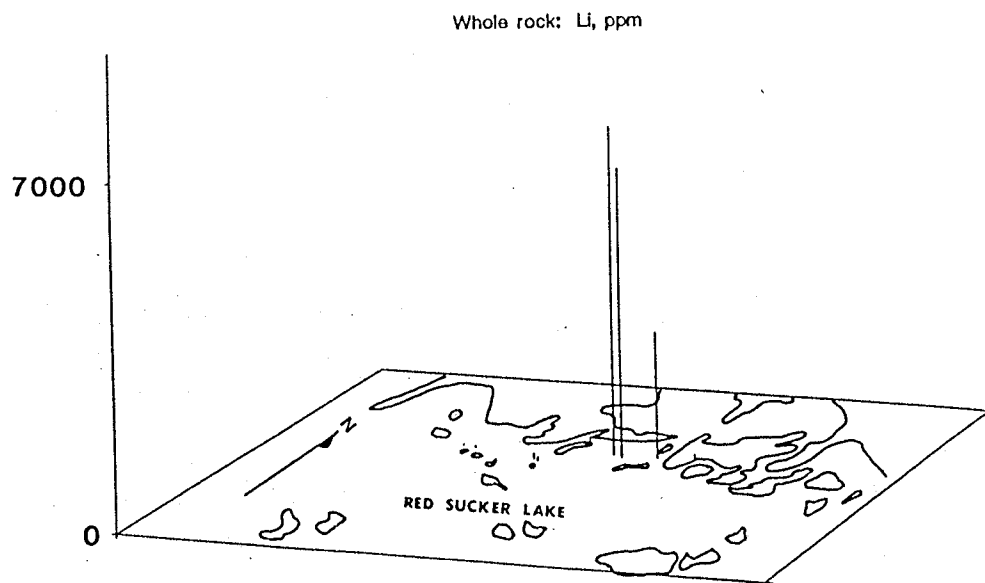
Figure 3.41: Li contents of whole-rock samples of pegmatitic leucogranite at Red Sucker Lake. The 3 extremely high Li values coincide with the petalite-bearing pegmatitic leucogranites.

Whole rock: Rb, ppm
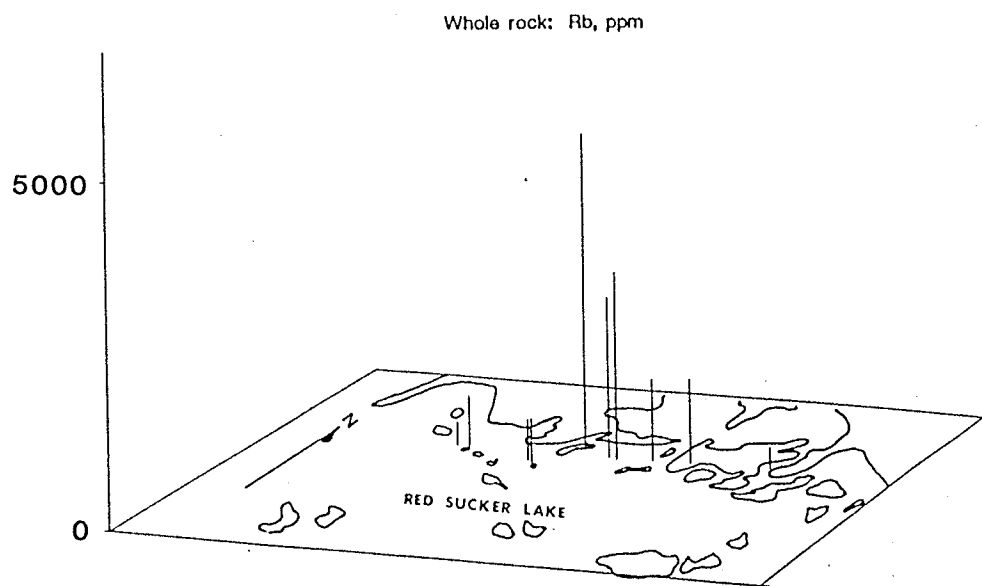
Figure 3.42: Rb contents of whole-rock samples of pegmatitic leucogranite at Red Sucker Lake. Highest values occur 1 km west of the petalite-bearing pegmatitic leucogranites.

Whole rock: Cs, ppm
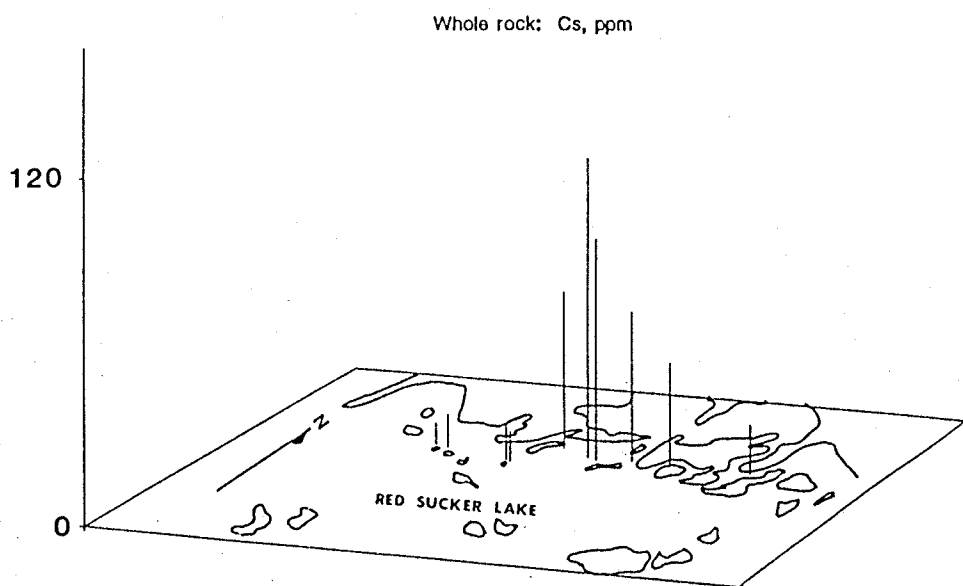
Figure 3.43: Cs contents of whole-rock samples of pegmatitic leucogranite at Red Sucker Lake. Highest values occur at the petalite-bearing pegmatitic leucogranites.

Whole rock: Be, ppm
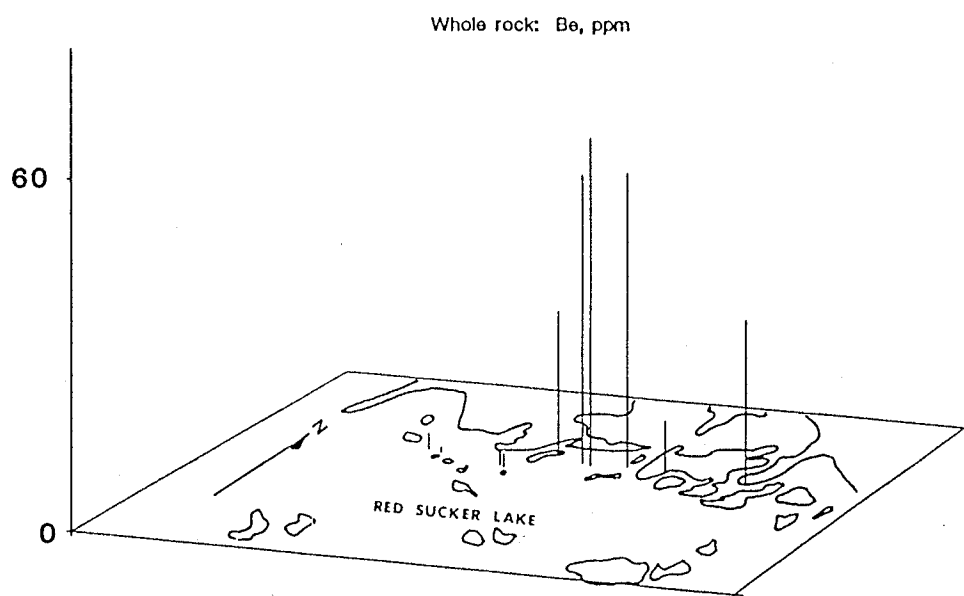
Figure 3.44: Be contents of whole-rock samples of pegmatitic leucogranite at Red Sucker Lake. Highest Be-values occur at the petalite-bearing pegmatitic leucogranites.

Whole rock: Ta, ppm
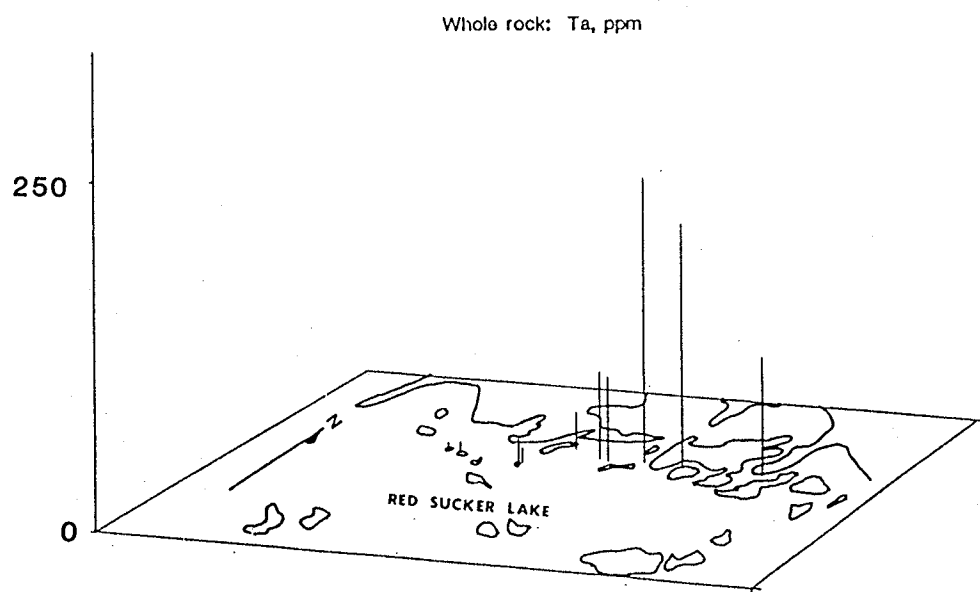
Figure 3.45: Ta contents of whole-rock samples of pegmatitic leucogranite at Red Sucker Lake. Highest values occur toward the eastern extent of the petalite-bearing pegmatitic leucogranites.

Chapter IV

PEGMATITES AT RED SUCKER LAKE

4.1 DISTRIBUTION AND INTRUSIVE RELATIONSHIPS

Pegmatites at Red Sucker Lake occur in three geographically and geochem-
ically distinct groups; a Northern series extending from location WP in
the west to GR in the east, a Western series at locations SQ, PK, TD and
BL, (Figure 4.1), and an additional small group of 7 narrow, intensely
sheared pegmatite dikes at location EE (the Eastern pegmatites).   The
Northern series pegmatites are not mineralized and are geochemically the
most primitive, least fractionated pegmatitic rocks in the study area.
In contrast, the Western pegmatites include the most highly fractionated
rocks encountered here.

Northern series

The Northern series pegmatites occur in a long, narrow, east-trending
zone north of and parallel to the pegmatitic granites. They intrude the
northern exposure of the Oxford Lake Group metasedimentary rocks.   They
are E-striking and subvertically dipping, generally to the north.
Structural deformation is intense in these pegmatites in relation to the
pegmatitic granites.   Ptygmatic folding and boudinage are seen at many
outcrops (Figure 4.2).   At pegmatite SC,   features that appear to be
boudins are in fact not lined up; they are separated by wall-rock bridg-
es and may represent individual fingers of the intrusion that have un-

- 70 -

dergone deformation (Figure 4.3).   Faulting, tight folding and moderate to intense shearing are also common in these pegmatites (Figures 4.4, 4.5 and 4.6).

Western series

The four pegmatites of the Western series intrude metabasalts of the Hayes River Group. They include a Li-rich pegmatite at SQ, a saccharoidal albite-rich cassiterite-bearing dike at TD, a beryl-bearing pegmatite at BL, and a narrow microlite-bearing pegmatite at PK.

   The SQ dike is exposed on a vertical face, 7 m wide by 5 m high. Contacts are obscured by overburden making strike measurements impossible.   The dike dips approximately 80° to the north and appears to be concordant to the dip of the schistosity of the basalt.   The 5 to 20 cm wide PK pegmatite is exposed for 4 m along strike.   It strikes N-S and dips steeply to the west, discordant to and deforming the metabasalts (Figure 4.7).   The dike at TD is also distinctly discordant to the schistosity of the basalt. It strikes approximately NW and appears vertical to subvertical.   The BL pegmatite could not be located during the 1984 field season.

Eastern pegmatites

The Eastern pegmatites intrude the Oxford Lake Group metasedimentary rocks at the far eastern end of the study area.   They strike E-W, dip 80° to 85° to the north, and are concordant to the schistosity of the host rocks.   The seven dikes range from 10 cm to 1 m wide and are exposed for up to 5 m along strike.   They are characterized by strong shearing; boudinage occurs in one of these dikes.
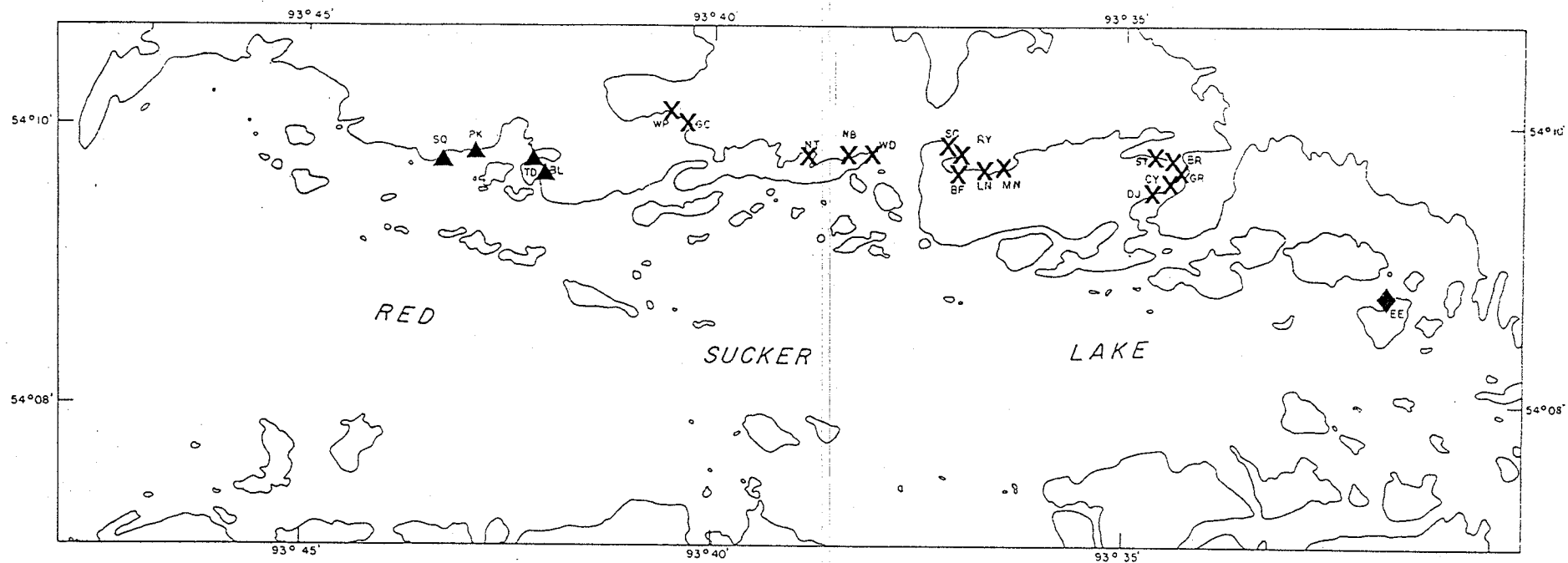
Figure 4.1: Distribution of pegmatite sampling locations at Red Sucker Lake. Modified after Chackowsky and Čerńy (1984).

Figure 4.2: Boudinaged pegmatite dike intruding metasedimentary rocks at location SC. Sharp intrusive contacts and lack of internal zoning are characteristic of the Northern series pegmatites.

Figure 4.3: Deformed pegmatite lenses resembling boudins, at location SC. Note that individual lenses are not lined up along the schistosity of the metasedimentary rocks. Pencil is 14 cm long in length.
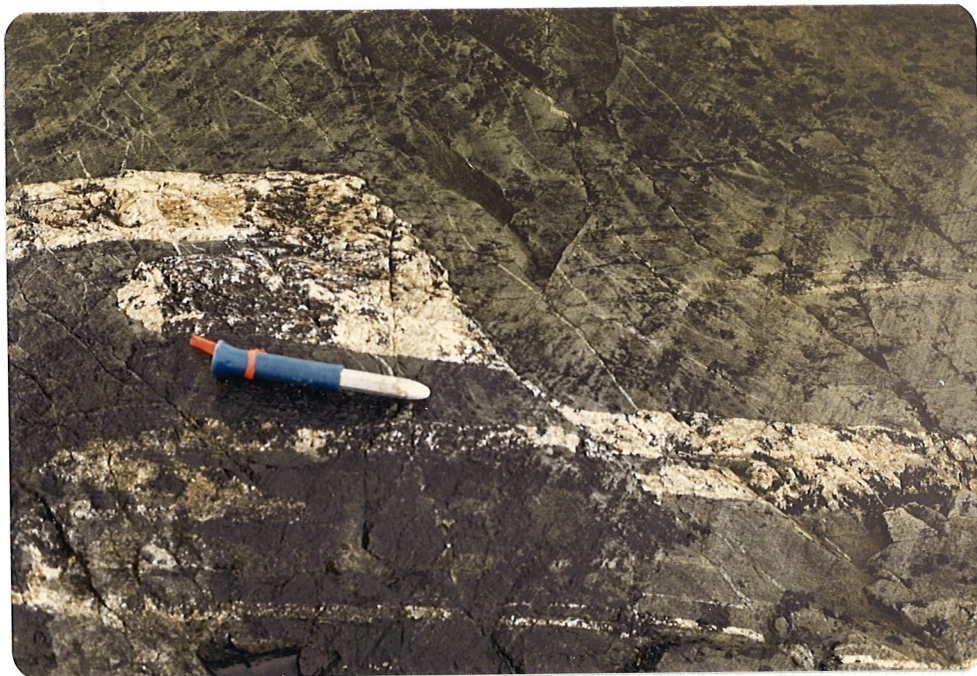
Figure 4.4: Faulted pegmatite dike intruding metasedimentary rocks at location GC. Chisel is 20 cm long.

Figure 4.5: Tight folds in pegmatite dike intruding metasedimentary rocks at location NT. Pencil is 14 cm long.
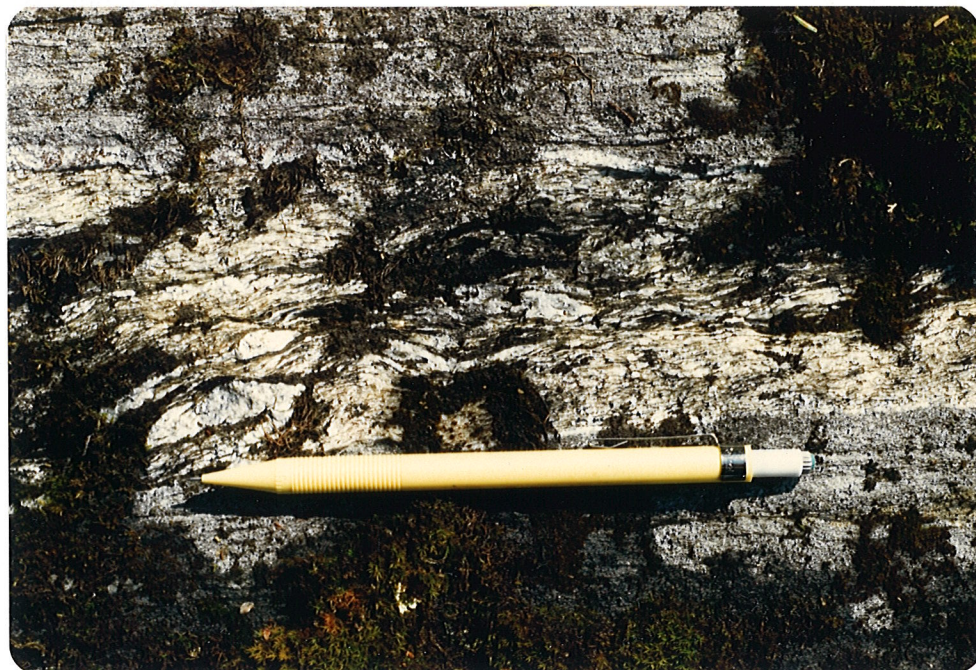
Figure 4.6: Intensely sheared pegmatite dike intruding metasedimentary rocks at location EE. Microcline phenocrysts are rotated and deformed. Pencil is 14 cm long.

Figure 4.7: Zoned pegmatite dike intruding metabasalts at location PK. The dike cross-cuts and deforms the schistosity of the metabasalts. Field book is 18 cm in length.

4.2   INTERNAL STRUCTURE

Northern pegmatites

The Northern pegmatites at Red Sucker Lake are texturally homogeneous. Variation in grain size is present at some pegmatites, but even at these locations systematic textural and mineralogical zoning are absent. Structural deformation has produced an internal foliation in some of these dikes.   Pegmatite is the only rock type observed at these loca- tions, except at GR where a banded aplite dike occurs within the pegma- tite.   Relatively coarse-grained blocky K-feldspar + quartz pods occur in many of the pegmatites, but do not contain any rare-element minerali- zation.

Western pegmatites

The pegmatites of the Western series are texturally and mineralogically heterogeneous.   Large grain size variation is present at locations SQ and PK, and symmetrical textural and mineralogical zoning is displayed by the PK pegmatite (Figure 4.8).

Grain size in the SQ pegmatite ranges from 1 to 10 cm, with blocky K-feldspar crystals up to 75 cm in maximum exposed dimension.   In the lower left corner of the exposed face massive fine-grained lithian mus- covite and spodumene + quartz intergrowth (pseudomorphic after petalite) occur.

The PK pegmatite is composed of 2 main zones - a thin (1 to 2 cm) fine-grained outer wall surrounding a thicker (5 to 20 cm) coarser inner zone (Figure 4.8).   The outer zone is composed of 0.1 to 2 mm grains of quartz, schorl, and K-feldspar laths that are approximately perpendicu-

lar to the intrusive contact. The inner zone is composed of abundant graphic K-feldspar + quartz intergrowth, blocky K-feldspar, quartz and plagioclase, subordinate schorl, and rare microlite.

The TD pegmatite is the most texturally and mineralogically homogeneous of the three observed Western pegmatites. Cassiterite and fine-grained muscovite occur in local banded concentrations, but their distribution is random.

Eastern pegmatites

The Eastern pegmatite dikes are texturally and mineralogically homogeneous. Intense shearing has produced internal foliation and deformed K-feldspar phenocrysts (Figure 4.6).

Figure 4.8: Textural and mineralogical zoning in pegmatite dike at location PK. Outer zone: fine-grained quartz + schorl + K-feldspar. Inner zone: blocky K-feldspar + massive quartz + plagioclase. Lens cap is 50 mm in diameter.

4.3 **PARAGENESIS**

Parageneses of the pegmatites at Red Sucker Lake are given in Table 4.1. Relative mineral abundances are based on field observations. Note the distinctly different paragenetic make-up of the highly fractionated Western series vs that of the barren Northern series. Muscovite, biotite, garnet and löllingite are much more abundant in the Northern series, whereas tourmaline, fine-grained lithian muscovite, beryl, spodumene, cassiterite and microlite occur only in the Western series. This correlates with the extreme levels of geochemical fractionation attained by these pegmatites.

The Northern pegmatites are composed of abundant perthitic K-feldspar, K-feldspar + quartz intergrowth, quartz, plagioclase, and subordinate biotite and muscovite. Accessory minerals include garnet, schorl, sillimanite, löllingite and arsenopyrite. Apatite, molybdenite and chalcopyrite are rare. Cobaltite and sphalerite were identified in a hand sample from pegmatite SC by microprobe.

The Western pegmatites are characterized by extremely diverse parageneses. The SQ pegmatite is composed of abundant blocky K-feldspar, quartz, platy muscovite, and accessory tourmaline (verdelite), fine-grained lithian muscovite and spodumene + quartz intergrowth. Fine-grained lithian muscovite and spodumene are unique to this pegmatite in the Red Sucker Lake area.

The PK pegmatite contains abundant blocky and graphic K-feldspar, quartz and plagioclase, subordinate schorl and rare microlite.

The TD dike consists of abundant fine-grained saccharoidal albite, subordinate quartz, and accessory cassiterite, garnet, muscovite and apatite. Rare minerals include microcline, dravite, arsenopyrite, fluorite and schorl.

Table 4.1: Paragenesis of pegmatites at Red Sucker Lake.

SERIES	WESTERN				NORTHERN															EE
LOCATION	SQ	PK	TD	BL	WP	GC	NT	NB	WD	SC	RY	BF	LN	MN	DJ	CY	GR	BR	ST	EE
MICROCLINE	A	A	r	A	A	A	A	A	A	A	A	A	A	A	A	A	A	A	A	A
PLAGIOCLASE	a	A	A		S	A	A	A	A	S	A	A	S	A	S	A	S	S	S	S
QUARTZ	A	A	A	A	A	A	A	A	A	A	A	A	A	A	A	A	A	A	A	A
MUSCOVITE	A		r	S	S	S	S	S	S	a	S	S	S	S	a	a	a		a	S
LEPIDOLITE	a																			
BIOTITE					a	S		a	S	A	S	S	S	S	S	S	S	S	S	
GARNET			a			a	a	a	a	a	a	a	a	a	r	a	a	a	a	r
SCHORL		a	a																	
DRAVITE			r																	
VERDELITE	a	a																		
SILLIMANITE												a								
BERYL				a																
SPODUMENE	a																			
FLUORITE			r																	
MICROLITE		r																		
CASSITERITE			a																	
ARSENOPYRITE		a	r												a	a	a			
LOLLINGITE						a						a			a	a				
CHALCOPYRITE										r										
MOLYBDENITE									r											
SPHALERITE										r										
COBALTITE										r										

A - abundant
S - subordinate
a - accessory
r - rare

4.4   MINERALOGY

K-feldspar

Graphic and blocky K-feldspar is abundant in all of the pegmatites, except at location TD. Blocky K-feldspars range up to 3 cm in size in the Northern series, and up to 75 cm at location SQ. They are equant to columnar and undeformed except in areas of intense structural deformation, as at pegmatites SC and EE. Coarse perthitic texture is visible in most specimens.

39 samples were selected for x-ray powder diffraction and partial chemical analysis. All samples turned out to be maximum microcline with Δ values ranging from 0.92 to 1.02. Five samples were selected from this group for determination of unit cell parameters. They were chosen so as to represent both series of pegmatites in terms of geographical distribution and variation in Δ and chemistry of the microcline samples. The refined unit cell parameters,   along with selected compostional parameters, are given in Table 4.2, and plotted on determination diagrams in Figures 4.9 to 4.12. All 5 samples plot close to the maximum microcline apices of the diagrams, and no systematic variations in chemistry or structural state of microcline samples from different pegmatites and pegmatite series are evident.

Partial chemical analyses and Δ values of the 39 microcline samples are given in Appendix B. Compositional parameters are plotted in Figures 4.13 to 4.18. Microcline from the Northern and Western series plot in distinctly different areas on these diagrams. The microcline samples display moderate to extreme levels of fractionation in terms of Li, Rb, Cs, K/Rb and Rb/Cs in the Western pegmatites, moderate fractionation in

the Eastern pegmatites,   and relatively low levels of fractionation in the Northern series.

The microcline samples range from Or_{75} at CY to Or_{94} at WD in the Northern series, and from Or_{87} at TD to Or_{92} at SQ in the Western series.   The most potassic microcline occurs in pegmatites SQ, PK, BL, WD and SC.

Li in these microcline samples ranges from 1 ppm at pegmatite WD to 26 ppm at pegmatite CY in the Northern series, and from 50 ppm at pegmatite PK to 290 ppm at pegmatite BL in the Western series.   Distinctly high Li values also occur at pegmatites SQ (89 to 139 ppm) and TD (97 ppm).

Rb in microcline ranges from 500 ppm at pegmatite WD to 1600 ppm at pegmatite GR in the Northern series, and from 9800 ppm at pegmatite TD to 18,800 ppm at pegmatite SQ in the Western series. Distinctly high Rb values also occur at pegmatites PK (13,800 ppm) and BL (11,400 ppm).

Cs in microcline ranges from less than 1 to 14 ppm in the Northern series, and from 326 ppm at pegmatite TD to 1250 ppm at pegmatite SQ in the Western series.   Distinctly high Cs values also occur at pegmatites PK (1180 ppm) and BL (455 ppm).

Figures 4.13 to 4.15 show discontinuous fractionation in terms of K/Rb vs Li, Rb and Cs.   The Eastern pegmatite data points tend to plot between those for the Western and Northern series.   All 3 diagrams show strong correlations between increasing rare alkali metals and increasing K/Rb fractionation.

Total Sr in microcline ranges from <6 ppm at pegmatite BF to 102 ppm at pegmatite WD in the Northern series, and from 75 ppm at pegmatite PK to 157 ppm at pegmatite SQ in the Western series. Total Sr tends to increase with increasing K/Rb fractionation, but when corrected for radiogenic ^{87}Sr the trend is reversed (Figure 4.16).

Ba in microcline ranges from 23 ppm at pegmatite LN to 760 ppm at pegmatite WD in the Northern series, and from 14 ppm at pegmatite BL to 325 ppm at pegmatite PK in the Western series. The K/Rb vs Ba diagram in Figure 4.17 shows two separate groups for the 2 series of pegmatites, but there is no significant variation in K/Rb with increasing Ba in microcline from these series.

Pb in microcline ranges from 32 ppm at pegmatite NT to 173 ppm at pegmatite WD in the Northern series, and from 16 ppm at pegmatite BL to 89 ppm at pegmatite SQ in the Western series. Figure 4.18 shows a moderate increase in Pb with decreasing K/Rb for the Northern pegmatites, and a very slight decrease in Pb with decreasing K/Rb for the Western series.

Microcline from the sheared Eastern pegmatites at location EE has values of Li (41 ppm), Rb (6500 ppm), Cs (240 ppm), Sr (60 ppm) and Pb (39 ppm) that are intermediate between corresponding values from the Northern and Western series of pegmatites. These values all plot between the separate areas covered by microcline analyses from the two series in Figures 4.13 to 4.18.

Triclinicities of the microcline samples are plotted against various compostional parameters in Figure 4.19. These diagrams show that there

is no systematic correlation between Δ and pegmatite series, although

the Western pegmatites cover a smaller range of Δ values than microcline

from the Northern pegmatites. Furthermore, there is no observable cor-

relation between Δ and concentrations of large cations in these micro-

cline samples.

Table 4.2: Unit cell parameters and selected geochemical parameters of microcline from pegmatites at Red Sucker Lake.

Series	Northern		Western		Eastern
Sample:	NT-10	WD-3	PK-5A	TD-17	EE-3
a	8.561(3)	8.565(5)	8.582(5)	8.585(5)	8.576(3)
b	12.970(4)	12.962(6)	12.965(5)	12.968(5)	12.965(3)
c	7.224(2)	7.223(3)	7.225(3)	7.223(2)	7.224(1)
α	90.65(3)	90.63(5)	90.63(4)	90.57(3)	90.61(2)
β	115.93(3)	115.96(3)	116.05(4)	115.97(3)	115.94(2)
γ	87.66(2)	87.73(4)	87.68(4)	87.70(3)	87.73(2)
vol.	720.8(3)	720.4(4)	721.7(4)	722.4(3)	721.7(3)
a*	.12999(5)	.12996(8)	.12980(9)	.12967(6)	.12977(4)
b*	.07717(2)	.07721(3)	.07719(3)	.07718(2)	.07720(2)
c*	.15392(5)	.15398(7)	.15406(4)	.15399(4)	.15394(3)
α*	90.42(3)	90.40(5)	90.43(4)	90.48(3)	90.43(2)
β*	64.08(3)	64.04(3)	63.96(4)	64.03(2)	64.06(2)
γ*	92.29(2)	92.22(4)	92.27(4)	92.28(3)	92.23(2)
Ba	37	325	325	53	<10
Ba+Sr+Ca	340	1200	690	920	350
Rb+Cs	1400	580	14900	10000	6700

a, b and c in Å; vol. in Å^3; a*, b* and c* in Å^{-1}. α, β, γ, α*, β* and γ* in degrees. All chemical data in ppm.
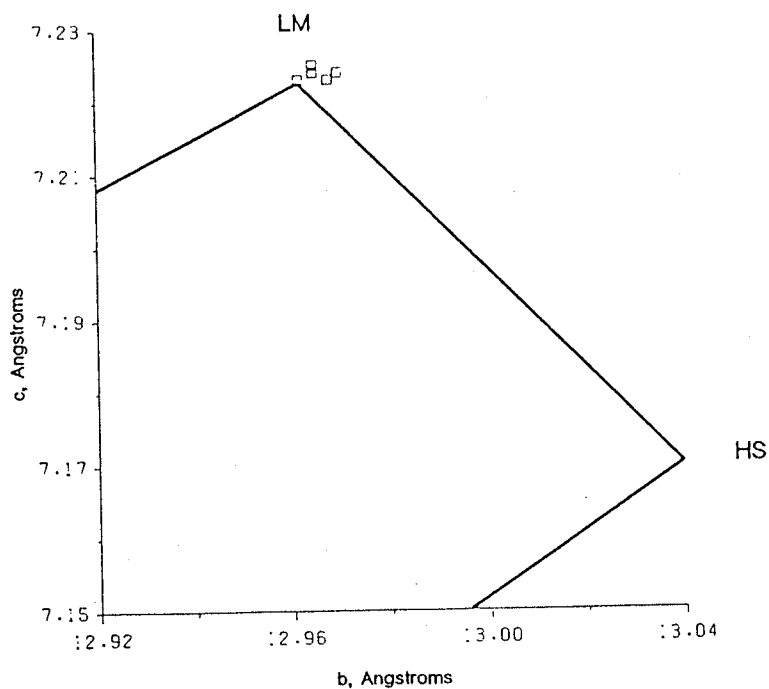
Figure 4.9 : c vs b cell parameters for maximum microcline from pegmatites at Red Sucker Lake. Modified after Kroll and Ribbe (1983).
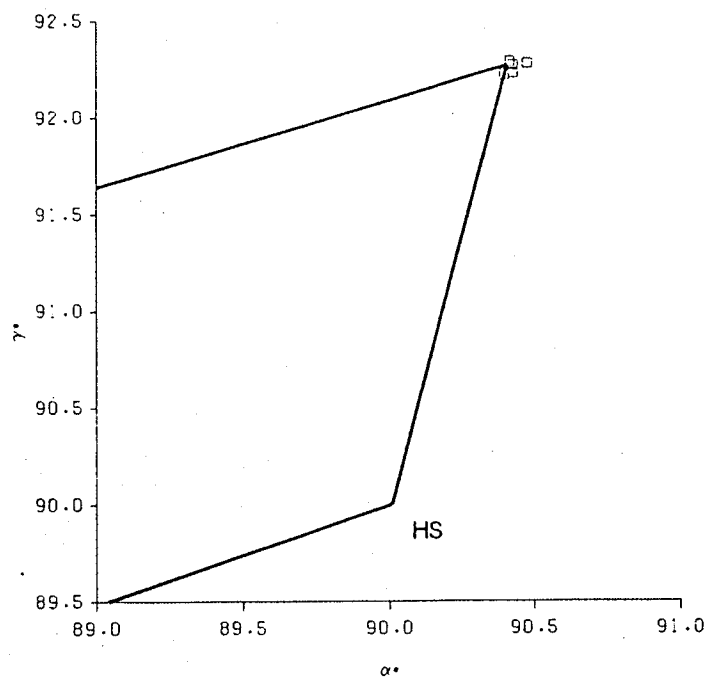
Figure 4.10 : γ^* vs α^* for maximum microcline from pegmatites at Red Sucker Lake. Modified after Kroll and Ribbe (1983).
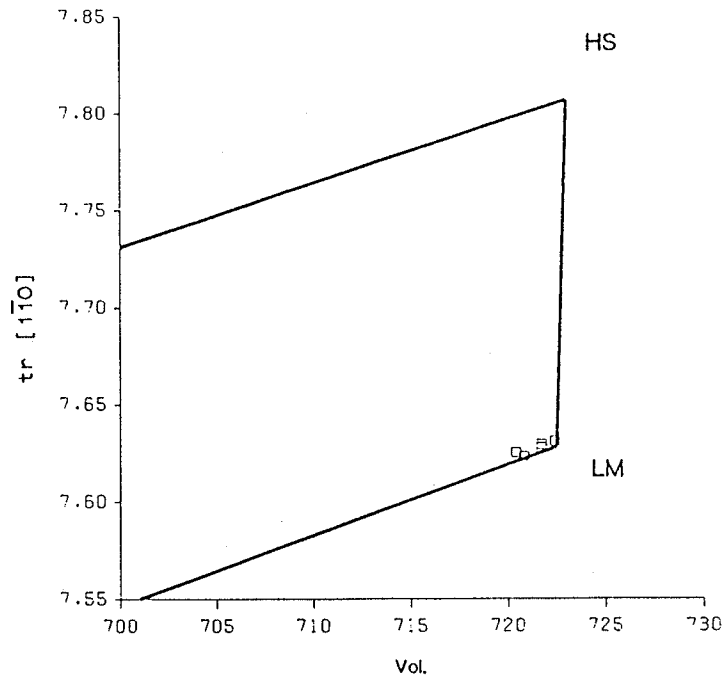
Figure 4.11 : tr[110] vs volume for maximum microcline from pegmatites at Red Sucker Lake. Modified after Kroll and Ribbe (1983).
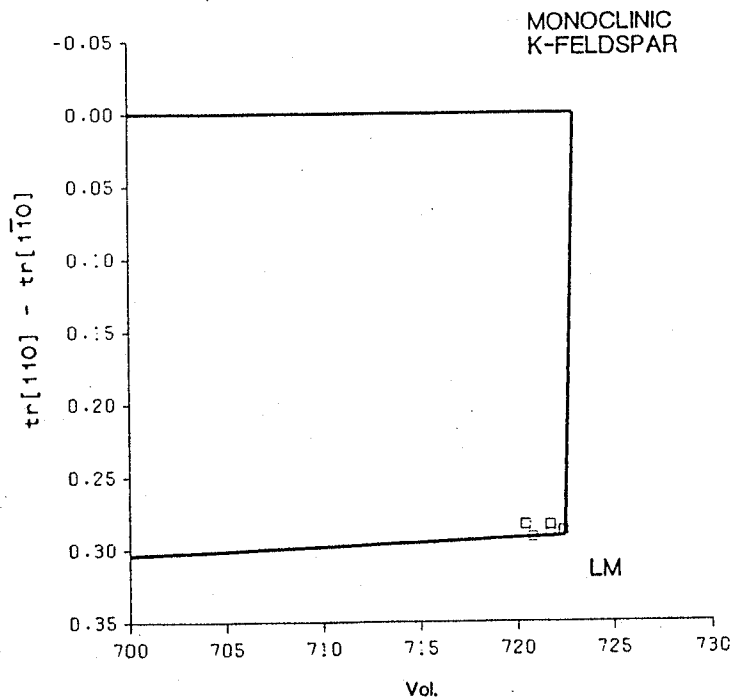
Figure 4.12 : tr[110] – tr[110] vs volume for maximum microcline from pegmatites at Red Sucker Lake. Modified after Kroll and Ribbe (1983).
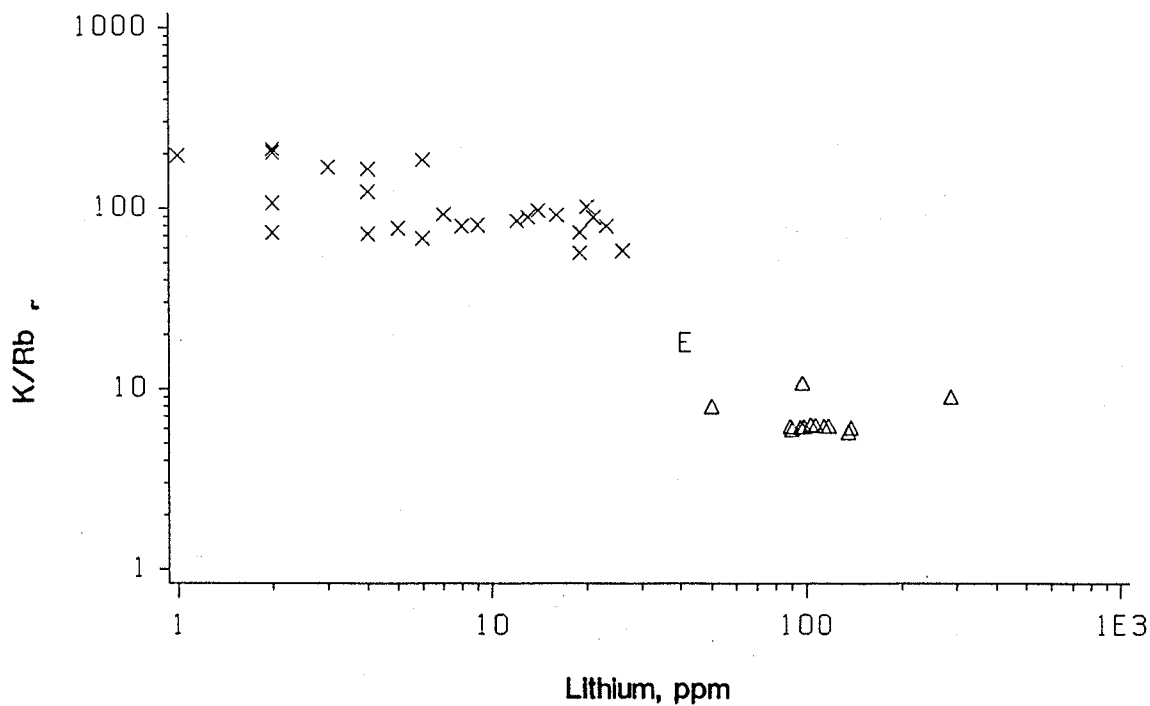
Figure 4.13 : K/Rb vs Li for microcline from pegmatites at Red Sucker Lake. Western pegmatites are extremely fractionated in terms of K-Rb ratio and Li content, in contrast to the geochemically barren Northern pegmatites. The sheared Eastern pegmatites plot between the Northern and Western pegmatites on this diagram. Data in this and following diagrams are grouped into the following units: Northern pegmatites (X's), Eastern pegmatites (E's) and Western pegmatites (triangles).
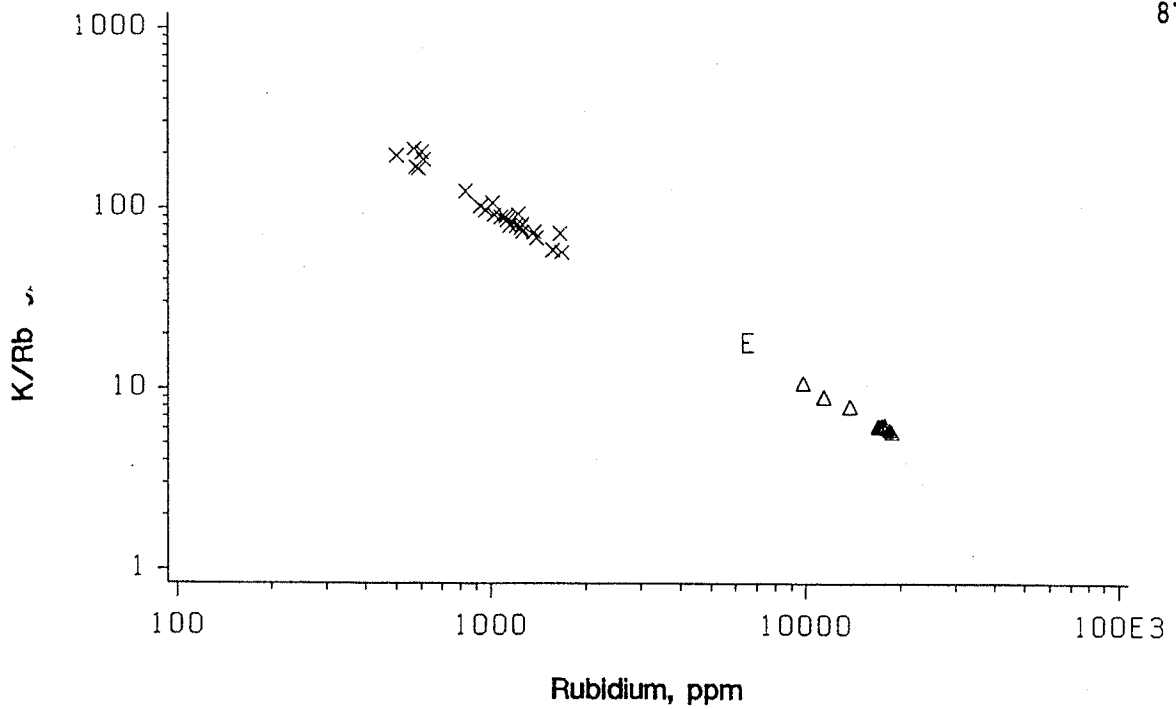
Figure 4.14 : K/Rb vs Rb for microcline from pegmatites at Red Sucker Lake. Symbols as in Figure 4.13. Note fractionation trend from barren Northern pegmatites to moderately fractionated Eastern pegmatites to extremely fractionated Western pegmatites.
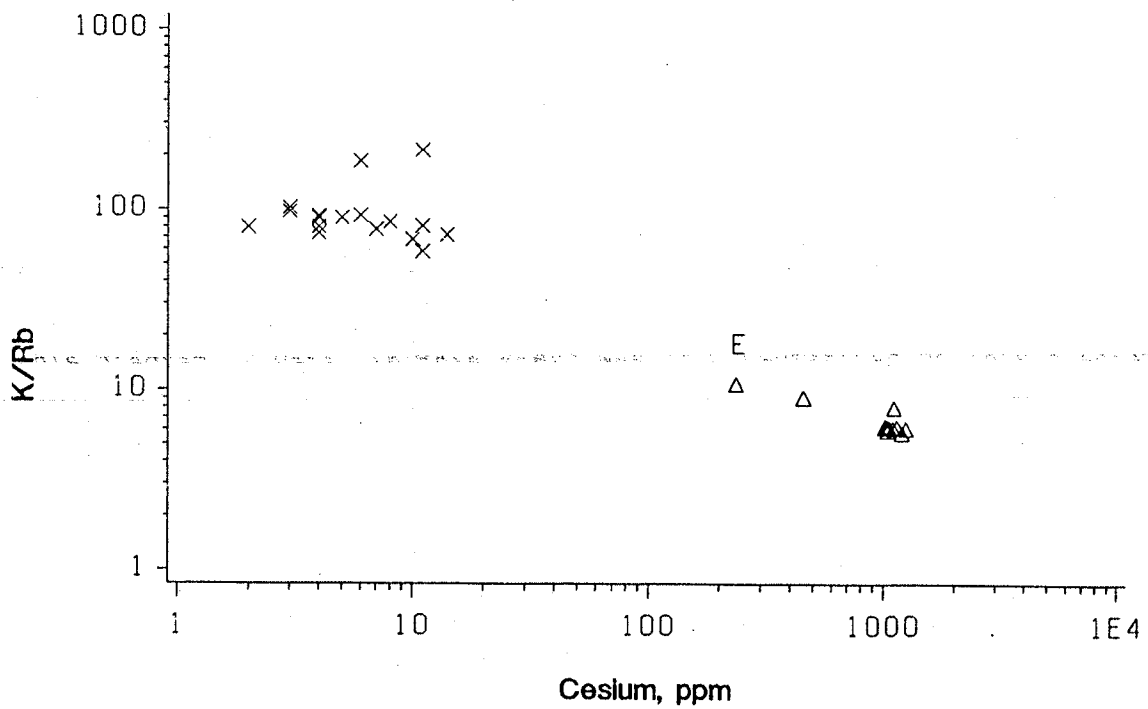
Figure 4.15 : K/Rb vs Cs for microcline from pegmatites at Red Sucker Lake, showing the extreme enrichment of Cs in the Western pegmatites. Symbols as in Figure 4.13.

(A)
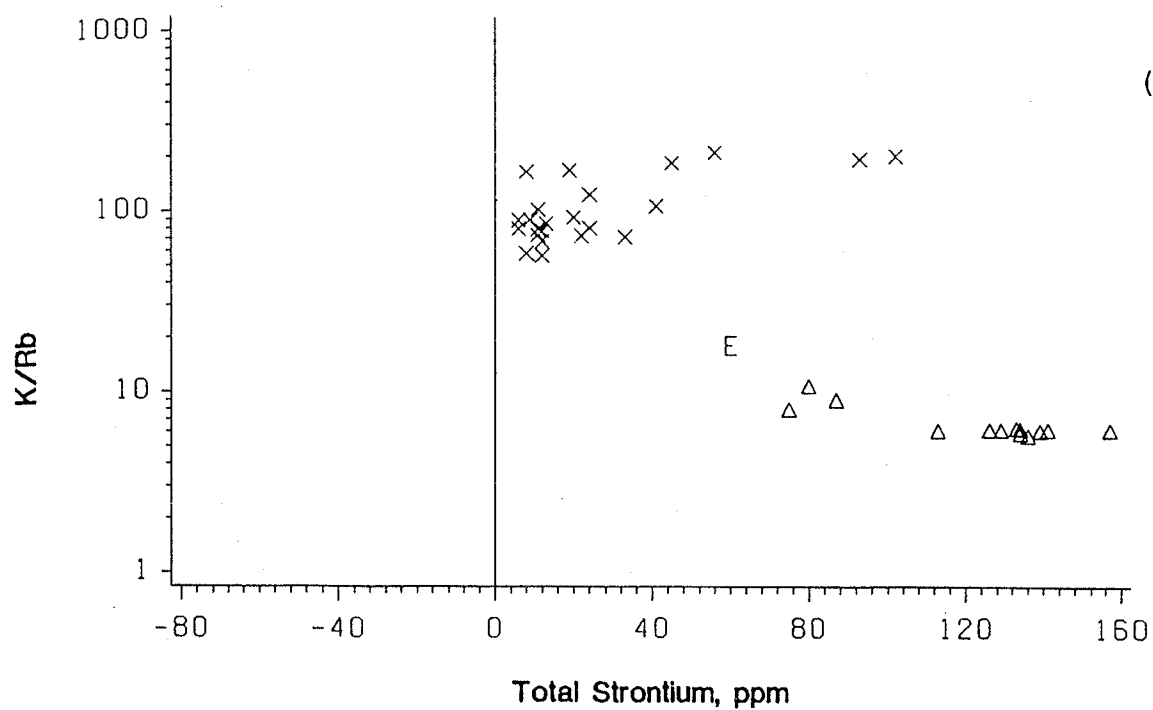
(B)
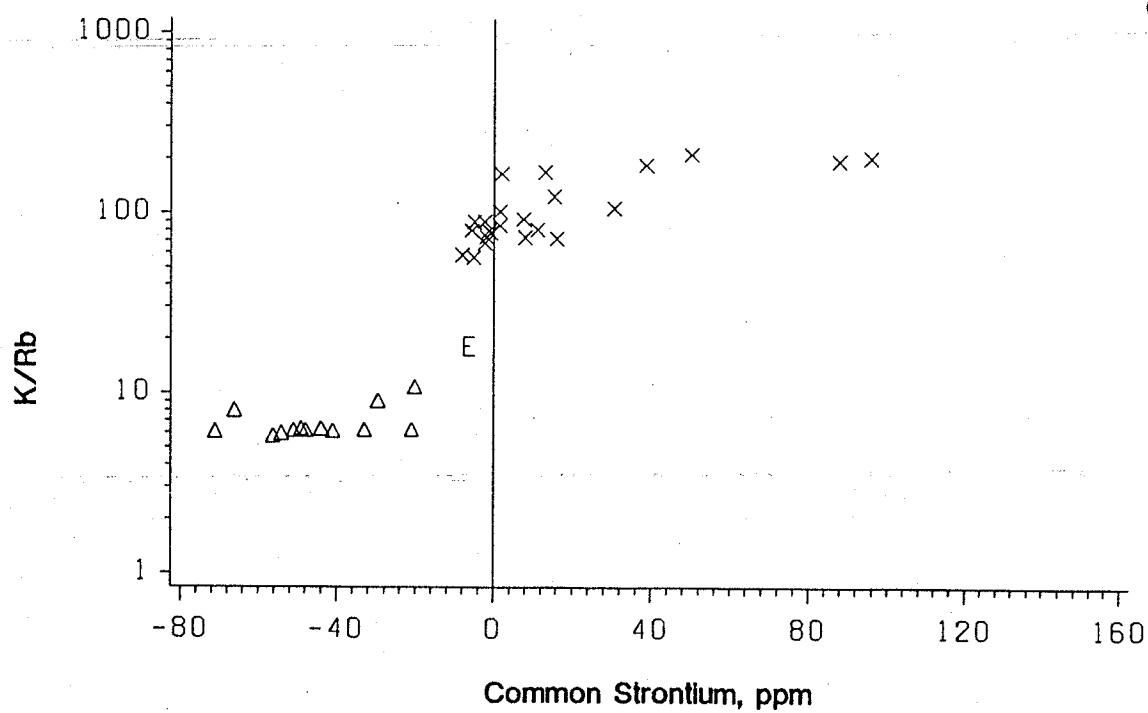
Figure 4.16 : K/Rb vs Sr for microcline from pegmatites at Red Sucker Lake. (A): Total Sr. (B): Common Sr (corrected for radiogenic ^{87}Sr). See text (p.27) for explanation of negative Sr values. Symbols as in Figure 4.13.
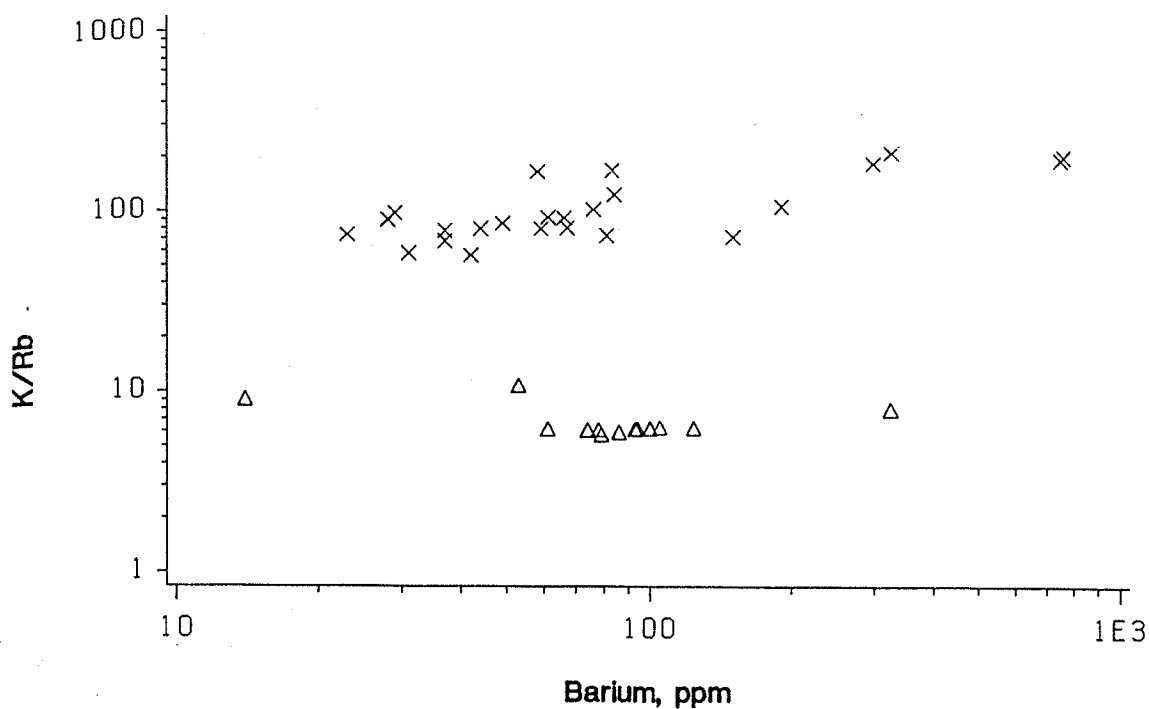
Figure 4.17 :   K/Rb vs Ba for microcline from pegmatites at Red Sucker
  Lake.   There is no correlation between K/Rb and within individual
  pegmatite series.   Ba content of a sample from the Eastern pegmatites
  is below detection (<10 ppm).   Symbols as in Figure 4.13.
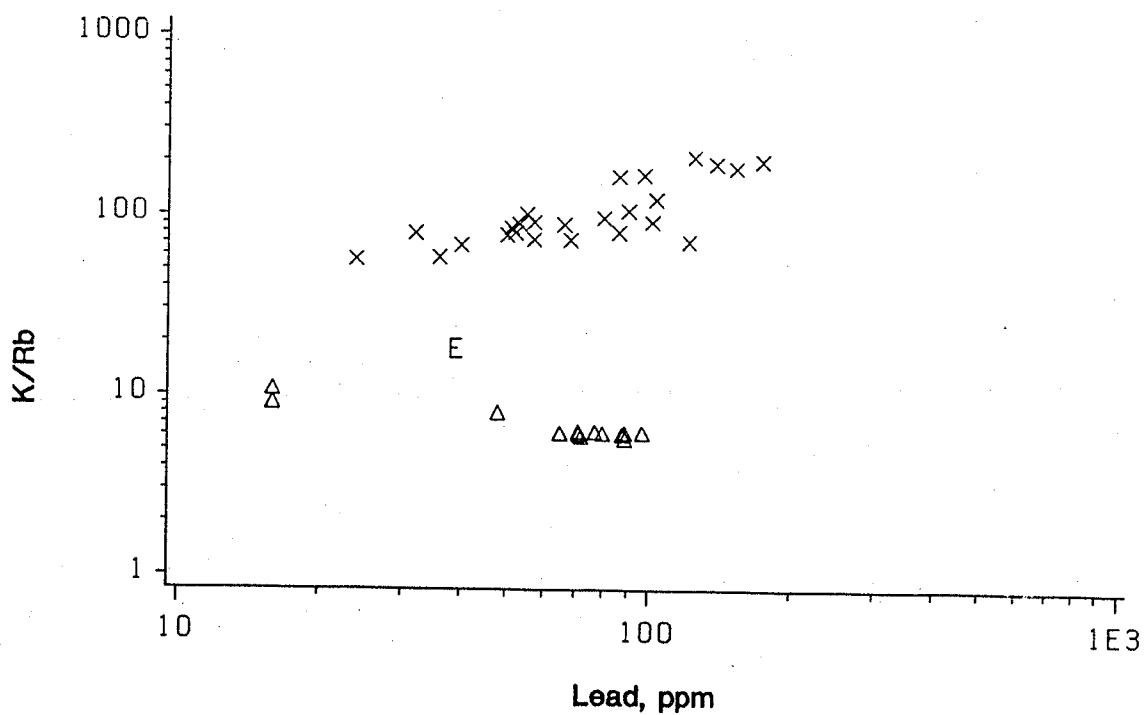
Figure 4.18 :   K/Rb vs Pb for microcline from pegmatites at Red Sucker
  Lake.   Pb decreases with decreasing K/Rb in the Northern pegmatites,
  and increases in the Western pegmatites.
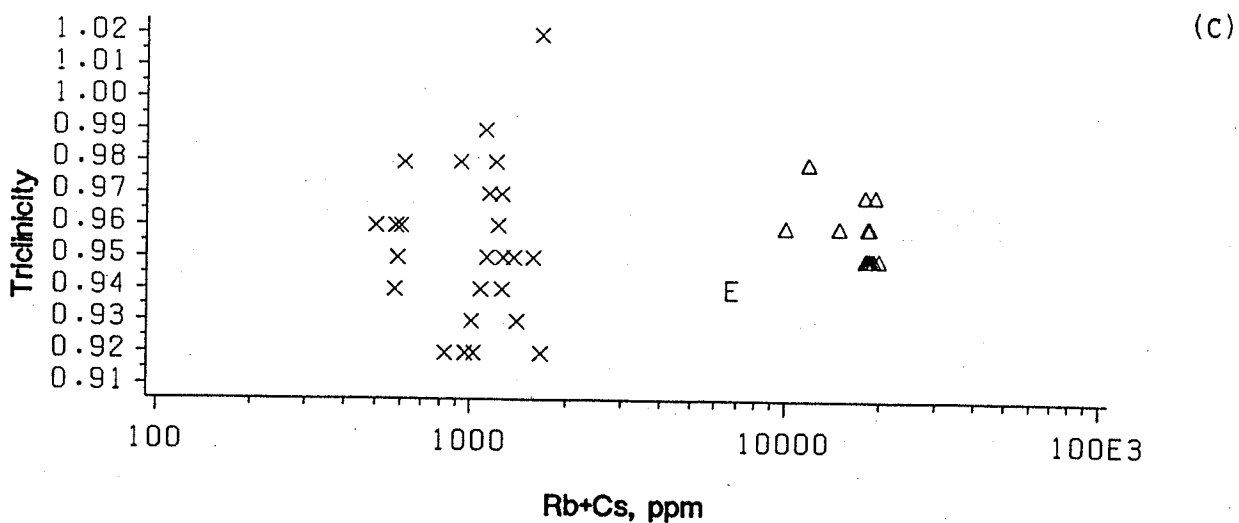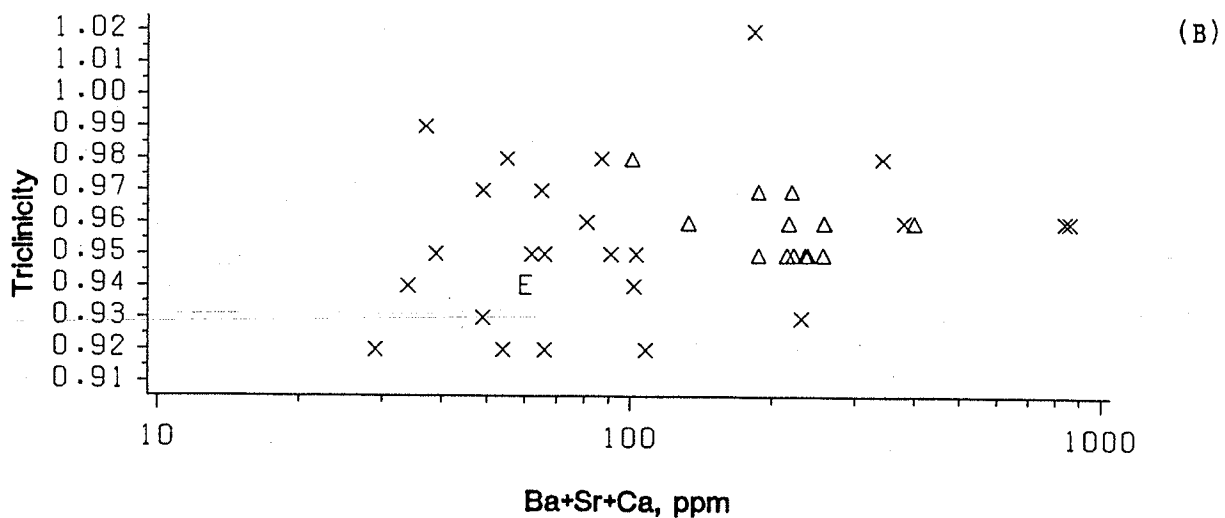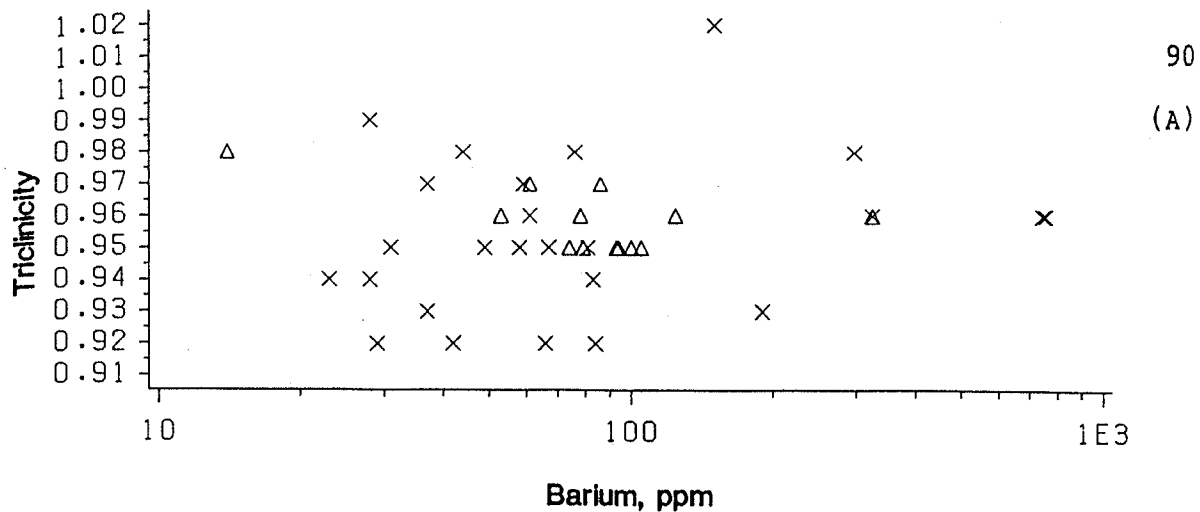
Figure 4.19 : Δ vs Ba (A), Δ vs Ca+Sr+Ba (B), and Δ vs Rb+Cs (C) for microcline from pegmatites at Red Sucker Lake. Western pegmatites show a smaller range of Δ than Northern pegmatites. Data show no correlation between Δ and concentrations of large cations. Symbols as in Figure 4.13.

Plagioclase

Plagioclase occurs as an interstitial phase in all of the pegmatites at
Red Sucker Lake.   It occurs as large blocky crystals only at location
SQ.   Table 4.3 lists the mol.% An contents of selected plagioclase sam-
ples from the pegmatites.   Samples range from calcic albites in the
Northern series to An_5 to An_7 in the Eastern and Western pegmatites.

Table 4.3:   Compositions of plagioclase in mol.% An from pegmatites at
   Red Sucker Lake.

Sample	Mol.% An	Series
EE-1	5	Eastern
GR-9	9	Northern
BF-9	10	"
LN-10	9 *	"
MN-30	7 *	"
TD-13	5	Western
SQ-19	7 *	"

* - Compositions determined by AAS analyses.
All other compositions determined optically.

Quartz

Quartz is abundant in all of the pegmatites, occurring as interstitial
grains, in quartz + blocky K-feldspar segregations, and as blebs and
graphic intergrowths in K-feldspar + quartz phenocrysts.   No distinct
quartz cores were observed in any of the pegmatites.

Muscovite

Muscovite occurs as a fine-grained interstitial phase in most of the pegmatites. It rarely forms books large enough for sampling. Partial analyses of ten book muscovite samples are given in Table 4.4. All of these muscovites are the $2M_1$ polytype. Relative to the Northern series, muscovites from pegmatite SQ are enriched in Fe, Mn, Li, Rb, Cs and Be. The SQ muscovites range up to 2.02 % Li_2O and are therefore lithian muscovites. The book muscovite at SQ occurs as thin plates, silver in colour, forming books 0.1 to 1 cm thick and 1 to 8 cm in maximum dimension. This is in contrast to the habit of lithian muscovite from southeastern Manitoba, which occurs in radial aggregates of lath- or wedge-shaped individuals, or in wedge-shaped curvilamellar crystals elongated parallel to $\underline{c}$ (Černý et al., 1981).

Table 4.4: Partial analyses of book muscovites from pegmatites at Red Sucker Lake.

Series	Northern					Western			
Sample	GR-2	LN-4	MN-3	NB-2	NT-3	SQ-3	SQ-9	SQ-22	SQ-25
wt.%:									
TiO_2	0.30	0.11	0.09	0.09	0.14	0.07	0.10	0.11	0.09
TFe_2O_3	1.63	1.97	1.72	1.56	1.65	2.63	2.67	2.73	2.67
MnO	0.01	0.01	0.01	0.01	0.01	0.94	0.92	0.98	0.95
MgO	0.42	0.44	0.34	0.35	0.33	1.48	1.56	1.10	1.53
CaO	0.04	0.18	0.01	0.02	0.01	0.02	0.03	0.03	0.02
Na_2O	0.69	0.83	0.73	0.73	0.68	0.46	0.53	0.46	0.39
K_2O	9.74	10.30	9.04	8.82	9.15	9.12	9.00	9.03	9.02
Li_2O	0.04	0.03	0.04	0.01	0.02	1.98	2.02	1.64	2.02
ppm:									
Rb	1870	454	599	938	950	19800	19400	20300	19300
Cs	80	15	16	27	24	1930	1810	1660	1950
Be	4	2	3	8	9	15	16	15	20
K/Rb	43.3	188	125	78.1	80.0	3.82	3.85	3.69	3.88
K/Cs	1000	5700	4700	2700	3200	39.3	41.2	45.2	38.4
Rb/Cs	23	30	37	35	40	10.3	10.7	12.2	9.90

TFe_2O_3 = total Fe calculated as Fe_2O_3

Fine-flaked lithian muscovite occurs at the SQ pegmatite in massive monomineralic aggregates of 0.5 to 3 mm pink to purple flakes (Figure 4.20). Analyses of three separate samples of this muscovite are given in Table 4.5. The fine-flaked lithian muscovite samples average 3.40 % Li_2O, 26,500 ppm Rb (2.90 % Rb_2O), and 4700 ppm Cs (0.50 % Cs_2O). The polytype is $2M_1$. It is distinctly enriched in rare alkali metals in relation to the platy muscovites from the same dike. This enrichment is similar to that of the fine-flaked pale pink to purple micas that occur in southeastern Manitoba in relation to the radial aggregates of lithian muscovite (Černý et al., 1981). The fine-flaked lithian muscovites from Red Sucker Lake have Li_2O contents in the lower range exhibited by similar micas from southeastern Manitoba.

Figure 4.20: Massive aggregate of fine-flaked lithian muscovite in SQ pegmatite at Red Sucker Lake. Pencil is 14 cm long.

Table 4.5: Partial analyses of fine-flaked lithian muscovite from pegmatite SQ, Red Sucker Lake.

Sample	SQ-5	SQ-10	SQ-80
wt.%:			
TiO_2	0.07	0.10	<0.01
TFe_2O_3	0.21	0.07	0.06
MnO	1.55	0.95	0.98
MgO	<0.01	<0.01	<0.01
CaO	0.02	0.09	0.01
Na_2O	0.27	0.35	0.27
K_2O	9.07	9.23	9.08
Li_2O	3.10	3.66	3.44
ppm:			
Rb	26000	27800	25700
Cs	4520	5180	4420
Be	11	14	10
K/Rb	2.90	2.76	2.65
K/Cs	16.7	14.8	15.3
Rb/Cs	5.75	5.37	3.76

TFe_2O_3 = total Fe calculated as Fe_2O_3

Biotite

Primary biotite was observed only in the Northern pegmatites. It occurs as interstitial flakes and rarely as large books, as at pegmatite DJ. Fine-flaked exomorphic biotite occurs at pegmatites BR, LN, WD, SQ and TD.   Partial chemical analyses of exomorphic biotite are given in Table 4.6.   These biotites are not overly enriched in rare alkali metals except for the sample from pegmatite TD which contains 2.38 wt.% Rb_2O (21,800 ppm Rb),   0.19 % Cs_2O (1760 ppm Cs), and 1.72 % Li_2O (7990 ppm Li). In comparison, exomorphic biotite from southeastern Manitoba ranges up to 1.87 % Rb_2O and 0.66 % Cs_2O (Černý et al., 1981).   Exomorphic biotite from the Tanco pegmatite ranges up to 4.61 % Rb_2O and 4.98 % Cs_2O (Morgan, 1986). The TD biotite occurs in a thin, 10 cm long monomineralic pod. The individual flakes are fresh looking, black in colour, and range from 0.2 to 3 mm in diameter.

Table 4.6: Partial chemical analyses of exomorphic biotite from pegmatites at Red Sucker Lake.

Series	Northern			Western	
Sample	BR-2	LN-2	WD-2	SQ-6	TD-9
wt.%:					
TiO_2	1.28	1.20	<0.01	0.61	1.19
TFe_2O_3	15.89	29.34	32.23	14.56	13.67
MnO	0.16	0.19	0.54	0.31	0.41
MgO	5.47	3.01	9.48	10.89	8.73
CaO	2.57	0.07	0.21	7.73	0.34
Na_2O	1.96	0.24	0.44	0.71	0.25
K_2O	5.19	8.37	8.10	3.33	7.86
Li_2O	0.06	0.27	0.06	0.36	1.72
ppm:					
Rb	1180	3100	120	2000	21800
Cs	48	61	<10	753	1760
Be	3	2	<1	11	8
K/Rb	36.4	22.4	560	13.8	2.99
K/Cs	900	——	——	36.7	37.0
Rb/Cs	25	51	——	2.66	12.4

TFe_2O_3 = total Fe calculated as Fe_2O_3

Beryl

Beryl was found only at the BL pegmatite. A beryl crystal from a hand sample collected in 1980 by P. Černý was analyzed, and a partial analysis is given in Table 4.7. This beryl is depleted in rare alkali metals compared to beryl from southeastern Manitoba (Černý et al., 1981). The sample is transparent, and pale green in colour. Crystals in the hand sample range up to 6 mm in diameter and are subhedral to euhedral.

Table 4.7: Partial chemical analysis of one beryl sample from the BL
pegmatite at Red Sucker Lake.

Sample:		BL-3		
wt.%			ppm	
TFe_2O_3	0.23	Li		2010
MnO	0.01	Rb		240
CaO	0.02	Cs		1100
Na_2O	0.92	Tl		<10
K_2O	0.06			

TFe_2O_3 = total Fe calculated as Fe_2O_3

Garnet

Garnet occurs at locations EE, TD, and in most of the Northern pegma-
tites.   The garnet crystals range up to 3 mm in diameter, are euhedral,
equant, and reddish brown to purple to black in colour.   Garnet at peg-
matite TD is distinguished by its orange colour.

All of these garnet samples are almandine-spessartines in composi-
tion; spessartines occur at pegmatites CY and TD and have MnO/(MnO+FeO)
values of 66 and 71 respectively.   Analyses of 26 garnet samples from
the TD and Northern series pegmatites are given in Appendix B and plot-
ted on geochemical diagrams in Figure 4.21. Except for two data points,
Ca increases with decreasing Fe/Mn ratio.   In contrast, Mg decreases
with increasing Mn content.   In both diagrams most of the Northern peg-
matite garnets plot near the FeO apices, and are distinctly separate
from the TD pegmatite.

(A)
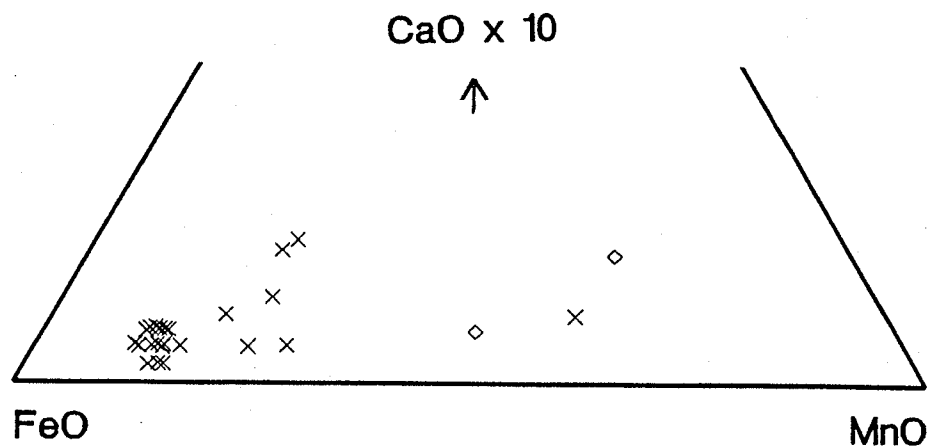
(B)
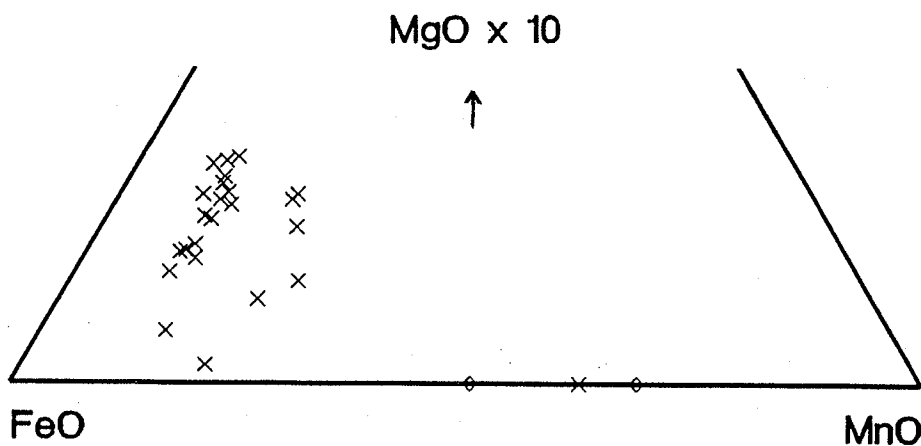
Figure 4.21: (A): FeO – MnO – CaOx10 diagram for garnet from pegmatites at Red Sucker Lake. Data points show weak negative correlation between Ca and Fe/Mn. (B): FeO – MnO – MgOx10 diagram for garnet from pegmatites at Red Sucker Lake. Symbols as in Figure 4.13.

Spodumene

Spodumene occurs at pegmatite SQ as spodumene + quartz intergrowth, pseudomorphic after petalite. Aggregates of parallel spodumene fibers (1 to 3 mm thick and 0.5 to 2 cm long) are interspersed with granular quartz in these pseudomorphs. It occurs in pods adjacent to massive fine-flaked lithian muscovite (Figure 4.22). A sample of separated spodumene contains 0.06 % Fe as Fe_2O_3, 0.02 % MnO, 0.09 % Na_2O and 0.16 % K_2O. This is comparable to spodumene from the Tanco pegmatite (London and Burt, 1982), but is Fe-poor compared to spodumene from southeastern Manitoba (Černý et al., 1981).

Figure 4.22: Spodumene + quartz intergrowth (squi), pseudomorphic after petalite, at pegmatite SQ. The squi is adjacent to a massive aggregate of fine-flaked lithian muscovite.

Tourmaline

Tourmaline occurs in the Western pegmatites as the schorl, dravite and verdelite varieties. It has not been observed in the Northern pegmatites. Schorl occurs as 1 to 5 mm grains at pegmatites TD and PK. At PK it occurs as 0.1 to 1 mm grains in the outer zone, and as 3 to 5 mm grains in the central zone. Dravite was identified by x-ray powder diffraction from a hand sample of the TD pegmatite. It occurs as 1 to 2 mm brownish transparent grains. Verdelite occurs as 2 to 4 mm grains in the central zone of the PK pegmatite, and as 0.5 to 5 cm long prisms intergrown with feldspar in the SQ pegmatite, near its northern contact.

Apatite

Apatite occurs as 0.2 to 1.5 mm grains at pegmatites BL, TD, NB and WD. Microprobe analyses of three apatite samples are given in Table 4.8. Significant Mn was detected in both samples from pegmatite TD, averaging 3.1% MnO which is comparable to values determined in apatites from the petalite-bearing pegmatitic leucogranites. Cl was detected only in the WD sample. No other subordinate elements were detected in these apatites.

Table 4.8: Microprobe analyses of apatites from pegmatites at Red Sucker Lake.

Sample	FeO	MnO	CaO	P_2O_5	Cl
TD-3	<0.1	3.0	49.5	28.9	<0.1
TD-11	<0.1	3.2	53.5	35.3	<0.1
WD-4	0.2	0.8	55.7	34.9	0.1

Microlite

One 0.5 by 3 mm grain of microlite was collected from the central zone of the PK pegmatite. It is associated with quartz and feldspar, and is dark brown in colour. The crystal is translucent and fairly fresh in appearance. A preliminary microprobe analysis of this grain is given in Table 4.9. Further examination and refinement is required, as $\Sigma(Ta+Nb+Ti) = 3.36$ is much below the expected value of 4.00. This stibio(?)microlite is the only Sb-bearing mineral found to date in the Red Sucker Lake area.

Table 4.9: Microprobe analysis of microlite from central zone of PK pegmatite, Red Sucker Lake.

Oxide	Wt.%	Cations per 13 oxygen atoms	
Ta_2O_5	48.8	Ta^{5+}	2.28
Nb_2O_5	8.4	Nb^{5+}	0.65
TiO_2	3.3	Ti^{4+}	0.43
Sb_2O_3	13.6	Sb^{3+}	0.96
SnO	8.0	Sn^{2+}	0.61
CaO	15.0	Ca^{2+}	2.76
Totals	97.1		7.70
Ta/Ta+Nb	0.778		

Cassiterite

Cassiterite occurs as 0.5 to 2 mm grains in the TD dike. The grains are subhedral to euhedral, equant to bladed in shape. Microprobe analyses of two grains are given in Table 4.10. As well as the Ta and Fe reported here, Sc (0.3 % Sc_2O_3) and Nb (0.1 % Nb_2O_5) were detected in partial analyses of two other cassiterite samples.

Table 4.10: Microprobe analyses of two cassiterite samples from pegmatite PK at Red Sucker Lake.

Sample	TDC-1	TDC-2
Wt.%		
Ta_2O_5	1.0	1.7
SnO_2	100.0	98.7
FeO	<0.1	0.5
Totals	101.0	100.9
Cations per 4 oxygens		
Ta^{5+}	0.01	0.02
Sn^{4+}	1.98	1.96
Fe^{2+}	——	0.02
Totals	1.99	2.00

Sulfides, sulfarsenides and arsenides

Arsenopyrite and löllingite are the most common sulfide / sulfarsenide phases present in the pegmatites at Red Sucker Lake. Arsenopyrite occurs as an accessory phase at pegmatites PK, TD, DJ, CY and GR. Löllingite occurs only in the Northern pegmatites, at NT, BF, DJ and CY. Other phases observed in the Northern pegmatites include molybdenite at pegmatite WD, and chalcopyrite, sphalerite and cobaltite at pegmatite SC which were detected by microprobe. No macroscopic grains of sphalerite or cobaltite were observed.

4.5   GEOCHEMISTRY

Whole-rock compositions of samples of three pegmatite dikes and one
aplite are given in Table 4.11.   The composition of sample TD-13 re-
flects the high content of albite, as well as the enrichment in cassi-
terite.

Average Li,   Rb ,   Cs,   K/Rb and Rb/Cs values for microcline, and
MnO/(MnO + FeO) ratios for garnet from the pegmatites are plotted on
geochemical diagrams in Figures 4.23 to 4.28.   The feldspar diagrams in
particular illustrate the extreme levels of geochemical fractionation
attained by the Western pegmatites,   in contrast to the geochemically
primitive nature of the Northern pegmatites.   The only significant geo-
chemical trend observed within the Northern pegmatites is a slight in-
crease in Li-content of microcline toward the eastern limit of the peg-
matite occurrences (Figure 4.23).   All of these K-feldspar diagrams
indicate that the Eastern pegmatites attain fractionation parameters
that are intermediate between those of the Western and Northern pegma-
tites.

Figures 4.23 to 4.27 show that the greatest levels of fractionation
attained by the pegmatites at Red Sucker Lake occur at the eastern and
especially the western limits of the pegmatite outcrops.   In contrast to
this, Figures 3.36 to 3.45 show that the reverse is true for the pegma-
titic granites; extreme fractionation occurs in the central parts of the
pegmatitic granite field, directly south of the proximal and geochemi-
cally barren Northern series pegmatites.

Table 4.11: Whole-rock analyses of pegmatites and one aplite sample (CY-06) from Red Sucker Lake.

	BF-09	CY-06	TD-13	EE-01			BF-09	CY-06	TD-13	EE-01
Wt. %:						ppm:				
SiO_2	77.13	75.92	68.97	74.65		Li	22	9	16	13
TiO_2	0.01	0.01	<0.01	<0.01		Rb	3	59	18	697
Al_2O_3	14.07	13.98	17.93	14.14		Cs	<1	1	6	20
Fe_2O_3	0.16	0.18	0.01	0.65		Be	5	1	4	46
FeO	0.53	0.95	0.07	0.22		Sr	41	35	12	17
MnO	0.06	0.23	0.02	0.28		Ba	72	68	28	51
MgO	0.09	0.16	0.08	0.00		Zn	22	27	5	24
CaO	1.10	0.99	0.77	0.15		Ga	54	56	101	65
Na_2O	4.85	5.96	9.81	5.28		U	4	9	5	8
K_2O	0.21	1.12	0.23	1.84		Th	7	11	6	9
P_2O_5	0.03	0.00	0.25	0.06		Zr	<10	26	106	22
CO_2	0.10	0.08	0.12	0.08		Hf	2	1	16	3
H_2O^+	0.10	0.10	0.10	0.05		Nb	30	44	35	93
S	0.01	<0.01	<0.01	0.02		Ta	7	13	110	162
F	<0.01	0.01	0.02	0.02		Sn	<1	7	4626	25
						Y	35	54	<10	<10
Σ:	98.45	99.69	98.37	97.42						

	BF-09	CY-06	TD-13	EE-01
A/CNK	3.75	2.69	2.72	2.83
K/Rb	581	158	110	22
K/Cs	——	9300	300	764
Rb/Cs	——	59	3	35
Ba/Rb	24	1.15	2.0	0.073
Al/Ga	1380	1320	940	1150
Nb/Ta	4	3.4	0.32	0.57

A/CNK = Al_2O_3 / (CaO + Na_2O + K_2O)
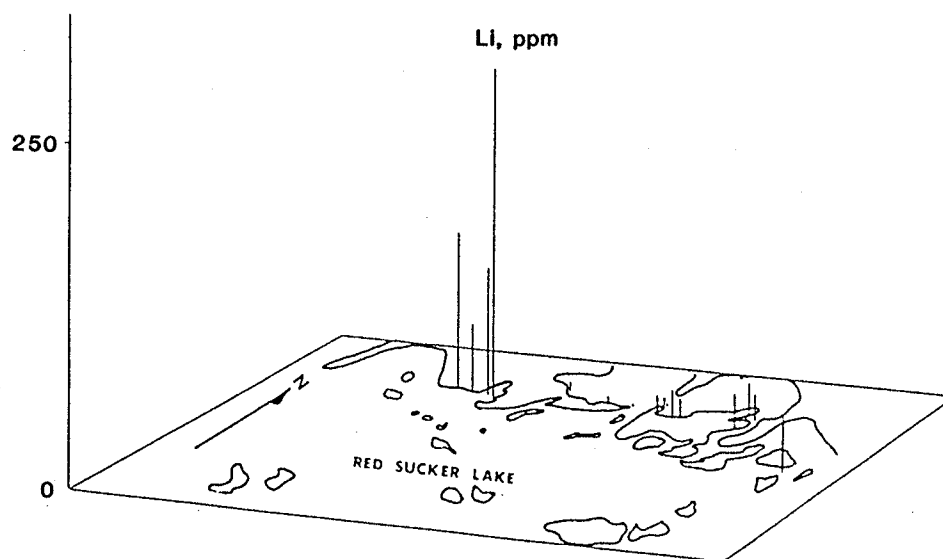
Figure 4.23: Li content of microcline from pegmatites at Red Sucker Lake. Western and Eastern pegmatites are highly fractionated with respect to Northern series. Li content increases toward the eastern extent of the Northern pegmatites.
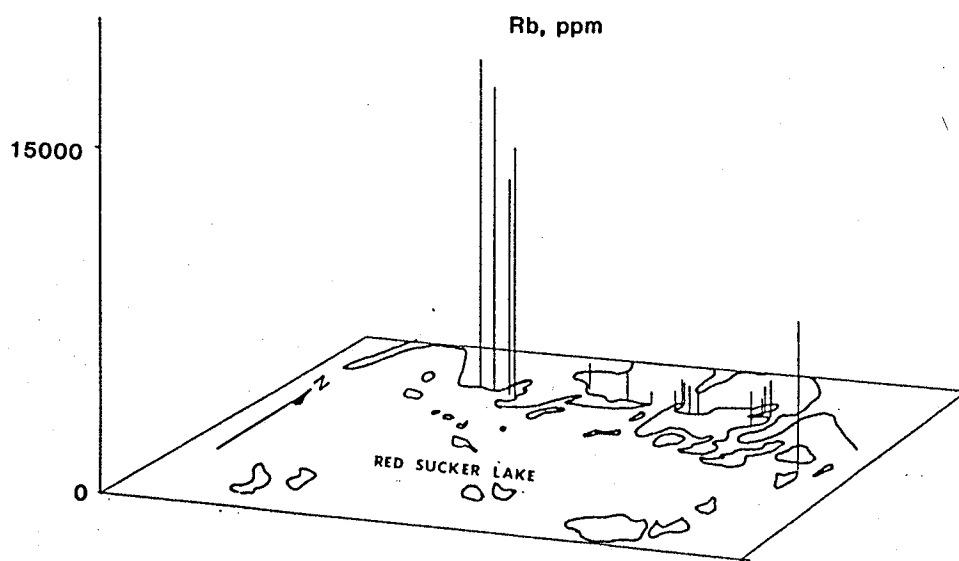
Figure 4.24: Rb content of microcline from pegmatites at Red Sucker Lake. Western pegmatites are extremely enriched, Eastern pegmatites moderately enriched in Rb in relation to the Northern pegmatites.
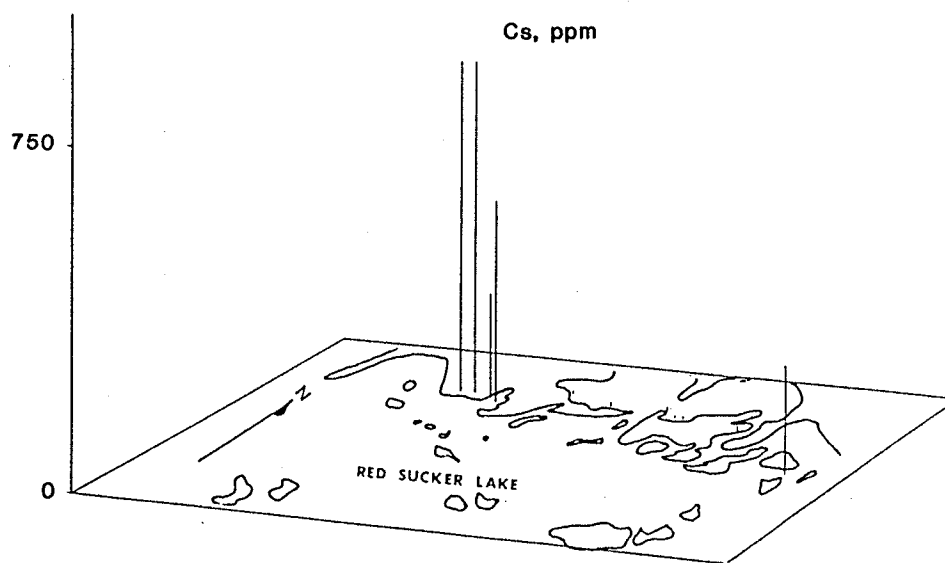
Figure 4.25: Cs content of microcline from pegmatites at Red Sucker Lake. Note the extreme contrast in Cs between the Western and Northern pegmatites.
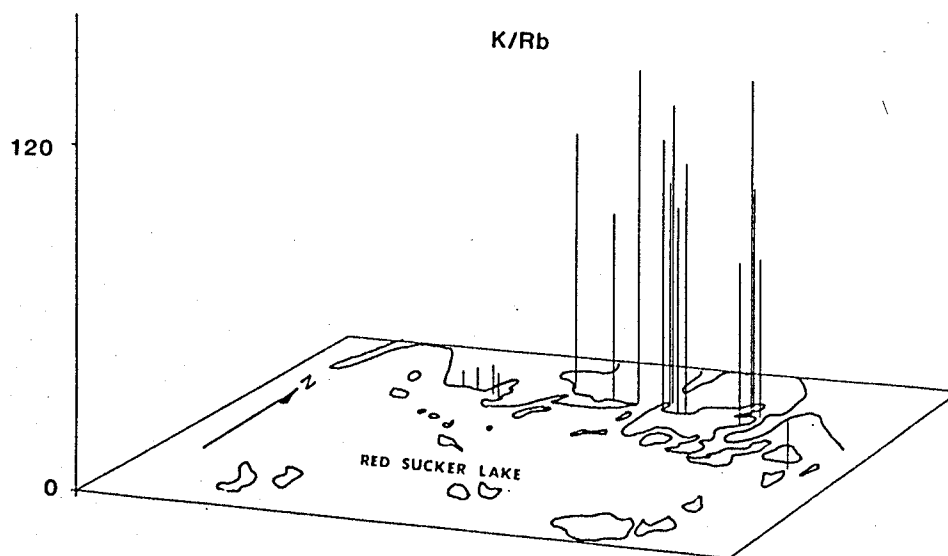
Figure 4.26: K/Rb ratios of microcline from pegmatites at Red Sucker Lake. Western and Eastern pegmatites display advanced levels of K/Rb fractionation.
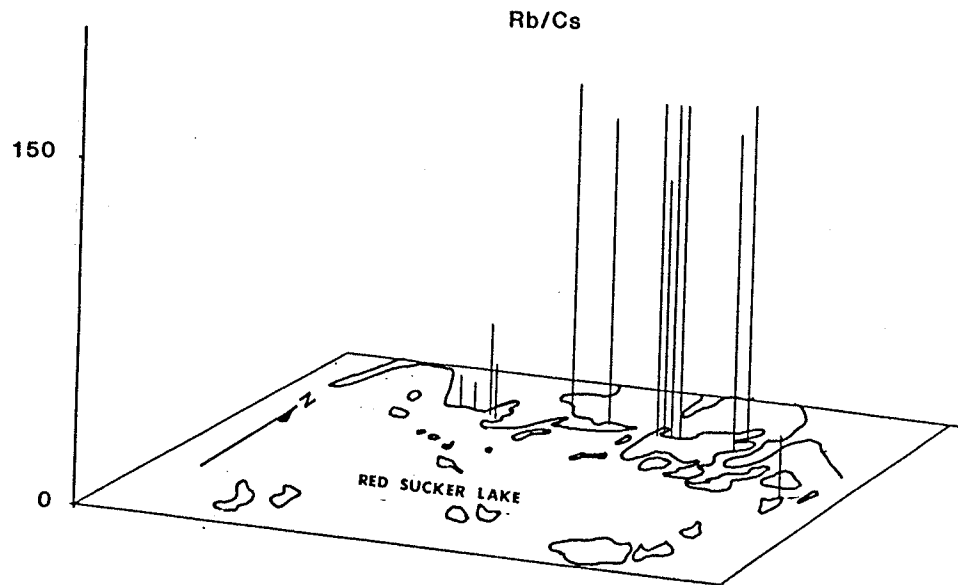
Figure 4.27: Rb/Cs ratios of microcline from pegmatites at Red Sucker Lake. Western and Eastern pegmatites display advanced levels of Rb/Cs fractionation.
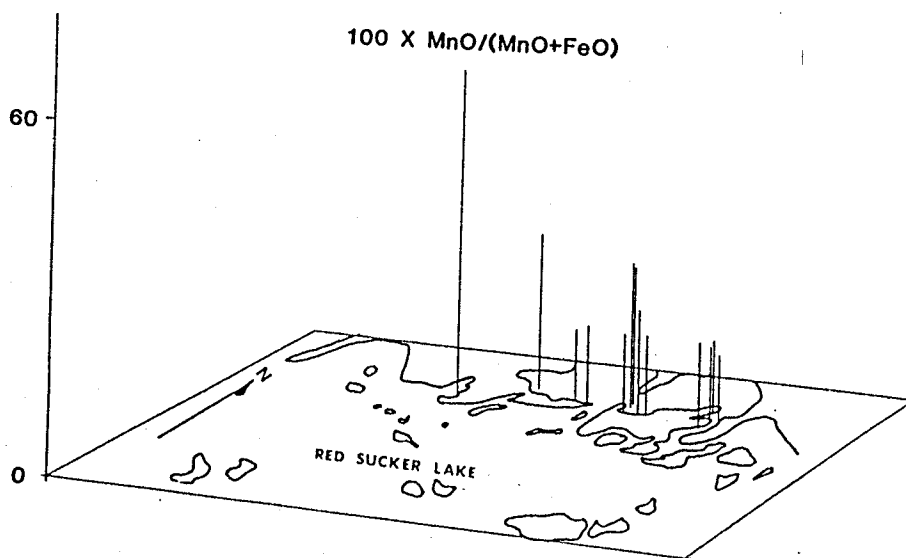
Figure 4.28: MnO/(MnO + FeO) ratios of garnet from pegmatites at Red Sucker Lake.

Chapter V

THE GODS RIVER PEGMATITE

5.1 LOCATION

The spodumene-rich Gods River pegmatite outcrops about 100 m inland from the NE shore of Johnson Bay, Gods Lake. It is situated about 6 km WNW of the town of Gods River, Manitoba (Figure 5.1).

5.2 INTRUSIVE RELATIONSHIPS

The Gods River pegmatite dike intrudes sheared metabasalts; the exposure is 3 to 10 m wide and 50 m in length. Diamond drilling by INCO in 1953 showed that the dike extends beneath the glacial drift for about 2 km eastward of the exposure, and dips steeply to the north to a depth of at least 250 m (Southard, 1977; see also Manitoba Department of Energy and Mines, Mineral Resources Division Open File #92618). The dike is discordant to the schistosity of the metabasalts which strike SE and dip 60° NE.

94°16'
54°52'
94°00'
54°52'

Gods River Pegmatite

Johnson

Bay

Gods River

GODS

LAKE

54°47'
94°16'
54°47'
94°00'
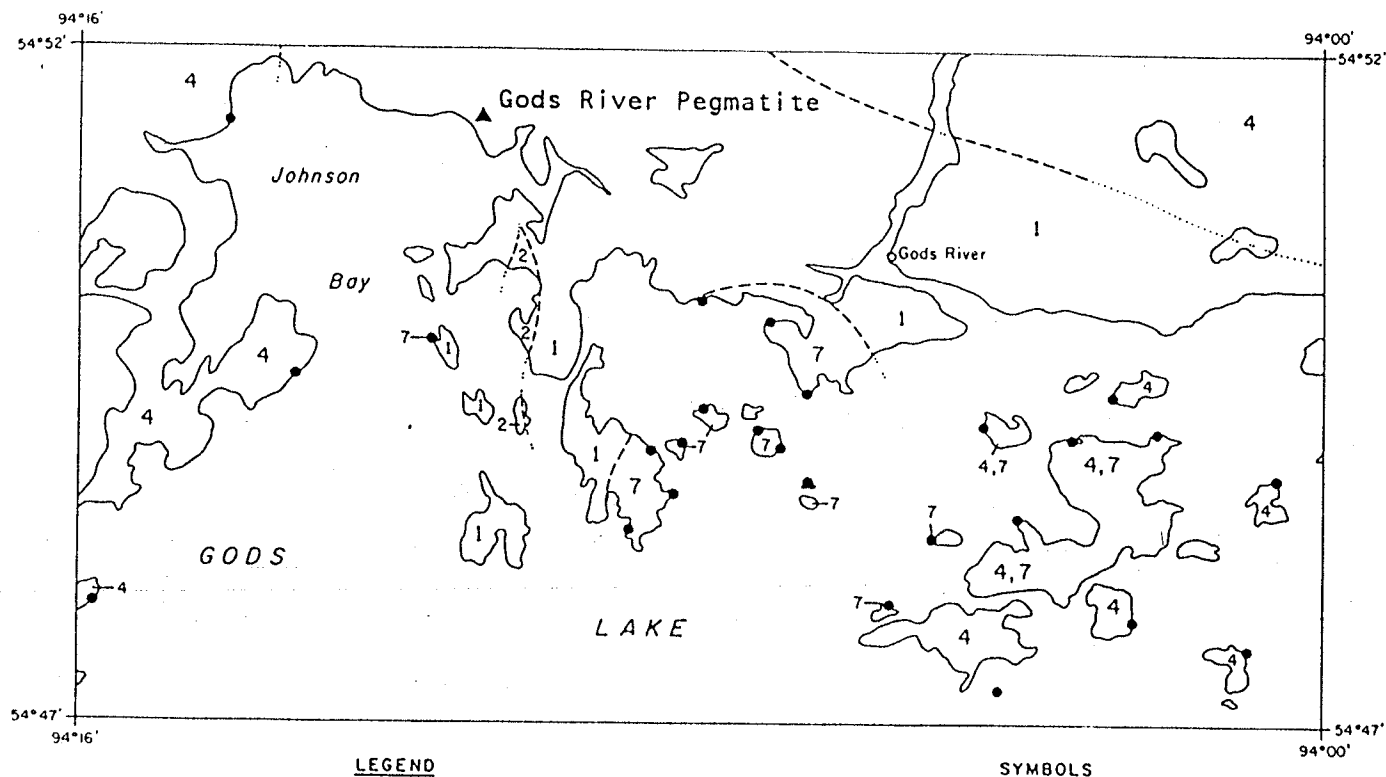
LEGEND

BAYLY LAKE COMPLEX

7   Metamorphosed granodiorite, minor granite
    and tonalite

4   Metamorphosed tonalite, minor granodiorite,
    gabbro, pegmatite and aplite

HAYES RIVER GROUP

2   Metamorphosed felsic to intermediate volcanic
    .fragmental rocks

1   Metamorphosed mafic volcanic and derived
    metasedimentary rocks

SYMBOLS

•   Plutonic rock sample locations

▲   Spodumene-bearing pegmatite

    Geological boundary (approx-
    imate, assumed, underwater)

0   1   2   3   4   5 km

Figure 5.1: Geological map of Gods Lake area showing the spodumene-
bearing Gods River pegmatite and sampling locations of plutonic
rocks. After Chackowsky and Černý, 1985.

5.3   INTERNAL STRUCTURE

The Gods River pegmatite is characterized by textural and mineralogical homogeneity.   The bladed spodumene crystals range from 2 to 10 mm in length and are strongly aligned, striking 150° to 160°.   This alignment is approximately concordant to the strike of the schistosity of the metabasalts, and oblique to the E-W strike of the pegmatite dike.   The alignment of the spodumene grains and interstitial white muscovite imparts a pervasive foliation to the pegmatite (Figure 5.2).   In places, columnar K-feldspar up to 1 m in length occurs parallel to the foliation of the pegmatite (Figure 5.3).

The spodumene grains appear somewhat altered in thin section, but undeformed.   In contrast, most plagioclase grains have deformation features such as kinks and undulatory extinction (Figure 5.4).

Younger, deep purple muscovite occurs locally in veins that are oblique to the foliation of the pegmatite (Figure 5.5).   These veins are oriented in an E-W direction which is approximately concordant to the strike of numerous narrow mylonitized shear zones that sporadically offset and somewhat deform the foliation of the pegmatite (Figure 5.6).
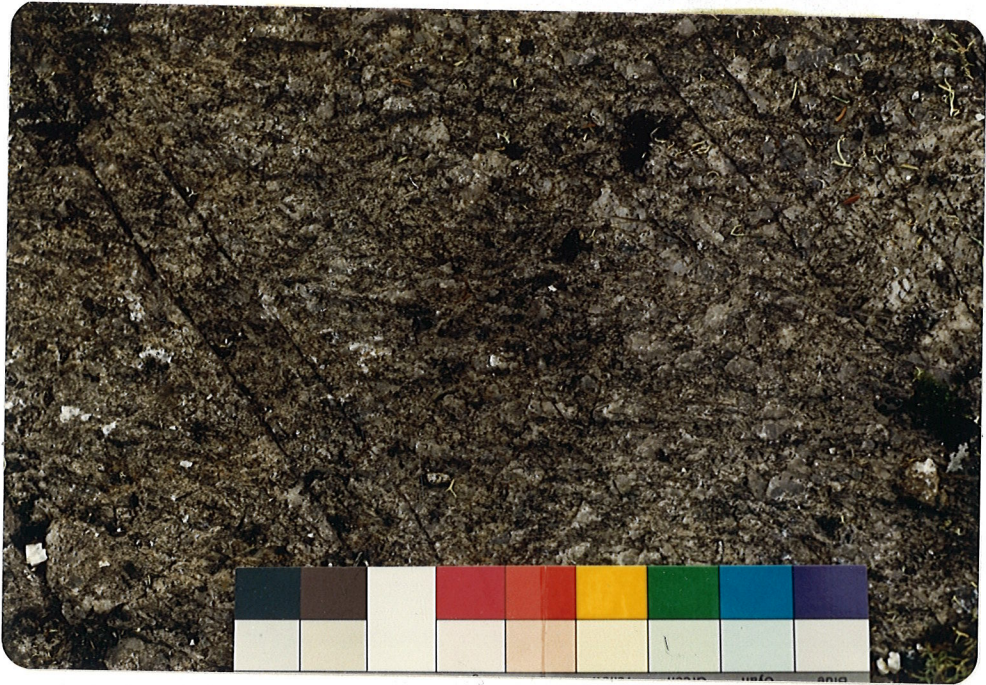
Figure 5.2: Pervasive E-W foliation (horizontal in the photograph) caused by oriented spodumene grains (pale grey). Late fractures obliquely cross-cut the foliation. Scale bar is 18 cm long.

Figure 5.3: Elongated K-feldspar parallel to the pervasive E-W foliation of the pegmatite (horizontal in the photo). Scale bar is 18 cm in length.
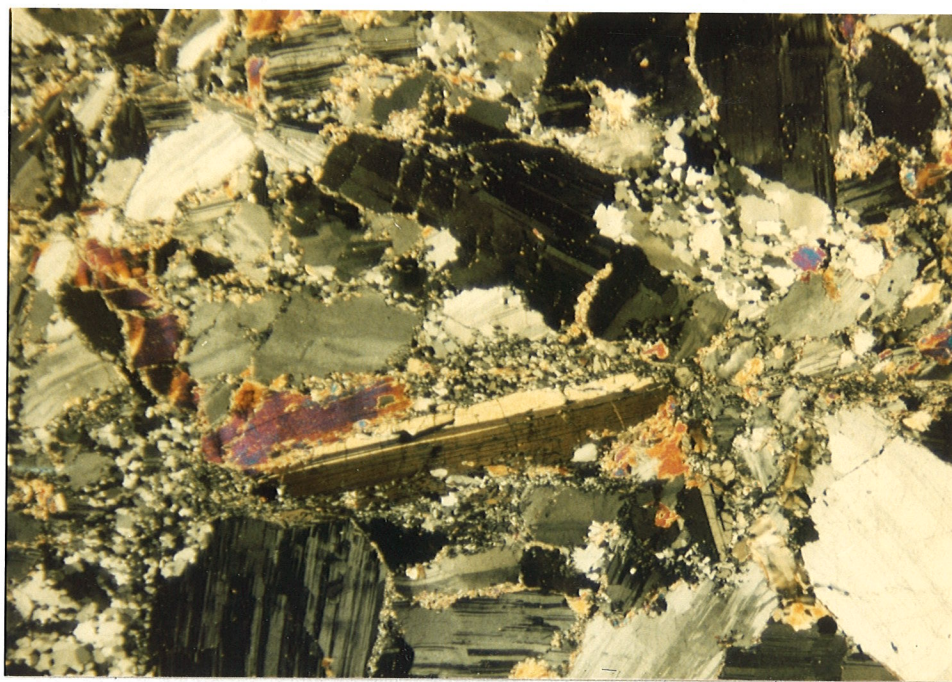
Figure 5.4: Photomicrograph showing altered, relatively undeformed, 4 mm long spodumene grain (twinned) and deformed plagioclase exhibiting undulatory extinction), suggesting that spodumene has undergone recrystallization after or during deformation, or that the deformation was not absorbed by the spodumene crystals.
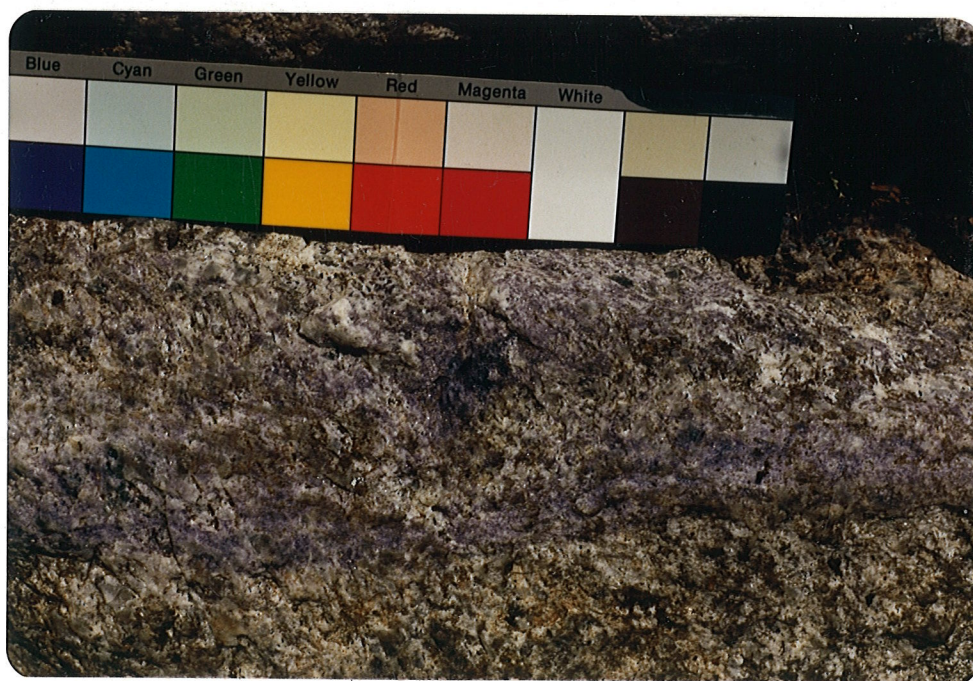
Figure 5.5: Late quartzo-feldspathic veins bearing deep purple muscovite in the eastern part of the pegmatite exposure. Scale bar is 18 cm long.
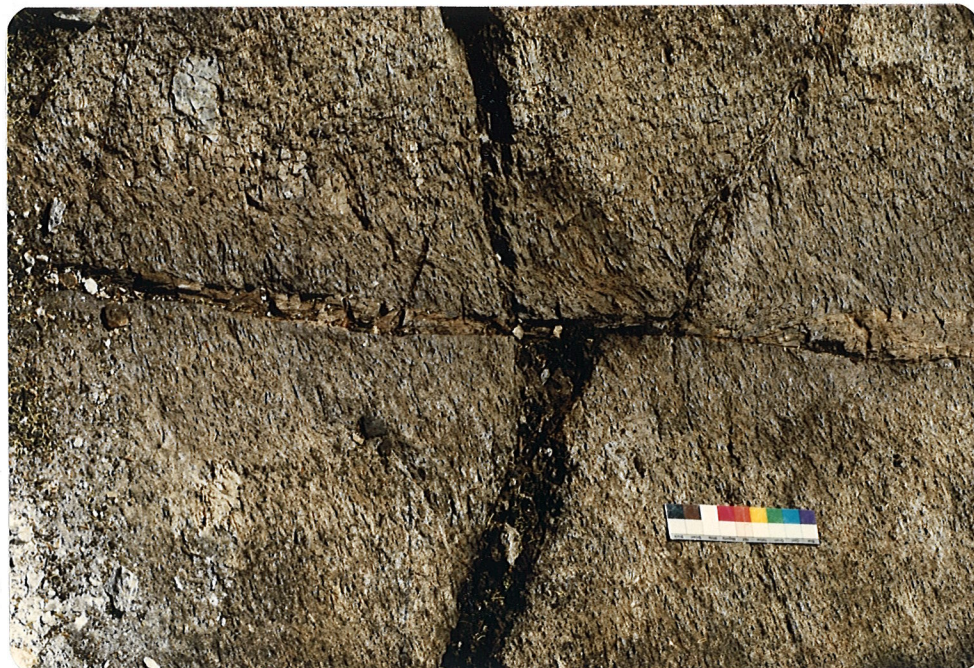
Figure 5.6: Mylonitized shear zone (horizontal in the photo) that off-
sets and slightly deforms the foliation of the pegmatite (vertical in
the photo). Scale bar is 18 cm in length.

5.4 PARAGENESIS AND MINERALOGY

The pegmatite dike is composed of abundant spodumene, quartz and white
muscovite, with subordinate K-feldspar and plagioclase. K-feldspar oc-
curs as blocky megacrysts 1 to 5 cm in size, and in places forms long
columnar rods (Figure 5.3). Accessory deep purple muscovite occurs lo-
cally in late cross-cutting veins. Heavy liquid separation of crushed
whole-rock samples in the 0.25 to 1 mm grain-size range failed to reveal
any other accessory mineral phases.

K-feldspar

Blocky K-feldspar is abundant in the pegmatite. Crystals range from 0.5 to 6 cm in size and are white to grey in colour. They are equant to columnar in shape, and are anhedral.

Thirteen samples were selected for x-ray powder diffraction and partial chemical analysis. All of these samples are maximum microcline with Δ values ranging from 0.90 to 0.95. 4 samples were chosen for unit cell refinements on the basis of their Δ values and rare alkali contents. The refined parameters are given in Table 5.1 along with selected chemical parameters, and plotted in Figures 5.7 to 5.10. All of the data plot near the maximum microcline apices in the diagrams. There are no correlations between chemistry and structural state in these microcline samples. Partial chemical analyses and Δ values of these samples are given in Table 5.2. Various compositional parameters are plotted in Figures 5.11 to 5.16. These microcline samples display extreme levels of fractionation in terms of Li, Rb and Cs contents and K/Rb and Rb/Cs ratios.

The microcline samples range from Or_{85} to Or_{77}. Contents of rare alkali metals range from 32 to 155 ppm Li, 11800 to 18700 ppm Rb, and 522 to 1350 ppm Cs indicating advanced levels of fractionation. The K/Rb ratios range from 5.4 to 8.8, and Rb/Cs from 13.5 to 26.6. These values are comparable to the rare alkali contents of microcline from the most fractionated pegmatitic granites and pegmatites at Red Sucker Lake, as well as those from the Tanco pegmatite. The diagrams in Figures 5.11 to 5.13 show fractionation trends of increasing Rb and Cs with decreasing K/Rb. Li contents do not show any significant correlation with K/Rb ratios.

Total Sr ranges from 106 to 151 ppm and shows a very slight increase with decreasing K/Rb (Figure 5.14). The data corrected for radiogenic ^{87}Sr show a reverse trend, with Sr decreasing with decreasing K/Rb, as would be expected during igneous fractionation.

The Ba content of the microcline samples ranges from 11 to 31 ppm. Pb ranges from 84 to 160 ppm. Neither element shows any significant correlation with K/Rb ratios.

Triclinicities of the microcline samples are plotted against various geochemical parameters in Figure 5.17. These diagrams show no correlation between Δ and concentrations of large cations, which is also the case for the microcline samples from Red Sucker Lake.

Table 5.1: Unit cell parameters and selected geochemical parameters of microcline from the Gods River pegmatite.

Sample:	7I-20	7I-26	7I-30	7I-34
a	8.567(10)	8.592(6)	8.576(5)	8.598(4)
b	12.946(13)	12.997(8)	12.956(7)	12.968(4)
c	7.246(4)	7.226(2)	7.216(6)	7.228(1)
α	90.77(11)	90.73(7)	90.64(4)	90.67(3)
ß	115.95(8)	115.96(5)	115.96(5)	115.99(3)
γ	87.60(9)	87.66(5)	87.64(4)	87.69(3)
vol.	721.0(8)	723.1(5)	720.3(5)	723.8(3)
a*	.12975(14)	.12996(8)	.12979(5)	.12949(5)
b*	.07731(8)	.0771953)	.07725(7)	.07718(3)
c*	.15390(12)	.15393(7)	.15413(6)	.15391(4)
α*	90.31(10)	90.33(7)	90.44(5)	90.38(3)
ß*	64.06(8)	64.04(5)	64.05(4)	64.01(3)
γ*	92.30(6)	92.25(5)	92.32(5)	92.25(3)
Ba	17	23	17	14
Ba+Sr+Ca	220	250	290	290
Rb+Cs	17200	16500	13100	20000

a, b and c in Å; vol. in Å^3; a*, b* and c* in Å^{-1}. α, ß, γ, α*, ß* and γ* in degrees. All chemical data in ppm.
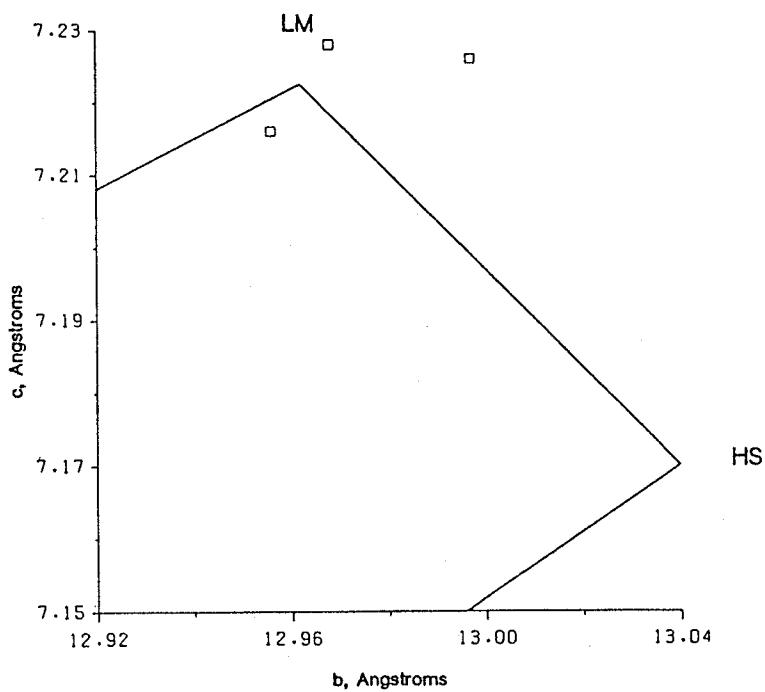
Figure 5.7 :   c vs b cell parameters for maximum microcline from the Gods River pegmatite. Modified after Kroll and Ribbe (1983).
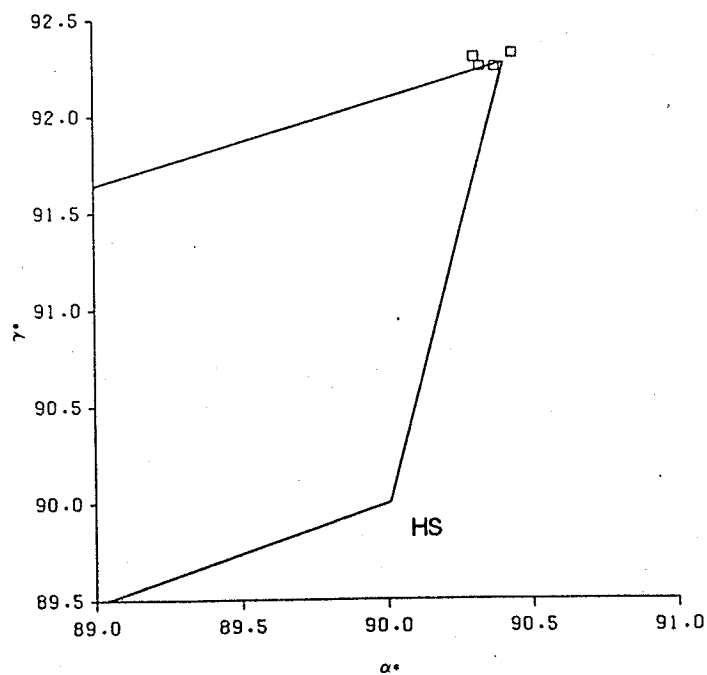
Figure 5.8 : γ* vs α* for maximum microcline from the Gods River pegmatite. Modified after Kroll and Ribbe (1983).
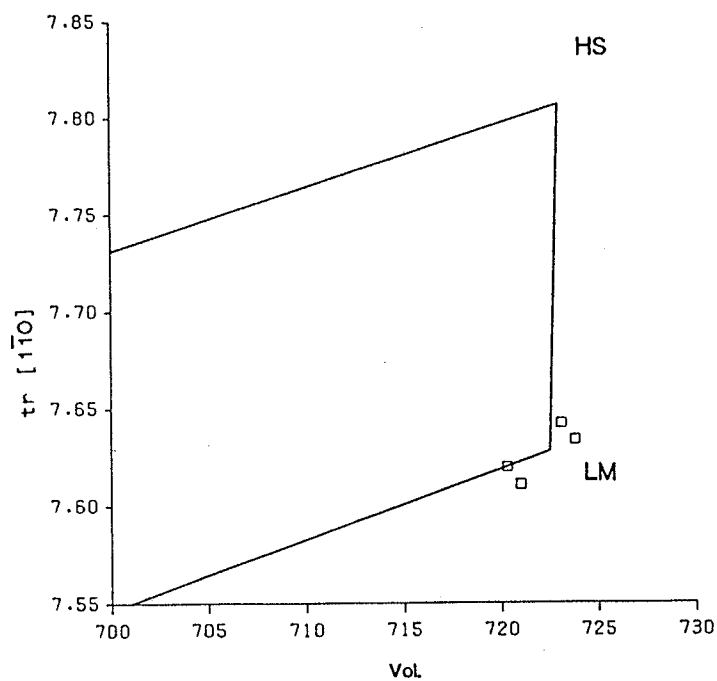
Figure 5.9 : tr[110] vs volume for maximum microcline from the Gods River pegmatite. Modified after Kroll and Ribbe (1983).
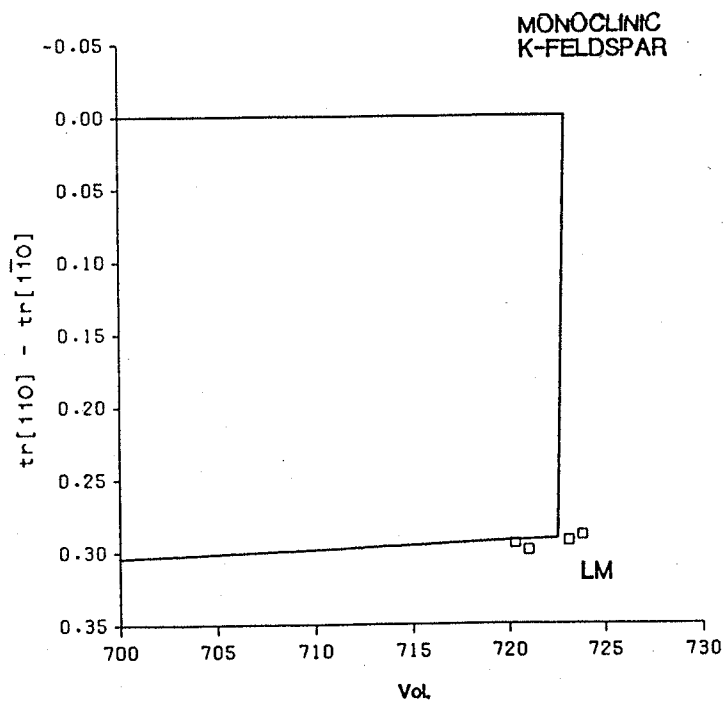
Figure 5.10 : tr[110] − tr[110] vs volume for maximum microcline from the Gods River pegmatite. Modified after Kroll and Ribbe (1983).
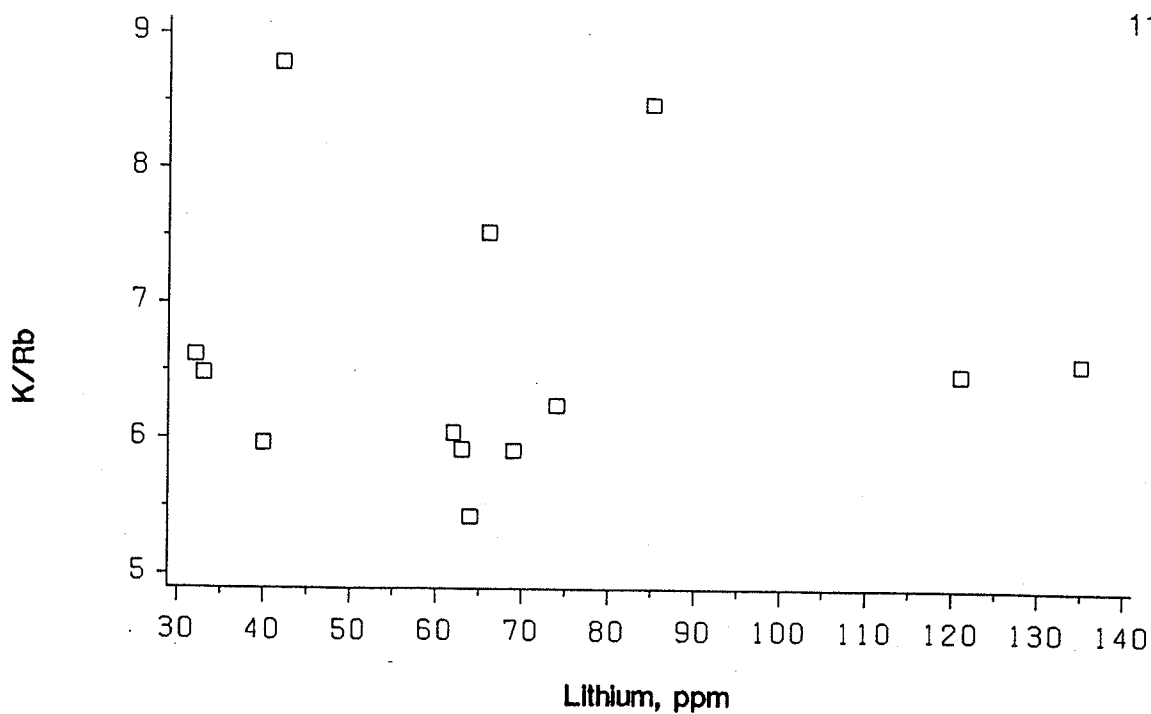
Figure 5.11:   K/Rb vs Li for microcline from the Gods River pegmatite.
There is no correlation between Li and K/Rb.
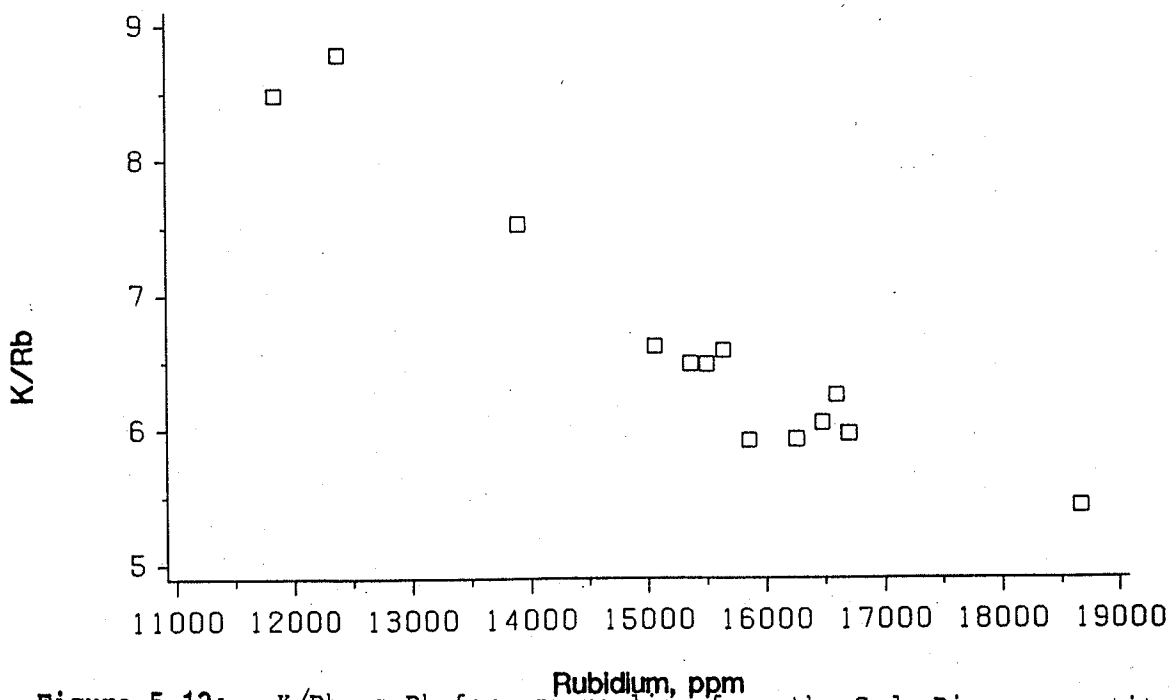
Figure 5.12:   K/Rb vs Rb for microcline from the Gods River pegmatite.
Increasing Rb is strongly correlated with decreasing K/Rb.
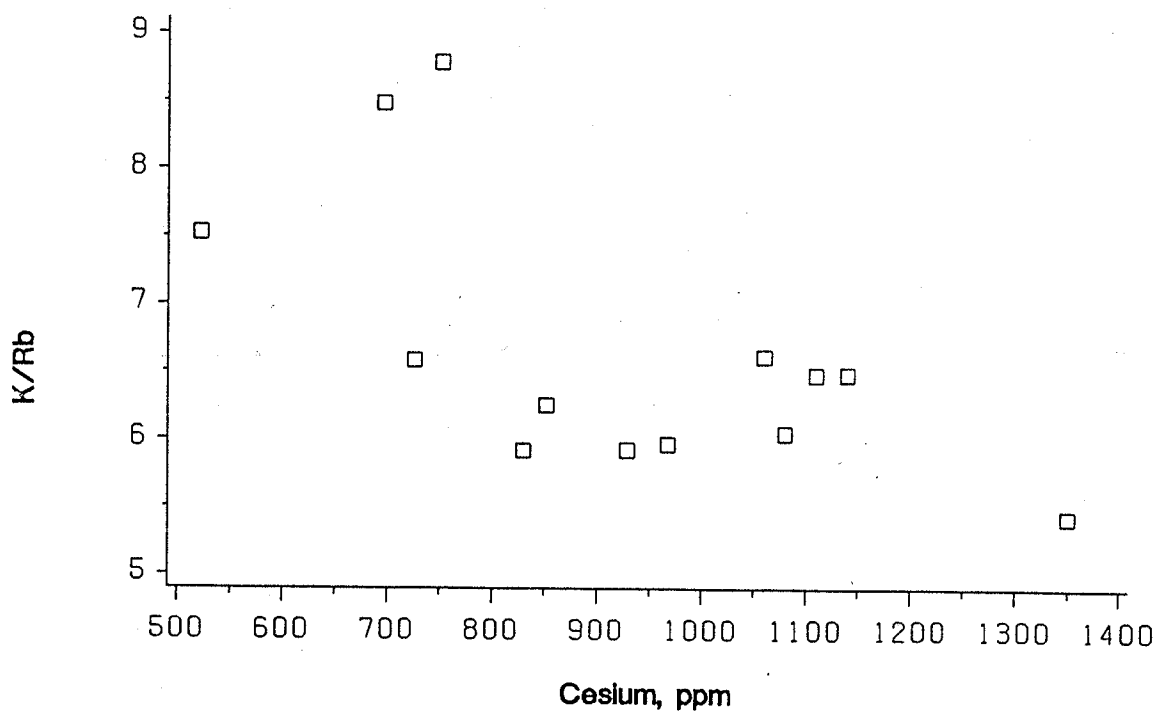
Figure 5.13: K/Rb vs Cs for microcline from the Gods River pegmatite. Increasing Cs is correlated with decreasing K/Rb.
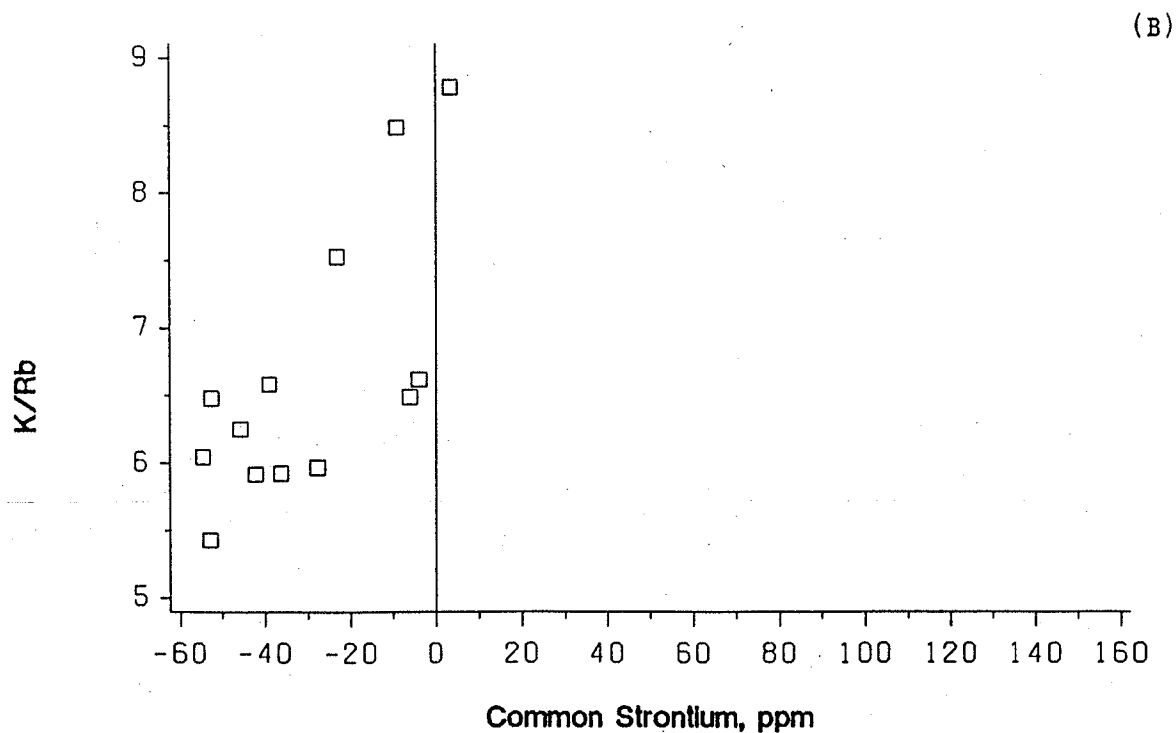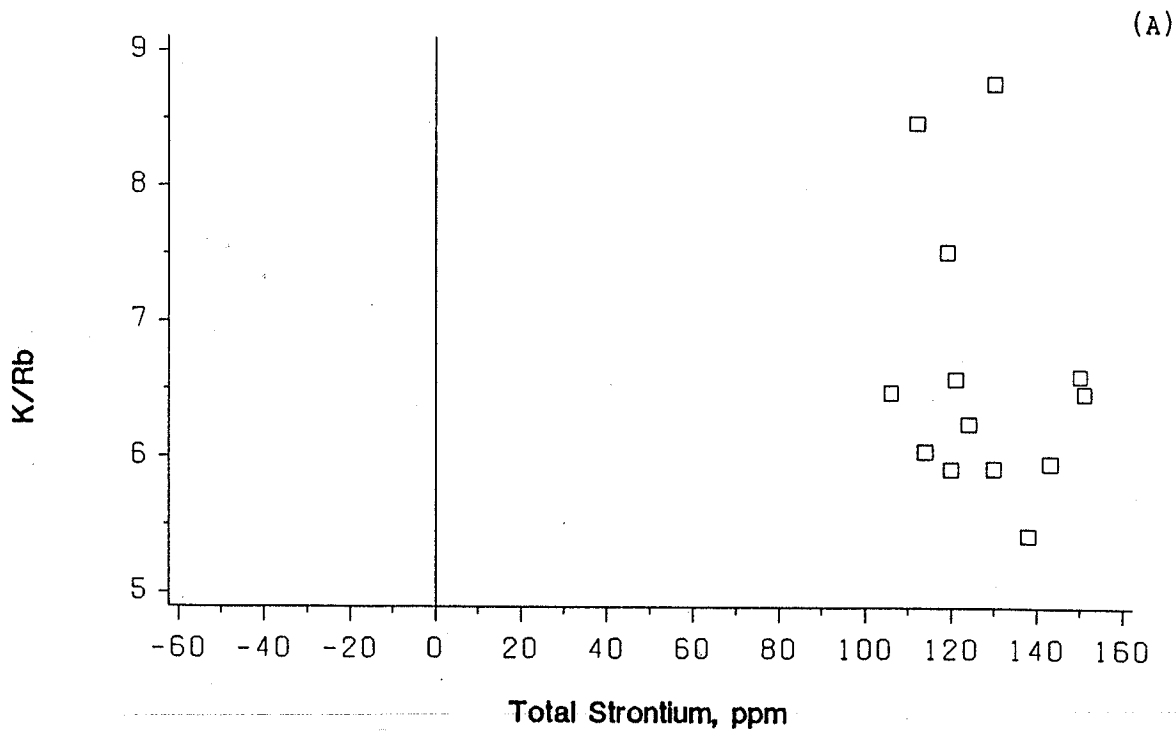
Figure 5.14: K/Rb vs Total Sr (A) and common Sr (B) for microcline from the Gods River pegmatite. Total Sr increases very slightly with decreasing K/Rb, whereas common Sr decreases significantly with decreasing K/Rb. See text (p.27) for explanation of negative Sr values.
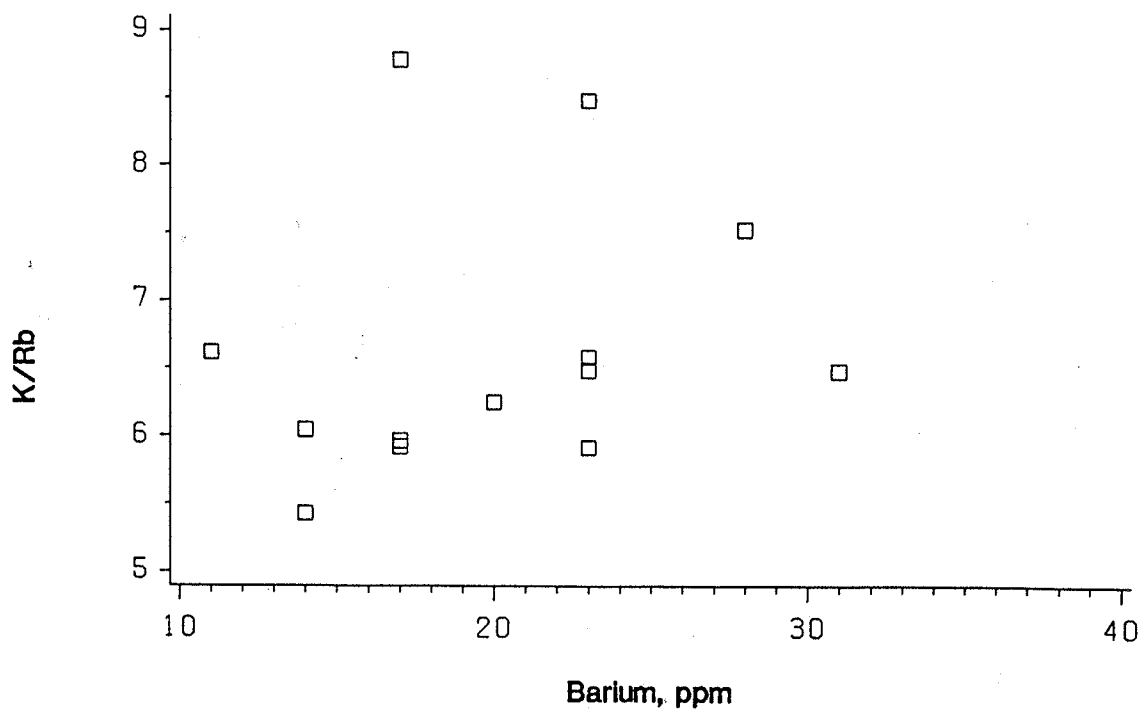
Figure 5.15:   K/Rb vs Ba for microcline from the Gods River pegmatite. There is no correlation between K/Rb and Ba.
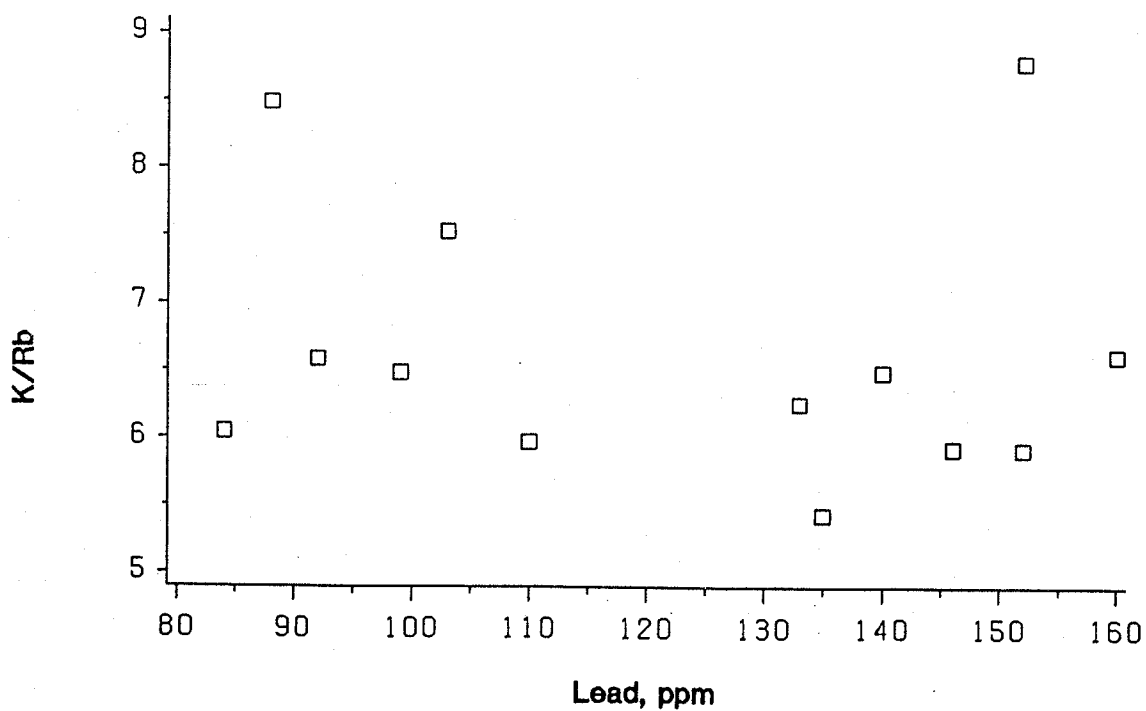
Figure 5.16:   K/Rb vs Pb for microcline from the Gods River pegmatite. There is no correlation between K/Rb and Pb.
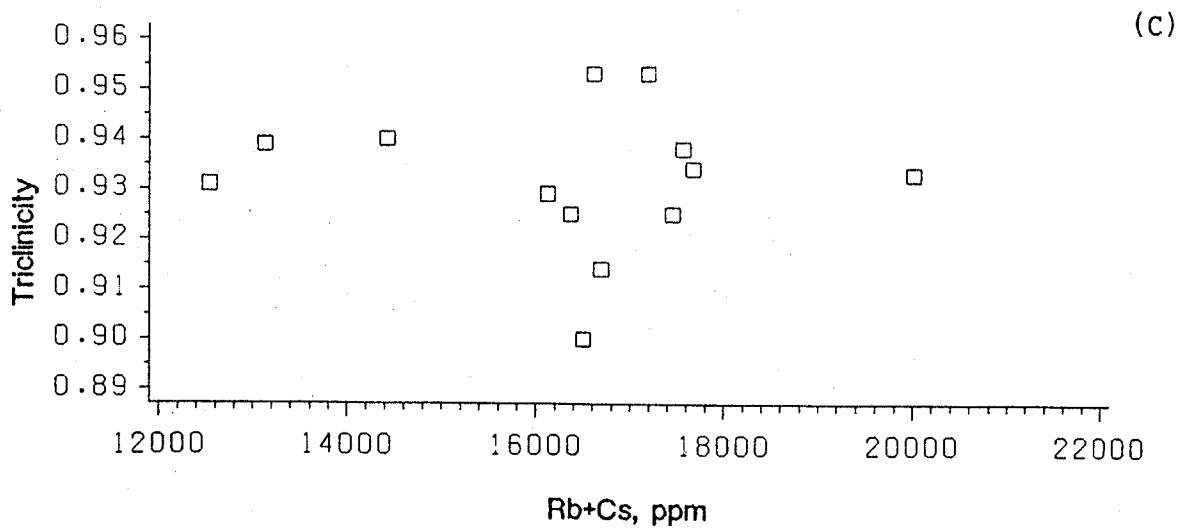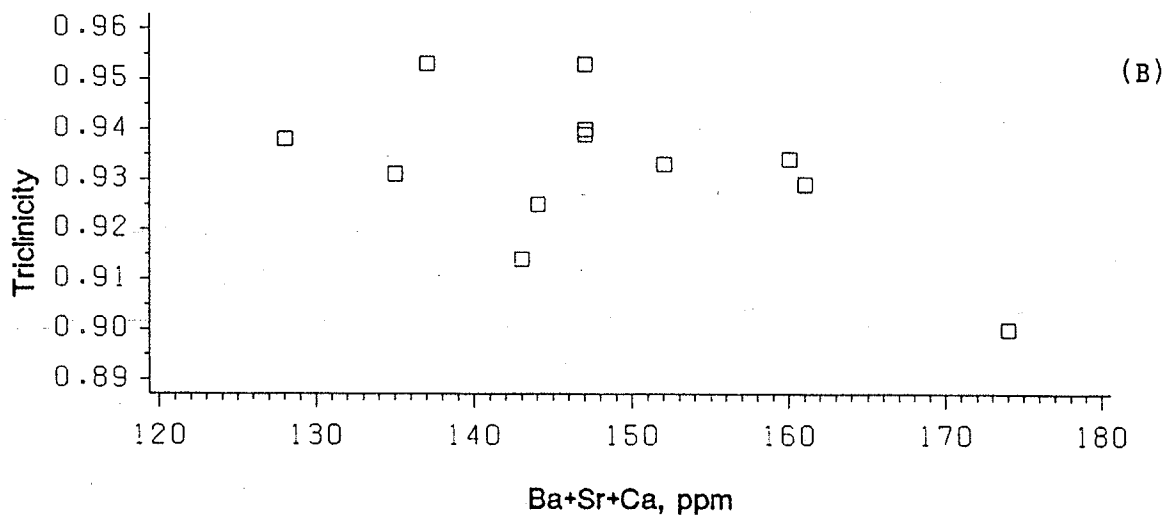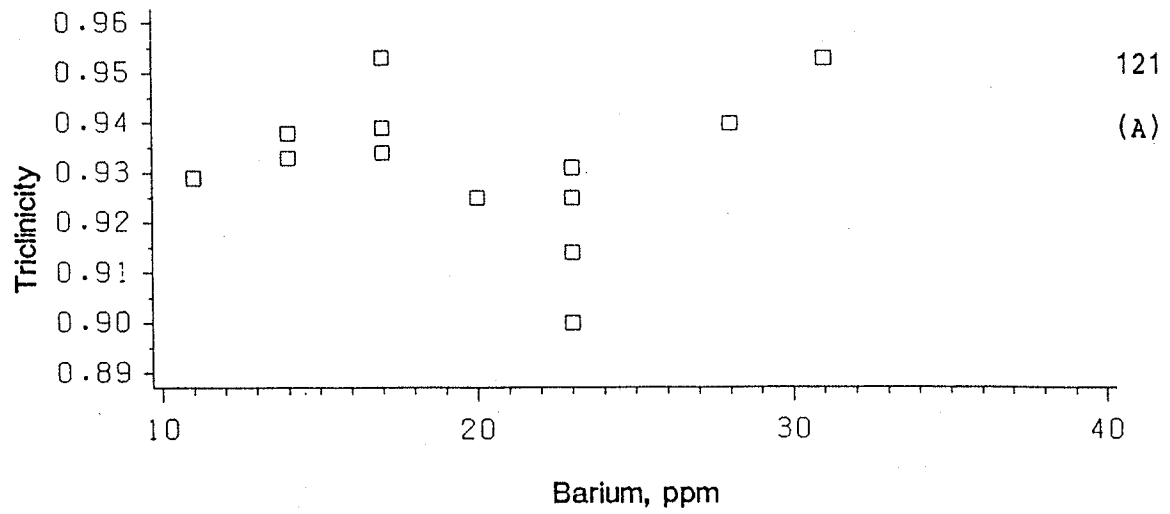
Figure 5.17: Δ vs Ba (A), Δ vs Ca+Sr+Ba (B), and Δ vs Rb+Cs (C) for microcline from the Gods River pegmatite. There is no correlation between Δ and concentrations of large alkali and divalent cations.

Table 5.2: Partial chemical analyses and triclinicities (Δ) of microcline from the Gods River pegmatite.

| | WT. % | | | | | PPM | | | | |
Sample	ΣFe_2O_3	CaO	Na_2O	K_2O	Li	Rb	Cs	Sr	Ba	Pb
GDL-7I-4B	0.02	0.03	1.86	12.60	66	13900	522	119	28	103
GDL-7I-7	0.02	0.04	1.99	12.40	135	15640	726	121	23	92
GDL-7I-9	0.02	0.01	2.32	12.10	85	11840	696	112	23	88
GDL-7I-10	0.03	0.03	1.45	12.50	74	16600	852	124	20	133
GDL-7I-12	0.03	0.02	1.69	12.00	40	16700	968	143	17	110
GDL-7I-16	0.02	0.01	2.14	11.30	69	15860	830	120	23	152
GDL-7I-20	0.02	0.01	1.36	11.60	63	16260	929	130	17	146
GDL-7I-26	0.03	0.01	1.35	12.00	121	15360	1140	151	23	140
GDL-7I-30	0.02	0.02	1.75	13.10	42	12380	751	130	17	152
GDL-7I-31	0.02	0.02	1.76	12.10	33	15500	1110	106	31	99
GDL-7I-32	0.05	0.02	1.62	12.00	32	15060	1060	150	11	160
GDL-7I-33	0.02	0.01	1.53	12.00	62	16480	1080	114	14	84
GDL-7I-34	0.02	0.02	1.53	12.20	64	18660	1350	138	14	135

Sample	K/Rb	K/Cs	K/Ba	Rb/Cs	Δ
GDL-7I-4B	7.5	200	3736	26.6	0.94
GDL-7I-7	6.6	142	4476	21.5	0.93
GDL-7I-9	8.5	144	4367	17.0	0.93
GDL-7I-10	6.3	122	5188	19.5	0.93
GDL-7I-12	6.0	103	5860	17.3	0.93
GDL-7I-16	5.9	113	4079	19.1	0.91
GDL-7I-20	5.9	104	5665	17.5	0.95
GDL-7I-26	6.5	87	4331	13.5	0.90
GDL-7I-30	8.8	145	6397	16.5	0.94
GDL-7I-31	6.5	90	3240	14.0	0.95
GDL-7I-32	6.6	94	9056	14.2	0.93
GDL-7I-33	6.0	92	7116	15.3	0.94
GDL-7I-34	5.4	75	7234	13.8	0.93

Plagioclase

Plagioclase is an abundant interstitial phase in this pegmatite. It occurs as anhedral lath-shaped crystals ranging from <0.1 to 3 mm in length. In thin section, most plagioclase grains appear unaltered but deformed, displaying kinks, fractures and undulatory extinction (Figure 5.4). Compositions of 5 crystals range from An_4 to An_6.

Quartz

Quartz is an abundant interstitial phase, occurring as anhedral equant grains ranging from <0.1 to 1 mm in diameter. No distinct quartz cores were observed in the outcrop.

Muscovite

Primary muscovite occurs as an abundant interstitial phase. Individual crystals are white in colour, appear fresh, and range from 0.5 to 3 mm in size. They occur in anhedral flakes up to 0.5 mm thick.

Secondary purple muscovite occurs in veins cross-cutting the foliation of the pegmatite near the eastern end of the exposure. This mica is very fine-grained with individual flakes ranging from 0.1 to 1 mm in size. Partial analyses of 2 samples are given in Table 5.3. Both samples are the $2M_1$ polytype. They average 0.30 wt.% Li_2O, 1.70 % Rb_2O (15600 ppm Rb), 0.53 % Cs_2O (4980 ppm Cs), and 290 ppm Be. Compared to the fine-flaked pink to purple lithian muscovite from the SQ pegmatite at Red Sucker Lake, these samples are enriched in Be, somewhat depleted in Rb and very poor in Li. Cs values are comparable in micas from the two pegmatites. MnO predominant over FeO corresponds with the purple

colour. The Na_2O content is surprisingly high, corresponding to 36.4 and 25.4 mol.% paragonite for the two samples, compared to 2.8 to 13.8 mol.% for late muscovite from the Tanco pegmatite (Rinaldi et al., 1972).

Table 5.3: Partial chemical analyses of fine-grained purple muscovite from the Gods River pegmatite.

Sample	7I-13	7I-14
Wt.%:		
TiO_2	<0.01	<0.01
TFe_2O_3	0.12	0.11
MnO	0.61	0.56
MgO	0.01	0.02
CaO	0.08	0.05
Na_2O	1.91	1.52
K_2O	5.07	6.80
Li_2O	0.01	0.59
ppm:		
Rb	14800	16300
Cs	3790	5990
Be	462	122
K/Rb	2.84	3.46
K/Cs	10.6	9.42
Rb/Cs	3.73	2.72

TFe_2O_3 = total Fe calculated as Fe_2O_3

Spodumene

Spodumene comprises 20 to 25 vol.% of the Gods River pegmatite, and is the most conspicuous phase in the outcrop. It occurs as dull grey, translucent, 2 to 15 mm long, anhedral to subhedral bladed crystals. An earthy reddish alteration is common on spodumene crystals at weathered surfaces of the exposure. In thin section, the spodumene grains appear altered at their edges but undeformed (Figure 5.4). This may indicate that the spodumene did not absorb any of the deformation, or that it re-

crystallized after the deformational event that affected the plagioclase. Solid-state recrystallization in a stress field may also explain the elongation of the spodumene crystals that is parallel to the schistosity of the metabasalts but oblique to the strike of the pegmatite.

5.5 GEOCHEMISTRY

Compositions of 4 whole-rock samples of the Gods River pegmatite are given in Table 5.4. The samples are all peraluminous. The high Li values reflect the high modal spodumene content of the pegmatite.

Whole-rock concentrations of SiO_2, Al_2O_3, Li_2O, Na_2O and K_2O were recalculated to 100% combined normative quartz, alkali feldspar and eucryptite (Figure 5.18). Chemical data for the Bikita (petalite-bearing) and Kings Mountain (spodumene-bearing) pegmatites (Stewart, 1978) are plotted for comparison. Three of the Gods River pegmatite samples plot in close proximity to the Bikita and Kings Mountain pegmatites. The average composition of the 4 Gods River samples plots very close to that of the Bikita data. Except for the feldspar-richest sample, all data fall within the general field of lithium-aluminosilicate-enriched units of zoned pegmatites, and the bulk compositions of the quasi-homogeneous albite-spodumene pegmatite type, as established by Stewart (1978).

The very low contents of Nb, Ta, Sn and Be suggest that no significant mineralization with these elements can be expected in the pegmatite. In contrast, the Zn and Ba contents seem to be exceptionally high, particularly compared to the pegmatites at Red Sucker Lake. However, reliable data on trace elements in whole-rock compositions of granitic pegmatites are scarce due to the difficulty in obtaining representative analyses of heterogeneous bodies (Černý, 1982a).

Table 5.4: Whole-rock composition of four samples of the Gods River pegmatite.

	7I-4	7I-19	7I-25	7I-37		7I-4	7I-19	7I-25	7I-37
Wt. %:					ppm:				
SiO_2	74.11	73.50	72.93	73.48					
TiO_2	0.01	0.01	0.01	0.01	Rb	3772	3328	5131	2843
Al_2O_3	16.18	16.57	16.57	16.83	Cs	297	250	793	315
Fe_2O_3	0.12	0.17	0.14	0.26	Be	105	61	127	110
FeO	0.10	0.12	<0.01	<0.01	Sr	36	29	51	32
MnO	0.29	0.23	0.27	0.24	Ba	542	491	725	457
MgO	0.06	0.04	0.05	0.06	Ga	227	240	177	222
CaO	0.13	0.12	0.20	0.15	Zn	332	229	227	260
Li_2O	1.32	1.61	0.65	1.30	U	4	4	<2	4
Na_2O	3.58	2.93	5.71	4.84	Th	2	2	1	2
K_2O	2.12	1.88	2.09	1.20	Zr	<10	<10	<10	<10
P_2O_5	<0.01	<0.01	<0.01	<0.01	Hf	<1	<1	<1	<1
CO_2	0.13	0.08	0.14	0.30	Sn	16	16	11	20
H_2O^+	0.10	0.10	0.05	0.10	Nb	43	31	32	53
H_2O^-	nd	nd	nd	nd	Ta	42	46	78	56
S	<0.01	0.01	0.01	0.01	Y	122	102	140	94
F	0.38	0.30	0.78	0.37					
Σ	98.47	97.54	99.27	98.99					
A/CNK	3.85	4.62	3.01	4.07					
K/Rb	4.67	4.69	3.38	3.50					
K/Cs	59.3	62.4	21.9	31.6					
Rb/Cs	12.7	13.3	6.47	9.03					
Ba/Rb	0.144	0.148	0.141	0.161					
Al/Ga	377	305	495	401					
Nb/Ta	1.0	0.67	0.41	0.95					

$A/CNK = Al_2O_3 / (CaO + Na_2O + K_2O)$
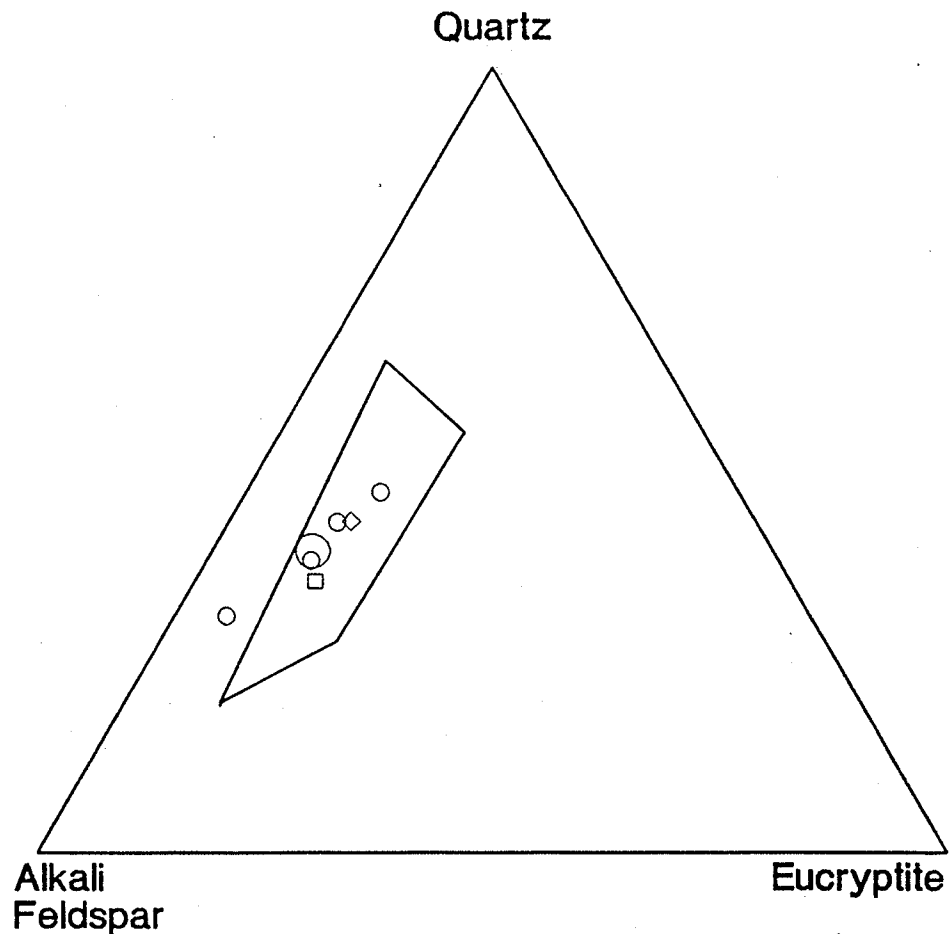
Figure 5.18: Compositions of the Gods River (circles), Bikita (square) and Kings Mountain (diamond) pegmatites recalculated to 100 wt.% normative alkali feldspar (Ab + Or), quartz and eucryptite. The 4 Gods River samples are shown by small circles; their average is shown by the large circle. Large field shows the range of bulk compositions of spodumene and petalite pegmatites from Stewart (1978).

Chapter VI

DISCUSSION AND CONCLUSIONS

6.1   GENERAL INTRODUCTION: PETROGENESIS OF GRANITIC PEGMATITES

Pegmatites generally have granitic compositions similar to those of associated pegmatitic granites. Studies of bulk composition, geothermobarometry, isotopes and fluid inclusions all indicate the origin of pegmatites from the late stages of crystallization of fertile granitic rocks (Černý, 1982b; Černý and Meintzer, 1987).   However, the current understanding of the generation of pegmatites by igneous fractionation of fertile granitoid rocks is far from complete.

Examples of physical continuity between granites and rare-element pegmatites are uncommon in the Precambrian shield because of the predominantly horizontal attitude of most of the exposures. However, many examples exist that illustrate the relationships between rare-element pegmatites and parental granitoid rocks.   For example,   the Ross Lake pegmatite group shows a regional zoning pattern that spreads west of, and roughly concentric to, the parental Redout Lake granite near Yellowknife, N.W.T. (Hutchinson, 1955; Černý, 1987), which strongly indicates their genetic relationship. The consanguinity of pegmatitic granites and pegmatites in the southern part of the Winnipeg River pegmatite field is suggested by their distinct mineralogical and geochemical signatures which are absent in the northern part of the field (Černý et al., 1981). Further examples may be found in Černý (1982b; 1987).

6.2   PETROGENESIS OF PEGMATITIC GRANITES AND PEGMATITES AT RED SUCKER LAKE

The tectonic setting and horizontal exposure at relatively shallow levels do not provide any information about deeper-seated roots of the granitic system at Red Sucker Lake. In better exposed terranes, the pegmatitic granites constitute the cupolas of complex intrusions that are more or less layered in terms of mineralogy, texture and fractionation (Černý et al., 1981; Černý and Meintzer, 1987). These systems suggest progressive upward fractionation and enrichment in volatile components. It can be assumed that a similar system underlies the highly fractionated pegmatitic granites and pegmatites at Red Sucker Lake.

Still, the pegmatitic granite-pegmatite system at Red Sucker Lake shows one special feature - concentration of the highly fractionated and rare element-enriched pegmatitic facies inside the pegmatitic granite body. The fractionated pegmatitic leucogranites fall under the general type of deposits related to highly evolved pegmatitic cupolas of granitic intrusions of the Montebras and Echassières type (Aubert, 1969; Burnol, 1974), but the mineralogy, geochemistry and textural style of the pegmatitic leucogranites are unique. They have no known analogs among other fertile granites worldwide, and there are no granitic rocks exposed in the Red Sucker Lake area that could possibly be parental to the pegmatitic granites.

In the examined terrane, the distribution of pegmatitic granites with fractionation increasing to extreme levels at the centre of the east-west line-up of exposures, and of highly fractionated pegmatites near the eastern and western extremities of the line-up may be interpreted by the model illustrated in Figure 6.1. This section shows a postulated

schematic E-W longitudinal profile through the pegmatitic granites and Western and Eastern pegmatites. The pegmatitic leucogranite crystallizes from the top of the cupola downward with progressively increasing fractionation. The present-day erosional surface exposes early, outermost and least fractionated pegmatitic leucogranite at the eastern and western flanks of the cupola, and progressively deeper and more fractionated pegmatitic leucogranite toward the centre. Late fractures in the roof of the intrusion allow the late volatile- and rare-element-enriched fluids to form a halo of highly fractionated pegmatites radiating upward from the intrusion. Most of the pegmatites have been removed by erosion, except at the eastern and western extremities. This explains the occurrence of the highly fractionated Eastern and Western series pegmatites.

Structural evidence indicates that the pegmatitic granites were intruded along an E-striking subvertically-dipping shear zone. A parallel shear zone would explain the alignment of the Northern series pegmatites (Figure 6.2). Assuming that the pegmatitic granites and pegmatites share a common granitic source at depth, the poorly fractionated nature of the Northern pegmatites can be explained by an overall higher level of emplacement of the granite-pegmatite system, relative to the pegmatitic granites to the south. Furthermore, field evidence shows much more syn- and post-crystallization structural deformation associated with these pegmatites than with the pegmatitic granites. The tectonic disturbances may have allowed later highly fractionated pegmatitic fluids to be emplaced at much higher levels, far above the erosional surface.

The consanguinity of the pegmatitic granites and pegmatites is supported by the geochemical evidence. K/Rb ratios in microcline are plotted against values and ratios of rare alkali metals in Figures 6.3 to 6.7. K/Rb in microcline is plotted against $MnO/(MnO+FeO)$ in garnet in Figure 6.10, and $MgO/(MgO+CaO)$ vs $MnO/(MnO+FeO)$ in garnet is plotted in Figure 6.11. All of these diagrams show several important features:

1. the Northern pegmatites overlap in part with the Eastern and Western pegmatitic granites, but

2. the Northern pegmatites show somewhat lower levels of fractionation than the poorest-fractionated pegmatitic granites;

3. the Western and Eastern pegmatites overlap with the Main and petalite-bearing pegmatitic leucogranites;

4. the Western pegmatites show the highest levels of fractionation in the Red Sucker Lake area;

5. the non-mineralized Main pegmatitic granites and the most fractionated Eastern and Western pegmatitic granites plot between the highly fractionated Western and Eastern pegmatites and the poorly fractionated Northern pegmatites; and

6. there are no major gaps or lateral shifts in the fractionation trend from the poorly fractionated Northern pegmatites through the pegmatitic granites to the most highly fractionated pegmatites.

From this one can conclude that the geochemical evidence does not contradict the hypothesis that the pegmatitic granites and pegmatites are consanguineous, and that the fractionation trends support the models illustrated in Figures 6.1 and 6.2. Geochemical indicators of separate evolution trends, such as lateral shifts in fractionation diagrams that

are demonstrated by chemically distinct, unrelated pegmatite groups in the Cross Lake pegmatite field (Anderson, 1984) and in the Winnipeg River district (Černý et al., 1981), are not in evidence here.

The only elements that may contradict the above conclusions are Ba and Pb in microcline. However, their behavior in pegmatitic systems is not well understood. The K/Rb vs Ba diagram of Figure 6.8 is difficult to interpret. It shows the overlap between the Northern pegmatites and the poorly fractionated pegmatitic granites, and somewhat separate fields for the non-mineralized pegmatitic granites, the petalite-bearing pegmatitic leucogranites, and the Western pegmatites. Ba tends to increase with deceasing K/Rb from the Northern pegmatites and Eastern and Western pegmatitic granites to the least fractionated Main pegmatitic granites, and from the petalite-bearing Main pegmatitic granites to the Eastern and Western pegmatites. However, Ba decreases with decreasing K/Rb within the Main pegmatitic granites. Similar difficulties are encountered in the Cross Lake data (Anderson, 1984). The bulk Ba content of pegmatites tends to increase with fractionation in highly evolved bodies, but it also tends to decrease during the progressive crystallization of individual pegmatites (Shearer and Papike, 1985).

The K/Rb vs Pb diagram of Figure 6.9 is also difficult to interpret. It illustrates the relationship between the pegmatites and pegmatitic granites, but shows a reversal from initial decrease in Pb to its increase at the lowest K/Rb ratios. There are no corresponding data from other pegmatite fields for comparison. It should be noted, however, that the concentration of Pb in K-feldspars is affected by sulfur fugacity from the magmatic stage onward (Stevenson and Martin, 1986); precip-

itation of sulfides or extraction of sulfur and transition elements in an aqueous fluid would undoubtedly affect the concentration trends of Pb in potassic silicates. The data of the present study do not allow evaluation of these factors.
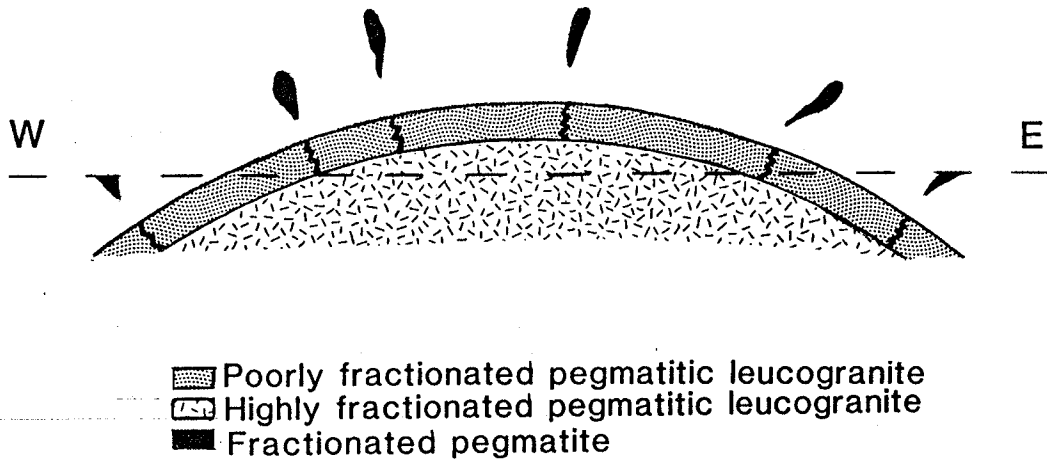
Figure 6.1: Postulated schematic E-W cross section through the line-up of pegmatitic granites and Eastern and Western pegmatites at Red Sucker Lake. Dashed line shows the present-day erosional surface.
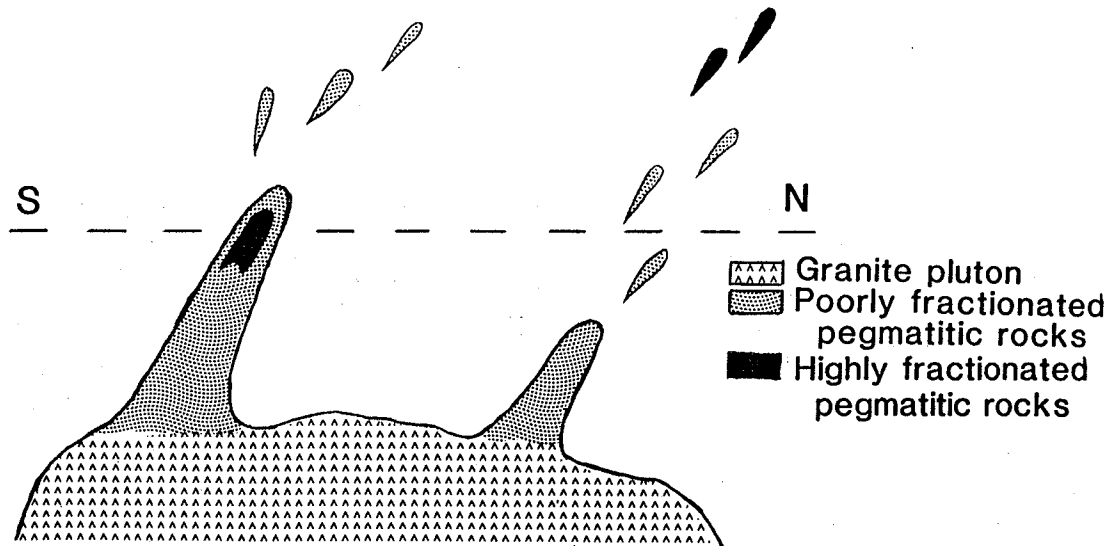
Figure 6.2: Postulated schematic N-S cross section through the pegmatitic granites and Northern pegmatites at Red Sucker Lake. Dashed line shows the present-day erosional surface.
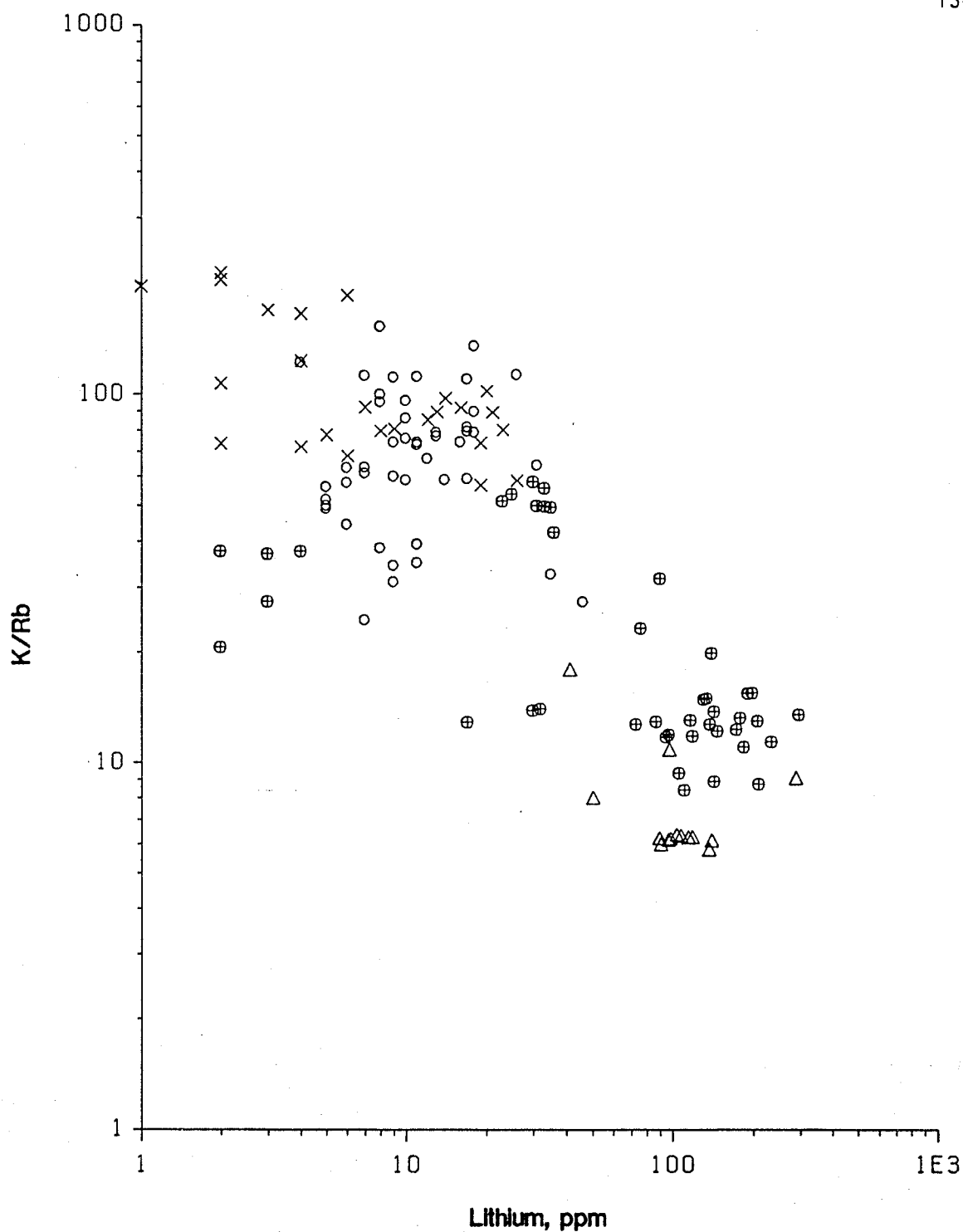
Figure 6.3: K/Rb vs Li in microcline from pegmatitic granites and pegmatites at Red Sucker Lake. Data in this and following diagrams are grouped into the following units: Eastern and Western pegmatitic granites (open circles), Main and petalite-bearing pegmatitic granites (crossed circles), Northern pegmatites (X's), and Western and Eastern pegmatites (triangles).
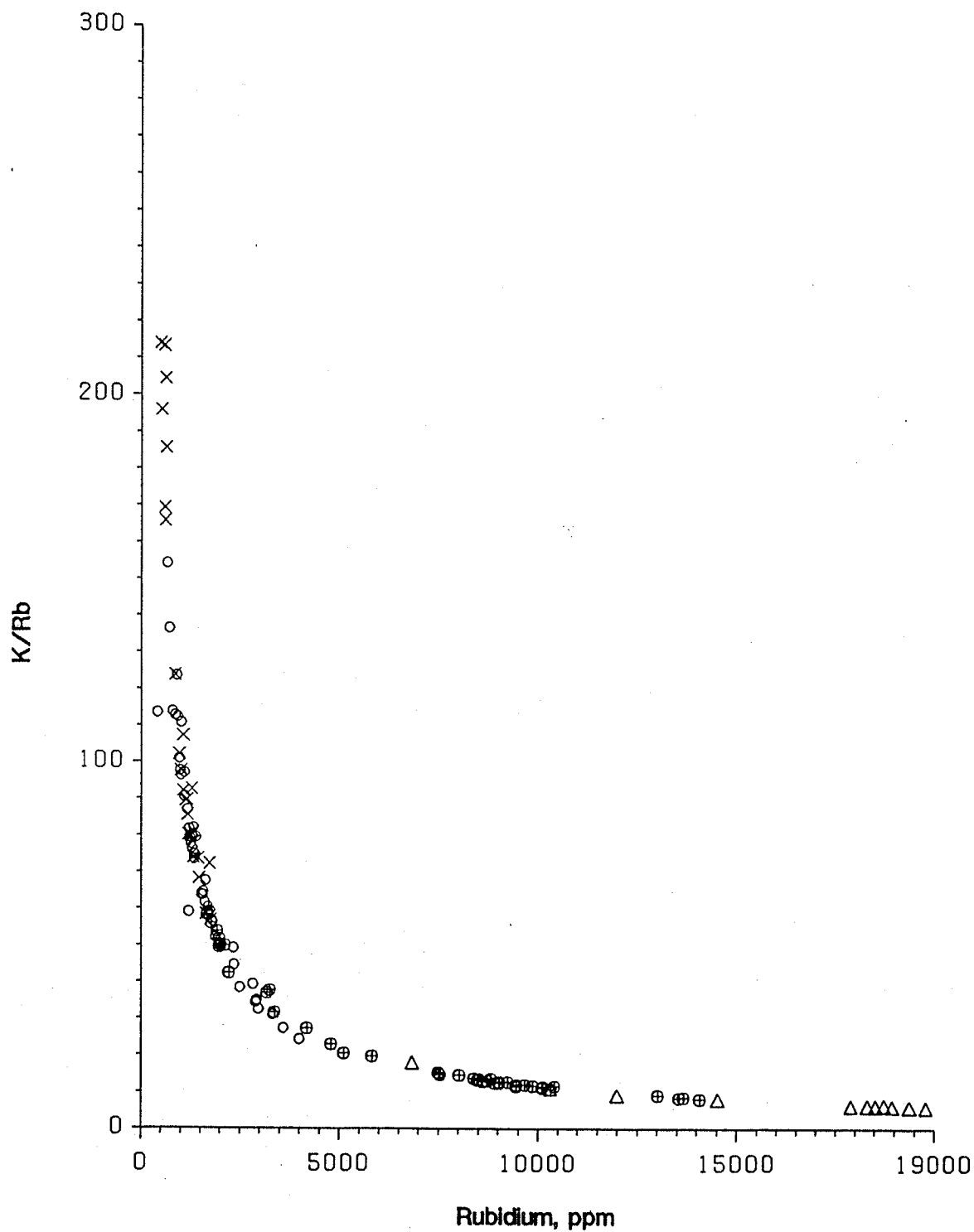
Figure 6.4: K/Rb vs Rb in microcline from pegmatitic granites and pegmatites at Red Sucker Lake. Symbols as in Figure 6.4.
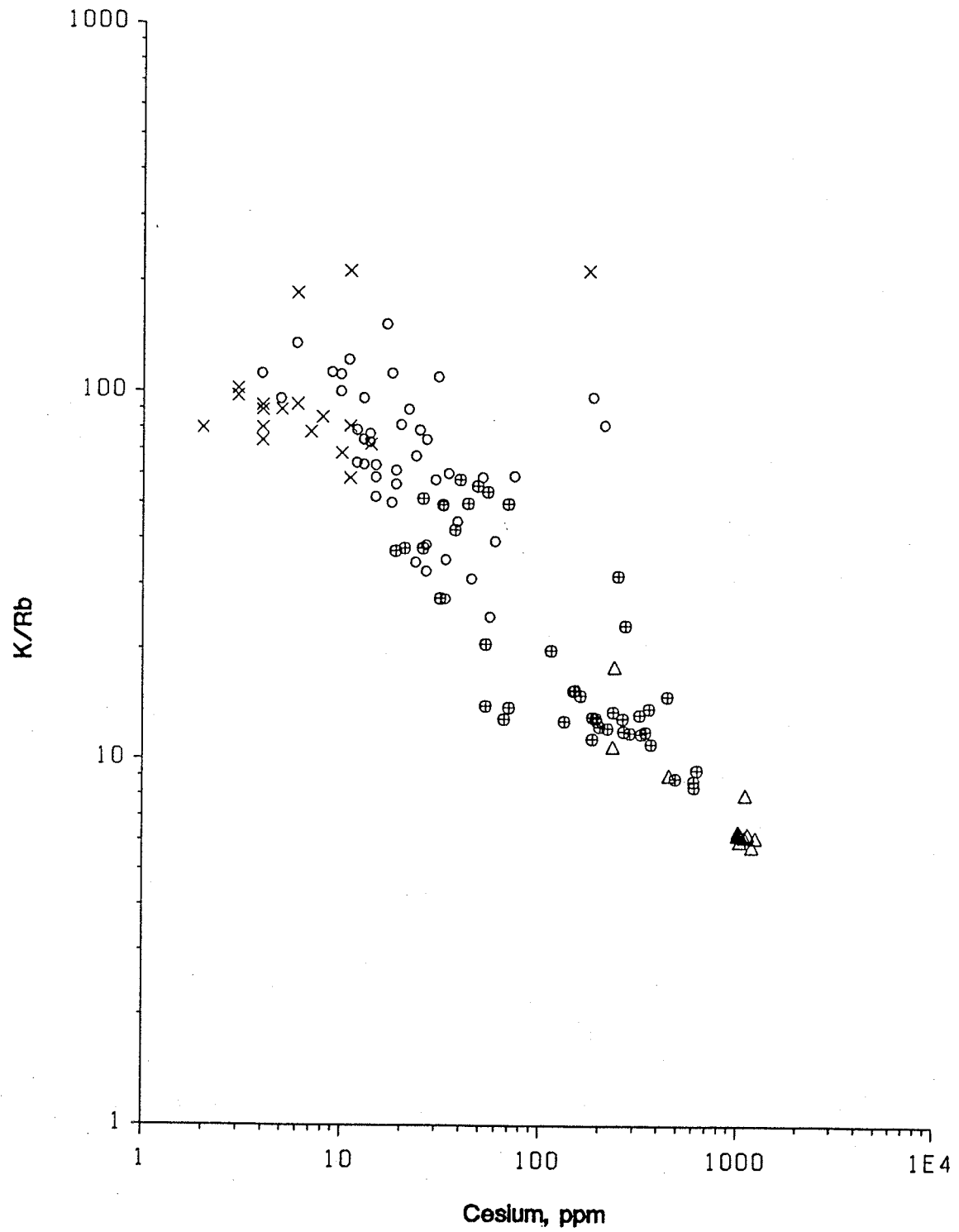
Figure 6.5: K/Rb vs Cs in microcline from pegmatitic granites and pegmatites at Red Sucker Lake. Symbols as in Figure 6.4.
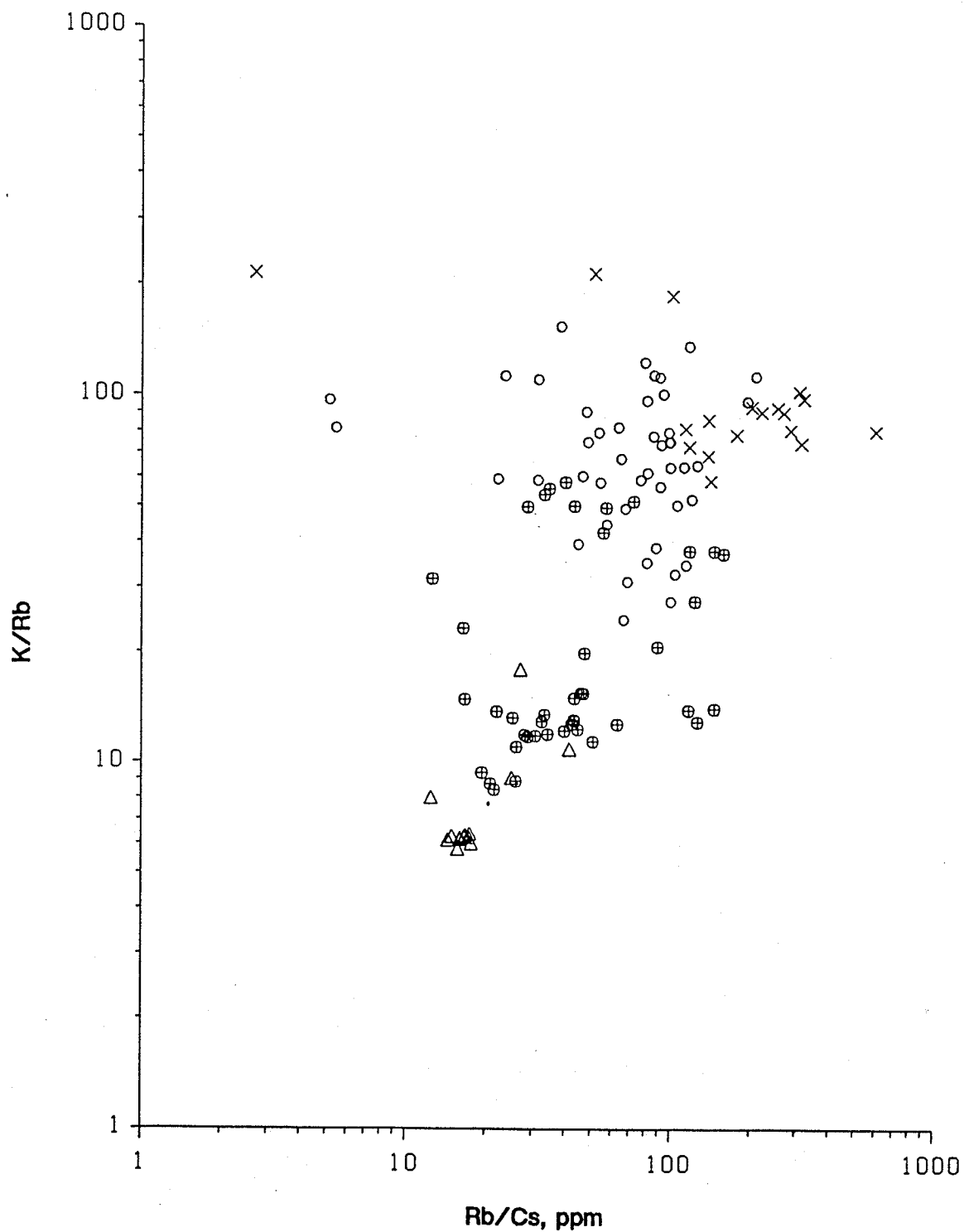
Figure 6.6: K/Rb vs Rb/Cs in microcline from pegmatitic granites and pegmatites at Red Sucker Lake. Symbols as in Figure 6.4.
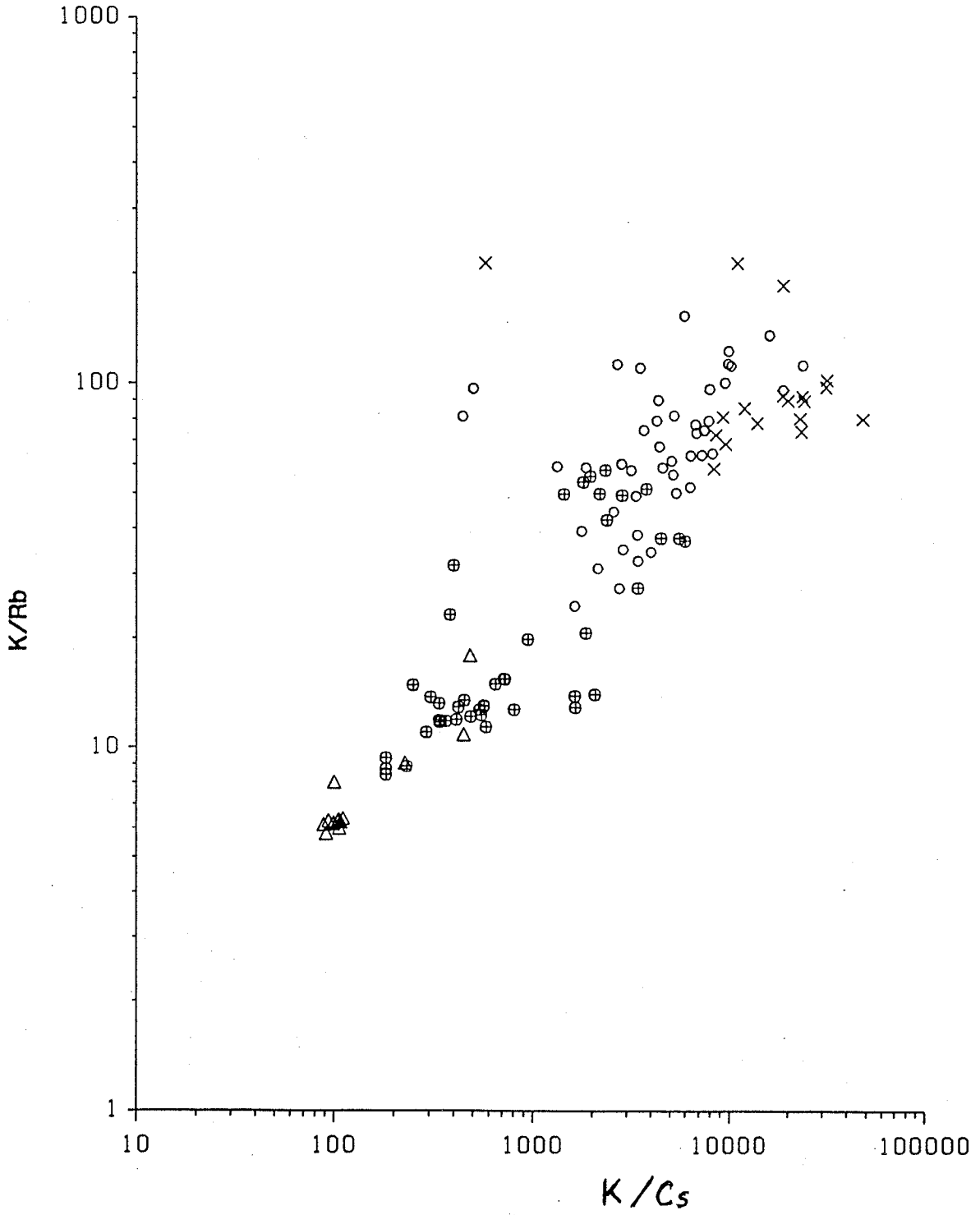
Figure 6.7: K/Rb vs K/Cs in microcline from pegmatitic granites and pegmatites at Red Sucker Lake. Symbols as in Figure 6.4.
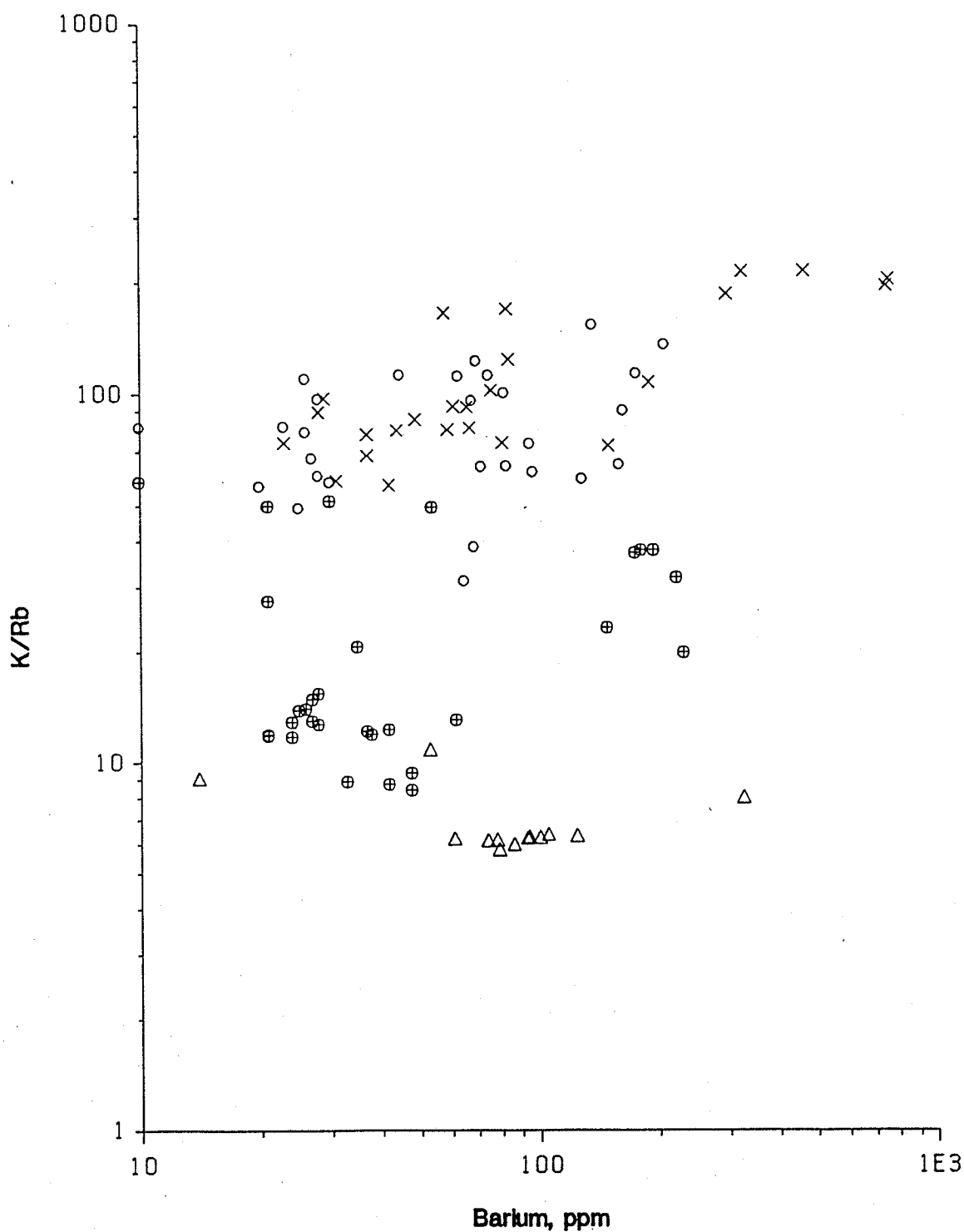
Figure 6.8: K/Rb vs Ba in microcline from pegmatitic granites and peg-
matites at Red Sucker Lake. Ba increases with decreasing K/Rb ratios
except within the Main and petalite-bearing pegmatitic granites.
Symbols as in Figure 6.4.
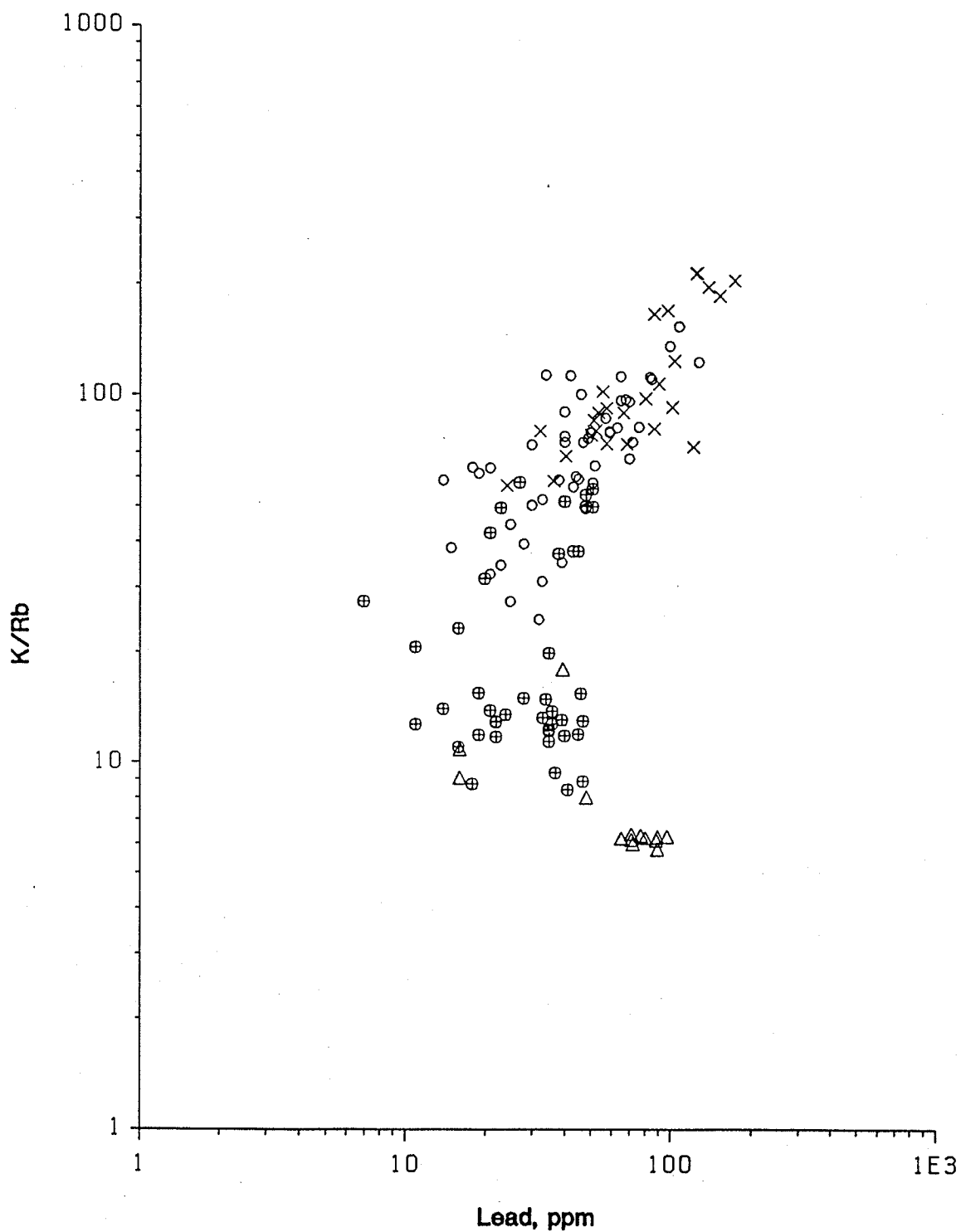
Figure 6.9: K/Rb vs Pb in microcline from pegmatitic granites and pegmatites at Red Sucker Lake. This diagram shows a reversal from initial decrease in Pb with decreasing K/Rb to an increase at the lowest K/Rb ratios. Symbols as in Figure 6.4.

Figure 6.10: K/Rb in microcline vs MnO/(MnO+FeO) in garnet from pegmatitic granites and pegmatites at Red Sucker Lake. Symbols as in Figure 6.4.
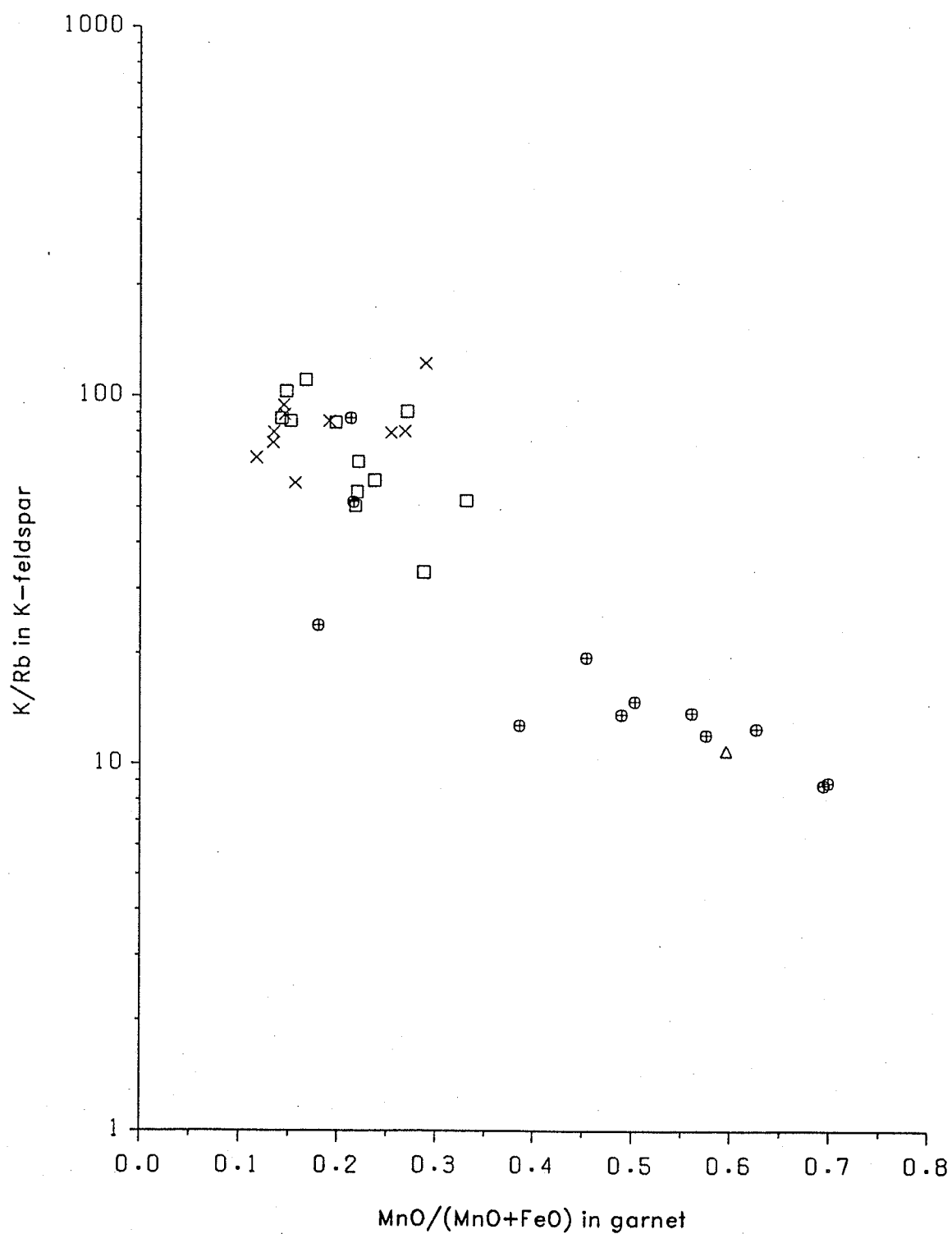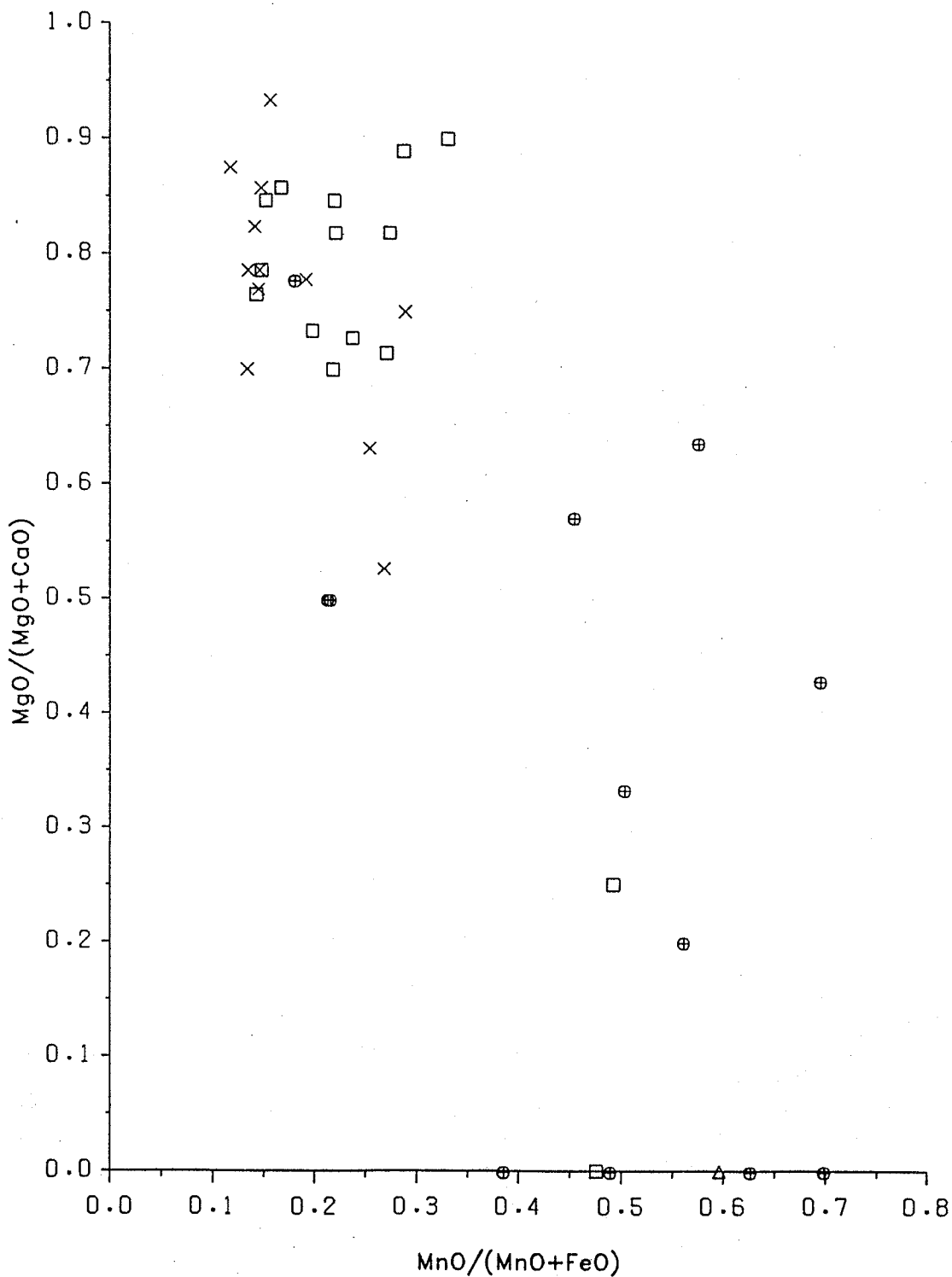
Figure 6.11: MgO/(MgO+CaO) vs MnO/(MnO+FeO) in garnet from pegmatitic granites and pegmatites at Red Sucker Lake. Symbols as in Figure 6.4.

6.3   PETROGENESIS OF THE GODS RIVER PEGMATITE

No leucogranites possibly parental to the Gods River pegmatite were ob-
served in the field.   The only plutonic granitoid rocks in the area are
the Bayly Lake complex granodiorites and tonalites, neither of which
show any pegmatitic texture or segregations.   Thick overburden of gla-
cial drift extensively covers most of the area to the east, north and
west of the pegmatite.   There is a potential for the occurrence of addi-
tional related pegmatitic rocks in the drift-covered area.

6.4   ECONOMIC CONSIDERATIONS

Red Sucker Lake pegmatitic granites

The rare element that attains potentially economic quantities in the
pegmatitic granites is lithium, which exceeds 6000 ppm in the geochemi-
cally anomalous petalite-bearing pegmatitic leucogranites. However, the
existing data are insufficient for estimating the potential reserves of
lithium for a number of reasons.   The character of the exposures does
not permit interpolation of the total outcrop area of the mineralized
pegmatitic leucogranite, and no information is available so far on its
vertical extent.   Also, the inhomogeneous nature of the pegmatitic leu-
cogranite precludes geochemical interpolation from the sparse distribu-
tion of the widely scattered sample locations.   Finally, the paucity of
outcrops on isolated islands does not permit a denser, more representa-
tive surface sampling.

Nevertheless, two kinds of parameters indicate a potential for sig-
nificant lithium mineralization. First, the areal extent of the mineral
finds and of the geochemical anomaly, if underlain by a more or less

continuous body of the petalite-bearing pegmatitic leucogranite, may represent a sizeable volume of the mineralized rock. Second, the degree of geochemical fractionation attained in the central parts of the anomaly compares favorably with the fractionation of other highly mineralized pegmatite deposits such as the Tanco pegmatite, and with the most fractionated pegmatite in the Red Sucker Lake field, the SQ body (see Table 3.11).

The only other element deserving attention is Ta. However, its concentration at the surface exposures is very low and much additional work would be needed to assess its potential.

The demand for lithium should increase in the future due to the projected increased use of the metal in the production of automotive and storage batteries, and the possible future use of liquid lithium metal as a coolant and tritium breeder in thermonuclear reactors (Gyongyossy and Spooner, 1979). However, the current production of lithium at the Kings Mountain pegmatite (Kunasz, 1982) and from the vast evaporite deposits in Chile (Kunasz, 1978) will probably satisfy most of the demand for lithium in the foreseeable future. Thus the local concentration in northern Manitoba may be significant only as a strategic reserve for the future.

Red Sucker Lake pegmatites

The only pegmatites in the Red Sucker Lake area that show extreme fractionation occur in the Western series. These can be classified as complex rare-element pegmatites (Černý, 1987). Tantalum contents are known from the PK and SQ pegmatites, and Sn is enriched in the TD body. How-

ever these pegmatites are all very small in outcrop, and diamond drilling at SQ and TD has failed to locate any sizeable mineralized rock bodies. No other rare elements occur in potentially economic quantities in these pegmatites. Unless additional and sizeable mineralized pegmatites are discovered by exploration in the drift-covered terrane, the pegmatites known at present have no economic significance.

Gods River pegmatite

The Gods River pegmatite is classified as an albite-spodumene rare-element pegmatite (Černý, 1987). It contains 20 to 25% spodumene (5000 ppm Li), is 3 to 10 m thick, and extends for 2 km along strike to a depth of at least 250 m (Southard, 1977). If the entire dike is homogeneous, as it is at the exposure, then this represents a significant deposit on the order of several tens of thousands of metric tons of lithium metal. The reserves may actually be much larger as the albite-spodumene type pegmatites are usually very extensive down-dip. However, due to the remote location of the pegmatite and the present and projected future market conditions for lithium, this deposit is not expected to become economically exploitable in the foreseeable future. No other rare elements occur in economic quantities in this pegmatite.

6.5 SUGGESTIONS FOR FURTHER RESEARCH

Red Sucker Lake area

Future research at Red Sucker Lake should concentrate on the petalite-bearing pegmatitic leucogranites as these are the only pegmatitic rocks outcroping in the area that have any potential for economic significance. A diamond-drilling program would have two major objectives; to

evaluate the horizontal and especially the vertical extents of the li-
thium reserves, and to test the petrogenetic model postulated in section
6.3. As a secondary target, drift-covered areas surrounding the Western
and Eastern pegmatites should be explored for possible additional pegma-
tite intrusions.

Understanding of the petrogenetic ralations will be supplemented by
the continuing work of R.E. Meintzer on REE and stable isotope abundanc-
es. The overall geological framework, especially in terms of structure
and metamorphism of the country rocks, would be greatly improved by de-
tailed geologic mapping within the Red Sucker Lake area, which, hopeful-
ly, be implemented in the near futurer by the Geological Services Branch
of Manitoba Department of Energy and Mines.

Gods Lake area

Further research associated with the Gods River pegmatite should include
exploration for and evaluating any additional albite-spodumene pegma-
tites that may occur in the vicinity of the known pegmatite, and to bet-
ter define the vertical extent of the Gods River pegmatite. Basal till
and/or stream sediment geochemical sampling would be the most practical
exploration techniques in this area. For further information on explo-
ration for lithium-bearing pegmatites see Trueman (1978) and Trueman and
Černý (1982).

REFERENCES

Anderson, A. (1984) The geochemistry, mineralogy and petrology of the Cross Lake pegmatite field, central Manitoba. M.Sc. thesis, University of Manitoba, Winnipeg, Manitoba, Canada.

Appleman, D.E., and Evans, H.T.Jr. (1973) Indexing and least-squares refinement of powder diffraction data. USGS Comp. Contr. **20**.

Aubert, G. (1969) Les coupoles granitiques de Montebras et d'Échassières (massif central française) et la genèse de leurs minéralisations. Bureau de Recherches Géologiques et Minières.

Bannatyne, B.B. (1985) Industrial minerals in rare-element pegmatites of Manitoba. Manitoba Department of Energy and Mines, Geological Services Branch, Economic Geology Report ER84-1.

Bannatyne, B.B. (1973) Pegmatite project. In: Summary of Geological Field Work, Manitoba Department of Energy and Mines, Mineral Resources Division, Geol. Paper 2/73.

Bateman, J.D. (1943) Tin in Manitoba. Canadian Mining Journal **64**, 50-53.

Burnol, L. (1974) Géochimie du béryllium et types de concentrations dans les leucogranites du massif central française. Bureau de Recherches Géologiques et Minières.

Černý, P. (1987) Rare-element granitic pegmatites. MMD-GAC Monograph Series on Geology of Mineral Deposits. Edited by A.C. Brown. In press.

Černý, P. (1982a) Anatomy and classification of granitic pegmatites. In: Granitic Pegmatites in Science and Industry. Edited by P. Černý. Mineralogical Association of Canada, Short Course Handbook **8**, 1-40.

Černý, P. (1982b) Petrogenesis of granitic pegmatites. In: Granitic Pegmatites in Science and Industry. Edited by P. Černý. Mineralogical Association of Canada, Short Course Handbook **8**, 405-450.

Černý, P. (1982c) The Tanco Pegmatite at Bernic Lake, Southeastern Manitoba. In: Granitic Pegmatites in Science and Industry. Edited by P. Černý. Mineralogical Association of Canada, Short Course Handbook **8**, 527-544.

Černý, P., and Hawthorne, F. (1982) Selected peraluminous minerals. In: Granitic Pegmatites in Science and Industry. Edited by P. Černý. Mineralogical Association of Canada, Short Course Handbook **8**, 163-186.

Černý, P., and Meintzer, R.E. (1987) Fertile granites in the Archean and Proterozoic fields of rare-element pegmatites: crustal environment, geochemistry and petrogenetic relationships. In Recent advances in the geology of granite-related mineral deposits. Edited by R.P. Taylor and D.F. Strong. Canadian Institute of Mining and Metallurgy, Special Volume 39 (in press).

Černý, P., Trueman, D.L., Ziehlke, D.V., Goad, B.E., and Paul, B.J. (1981) The Cat Lake-Winnipeg River and the Wekusko Lake Pegmatite Fields, Manitoba; Manitoba Mineral Resources Division, Economic Geology Report ER80-1.

Chackowsky, L.E., and Černý, P. (1986) Mineralized pegmatitic granites at Red Sucker Lake, northeastern Manitoba. In: Manitoba Mineral Resources Division, Report of Field Activities 1986, 184-190.

Chackowsky, L.E., and Černý, P. (1984) Pegmatitic granites and pegmatites at Red Sucker Lake, Manitoba. In: Manitoba Mineral Resources Division, Report of Field Activities 1984, 133-135.

Chackowsky, L.E., Wang, X.J., Eby, R., and Černý, P. (1985) Pegmatitic granites, pegmatites and other felsic plutonic rocks at Gods Lake and Red Cross Lake, Manitoba. In: , Manitoba Mineral Resources Division, Report of Field Activities 1985, 209-211.

Clark, G.S., and Černý, P. (1987) Radiogenic ^{87}Sr, its mobility and their effect on deciphering Rb-Sr fractionation in rare-element pegmatites. Geochimica et Cosmochimica Acta **51**, in press.

Clark, G.S., and Cheung, S.-P. (1980) Rubidium-strontium ages from the Oxford Lake - Knee Lake greenstone belt, northern Manitoba. Canadian Journal of Earth Sciences **17**, 560-568.

Clark, G.S., and Meintzer, R.E. (1987) Rb-Sr isotopic systematics of leucogranites of the Cross Lake pegmatite field, central Manitoba, Canada. In preparation.

Clark, G.S., and Weber, W. (1987) Rubidium-strontium age and origin of uraniferous granite, Molson Lake-Red Sucker Lake area, northwestern Superior Province, Manitoba. Canadian Journal of Earth Sciences **25**,

Deer, W.A., Howie, R.A., and Zussman, J. (1966) An Introduction to the Rock-forming Minerals. Longman.

Downie, D.L. (1936) Stull Lake sheet (West half), Manitoba and Ontario; Geological Survey of Canada, Map 452A.

Ercit, T.S. (1986) The simpsonite paragenesis: the crystal chemistry and geochemistry of extreme tantalum fractionation. Ph.D. thesis, University of Manitoba.

Ermanovics, I.F., McRitchie, W.D., and Houston, W.N. (1979) Petrochemistry and tectonic setting of plutonic rocks of the Superior Province in Manitoba. In: Trondhjemites, Dacites and Related Rocks. Edited by F. Barker. Elsevier Publishing Company, p. 323-362.

Ermanovics, I.F., and Wanless, R.K. (1983) Isotopic age studies and tectonic interpretation of Superior Province in Manitoba. Geological Survey of Canada, Paper 82-12, 22p.

Gilbert, H.P. (1985) Geology of the Knee Lake-Gods Lake area. Manitoba Department of Energy and Mines, Geological Services Branch, Geological Report GR83-1b.

Goad, B.E., and Černý, P. (1981) Peraluminous pegmatitic granites and their pegmatite aureoles in the Winnipeg River District, southeastern Manitoba. Canadian Mineralogist **19**, 177-194.

Gyongyossy, Z.D., and Spooner, E.T.C. (1979) Lithium: an energy element. Minerals Sci. Engng. **11**, 155-176.

Hutchinson, R.W. (1955) Regional zonation of pegmatites near Ross Lake, District of Mackenzie, Northwest Territories. Geol. Survey 29, Canada Bull. 34.

Kroll, H., and Ribbe, P.H. (1983) Lattice parameters, composition and Al,Si order in alkali feldspars. In: Feldspar Mineralogy, Vol. 2, 2nd Edition. Mineralogical Society of America.

Kunasz, I.A. (1982) Foote Mineral Company - Kings Mountain operation. In: Granitic Pegmatites in Science and Industry. Edited by P. Černý. Mineralogical Association of Canada, Short Course Handbook **8**, 505-512.

Kunasz, I.A. (1978) Quo vadis, Lition? Energy **3**, 387-390.

London, D., and Burt, D.M. (1982) Lithium minerals in pegmatites. In: Granitic Pegmatites in Science and Industry. Edited by P. Černý. Mineralogical Association of Canada, Short Course Handbook **8**, 99-134.

Morgan, G.B. IV (1986) Alteration of amphibolitic wallrocks around the Tanco rare-element pegmatite, southeastern Manitoba. M.Sc. thesis, School of Geology and Geophysics, University of Oklahoma.

Phillips, W.R. (1971) Mineral Optics. W.H. Freeman and Co.

Rinaldi, R., Černý, P., and Ferguson, R.B. (1972) Lithium-rubidium-cesium micas. Canadian Mineralogist **11**, p. 690-707.

Schledewitz, D.C.P., and Kusmirski, R. (1979) Boulton Lake-Red Sucker Lake area; Manitoba Mineral Resources Division, Report of Field Activities 1979, 32-37.

Schledewitz, D.C.P. (1980) Stull Lake, Southwest; Manitoba Mineral Resources Division, Preliminary Geological Map 1980 K-5.

Shearer, C.K., Papike, J.J., and Laul, J.C. (1985) Chemistry of potassium feldspars from three zoned pegmatites, Black Hills, South Dakota: Implications concerning pegmatite evolution. Geochimica et Cosmochimica Acta **34**, 663-673.

Southard, G.G. (1977) Exploration history, compilation and review including exploration data from cancelled assessment files for the Gods, Knee and Oxford Lake areas, Manitoba. Manitoba Mineral Resources Division, Open File Report 77/5.

Steiger, R.H., and Jäger, E. (1977) Subcommission on geochronology: convention on the use of decay constants in geocosmochronology. Earth and Planetary Science Letters **36**, 359-362.

Stevenson, R.K., and Martin, R.F. (1986) Implications of the presence of amazonite in the Broken Hill and Geco metamorphosed sulfide deposits. Canadian Mineralogist **24**, 729-746.

Stewart, D.B. (1978) Petrogenesis of lithium-rich pegmatites. American Mineralogist **63**, 970-980.

Trueman, D.L., and Černý, P. (1982) Exploration for rare-element granitic pegmatites. In: Granitic Pegmatites in Science and Industry. Edited by P. Černý. Mineralogical Association of Canada, Short Course Handbook **8**, 463-491.

Trueman, D.L. (1978) Exploration methods in the Tanco mine area of southeastern Manitoba, Canada. Energy **3**, 293-298.

Turekian, K., and Wedepohl, K.H. (1961) Distribution of the Elements in Some Major Units of the Earth's Crust. Geological Society of America Bulletin **72**, 175-212.

Weber, W., Schledewitz, D.C.P., and Soonawala, N.M. (1982) Airborne radiometric anomalies caused by late kinematic granitic rocks in the Molson lake-Red Sucker Lake area, east-central Manitoba. In: Uranium in Granites. Edited by Y.T. Maurice. Geological Survey of Canada, Paper 81-23, 119-124.

Appendix A

MICROCLINE AND GARNET ANALYSES FROM PEGMATITIC GRANITES AT RED SUCKER LAKE

Table A.1: Microcline analyses from pegmatitic granites at Red Sucker Lake.

Sample	WT. %					PPM									
	ΣFe_2O_3	CaO	Na_2O	K_2O	Li	Rb	Cs	Sr	Ba	Pb	K/Rb	K/Cs	K/Ba	Rb/Cs	Δ
RSL-A-04	<0.01	0.03	1.51	13.71	111	13400	616	87	48	41	8.5	185	2371	21.8	0.95
RSL-A-14-B	<0.01	0.03	1.20	14.03	143	13000	495	78	33	47	9.0	235	3529	26.3	0.98
RSL-A-15	<0.01	0.05	1.17	14.10	106	12400	635	77	48	37	9.4	184	2439	19.5	0.94
RSL-B-05	0.01	0.02	1.97	13.28	138	8600	135	42	28	36	12.8	817	3937	63.7	0.97
RSL-B-12	<0.01	0.03	1.87	12.93	119	9000	290	35	21	40	11.9	370	5111	31.0	0.98
RSL-B-13	0.01	0.05	1.36	13.55	143	8100	364	63	<20	36	13.9	309	******	22.3	0.96
RSL-B-14	0.01	0.05	1.22	13.80	131	7640	452	62	27	34	15.0	253	4243	16.9	0.94
RSL-B-19	0.01	0.03	1.66	13.46	199	7150	154	51	<20	19	15.6	726	******	46.4	0.96
RSL-B-22	0.01	0.04	1.73	13.05	134	7190	164	52	<20	28	15.1	661	******	43.8	0.96
RSL-B-28	0.01	0.02	1.55	13.36	179	8320	325	62	<20	33	13.3	341	******	25.6	0.97
RSL-C-02	0.01	0.01	1.89	13.32	147	9000	224	39	37	35	12.3	494	2989	40.2	0.99
RSL-C-05	0.01	0.01	1.48	13.02	117	8200	188	36	62	39	13.2	575	1743	43.6	0.92
RSL-C-11	0.01	<0.01	1.87	13.62	97	9400	271	60	38	45	12.0	417	2975	34.7	0.97
RSL-C-24	0.01	0.01	1.83	13.56	209	8600	196	49	27	47	13.1	574	4169	43.9	0.96
RSL-C-25	0.01	<0.01	1.56	13.75	174	9200	204	51	42	35	12.4	560	2718	45.1	0.94
RSL-D-06	0.01	0.02	1.25	14.15	30	8400	71	41	25	21	14.0	1654	4699	118.3	1.00
RSL-D-07	0.01	0.01	1.64	13.62	32	8000	54	32	26	14	14.1	2094	4349	148.1	0.96
RSL-D-11	0.01	0.01	1.80	13.46	17	8600	67	31	24	22	13.0	1668	4656	128.4	0.96
RSL-E-04	0.01	0.03	1.77	13.73	3	3048	19	39	175	38	37.4	5999	651	160.4	0.97
RSL-E-05	0.01	0.03	1.51	14.26	4	3111	21	37	181	45	38.1	5637	654	148.1	0.97
RSL-E-06	0.01	0.03	1.53	14.23	2	3105	26	40	195	43	38.0	4543	606	119.4	0.99
RSL-F-03	0.01	0.01	3.43	11.43	35	1902	33	12	54	23	49.9	2875	1757	57.6	0.93
RSL-F-08	0.01	<0.01	3.13	11.43	30	1618	40	44	10	27	58.6	2372	9489	40.4	0.97
RSL-F-11	0.01	0.03	3.23	11.95	23	1906	26	12	30	40	52.0	3815	3307	73.3	0.95
RSL-F-12	0.01	0.06	3.03	12.30	33	2030	70	12	21	51	50.3	1459	4862	29.0	0.98
RSL-G-10	0.02	0.07	3.05	11.72	31	1926	44	16	<20	48	50.5	2211	******	43.8	0.94
RSL-G-14	0.04	0.08	3.07	11.67	33	1719	49	10	<20	51	56.4	1977	******	35.1	0.93
RSL-G-17	0.02	0.06	2.54	12.11	25	1853	55	12	<20	48	54.3	1828	******	33.7	0.96
RSL-G-22	0.02	0.02	3.79	11.02	36	2139	38	14	<20	21	42.8	2407	******	56.3	0.97
RSL-I-04	0.04	0.14	2.93	11.51	< 1	975	188	14	28	68	98.0	508	3413	5.2	0.00
RSL-I-10	0.02	0.12	3.43	10.80	26	786	9	21	177	34	114.1	9962	507	87.3	0.94
RSL-I-11	0.03	0.10	3.08	11.96	31	1530	12	11	160	52	64.9	8274	621	127.5	0.96
RSL-I-17	0.04	0.06	2.91	11.67	< 1	1180	215	10	10	63	82.1	451	9688	5.5	0.00
RSL-J-04	0.02	0.05	2.83	12.13	17	1685	75	15	<20	45	59.8	1343	******	22.5	0.96
RSL-J-05	0.02	0.13	3.47	11.70	18	1068	22	18	164	40	90.9	4415	592	48.5	0.96
RSL-J-11	0.02	0.21	2.69	12.11	17	1253	< 1	13	<20	59	80.2	******	******	*********	0.95
RSL-J-17	0.02	0.06	2.72	12.07	9	3191	46	17	65	33	31.4	2178	1542	69.4	0.96
RSL-J-18	0.02	0.02	2.69	11.92	11	2803	34	15	<20	39	35.3	2910	******	82.4	0.99
RSL-J-21	0.02	0.06	1.77	13.00	11	2718	60	12	<20	28	39.7	1799	******	45.3	0.97
RSL-J-35	0.02	0.09	2.09	13.01	13	1355	25	9	26	59	79.7	4320	4154	54.2	0.95

Sample	WT. %				PPM						K/Rb	K/Cs	K/Ba	Rb/Cs	Δ
	ΣFe_2O_3	CaO	Na_2O	K_2O	Li	Rb	Cs	Sr	Ba	Pb					
RSL-K-02	0.02	0.02	3.09	11.37	7	3826	57	17	<20	32	24.7	1656	******	67.1	0.97
RSL-K-03	0.04	0.02	3.30	11.65	9	2784	24	10	<20	23	34.7	4030	******	116.0	0.96
RSL-K-09	0.02	0.14	3.09	11.60	11	1304	14	9	95	30	73.8	6878	1014	93.1	0.96
RSL-K-11	0.01	0.06	3.35	11.44	46	3442	34	16	<20	25	27.6	2793	******	101.2	0.97
RSL-K-13	0.02	0.02	3.66	11.24	35	2839	27	8	<20	21	32.9	3456	******	105.1	0.97
RSL-L-02	0.01	0.07	2.85	12.04	9	1646	35	11	28	44	60.7	2856	3570	47.0	0.97
RSL-L-03	0.02	0.07	3.01	11.57	6	1647	30	11	30	51	58.3	3202	3202	54.9	0.95
RSL-M-05	0.02	0.15	2.68	11.80	18	716	6	21	208	100	136.8	16326	471	119.3	0.95
RSL-M-06	<0.01	0.11	2.52	12.73	17	1283	20	14	23	76	82.4	5284	4595	64.1	0.95
RSL-M-10	0.01	0.08	3.01	11.85	16	1310	13	11	<20	72	75.1	7567	******	100.8	0.96
RSL-N-17	0.01	0.05	3.16	11.76	5	1927	18	9	<20	30	50.7	5424	******	107.1	0.96
RSL-N-18	0.01	0.11	3.14	11.54	5	1824	15	10	<20	33	52.5	6387	******	121.6	0.95
RSL-N-19	0.01	0.05	2.71	12.00	5	1755	19	10	20	43	56.8	5243	4981	92.4	0.97
RSL-N-20	0.01	0.10	1.90	13.47	5	2254	33	13	25	48	49.6	3389	4473	68.3	0.97
RSL-AE-20	0.01	0.13	1.70	13.25	17	990	31	12	26	85	111.1	3548	4231	31.9	0.92
RSL-BE-01	0.01	0.09	2.90	11.59	8	950	10	10	82	46	101.3	9621	1173	95.0	0.97
RSL-BE-07	0.01	0.09	2.91	11.53	8	990	5	9	68	70	96.7	19143	1408	198.0	0.95
RSL-BE-10	0.01	0.08	2.69	11.58	11	850	4	11	75	65	113.1	24033	1282	212.5	0.96
RSL-CE-06	0.01	0.05	3.07	11.46	18	1192	12	10	<20	50	79.8	7928	******	99.3	0.94
RSL-CE-07	0.01	0.04	2.98	11.57	10	1249	< 1	12	<20	49	76.9	******	******	*********	0.93
RSL-CE-12	0.02	0.05	2.84	11.77	9	1299	13	8	<20	47	75.2	7516	******	99.9	0.97
RSL-CE-13	0.03	0.07	2.52	12.08	10	1149	< 1	12	<20	57	87.3	******	******	*********	0.94
RSL-DE-02	0.01	0.04	3.05	11.46	13	1220	14	8	<20	40	78.0	6795	******	87.1	0.93
RSL-DE-03	0.01	0.03	2.43	12.03	11	1330	27	8	<20	40	75.1	3699	******	49.3	0.95
RSL-DE-05	0.02	0.03	2.27	11.80	14	1652	52	11	<20	38	59.3	1884	******	31.8	0.91
RSL-FE-05	0.03	0.02	1.59	13.15	73	8500	199	63	<20	11	12.8	549	******	42.7	0.95
RSL-HE-03	0.03	0.02	1.91	13.35	3	4001	32	32	21	7	27.7	3463	5277	125.0	0.96
RSL-HE-05	0.01	0.04	2.11	12.26	2	4880	54	34	35	11	20.9	1885	2908	90.4	0.94
RSL-IE-04	0.01	0.05	1.18	13.38	192	7150	151	69	28	46	15.5	736	3967	47.4	0.95
RSL-IE-06	0.01	0.07	1.40	13.40	140	5550	116	54	232	35	20.0	959	479	47.8	0.95
RSL-IE-13	0.01	0.05	1.35	13.32	235	9620	187	71	<20	35	11.5	591	******	51.4	0.93
RSL-KE-03	0.01	0.06	0.98	13.72	95	9630	331	79	24	22	11.8	344	4746	29.1	0.95
RSL-KE-04	<0.01	0.05	0.63	14.33	97	9920	349	77	21	19	12.0	341	5665	28.4	0.96
RSL-KE-11	0.01	0.05	1.40	13.24	297	8075	240	57	<20	24	13.6	458	******	33.6	0.97
RSL-KE-13	0.01	0.06	1.46	13.17	185	9830	372	78	<20	16	11.1	294	******	26.4	0.94
RSL-ME-04	0.08	0.08	1.30	12.90	76	4580	275	37	149	16	23.4	389	719	16.7	0.99
RSL-ME-06	0.04	0.11	1.71	12.40	90	3220	253	33	223	20	32.0	407	462	12.7	0.96
RSL-ME-07	<0.01	0.04	0.99	13.82	87	8800	267	63	<20	22	13.0	430	******	33.0	0.97
RSL-NE-04	0.01	0.05	1.18	13.67	211	12900	613	61	42	18	8.8	185	2702	21.0	0.96
RSL-RE-06	0.02	0.07	2.78	8.37	10	1170	15	13	129	14	59.4	4632	539	78.0	0.96

Sample	WT. %				PPM						K/Rb	K/Cs	K/Ba	Rb/Cs	Δ
	ΣFe_2O_3	CaO	Na_2O	K_2O	Li	Rb	Cs	Sr	Ba	Pb					
RSL-RE-07	0.01	0.07	3.20	11.65	6	1510	15	13	72	21	64.0	6447	1343	100.7	0.96
RSL-RE-09	0.01	0.07	3.52	11.45	7	1480	13	12	83	18	64.2	7312	1145	113.8	0.96
RSL-RE-11	0.01	0.07	3.30	11.72	7	1570	19	9	97	19	62.0	5121	1003	82.6	0.93
RSL-RE-12	0.01	0.05	3.77	11.22	8	2400	27	13	69	15	38.8	3450	1350	88.9	0.97
RSL-SE-03	0.01	0.09	2.57	12.48	9	920	10	20	63	84	112.6	10360	1644	92.0	0.95
RSL-SE-04	0.01	0.09	2.76	12.29	8	660	17	20	137	108	154.6	6001	745	38.8	0.96
RSL-SE-06	0.02	0.09	2.45	12.87	12	1574	24	15	27	70	67.9	4452	3957	65.6	0.97
RSL-SE-07	0.01	0.06	2.78	12.24	6	2260	39	14	<20	25	45.0	2605	******	57.9	0.95
RSL-SE-08	0.01	0.06	2.52	12.56	10	1070	13	6	<20	65	97.4	8021	******	82.3	0.96
RSL-SE-09	0.01	0.08	1.93	13.28	4	890	11	14	70	128	123.9	10022	1575	80.9	0.96
RSL-SE-17	0.01	0.05	2.04	5.90	7	430	18	11	45	42	113.9	2721	1088	23.9	0.98

Table A.2: Garnet analyses from pegmatitic granites at Red Sucker Lake.

SAMPLE	SiO_2	Al_2O_3	Fe_2O_3	FeO	MnO	MgO	CaO	TOTAL	Si	Al	Fe^{3+}	Fe^{2+}	Mn	Mg	Ca	TOTAL	MnO*
						Wt. %					Number of cations per 12 oxygens						
RSL-A-02-B	37.00	21.30	0.00	10.10	32.00	<0.10	0.30	100.70	3.01	2.04	0.00	0.69	2.20	0.00	0.02	7.96	76
RSL-A-07-A	33.30	20.80	4.47	9.68	29.50	<0.10	0.30	98.05	2.82	2.07	0.28	0.68	2.11	0.00	0.02	7.99	75
RSL-A-12-A	34.00	20.80	0.04	13.76	26.20	0.10	0.30	95.20	2.94	2.12	0.00	0.99	1.91	0.01	0.02	7.99	66
RSL-B-06	34.80	21.40	1.27	18.56	22.40	<0.10	0.40	98.83	2.90	2.11	0.08	1.30	1.58	0.00	0.03	7.99	55
RSL-B-07	34.80	21.10	3.39	17.75	23.20	<0.10	0.40	100.64	2.87	2.05	0.21	1.22	1.62	0.00	0.03	7.99	57
RSL-B-15	34.40	21.10	1.28	23.45	17.10	0.10	0.30	97.73	2.90	2.10	0.08	1.66	1.22	0.01	0.02	7.99	42
RSL-B-18	36.60	21.10	0.00	21.50	20.80	<0.10	0.40	100.40	3.00	2.04	0.00	1.47	1.44	0.00	0.03	7.98	49
RSL-B-29	34.30	21.30	3.32	10.11	29.80	0.40	0.40	99.63	2.84	2.08	0.21	0.70	2.09	0.02	0.03	7.98	75
RSL-C-03	36.30	20.80	0.00	22.60	19.40	<0.10	0.40	99.50	3.00	2.03	0.00	1.56	1.36	0.00	0.03	7.98	46
RSL-C-12-B	34.20	21.00	0.65	15.71	24.60	<0.10	0.30	96.47	2.92	2.11	0.04	1.12	1.78	0.00	0.02	8.00	61
RSL-C-13	34.50	21.40	1.74	13.03	27.60	<0.10	0.30	98.57	2.89	2.11	0.11	0.91	1.96	0.00	0.02	8.00	68
RSL-C-15	34.30	21.10	3.91	11.68	28.70	<0.10	0.30	99.99	2.84	2.06	0.24	0.81	2.01	0.00	0.02	8.00	71
RSL-C-21	36.90	21.20	0.00	17.20	25.40	<0.10	0.30	101.00	3.00	2.03	0.00	1.17	1.75	0.00	0.02	7.97	60
RSL-C-23	36.80	21.20	0.00	15.90	26.80	0.10	0.30	101.10	2.99	2.03	0.00	1.08	1.84	0.01	0.02	7.98	63
RSL-D-03	34.30	21.10	3.15	18.77	21.70	<0.10	0.30	99.32	2.86	2.07	0.20	1.31	1.53	0.00	0.02	8.00	54
RSL-D-08	34.50	21.20	0.64	20.93	19.80	<0.10	0.30	97.36	2.92	2.11	0.04	1.48	1.42	0.00	0.02	8.00	49
RSL-F-05	33.90	20.90	4.07	28.94	11.00	0.20	0.30	99.31	2.84	2.06	0.26	2.02	0.78	0.01	0.02	7.99	28
RSL-F-06	34.00	20.90	3.33	32.30	7.80	0.30	0.20	98.83	2.85	2.07	0.21	2.27	0.55	0.02	0.01	7.98	19
RSL-G-01	34.60	21.10	2.47	30.18	10.60	0.20	0.30	99.45	2.88	2.07	0.15	2.10	0.75	0.01	0.02	7.99	26
RSL-G-03	34.70	21.20	1.62	34.24	6.80	0.20	0.20	98.96	2.90	2.09	0.10	2.39	0.48	0.01	0.01	7.99	17
RSL-G-09-B	34.50	21.10	2.29	30.24	10.60	0.10	0.20	99.03	2.88	2.08	0.14	2.11	0.75	0.01	0.01	7.99	26
RSL-G-09-C	34.20	21.00	3.11	30.40	10.00	0.20	0.20	99.11	2.86	2.07	0.20	2.13	0.71	0.01	0.01	7.99	25
RSL-G-18	35.00	21.50	2.46	33.59	7.80	0.20	0.20	100.75	2.88	2.08	0.15	2.31	0.54	0.01	0.01	7.99	19
RSL-G-23	35.30	21.50	2.41	32.03	9.60	0.30	0.20	101.34	2.88	2.07	0.15	2.19	0.66	0.02	0.01	7.99	23
RSL-H-01	34.90	21.60	1.23	29.19	11.40	0.90	0.20	99.42	2.89	2.11	0.08	2.02	0.80	0.06	0.01	7.96	28
RSL-I-02	34.70	21.60	1.43	33.12	7.10	0.90	0.40	99.24	2.88	2.11	0.09	2.30	0.50	0.06	0.03	7.96	18
RSL-I-09	34.40	21.60	1.75	31.92	8.20	0.80	0.20	98.88	2.87	2.12	0.11	2.22	0.58	0.05	0.01	7.96	20
RSL-I-16	34.40	21.20	2.67	32.90	7.50	0.50	0.20	99.37	2.86	2.08	0.17	2.29	0.53	0.03	0.01	7.98	19
RSL-I-18	35.10	21.80	1.32	29.41	9.80	2.20	0.70	100.33	2.86	2.10	0.08	2.01	0.68	0.13	0.05	7.90	25
RSL-J-03	34.50	21.00	2.08	31.93	8.40	0.60	0.30	98.81	2.89	2.07	0.13	2.23	0.59	0.04	0.02	7.97	21
RSL-J-10	34.60	21.40	2.22	30.50	10.20	0.40	0.20	99.52	2.87	2.09	0.14	2.12	0.72	0.02	0.01	7.98	25
RSL-J-12	35.40	21.80	2.00	28.60	12.20	0.80	0.70	101.50	2.87	2.09	0.12	1.94	0.84	0.05	0.04	7.96	30
RSL-J-28-B	34.80	21.60	1.44	30.70	9.70	1.00	0.20	99.44	2.88	2.11	0.09	2.13	0.68	0.06	0.01	7.96	24
RSL-J-38	34.90	21.60	1.84	33.05	7.50	0.90	0.30	100.08	2.87	2.10	0.11	2.28	0.52	0.06	0.02	7.96	18
RSL-J-40	34.40	21.40	2.40	32.94	7.10	0.70	0.40	99.34	2.86	2.10	0.15	2.29	0.50	0.04	0.03	7.97	18
RSL-K-05	35.40	21.70	1.48	30.47	11.00	0.70	0.10	100.85	2.89	2.09	0.09	2.08	0.76	0.04	0.01	7.97	27
RSL-K-07	34.90	21.40	1.80	29.38	11.40	0.80	0.10	99.78	2.88	2.08	0.11	2.03	0.80	0.05	0.01	7.97	28
RSL-K-12	34.80	21.40	1.86	26.33	14.20	0.80	0.20	99.59	2.88	2.09	0.12	1.82	0.99	0.05	0.01	7.96	35
RSL-L-05-A	37.70	24.40	8.72	25.96	12.70	3.50	3.30	116.27	2.67	2.04	0.46	1.54	0.76	0.19	0.18	7.84	33
RSL-L-05-B	34.40	21.30	1.99	30.11	9.90	0.80	0.30	98.80	2.87	2.10	0.13	2.10	0.70	0.05	0.02	7.96	25

| | Wt. % | | | | | | | | Number of cations per 12 oxygens | | | | | | | | |
SAMPLE	SiO$_2$	Al$_2$O$_3$	Fe$_2$O$_3$	FeO	MnO	MgO	CaO	TOTAL	Si	Al	Fe^{3+}	Fe^{2+}	Mn	Mg	Ca	TOTAL	MnO*
RSL-M-01	34.50	21.20	1.77	28.81	11.30	0.80	0.30	98.68	2.88	2.09	0.11	2.01	0.80	0.05	0.02	7.96	28
RSL-M-08	34.70	21.40	3.91	28.28	11.70	1.10	0.40	101.49	2.83	2.06	0.24	1.93	0.81	0.07	0.03	7.95	29
RSL-N-01	34.60	21.30	1.76	26.92	13.30	1.00	0.10	98.98	2.88	2.09	0.11	1.87	0.94	0.06	0.01	7.96	33
RSL-N-06	34.70	21.40	1.91	26.08	14.60	0.60	0.10	99.39	2.88	2.09	0.12	1.81	1.03	0.04	0.01	7.97	36
RSL-N-09	34.30	21.60	1.50	26.35	13.50	1.00	0.10	98.35	2.87	2.13	0.09	1.84	0.96	0.06	0.01	7.96	34
RSL-N-16	34.10	21.70	1.41	34.33	6.00	0.20	0.20	97.94	2.87	2.15	0.09	2.42	0.43	0.01	0.01	7.99	15
RSL-O-02-A	34.40	21.00	2.24	27.88	12.00	0.70	0.50	98.72	2.88	2.07	0.14	1.95	0.85	0.04	0.03	7.96	30
RSL-O-02-B	34.50	21.30	1.65	27.52	12.20	0.70	0.80	98.66	2.88	2.10	0.10	1.92	0.86	0.04	0.05	7.96	31
RSL-O-03	34.90	21.60	2.10	28.41	11.70	0.80	0.80	100.31	2.87	2.09	0.13	1.95	0.81	0.05	0.05	7.96	29
RSL-AE-06	35.00	21.50	1.23	32.69	7.80	1.30	0.10	99.62	2.89	2.09	0.08	2.26	0.54	0.08	0.01	7.95	19
RSL-AE-11-B	35.00	21.50	2.29	34.74	5.50	1.40	0.30	100.73	2.86	2.07	0.14	2.38	0.38	0.09	0.02	7.94	14
RSL-AE-13	35.10	21.70	1.74	33.23	7.20	1.40	0.20	100.57	2.87	2.09	0.11	2.27	0.50	0.09	0.01	7.94	18
RSL-AE-17-A	35.20	21.60	1.19	34.03	6.80	1.20	0.10	100.12	2.89	2.09	0.07	2.34	0.47	0.07	0.01	7.95	17
RSL-AE-18A	34.80	21.60	3.19	32.53	7.80	1.00	0.30	101.22	2.84	2.08	0.20	2.22	0.54	0.06	0.02	7.96	19
RSL-AE-18-B	34.70	21.10	1.55	32.20	8.10	1.00	0.20	98.86	2.89	2.07	0.10	2.25	0.57	0.06	0.01	7.96	20
RSL-AE-18-C	34.80	21.20	1.56	33.99	6.00	1.40	0.30	99.26	2.89	2.07	0.10	2.36	0.42	0.09	0.02	7.94	15
RSL-BE-05-B	34.70	21.40	1.52	34.33	6.00	1.00	0.20	99.15	2.88	2.10	0.10	2.39	0.42	0.06	0.01	7.96	15
RSL-BE-06	35.10	21.70	1.87	34.32	6.30	1.10	0.30	100.69	2.87	2.09	0.12	2.35	0.44	0.07	0.02	7.95	16
RSL-CE-01	34.90	21.40	2.10	11.31	29.60	0.20	0.30	99.81	2.89	2.09	0.13	0.78	2.07	0.01	0.02	7.99	72
RSL-CE-01-B	34.10	20.90	1.56	32.40	7.20	1.00	0.20	97.36	2.89	2.08	0.10	2.29	0.52	0.06	0.01	7.96	18
RSL-CE-02	34.70	21.50	1.29	34.54	5.70	1.10	0.20	99.03	2.88	2.11	0.08	2.40	0.40	0.07	0.01	7.95	14
RSL-CE-08-A	34.80	21.30	1.06	33.85	6.50	1.00	0.30	98.81	2.90	2.09	0.07	2.36	0.46	0.06	0.02	7.96	16
RSL-CE-08-B	35.10	21.80	1.97	34.73	5.90	1.20	0.20	100.90	2.87	2.10	0.12	2.37	0.41	0.07	0.01	7.95	15
RSL-CE-15	34.80	21.40	1.50	33.95	6.40	1.00	0.30	99.35	2.89	2.09	0.09	2.35	0.45	0.06	0.02	7.96	16
RSL-DE-06	34.60	21.20	1.59	32.57	7.80	0.80	0.20	98.76	2.89	2.09	0.10	2.27	0.55	0.05	0.01	7.96	19
RSL-DE-07	34.70	21.30	1.67	28.50	12.30	0.50	0.10	99.07	2.89	2.09	0.10	1.99	0.87	0.03	0.01	7.98	30
RSL-DE-10	35.40	21.40	0.80	32.88	7.90	1.30	0.30	99.98	2.91	2.07	0.05	2.26	0.55	0.08	0.02	7.94	19
RSL-DE-12	34.70	21.40	1.55	31.40	8.80	1.10	0.20	99.16	2.88	2.09	0.10	2.18	0.62	0.07	0.01	7.95	22
RSL-FE-04	34.90	21.30	2.30	24.63	16.80	<0.10	0.10	100.03	2.89	2.08	0.14	1.70	1.18	0.00	0.01	8.00	41
RSL-IE-08-B	35.20	21.40	1.68	19.59	21.40	0.30	0.60	100.17	2.90	2.08	0.10	1.35	1.49	0.02	0.04	7.98	52
RSL-KE-01	34.80	21.80	2.66	15.70	24.60	0.70	0.40	100.67	2.85	2.10	0.16	1.08	1.70	0.04	0.03	7.97	61
RSL-ME-01	34.00	21.10	2.88	9.91	30.10	<0.10	0.30	98.29	2.86	2.09	0.18	0.70	2.14	0.00	0.02	7.99	75
RSL-ME-05	34.90	21.50	1.31	32.33	8.30	0.80	0.30	99.43	2.89	2.10	0.08	2.24	0.58	0.05	0.02	7.96	20
RSL-NE-01	34.60	21.10	1.92	11.07	29.30	0.30	0.40	98.69	2.89	2.08	0.12	0.77	2.07	0.02	0.03	7.98	73
RSL-OE-03	34.60	21.20	3.08	20.13	20.80	<0.10	0.20	100.01	2.87	2.07	0.19	1.40	1.46	0.00	0.01	8.00	51
RSL-PE-03	34.80	21.50	1.91	19.98	21.00	0.10	0.30	99.59	2.89	2.10	0.12	1.39	1.47	0.01	0.02	7.99	51
RSL-RE-05	35.20	21.50	1.34	31.60	9.20	1.10	0.20	100.13	2.89	2.08	0.08	2.17	0.64	0.07	0.01	7.95	23
RSL-SE-01-A	34.70	21.40	1.13	33.49	6.20	1.50	0.40	98.81	2.88	2.10	0.07	2.33	0.44	0.09	0.03	7.93	16
RSL-SE-02	35.00	21.40	1.77	34.90	5.60	1.00	0.40	100.08	2.88	2.08	0.11	2.40	0.39	0.06	0.03	7.95	14

Appendix B

MICROCLINE AND GARNET ANALYSES FROM PEGMATITES AT RED
SUCKER LAKE

Table B.1: Microcline analyses from pegmatites at Red Sucker Lake.

Sample	ΣFe_2O_3	CaO	Na_2O	K_2O	Li	Rb	Cs	Sr	Ba	Pb	K/Rb	K/Cs	K/Ba	Rb/Cs	Δ
	WT. %				PPM										
RSL-BL	0.01	0.03	1.70	12.46	288	11400	455	87	14	16	9.1	227	7388	25.1	0.98
RSL-BF-02	0.01	0.08	3.66	11.34	16	1022	4	< 6	66	57	92.1	23535	1426	255.5	0.92
RSL-BF-03	0.02	0.09	3.79	11.30	14	961	3	< 6	29	80	97.6	31269	3235	320.3	0.92
RSL-CY-02	0.01	0.03	4.13	11.03	26	1567	11	8	31	36	58.4	8324	2954	142.5	0.95
RSL-DJ-01	0.01	0.08	3.96	11.04	23	1143	4	6	59	52	80.2	22912	1553	285.8	0.97
RSL-GC-03	0.01	0.12	2.11	13.66	6	611	6	45	298	152	185.6	18900	381	101.8	0.98
RSL-GC-06	0.01	0.11	2.31	13.60	7	1219	6	20	61	101	92.6	18817	1851	203.2	0.96
RSL-GR-03	0.01	0.05	3.71	11.54	12	1120	8	13	49	51	85.5	11975	1955	140.0	0.95
RSL-GR-06	0.01	0.12	3.63	11.45	19	1672	< 1	12	42	24	56.8	******	2263	*********	0.92
RSL-LN-01	0.01	0.07	3.88	11.38	20	925	3	11	76	55	102.1	31490	1243	308.3	0.98
RSL-LN-11	0.01	0.06	4.00	11.19	19	1257	4	11	23	57	73.9	23223	4039	314.3	0.94
RSL-MN-01	0.01	0.07	3.67	11.58	21	1075	4	6	28	66	89.4	24033	3433	268.8	0.94
RSL-MN-05	0.01	0.09	3.18	11.99	13	1110	5	9	28	53	89.7	19907	3555	222.0	0.99
RSL-NT-02	0.01	0.09	3.79	11.55	8	1200	2	11	44	32	79.9	47941	2179	600.0	0.98
RSL-NT-09	0.01	0.05	3.61	11.70	5	1246	7	12	37	50	78.0	13875	2625	178.0	0.97
RSL-NT-10	0.01	0.04	3.47	11.46	6	1393	10	12	37	40	68.3	9514	2571	139.3	0.93
RSL-PK-05-A	0.02	0.04	1.44	13.35	50	13800	1106	75	325	48	8.0	100	341	12.5	0.96
RSL-RY-01	0.01	0.13	2.83	12.26	9	1257	11	24	67	86	81.0	9252	1519	114.3	0.95
RSL-SC-04	0.01	0.08	1.58	14.37	4	1651	14	33	150	121	72.3	8521	795	117.9	1.02
RSL-SC-07	0.01	0.11	3.03	12.16	2	1371	< 1	22	81	68	73.6	******	1246	*********	0.95
RSL-SC-10	0.01	0.22	2.21	13.04	2	1010	< 1	41	190	90	107.2	******	570	*********	0.93
RSL-SC-13	0.06	0.10	1.59	12.24	< 1	475	176	57	465	125	213.9	577	219	2.7	0.00
RSL-SQ-01	<0.01	0.09	1.41	13.30	139	18000	1246	113	74	88	6.1	89	1492	14.4	0.95
RSL-SQ-07	<0.01	0.07	1.29	13.65	103	17800	1020	133	105	71	6.4	111	1079	17.5	0.95
RSL-SQ-11	<0.01	0.11	2.00	12.70	98	17000	1058	126	61	65	6.2	100	1728	16.1	0.97
RSL-SQ-12	<0.01	0.03	1.62	13.05	96	17600	1098	139	78	71	6.2	99	1389	16.0	0.96
RSL-SQ-13	<0.01	0.03	1.39	13.28	90	18400	1039	134	86	72	6.0	106	1282	17.7	0.97
RSL-SQ-14	0.01	0.03	1.57	13.19	89	17600	1014	129	93	80	6.2	108	1177	17.4	0.95
RSL-SQ-15	<0.01	0.04	1.42	13.24	107	17400	1037	134	124	77	6.3	106	886	16.8	0.96
RSL-SQ-16	<0.01	0.02	1.47	13.12	136	18800	1196	136	79	89	5.8	91	1379	15.7	0.95
RSL-SQ-17	<0.01	<0.01	1.56	13.12	114	17400	1046	157	100	89	6.3	104	1089	16.6	0.95
RSL-SQ-18	0.01	0.06	1.92	12.85	118	17000	1139	141	94	97	6.3	94	1135	14.9	0.95
RSL-ST-01	0.01	0.13	3.21	11.76	4	589	< 1	8	58	86	165.7	******	1683	*********	0.95
RSL-ST-04	0.01	0.08	3.62	11.79	3	578	< 1	19	83	97	169.3	******	1179	*********	0.94
RSL-ST-05	0.01	0.09	2.75	12.39	4	831	< 1	24	84	103	123.8	******	1224	*********	0.92
RSL-TD-17	0.01	0.11	2.17	12.80	97	9800	236	80	53	16	10.8	450	2005	41.5	0.96
RSL-WD-03	0.01	0.12	1.33	14.62	2	569	11	56	325	124	213.3	11033	373	51.7	0.96
RSL-WD-09	0.01	0.13	2.44	11.82	1	501	< 1	93	746	138	195.9	******	132	*********	0.96
RSL-WD-10	0.01	0.10	1.15	14.87	2	604	< 1	102	757	173	204.4	******	163	*********	0.96
RSL-EE-03	0.03	0.04	1.07	14.03	41	6500	240	60	<20	39	17.9	485	******	27.1	0.94

Table B.2: Garnet analyses from pegmatites at Red Sucker Lake.

| | Wt. % | | | | | | | | Number of cations per 12 oxygens | | | | | | | | |
SAMPLE	SiO_2	Al_2O_3	Fe_2O_3	FeO	MnO	MgO	CaO	TOTAL	Si	Al	Fe^{3+}	Fe^{2+}	Mn	Mg	Ca	TOTAL	MnO*
RSL-BF-01	36.80	21.10	0.00	34.30	5.10	0.80	0.30	98.40	3.04	2.05	0.00	2.37	0.36	0.05	0.02	7.88	13
RSL-BF-06-B	37.20	21.70	0.00	33.80	5.50	1.40	0.20	99.80	3.02	2.07	0.00	2.29	0.38	0.09	0.01	7.86	14
RSL-BF-07-B	34.70	21.50	1.32	32.22	8.70	0.10	0.40	98.93	2.90	2.12	0.08	2.25	0.61	0.01	0.03	7.99	21
RSL-BF-10-A	36.40	21.20	0.00	35.10	5.40	1.60	0.20	99.90	2.98	2.04	0.00	2.40	0.37	0.10	0.01	7.90	13
RSL-BR-01-B	34.80	21.80	1.23	34.20	5.80	1.40	0.30	99.52	2.87	2.12	0.08	2.36	0.41	0.09	0.02	7.94	15
RSL-CY-01-A	34.80	21.50	0.71	33.46	6.80	1.20	0.20	98.67	2.90	2.11	0.04	2.33	0.48	0.08	0.01	7.95	17
RSL-CY-01-B	34.60	21.40	2.37	13.87	26.80	<0.10	0.40	99.44	2.87	2.10	0.15	0.96	1.88	0.00	0.03	7.99	66
RSL-CY-03-B	37.20	21.70	0.00	33.70	5.90	1.60	0.10	100.20	3.01	2.07	0.00	2.28	0.40	0.10	0.01	7.86	15
RSL-CY-03-C	36.50	20.70	0.00	34.30	6.30	1.30	0.10	99.20	3.01	2.01	0.00	2.36	0.44	0.08	0.01	7.91	16
RSL-DJ-03	36.60	21.10	0.00	35.30	5.50	1.10	0.30	99.90	3.00	2.04	0.00	2.42	0.38	0.07	0.02	7.91	13
RSL-GC-05	37.30	21.80	0.00	28.60	11.60	0.60	0.20	100.10	3.02	2.08	0.00	1.94	0.80	0.04	0.01	7.89	29
RSL-GR-09	37.00	21.40	0.00	36.20	4.90	1.30	0.20	101.00	2.99	2.04	0.00	2.45	0.34	0.08	0.01	7.91	12
RSL-GR-10	36.50	21.30	0.00	34.30	4.40	1.50	0.20	98.20	3.01	2.07	0.00	2.37	0.31	0.09	0.01	7.86	11
RSL-LN-03	36.40	20.40	0.00	31.60	10.20	0.50	0.20	99.30	3.01	1.99	0.00	2.19	0.72	0.03	0.01	7.95	24
RSL-LN-05	34.60	21.30	1.78	34.60	5.80	0.90	0.10	99.08	2.88	2.09	0.11	2.41	0.41	0.06	0.01	7.96	14
RSL-MN-02	34.60	21.40	1.97	33.92	6.10	1.10	0.30	99.40	2.87	2.09	0.12	2.35	0.43	0.07	0.02	7.95	15
RSL-NB-01	36.30	21.20	0.00	33.60	5.80	1.20	0.20	98.30	3.00	2.07	0.00	2.32	0.41	0.07	0.01	7.89	15
RSL-NT-04-B	35.00	21.40	1.71	34.66	6.20	0.80	0.20	99.97	2.89	2.08	0.11	2.39	0.43	0.05	0.01	7.96	15
RSL-NT-04-C	34.20	21.40	0.19	34.93	4.90	0.80	0.30	96.72	2.90	2.14	0.01	2.48	0.35	0.05	0.02	7.96	12
RSL-NT-06-A	36.80	21.40	0.00	36.10	6.20	0.30	0.20	101.00	2.99	2.05	0.00	2.46	0.43	0.02	0.01	7.96	15
RSL-NT-07	34.30	21.00	2.74	34.94	5.10	0.70	0.30	99.07	2.86	2.07	0.17	2.44	0.36	0.04	0.02	7.97	13
RSL-RY-02-A	36.80	21.30	0.00	29.50	10.80	1.00	0.90	100.30	2.99	2.04	0.00	2.01	0.74	0.06	0.06	7.91	27
RSL-SC-05-A	36.60	21.20	0.00	30.50	10.50	1.30	0.50	100.60	2.98	2.03	0.00	2.07	0.72	0.08	0.03	7.92	26
RSL-SC-05-B	34.20	21.00	0.51	29.04	9.90	1.20	0.80	96.65	2.90	2.10	0.03	2.06	0.71	0.08	0.05	7.94	25
RSL-TD-01	34.70	21.00	0.90	11.99	28.40	<0.10	0.80	97.79	2.92	2.09	0.06	0.84	2.02	0.00	0.05	7.99	70
RSL-TD-12	37.00	21.30	0.00	21.20	21.70	<0.10	0.30	101.50	3.00	2.03	0.00	1.44	1.49	0.00	0.02	7.98	51